JOURNAL OF BIOLOGICAL REGULATORS & HOMEOSTATIC AGENTS
Volume 28, Number 1, January – March 2014

CONTENTS

Editorial

M. Carmignani, A.R. Volpe, M. Aldea, O. Soritau, A. Irimie, I.S. Florian, C. Tomuleasa, A. Baritchii, B. Petrushev, G. Crişan and G. Valle. Glioblastoma stem cells: a new target for metformin and arsenic trioxide..... 1

S.K. Kritas, A. Saggini, G. Cerulli, A. Caraffa, P. Antinolfi, A. Pantalone, R. Saggini, S. Frydas, M. Rosati, M. Tei, A. Speziali, F. Pandolfi and P. Conti. Interrelationship between IL-3 and mast cells..... 17

Original Articles

Q. Li, M. Kobayashi and T. Kawada. Carbamate pesticide-induced apoptosis and necrosis in human natural killer cells 23

L. Turin, G. Manarolla, T. Rampin and F. Riva. The innate immunity receptor TIR8/SIGIRR is expressed in the early developmental stages of chicken embryos..... 33

M. Agallou, E. Dotsika, S. Frydas and E. Karagouni. Toll-like receptor 4 promotes control of *Leishmania infantum* infection through inducement of leishmanicidal activity in host macrophages: role of mitogen activated kinases..... 43

G. Bertuccelli, F. Marotta, N. Zerbinati, A. Cabeca, F. He, S. Jain, A. Lorenzetti, H. Yadav, M. Milazzo, F. Calabrese, C. Tomella and R. Catanzaro. Iron supplementation in young iron-deficient females causes gastrointestinal redox imbalance: protective effect of a fermented nutraceutical..... 55

C. Zoccali, V. Anelli, G. Chichierchia, F. Erba and R. Biagini. The use of engineered biomaterial Bone Plexur M® in benign epiphyseal tumors: our experience at 20 months of follow-up..... 67

M. Golec, C. Reichel, M. Lemieszek, J. Buczkowski, B. Mackiewicz, C. Skórska, J. Dutkiewicz, A. Góra, R. Ziesche and J. Milanowski. Cathelicidin LL-37 in bronchoalveolar lavage and epithelial lining fluids from healthy individuals and sarcoidosis patients..... 75

S. Buccheri, G. Guggino, N. Caccamo, P. Li Donni and F. Dieli. Efficacy and safety of gd T cell-based tumor immunotherapy: a meta-analysis..... 83

D. Poddighe, C.B. Mathias, E.J. Freyschmidt, D. Kombe, B. Caplan, G.L. Marseglia and H.C. Oettgen. Basophils are rapidly mobilized following initial aeroallergen encounter in naïve mice and provide a priming source of IL-4 in adaptive immune responses..... 93

C. Muscoli, F. Lauro, C. Dagostino, S. Ilari, L.A. Giancotti, M. Gliozzi, N. Costa, C. Carresi, V. Musolino, F. Casale, D. Ventrice, E. Oliverio, E. Palma, S. Nisticò, A. Procopio and V. Mollace. Olea Europea-derived phenolic products attenuate antinociceptive morphine tolerance: an innovative strategic approach to treat cancer pain..... 107

C. Valsecchi, A. Marseglia, L. Montagna, S.C. Tagliacarne, M. Elli, A. Licari, G.L. Marseglia and A.M. Castellazzi. Evaluation of the effects of a probiotic supplementation with respect to placebo on intestinal microflora and secretory IgA production, during antibiotic therapy, in children affected by recurrent airway infections and skin symptoms..... 119

V. Pesce, G. Maccagnano, G. Vicenti, A. Notarnicola, L. Moretti, S. Tafuri, D. Vanni, V. Salini and B. Moretti. The effect of hydroxyapatite coated screw in the lateral fragility fractures of the femur. A prospective randomized clinical study..... 127

M.L. Roberti, L. Ricottini, A. Capponi, E. Sclauzero, P. Vicenti, E. Fiorentini, C. Savoia, G. Scornavacca, D. Brazioli, L. Gaio, R. Giannetti, C. Ignazzi, G. Meloni and L.M. Chinni. Immunomodulating treatment with low dose interleukin-4, interleukin-10 and interleukin-11 in psoriasis vulgaris..... 135

Letters to the Editor

G. Da Villa, G. Ianiro, F. Mangiola, E. Del Toma, A. Vitale, A. Gasbarrini and G. Gasbarrini. White mulberry supplementation as adjuvant treatment of obesity..... 143

R. Pippi, R. Patini, C.M. Ghiciuc, R.B. Sandu, V. Pasquali, S. Scaccianoce, L.C. Dima-Cozma and F.R. Patacchioli. Diurnal trajectories of salivary cortisol, salivary α-amylase and psychological profiles in oral lichen planus patients..... 149

C. Rossi, A. Reginelli, M. D'Amora, G. Di Grezia, Y. Mandato, A. D'Andrea, L. Brunese, R. Grassi and A. Rotondo. Safety profile and protocol prevention of adverse reactions to uroangiographic contrast media in diagnostic imaging..... 157

EDITORIAL

GLIOBLASTOMA STEM CELLS: A NEW TARGET FOR METFORMIN AND ARSENIC TRIOXIDE

M. CARMIGNANI[1], A.R. VOLPE[1], M. ALDEA[2], O. SORITAU[3], A. IRIMIE[4], I.S. FLORIAN[5], C. TOMULEASA[6], A. BARITCHII[7], B. PETRUSHEV[8], G. CRIŞAN[9] and G. VALLE[10]

[1]Laboratory of Pharmacology and Toxicologyy, Department of Life, Health and Environmental Sciences, University of L'Aquila, Coppito, Italy; Departments of [4]Surgery, [5,7]Neurosurgery and [9]Pharmaceutical Botany, [2,8]"Iuliu Haţieganu" University of Medicine and Pharmacy and [3]Department of Immunology, Ion Chiricuta Comprehensive Cancer Center, Cluj Napoca, Romania; [6]Department of Medicine, Division of Gastroenterology and Hepatology, the Johns Hopkins University School of Medicine, Baltimore, MD, USA; [10]Nuclear Medicine Unit, Scientific Institute "Casa Sollievo della Sofferenza", San Giovanni Rotondo, Italy

Received November 8, 2013 – Accepted January 30, 2014

The high malignancy of glioblastoma has been recently attributed to the presence, within the tumor, of glioblastoma stem cells (GSC) poorly responsive to chemo- and radiotherapy. Here, the potential employment of metformin and arsenic trioxide (ATO) in glioblastoma therapy is discussed focusing on their effects on GSC. Metformin exerts anticancer effects by primarily blocking the pivotal LKB1/AMPK/mTOR/S6K1 pathway-dependent cell growth, induces selective lethal effects on GSC by impairing the GSC-initiating spherogenesis and inhibits the proliferation of $CD133^+$ cells, while having a low or null effect on differentiated glioblastoma cells and normal human stem cells. Metformin and ATO induce autophagy and apoptosis in glioma cells by inhibiting and stimulating the PI3K/Akt and the mitogen-activated protein kinase pathways, respectively. Both drugs promote differentiation of GSC into non-tumorigenic cells. In this regard, metformin acts via activation of the AMPK-FOXO3 axis, whereas ATO blocks the interleukin 6-induced promotion of STAT3 phosphorylation. Blood-brain barrier, easily crossed by metformin but not by ATO, undergoes important glioblastoma-induced alterations that increase its permeability, thus allowing ATO to distribute more into the glioblastoma bulk than in the normal brain parenchyma. A prompt clinical assessment of metformin and ATO in glioblastoma patients would represent a valid attempt to improve their survival.

Malignant gliomas remain some of the most devastating and difficult to treat human cancers with an incidence of 5 cases per 100,000 persons each year in western countries. Glioblastoma, the most common primary brain tumor, accounts for about 60-70% of such neoplasms. It originates *de novo* (primary glioblastoma) in about 90% of cases, while secondary glioblastoma originates from low-grade gliomas. Glioblastoma infiltrates the brain early in its course and makes a complete neurosurgical resection almost impossible. Recent years have brought significant advances in tumor biology

Key words: Glioblastoma, stem cells, metformin, arsenic trioxide

Mailing address: Prof. Marco Carmignani, MD, Laboratory of Pharmacology and Toxicology, Dept. of Life, Health and Environmental Sciences, University of L'Aquila, Via Vetoio 2, 67010 Coppito (AQ), Italy
Tel.: +39 862 433265 Fax: +39 862 433273
e-mail: marco.carmignani@univaq.it

0393-974X (2014)

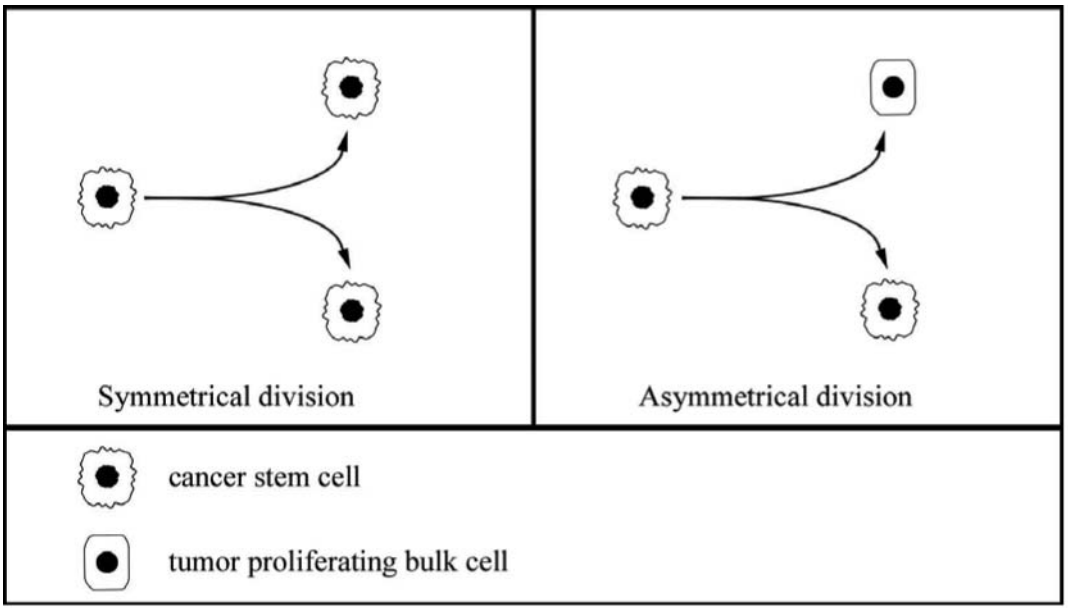

Fig. 1. *Symmetrical and asymmetrical division of cancer stem cells. Symmetrical division originates identical cancer stem cells. Asymmetrical division gives rise to two different kinds of cells: cancer stem cells and tumor proliferating bulk cells.*

including the discovery that many cancers, such as gliomas, contain cells with stem-like properties (1). Since the late 1970s, alkylating agents such as nimustine, carmustine and lomustine have been used, besides surgery and together with radiotherapy, to prolong the survival of glioblastoma patients (2). A methylating agent, temozolomide (TMZ), is nowadays the most important and widely employed drug in glioblastoma pharmacopoeia. However, the clinical efficacy of TMZ is scant and, despite chemo- and radiotherapy, the median survival after diagnosis of glioblastoma is in the order of 15 months (1). Therefore, the quest for new treatments against glioblastoma is a very stimulating challenge. The lack of efficacious pharmacological treatments for glioblastoma has been recently attributed to the presence, within the tumor, of glioblastoma stem cells (GSC), which are poorly responsive to antineoplastic drugs because of their chemoresistant properties and ability to stimulate neoangiogenesis. GSC are also able to survive radiotherapy, thus originating tumor relapses (3). The presence of these apparently invulnerable cells confers glioblastoma the capacity of re-growth even after heavy debulking treatment. So far, to fight GSC resembles the myth of the Lernaean Hydra and a hopeless struggle of any hero. GSC, although accounting for only 1% - 3% of the whole glioblastoma cell population, represent the real core of glioblastoma malignancy (1,3). GSC targeting is actually the goal to which the pharmacological research in glioblastoma therapy is aimed to.

Recently, metformin and arsenic trioxide have been shown to be provided with antineoplastic activity against GSC and to possibly become promising candidates to prolong survival in glioblastoma patients. Although their mechanisms of action are not entirely determined, it has been proved that they share an antiproliferative action and possibly promote GSC differentiation (4, 5). Here, we focus on the possible extension of these drugs to glioblastoma therapy for which other drugs, such as mebendazole (6) and valproic acid (7), are actually being under clinical investigation.

CANCER STEM CELLS, THE CORE OF GLIOBLASTOMA

Since nearly a decade, cancer research has gained new insights into the role of stem cells in the oncogenic

processes. The remarkable similarities between stem cells and cancer cells have led to the hypothesis that tumors may originate from neoplastic transformation of normal stem cells and that tumors include cancer stem cells (CSC) possibly also originating from cells having acquired stem cell characteristics. Reya et al. proposed a hierarchical growth pattern where CSC are the apex that drives into two directions: a symmetrical and an asymmetrical division (8). The symmetrical division is a clonal proliferation that originates other identical CSC. The asymmetrical division results in two different cell populations: progenitor CSC, representing only a small fraction of the total tumor burden, and more differentiated cells representing the bulky mass of the tumor (Fig. 1). Accordingly, a solid tumor contains heterogenic cell populations favouring the accumulation of genetic abnormalities. Although GSC are a small fraction of the whole tumor population, they have a self-renewal capacity, are more resistant to radio- and chemotherapy than differentiated tumor cells, survive intensive oncological therapies, and are responsible for tumor recurrences (8).

The "stem cell theory" of carcinogenesis well agrees with the aggressive behaviour of glioblastoma (1, 2). Malignant gliomas, respecting the hierarchical model of this theory, contain proliferating and differentiating cells showing different morphological and functional characteristics. Proposed cells for the origin of GSC are neural stem cells, astrocytes and glial precursors (including oligodendrocytes) (9). Stem cells are not the only target for malignant transformation because, under microenvironment stress conditions, even fully differentiated cells may undergo oncogenic mutations and acquire stem-like properties (1, 3). The literature, starting from the initial isolation of GSC from primary human brain tumors by using selection in neurosphere cultures, brings strong evidence for the existence of GSC within glioblastoma. The neurosphere formation by GSC is a predictor of the glioblastoma outcome and correlates with both aggressiveness and poor prognosis of such neoplasm (1). GSC show abnormal growth properties and ability to express markers of differentiated neural lineages (10).

GSC Markers and Mutations

GSC are responsive to epidermal growth factor (EGF) and fibroblast growth factor-2, and express specific markers for stem cells such as cluster of differentiation 44 (CD44), CD90, CD105, CD133, C-X-C chemokine receptor type 4, Nanog, Oct ¾, Oct4, Olig2 and breast cancer resistance protein/ adenosine triphosphate-binding cassette (ABC) sub-family G member 2 transporter (BCRP/ABCG2) (1, 3, 11). Other markers for GSC have been identified such as aldehyde dehydrogenase, a likely new marker of resistance to TMZ, and heat shock protein 90 (12). GSC also express markers for astroglial cells (e.g., glial fibrillary acidic protein) and anti-apoptotic factors such as B-cell lymphoma-gene-2 (Bcl-2), survivin, and inhibitor of apoptosis proteins (13). On the other hand, the cell surface marker CD133 has been questioned as a specific stem cell marker in the identification and isolation of GSC. In this respect, Beier et al. compared the behaviour of CD 133^- and CD 133^+ glioblastoma cells and concluded that both cell populations satisfied stem cell criteria. Such populations were shown to be provided with a similar tumorigenic ability in nude mice while exhibiting, both *in vitro* and *in vivo,* distinct biomolecular profiles and growth characteristics (14). A quantitative correlation between the glioma grade and the presence of $CD133^+$ cells was reported by Thon et al. (15). $CD133^+$ glioblastoma cells were found to express higher levels of BCRP/ABCG2 and O-6-methylguanine-DNA methyltransferase (MGMT) mRNA, to present higher mRNA levels of genes that inhibit apoptosis, and to result to be more resistant to chemotherapeutic agents (such as TMZ, carboplatin, etopoxide and paclitaxel) than the $CD133^-$ cells. GSC from primary or recurrent gliomas did not reach the terminal differentiation stage, while their retro-differentiation was observed *in vitro*, i.e. the partial differentiation observed in $CD133^-$ GSC was reversed along with the re-acquisition of CD133 expression ($CD133^+$). A study by Brescia et al. showed that, in addition to the surface marker CD133, GSC contain an intracellular CD133 located in the cytoplasm of neurosphere cells (16). GSC have the capacity of re-expressing CD133 at the cell surface, thus regaining their enhanced self-renewal capacity and tumorigenic potential. This interconvertible state between cytoplasmatic and surface localization of CD133 could explain the GSC capacity of losing, maintaining and re-acquiring

Table I. *Mechanisms of Chemoresistance in Glioblastoma Stem Cells[a]. [a]either maintenance of the "stemness" character or re-acquisition of the stem cell properties by non-stem cells lead to chemoresistance (8).*

Intrinsic mechanisms		Extrinsic mechanisms	
MGMT	It protects cells from alkylating agents by removing the methyl adduct.	Blood-brain barrier	It reduces the efficacy of chemotherapy by limiting the drug distribution within the brain.
ABC transporters (Efflux pumps)	They extrude TMZ outside the cell, thus inducing resistance to treatment. MDR1 (ABCB1) gene single nucleotide polymorphism is an independent predictor for TMZ responsiveness (18).	Direct cell-cell interactions	They influence the cell behaviour, proliferation and differentiation.
Over-expression of Hedgehog and Notch pathways	It contributes to the TMZ resistance. The blockade of these pathways increases the cytotoxic effects of TMZ, whereas the activation of such pathways enhances the resistance to TMZ (19).	Local cytokine levels	High levels of LIF induce overexpression of TGF-β2 and neuroprogenitor cell markers (22).
		Hypoxia	It impairs the formation of reactive oxygen species.
Over-expression of EGF	It increases cell proliferation, neoangiogenesis and tissue invasion, and inhibits apoptosis (20).		
MicroRNA-328 (miR-328)	It controls proliferation, apoptosis and cell differentiation. It is underexpressed in glioblastoma multiforme and in other cancers, thus contributing to chemoresistance (21).		

MGMT:O-6-methylguanine-DNA methyltransferase; ABC: adenosine triphosphate-binding cassette; EGF: epidermal growth factor; TMZ: temozolomide; LIF: leukemia inhibitory factor; TGF-β2: transforming growth factor-beta2.

their stemness character in the presence of various stimuli. In this regard, the silencing of CD133 gene expression with a lentivirus-mediated short hairpin RNA imparted both self renewal and tumorigenic potential of GSC, thus confirming the role of CD133 in maintaining the "stemness" character (16).

GSC also express elements of the Hedgehog signaling pathway like sonic hedgehog (SHH), protein-patched homolog, glioma-associated oncogene homolog and transcriptional repressor of E-cadherin (17). Importantly, all brain tumor stem cells are able, when transferred in immuno-compromised mice, to initiate tumors that phenocopy the original neoplasm (3). Also genetic alterations were observed such as amplification of the EGF-receptor (EGF-R) oncogene and deletion of the tumor suppressor phosphatase and tensin homolog (PTEN), while amplification of the metastasis-associated gene 1 (MTA1) only occurred in GSC derived from recurrent tumors (11). These data suggest that malignancy progression also occurs in GSC.

Differences between GSC and neural stem cells are still not clearly demarcated. A unique characteristic of GSC is their ability to survive and proliferate independently from exogenous mitogenic stimulation and to likely undergo a dynamic adaptation to environmental factors. On the other hand, different anticancer treatments may select preexisting glioblastoma cell subclones displaying characteristics of GSC (2). For clinical practitioners, the most important feature of GSC is their high resistance to radio- and chemotherapy needing identification of drugs acting selectively against these cells (2, 13).

Mechanisms of Chemo- and Radioresistance in GSC

The prognosis of glioblastoma still remains highly unfavourable despite the standard adjuvant treatment including radiotherapy and TMZ. The most compelling evidence of the existence of chemo- and radioresistance by GSC is given by glioblastoma recurrence within a few months starting from the initial response to treatment. The unresponsiveness of malignant gliomas to the conventional treatment depends on both intrinsic properties of GSC and tumor microenvironment favouring the "stemness" (Table I).

TMZ methylates the O-6-position of guanine causing DNA damage. MGMT, frequently over-expressed in GSC and especially in those located in the inner core of the tumor mass, restores guanine by removing the methyl adduct. However, the DNA mismatch repair system exclusively recognizes the mispaired thymine and excises it. As a consequence, the methylation of the O-6-position of guanine persists in the template strand, while thymine is continuously re-inserted and re-excised with the result of persistent single-stranded gaps in newly replicated DNA. Therefore, the efficacy of TMZ in glioblastoma treatment requires low cell levels of MGMT. Although a few studies investigated the DNA repair system in GSC, none of them obtained conclusive results. Bai et al. suggested that GSC are resistant to radiotherapy because of a DNA repair system more efficient than that of non-stem cells (6). Conversely, a recent report evidenced that only the enhanced activation of check-point proteins can contribute to radioresistance, whereas an enhanced DNA repair is not a common feature of GSC (23). MGMT, probably the most important modulator of chemoresistance in glioblastoma, rapidly prevents the formation of cross-links and thereby causes resistance to alkylating drugs.

Another mechanism of GSC chemoresistance is likely to be the extrusion of cytotoxic drugs outside the cell. In this respect, the ABC transporters, able to extrude drugs through energy consumption, play a primary role. Such a mechanism seems to contribute to protect GSC from drug-induced death or damage, thus assuring the maintenance of glioblastoma growth (24). Since the ABC efflux pumps operate also in normal stem cells, it would be of interest to characterize the activity of such pumps during stem cell neoplastic differentiation.

Other cell pathways involved in GSC drug resistance include the SHH pathway, operating in neural progenitors, the Notch pathway, modulating angiogenesis and hypoxia, and the Wnt-β-catenin pathway. All these pathways are over-expressed in GSC and are involved in gliomas' resistance to TMZ and/or in maintenance of the "stemness" feature (19). Aberrant Notch signaling activation was found in glioblastoma, while an increased expression of Notch1 and Notch2 protected glioma cells against radiation-induced DNA damage by activation of protein kinase B (Akt) and its downstream effector mammalian target of rapamycin (mTOR) (25). Autocrine activation of the SHH pathway up-regulates the insulin-receptor substrate-1, a key protein in the insulin-like growth factor receptor (IGF-R)/phosphatidylinositol-3-kinase (PI3K)-Akt pathway, and sustains the growth of GSC population and its expansion in glioblastoma. Additionally, such an activation can initiate a paracrine signaling upon stromal cells present in the microenvironment which, in turn, produce factors that amplify the Hedgehog signaling. Both survival and radioresistance of GSC are dependent on increased expression of the transmembrane protein L1CAM (CD171), a neuronal cell adhesion glycoprotein shown to regulate DNA damage check-point responses through nuclear translocation of its intracellular domain (26). The SHH and Notch pathways contribute to GSC radioresistance as shown by the employment of SHH and Notch inhibitors, which improve the radiation efficacy upon GSC. The main radioresistance mechanisms in GSC are summarized in Table II.

Table II. *Mechanisms of Radioresistance in Glioblastoma Stem Cells*[a].

Over-expression of Wnt-β-catenin pathway	It is preferentially activated after irradiation (19).
Over-expression of Notch pathway	It protects GSC against radiations, whereas its inhibition by γ-secretase inhibitors makes GSC more sensitive to radiotherapy (19).
Over-expression of SHH pathway	The SHH inhibitor cyclopamine improves the radiation effects on GSC (19).
Increased expression of L1CAM protein	It is a surface protein that regulates cell adhesion, survival, migration and invasion. It protects GSC against irradiation-induced DNA damage by activating ATM-Chk2 checkpoints through NBS1 up-regulation. L1CAM targeting by RNA interference sensitizes GSC to radiation (26).
Hypoxia	It impairs the formation of reactive oxygen species, thus opposing the radiation-induced DNA damage. In the absence of oxygen, the radiation dose required to achieve the biologic effect obtained in the presence of normal oxygen levels is three times higher.

SHH: Sonic Hedgehog; GSC: glioblastoma stem cells; NBS1: a gene regulator involved glioblastoma. [a]*either maintenance of the "stemness" character or re-acquisition of the stem-cell properties by non-stem cells lead to radioresistance.*

Glioblastoma: Stemness and Hypoxia

The tumor microenvironment, influencing the phenotypic and biomolecular characteristics of GSC, has a major clinical relevance. In fact, in favorable conditions, non-stem cancer cells possess the capacity to convert to GSC which need, by themselves, adequate conditions to preserve their "stemness" (Table III).

The hypoxia within glioblastoma tissue promotes both self-renewal capability of stem and non-stem cell populations and evolution of the non-stem cell population towards a more stem-like phenotype. GSC are preferentially located within the hypoxic core of the tumor mass, while the more differentiated cells are mainly present within the more vascularized peripheral part of the tumor (Fig. 2). The poor vascularization of the central core does not favour the drug distribution within it and hypoxia increases GSC resistance to radiotherapy. Therefore, the resistance of GSC to radio- and chemotherapy is related not only to their intrinsic characteristics but also to their location within the tumor mass.

The Quest for Drugs Targeting GSC

As GSC are the re-generating cell reservoir of glioblastoma, a rational therapeutic approach should try to target and silence this relatively small but extremely resistant and re-populating cell compartment. Drugs against GSC are not expected to appreciably reduce the overall glioblastoma burden in a short time but, by removing the neoplastic cellular spring, to hinder tumor re-growth after conventional chemo- and radiotherapy, thus avoiding relapses (Fig. 3).

METFORMIN

Metformin (dimethylbiguanide) was developed in the 1950's starting from galegine, a guanidine derivative found in *Galega officinalis* (goat rue also known as French lilac, Italian fitch, Spanish sainfoin) which, since Middle Age times, was used to relieve polyuria, a typical symptom of hyperglycemia. Considering the hypoglycemic effect of guanidine, Sterne proposed the name of *Glucophage* (glucose

Table III. *Pathways and Factors Involved in Stemness.*

PI3K/mTor	It is critical for maintaining the properties of GSC and plays a central role in the regulation of cell proliferation, differentiation and survival. Dysregulation of this pathway frequently occurs in glioblastoma. Inhibitors of PI3K/ mTor reduce the self-renewal of GSC, promote differentiation of GSC and reduce their oncogenic potential in mice (27).
TGF-β and LIF	They stimulate the self-renewal capacity and prevent the differentiation of GSC (22).
Transcription factor Sox-2	Loss of the Sox-2 function limits the self-renewal capacity of human glioma cells[44] and decreases their cancerogenic potential when transplanted into the rodent brain (28).
Hypoxia	It promotes the self-renewal capacity of both stem and non-stem cell populations, and induces a more stem-like phenotype in the non-stem cell population (27).
STAT3	It regulates the self-renewal of GSC. STAT3 inhibition (e.g., by STA-21 and S3I-201) causes loss of the stem-like characteristics of GSC.
MEF/Sox2	The absence of this signaling pathway hinders glioma genesis and impacts the formation of neurospheres (28).
MEF/Wnt/β-catenin	It is over-activated in GSC, highly expressing the tyrosine kinase MET receptor, and is part of the MET downstream signaling pathway. It contributes to the maintenance of the stemness character (29).
Frizzled 4	It is a member of the Wnt signaling family. Its up-regulation in GSC promotes neurosphere formation and expression of the epithelial to mesenchymal transition regulator SNAI1 as well as acquisition of a mesenchymal phenotype (30).
Girdin	It is an actin binding protein over-expressed in glioblastoma and shown to be a novel substrate of Akt. Its knock-down in GSC leads to reduced expression of stem cell markers, induces neural differentiation and inhibits cell motility, cell invasion, neurosphere formation and *in vivo* tumor formation (31).
Autocrine endothelin-3/endothelin receptor B	It is highly expressed in GSC. Blocking this pathway reduces the stemness, as proven by the inibition of neurosphere formation, cell migration and loss of tumorigenic capacity in vivo.
CXCR4	The blockade of CXCR4 with its specific antagonist AMD3100 inhibits the highly invasive growth of GSC xenografts in vivo and cell migration in vitro (32).

PI3K/mTor: phosphatidyl-inositol 3-kinase/mammalian target of the rapamycin signaling pathway; TGF-β: transforming growth factor-beta; LIF:leukemia inhibitory factor; STAT3: the signal transducer and activator of transcription-3; GSC: glioblastoma stem cells; CXCR4: C-X-C chemokine receptor type 4; Sox-2: sex determining region Y-box 2; MEF: transcription factor myeloid Elf-1 like factor (ELF4); MET: hepatocyte growth factor receptor.

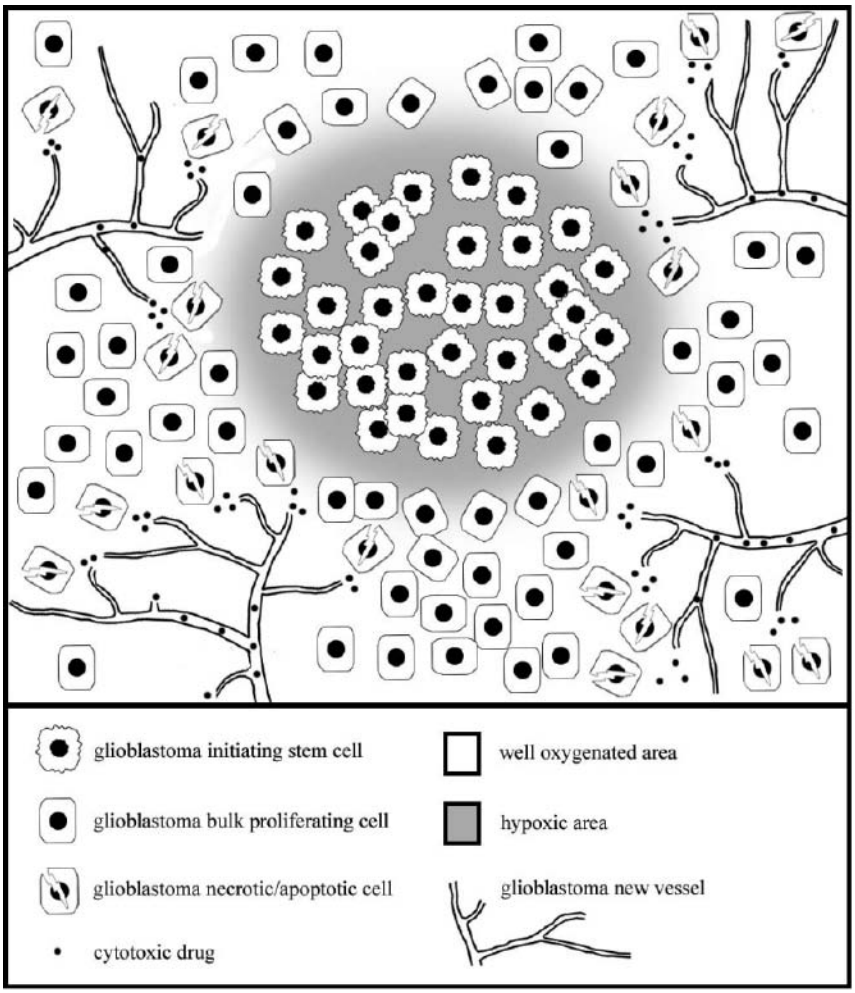

Fig. 2. *Preferential localization of glioblastoma stem cells in glioblastoma hypoxic areas. Glioblastoma is highly vascularized at its periphery, while its center (core) is a hypoxic area sharing a limited vascularization. Glioblastoma stem cells are concentrated in the core. Due to this vessel distribution, the antineoplastic drugs accumulate at the periphery of the tumor, with a limited supply to the core. Hypoxia in the core leads to a low formation of reactive oxidative species, thus contributing to an impaired radiotherapy response.*

eater) for the first commercial formulation of metformin. While other biguanides (phenformin and buformin) have been discontinued in most countries since the end of 1970s because of the frequently induced lactic acidosis, metformin is nowadays the only marketed biguanide that is employed by almost 120 million people worldwide with type II diabetes. Recently, metformin has been used in the treatment of polycystic ovary syndrome. The concept that antidiabetic biguanides can act as anticancer and geroprotector drugs ("metabolic rehabilitation") was introduced more than thirty years ago (34). Despite prolonged serious reservations on this issue, scientific acquisitions obtained in the last years have given credit to the therapeutic effectiveness of metformin against neoplasms.

The anticancer effects of metformin are thought to be partly due to its insulin lowering action because insulin and insulin secretagogues like sulfonylurea-related drugs exert cancer promoting actions. High insulin levels up-regulate growth hormone (GH) receptors and the augmented GH receptor signaling leads to an increased production of IGF. In turn, IGF-R stimulation favours cell growth processes

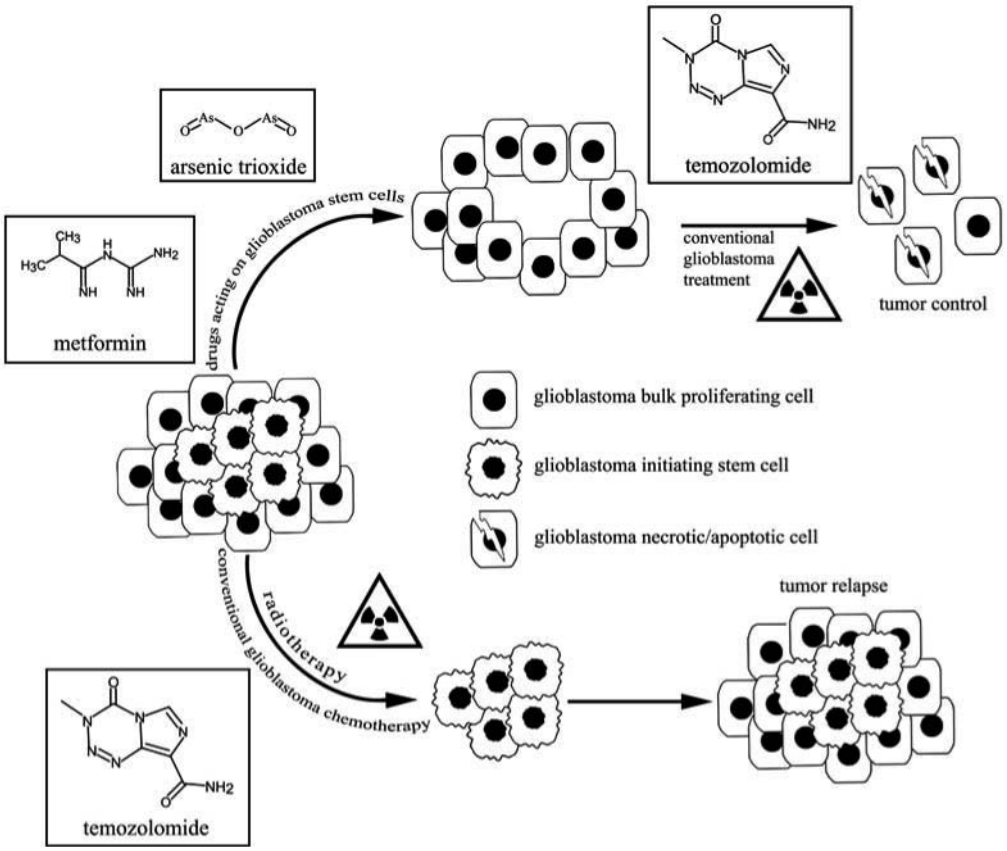

Fig. 3. *Expected effects of the association of drugs (arsenic trioxide and/or metformin) acting on glioblastoma stem cells (GSC) to the conventional glioblastoma treatment (temozolomide plus radiotherapy) in comparison with the conventional treatment alone. Treatment with drugs targeting GSC wouldn't induce a significant reduction of the tumor bulk. However, the removal of GSC is expected to hinder relapses after conventional chemo- and radiotherapeutic treatments. Adapted, with permission, from Martin-Castillo et al (33).*

and cell cycle progression, and inhibits apoptosis. Moreover, increased serum IGF concentrations are associated with an increased risk of developing cancers and, along with hyperinsulinemia secondary to insulin resistance, contribute to explain the causal relationships among obesity, type II diabetes and cancer. IGF receptors are expressed in glioblastoma cells and IGF receptor targeting has been reported as a successful anticancer approach in experimental studies on these cells. Epidemiological data support a positive relationship between obesity and glioblastoma occurrence. The risk of developing gliomas is twice higher in tall (> 1.90 m) than in small subjects (< 1.60 m) and four times higher in obese at age 18 [body mass index (BMI): 30.0-34.9] than in normal weight persons (BMI: 18.5-24.9). An epidemiological study on over a million women showed, with reference to all tumors of the central nervous system, an about 20% increase of the risk per 10 cm increase in height and an about 20% increase of the risk per 10 kg/m^2 body weight increase.

In vitro studies showed the anticancer effects of metformin to be linked to its inhibitory action on cell growth through a blockade of the pivotal liver kinase B1 (LKB1)/AMP-dependent kinase (AMPK)/mTOR /S6 kinase 1 (S6K1) pathway. Since metformin impairs mitochondrial respiratory chain by interfering at level of the complex I, both reduction of adenosine triphosphate (ATP) production and increase of the adenosine monophosphate (AMP)/

ATP ratio occur. Consequently, there is an enhanced AMPK activity due to the direct allosteric activating effects of AMP on AMPK, in which AMP promotes phosphorylation of Thr 172 by LKB1 and inhibits Thr 172 dephosphorylation. It is noteworthy that AMPK activation by the agonist AICAR (5-amino-1-β-D-ribofuranosyl-imidazole-4-carboxamide), with consequent mTOR signaling inhibition, provokes the arrest of cell growth in glioblastoma cells (expressing the activated EGF-R mutant EGF-RvIII) through inhibition of cholesterol and fatty acid synthesis.

The blockade of the LKB1/AMPK/mTOR/S6K1 pathway is responsible for a reduced activity of protein kinases other than AMPK also depending on activation of tyrosine kinase receptors like HER and HER1 (35). Such receptors, together with the EGF ones, are often over-expressed in glioblastoma and their signaling favours tumourigenesis by promoting cell proliferation, tissue invasion, neoangiogenesis and tumor cell resistance, and by inhibiting apoptosis. Metformin has been recently shown to silence the HER signaling, while mTOR inhibition promotes differentiation of human embryonic stem cells (20). In this regard, considering that a small population of cells within the neoplastic tissues has stem-like properties, one may presume that the ability of metformin to inhibit mTOR can allow GSC to differentiate in "bulk" malignant glioma cells much more sensitive to the anticancer effects of chemo- and radiotherapy. Accordingly, we showed that, in seven of eight glioblastoma cultured primary cell lines obtained from our patients, the cytotoxicity of TMZ, evaluated by the 3-(4,5-dimethylthiazol-2-yl)-2,5-diphenyltetrazolium bromide (MTT) viability assay, was significantly increased by metformin to which cells were exposed 24 h prior TMZ administration (36). If a collateral metformin-favoured differentiation of the neural stem cells in the subventricular zone of the brain may occur, such a differentiation is unlikely to cause physiopathological alterations by itself. As shown in *ex vivo* studies, these stem cells are much less sensitive, as compared to glioma stem-like cells, to the cytotoxic effects of antineoplastic drugs including TMZ.

Metformin has inhibitory effects on cell cycle progression. In low density cultures of rat C6 chemoresistant glioma cells, it blocked cell cycle in G0/G1 phase without inducing cell death. Conversely, in confluent cultures of the same cells, metformin induced caspase-dependent apoptosis accompanied by c-Jun N-terminal kinase activation, mitochondrial depolarization and oxidative stress. All these actions of metformin were not observed on primary rat astrocytes. As shown in prostate cancer cell lines, metformin induces AMPK-independent mTOR inhibition and cell cycle arrest through regulated in development and DNA damage response 1 (REDD1) (37). Further anticancer mechanisms of metformin in glioblastoma likely include an increased glucose accumulation within GSC leading to activation of the polyol pathway, in turn compromising the recycling of glutathione disulphide to reduced glutathione. As a consequence, there may be, similarly to diabetes, an increased susceptibility to oxidative stress and an impairment of DNA repair mechanisms (38). Recent *ex vivo* studies on glioblastoma cells have shown metformin alone, and even more when associated with TMZ, to increase cell oxidative stress by raising the lipid peroxide levels and decreasing those of reduced glutathione so that an inverse relationship between the grade of oxidative stress and the cell proliferation rate has been established (Aldea, unpublished data). Another mechanism may be ascribed to the metformin-induced fall of serum levels of leptin, which shares promoting effects on glioblastoma and other cancers, and plays a role in the increased risk of cancer associated to obesity. Recently, in breast cancer cells, metformin has been found to inhibit the signal transducer and activator of transcription 3 (STAT3) activation (P-STAT3) at Tyr705 and Ser727 and to induce apoptosis (39).

In vitro studies also showed that metformin selectively kills GSC, while having a low or null effect on differentiated glioblastoma cells or normal human stem cells. In a study performed on GSC isolated from 4 human glioblastomas, metformin impaired GSC-initiating spherogenesis and highly reduced proliferation of $CD133^+$ cells, thus evidencing its selectivity for CSC. The low effect on differentiated cells was explained through the poor ability of metformin to affect the Akt-dependent cell survival pathway that, on the contrary, was greatly inhibited in GSC. Strikingly, in umbilical cord-derived mesenchymal stem cells but not in normal cells, metformin induced cytotoxic effects by

increasing Akt phosphorylation (5). The spearing of normal stem cells by metformin is of high relevance when considering its low or absent toxicity for other human body cells. Moreover, *in vitro* and *in vivo* studies showed metformin to promote differentiation of GSC into non-tumorigenic cells via activation of the AMPK-forkhead box protein O3 (FOXO3) axis. Sato et al. concluded that metformin is "the most clinically relevant drug ever reported for targeting of glioma-initiating cells" (40).

If the above anticancer effects of metformin will be confirmed on high-grade glioblastoma patients, this drug might represent the Ehrlich's "magic bullet" in glioblastoma therapy. Interestingly, the LKB1/AMPK/mTOR/S6K1 pathway is widely recognized as the target of several "new" anticancer agents like everolimus and sirolimus that proved their clinical usefulness, together with somatostatin, in the therapy of tumors of neuroectodermal derivation. Metformin presents positive characteristics such as easy and rapid crossing of the blood-brain barrier (BBB), safety and low cost. Its side effects, as observed in diabetic patients, are well known: anorexia, nausea, emesis and abdominal pain that occur up to 20% of these subjects. Such effects are dose-dependent, tend to appear at the beginning of treatment and are often transitory. On the other hand, metformin has to be suspended in 3-5% of cases because of persistent diarrhoea. Long-term therapy with metformin seems to reduce the absorption of vitamin B_{12}.

A phase I trial (NCT01430351) is being actually performed in the University of Texas MD Anderson Cancer Center (Houston, TX, USA) on post-radiation therapy glioblastoma patients. This trial is aimed to study the maximum tolerated dose levels of TMZ plus metformin and/or memantine and/or mefloquine and to determine the survival associated to these treatments. The completion of this study is expected for September 2015. Metformin has been recently assessed for breast cancer therapy also in patients without metabolic syndrome.

ARSENIC TRIOXIDE

Arsenic trioxide (ATO) was approved in September 2000 by the Food and Drug Administration for use in the treatment of relapsed/refractory acute promyelocytic leukemia. In solid malignancies ATO down-regulates Bcl-2 levels, interferes with the Notch signaling pathway, promotes cell differentiation followed by apoptosis (through mitochondrial mechanisms determining cytochrome c release and caspase activation), and arrests the cell cycle in G2M or G1/G2M phases (41). The *in vitro* survival of GSC, unaffected by the exposure to ionizing radiation and chemotherapeutic agents, was significantly reduced if such treatments were preceded by the exposure to a subtoxic concentration of ATO (0.5 μM). In this model, the exposure to ATO alone did not change the survival of GSC as compared to the control (no ATO treatment). Therefore, low-level ATO was thought not to act by itself but to potentiate the effects of either ionizing radiation or anticancer drugs (41). In *ex vivo* studies on glioma cells, ATO depleted the population of GSC, in which it reduced the levels of Notch1 and hairy and enhancer of split-1 (Hes1) and diminished the number of nestin-positive GSC (42). Moreover, *ex vivo* and *in vitro* studies found ATO to stimulate the generation of reactive oxygen species through nicotinamide adenine dinucleotide phosphate (NADPH) oxidase, to reduce the activity of antioxidant enzymes such as glutathione peroxidase and thioredoxin reductase, to inhibit the mitochondrial electron transport chain, and to disturb redox homeostasis. The observation that ATO increases the sensitivity of GSC to both chemo- and radiotherapy through cell differentiation effects prompted to hypothesize its employment in the management of inoperable glioblastoma (41).

Several mechanisms have been proposed to explain how ATO induces differentiation and growth inhibition in GSC. One should first consider that arsenic is provided with high affinity for the sulphydryl groups, thus likely interacting with many proteins involved in cytotoxic, apoptotic and cancerogenic processes. *Ex vivo* and *in vitro* studies suggested that the interleukin-6 (IL-6)/Janus kinase (JAK)/STAT pathway (IJSP) inhibition seems to play a primary role in the ATO-induced reduction of GSC survival. In this context, IL-6 exerts a pro-neoplastic action in promoting STAT3 phosphorylation via JAK activation, being STAT3 essential for the maintenance of stem cells in glioblastoma patients. In fact, the blockade of STAT3 signaling pathway with a decoy oligonucleotide suppressed growth of GSC, while knock-down of the STAT3 expression

by RNAi (ribonucleic acid interference) suppressed growth and induced apoptosis and differentiation in GSC (43). Moreover, in a glioblastoma cell line, STAT3 was required for the expression of the anti-apoptotic genes survivin and Bcl-xL (B-cell lymphoma-extra large). An explanation for the ATO inhibitory effects on GSC may be found in the interaction between arsenic and JAK tyrosine kinases leading to IJSP inhibition. IJSP inhibition by ATO is also important for the amplifying mechanism that exists in glioblastomas between the $CD133^+$ and $CD133^-$ cell populations. In this respect, it is known that $CD133^-$ cells produce IL-6 but do not express IL-6 receptors, whereas $CD133^+$ cells do not produce IL-6 but do express IL-6 receptors (44). Therefore, $CD133^-$ cells stimulate the maintenance of $CD133^+$ population via IJSP and, on their behalf, $CD133^+$ cells repopulate the $CD133^-$ cell compartment.

Other mechanisms for the ATO inhibitory effects on GSC have been reported by *in vitro* and *ex vivo* studies. One of them concerns the inhibition, in glioblastoma cell lines, of cell proliferation through a decreased expression of cyclin B1 and cyclin D1 with cell cycle arrest at the G2/M or G1 phases, respectively. Another mechanism may be identified in the down-regulation of the stem cell marker Sox2 (sex determining region Y-box 2) (45). The direct inhibition by ATO of nuclear factor kappa B (NF-κB), that results to be more pronounced in astrocytoma cells than in normal astrocytes, has also to be considered. The inhibitory effects of ATO on STAT3, as shown in chronic lymphocytic leukemia cells, further inhibit NF-κB because of the STAT3-induced NF-κB activation (46). ATO affects the apoptotic pathways, being the glioblastoma cell apoptosis promoted by ATO through induction of mitochondrial damage. Moreover, ATO induces autophagy and apoptosis in glioma cells by inhibiting the PI3K/Akt pathway and activating the mitogen-activated protein kinase (MAPK) pathway with consequent down-regulation of survivin. This protein, a member of the inhibitor apoptosis protein family, is expressed in glioma cells where it acts by specifically binding to and inhibiting the activity of caspase-3 and caspase-7. Such a protein is an important target for anticancer therapies also because it enhances cell proliferation and promotes tumor angiogenesis (47). Interestingly, silibilin, a compound obtained from the milk thistle (*Sibylum marianum*), potentiates both inhibitory metabolic effects and pro-apoptotic actions of ATO (48).

From a clinical point of view, it is noteworthy that BBB is not easily crossed by arsenic. Entry of arsenic into the central nervous system, however, is favoured when the integrity of BBB is compromised by pathological processes. For example, therapeutically meaningful levels of arsenic were found in the cerebrospinal fluid of an ATO-treated leukemic patient presenting diffuse meningeal damage. Moreover, BBB has been reported to be essentially normal at micro-tumor sites but, as the tumor grows, it is progressively disrupted (49). In human glioblastoma, BBB breakdown is reflected by changes of the molecular compositions of both endothelial tight junctions and basal lamina. It is also known that glioblastoma cells release factors altering BBB features. Therefore, since the altered structure of BBB in glioblastoma implies an increase of its permeability, one may reasonably presume that the administration of ATO allows arsenic to distribute into the glioblastoma bulk more than in the normal brain parenchyma.

Minor side effects of ATO including sense of fatigue, gastrointestinal upset, hepatitis and a syndrome characterized by skin rashes, water retention and increase in weight have been reported. Such effects are successfully faced by symptomatic treatments or temporary drug cessation, and do not compromise the resumption of therapy. In some cases, however, kidney damage may occur along with impairment of the cardiac function, which is often characterized by arrhythmias or QT prolongation and *torsade de points* possibly resulting in sudden cardiac death. Reduction of the ATO doses may be useful in the case of nephropathy, whereas the *per os* administration of this compound may result beneficial to prevent heart side effects. The opportunity of ATO therapy, however, must be carefully evaluated in patients with cardiac and pulmonary diseases as well as electrolyte disturbances.

A pivotal study by Ryu et al. on a limited group of patients showed that the association of radiotherapy and ATO induced a differential delay of blood flow in glioblastoma as compared to normal brain (50). A phase I-II multicenter clinical study (NCT00275067) is actually ongoing in the United States of America to assess the efficacy of the association of ATO and

TMZ, employed together with radiation therapy, in patients after surgical removal of malignant glioma. Besides the appraisal of the maximum tolerated doses of ATO and TMZ during radiotherapy, another goal of this study is the determination of the glioma progression-free survival and of the overall survival. The completion of the study is expected for May 2014.

Taken together, the above findings lead to believe that ATO will be able to enter the panel of glioblastoma medical therapy.

CONCLUSIONS

Despite progresses in chemo- and radiotherapy, the outcome of glioblastoma patients maintains a median survival time of about 15 months. The availability of drugs improving the conventional glioblastoma therapy and the life expectancy of glioblastoma patients represents a compelling clinical need. Metformin and ATO appear to be very promising candidates to enter the glioblastoma pharmacopoeia as "Ehrlich's magic bullets" favouring an adequate cancer control and minimizing the heavy side effects of the current therapies. Broad pre-clinical findings support an anticancer activity of metformin in glioblastoma patients as in non-diabetic women diagnosed with breast cancer. A clinical assessment in glioblastoma patients of metformin in association to the conventional therapy appears largely justified independently from a diabetic condition.

In vitro studies evidenced important anti-GSC effects of ATO in sensitizing these cells to chemo- and radiotherapy (41). The clinical efficacy of ATO against leukemic disorders (48) and other neoplasms (41) gives further credit to its useful employment in glioblastoma therapy. Attempts to introduce in glioblastoma therapy drugs employed in other diseases (e.g., mebendazole and valproic acid) yielded interesting preliminary results that, however, need further clinical validation (6).

ACKNOWLEDGEMENTS

This study, patronized by the Italian National Military Health Association, Section of Rome, has been supported by grants of the Romanian Ministry of Research and Education (Project of Exploratory Research, Contract ID 1161 to Ioan-Stefan Florian), and of the "Iuliu Hatieganu" University of Medicine and Pharmacy, Cluj Napoca, Romania (grants No 22714/38/06.10.2011 to Mihaela Aldea and No 22714/37/06.10.2011 to Bobe Petrushev). The authors declare that study sponsors have had no role in the study design, in the collection, analysis and interpretation of data, in the writing of the manuscript, and in the decision to submit the manuscript for publication. The authors gratefully thank professor Gianmarco Mischitelli for helping in computer graphics and colonel Nunzio Scolamacchia for organization support. There was no writing assistance.

REFERENCES

1. Heywood RM, Marcus HJ, Ryan DJ, Piccirillo SGM, Al-Mayhani TMF, Watts C. A review of the role of stem cells in the development and treatment of glioma. Acta Neurochir 2012; 154:951-69.
2. Haar CP, Hebbar P, Wallace IV GC, Das A, William A, Vandergrift III WA, Smith JA, Giglio P. Drug resistance in glioblastoma: a Mini Review. Neurochem Res 2012; 37:1192-200.
3. Zhang M, Song T, Yang L, Chen R, Wu L, Yang Z, Fang J. Nestin and CD133 valuable stem cell specific markers for determining clinical outcome of glioma patients. J Exp Clin Cancer Res 2008; 27:85-92.
4. Grimm S.A, Marymont M, Chandler JP, et al. Phase I study of arsenic trioxide and temozolomide in combination with radiation therapy in patients with malignant gliomas. J Neuro-Oncol 2012; 10:237-43.
5. Würth R, Pattarozzi A, Gatti M, et al. Metformin selectively affects human glioblastoma tumor-initiating cell viability: A role for metformin-induced inhibition of Akt. Cell Cycle 2013; 12:145-56.
6. Bai RY, Staedtke V, Aprhys CM, Gallia GL, Riggines GJ. Antiparasitic mebendazole shows survival benefit in 2 preclinical models of glioblastoma multiforme. Neuro-Oncology 2011; 13:974-82.
7. Tsai HC, Wei KC, Tsai CN, Huang YC, Chen PY, Chen SM, Lu YJ, Lee ST. Effect of valproic acid on the outcome of glioblastoma multiforme. Br J Neurosurg 2012; 26:347-54.
8. Reya T, Morrison SJ, Clark MF, Weissman IL. Stem cells, cancer, and cancer stem cells. Nature 2001; 414:105-11.
9. Zong H, Verhaak RG, Canolk P. The cellular origin

for malignant glioma and prospects for clinical advancements. Expert Rev Mol Diagn 2012; 12:383-94.
10. Laks DR, Masterman-Smith M, Visnyei K, et al. Neurosphere formation is an independent predictor of clinical outcome in malignant glioma. Stem Cells 2009; 27:980-7.
11. Jin X, Jin X, Sohn YW, et al. Blockade of EGFR signaling promotes glioma stem-like cell invasiveness by abolishing ID3-mediated inhibition of p27KIP1 and MMP3 expression. Cancer Lett 2013; 328:235-42.
12. Rappa F, Cappello F, Halatsch ME, Scheuerle A, Kast RE. Aldehyde dehydrogenase and HSP90 co-localize in human glioblastoma biopsy cells. Biochimie 2013; 95:782-6.
13. Tomuleasa C, Soritau O, Rus-Ciuca D, et al. Functional and molecular characterization of glioblastoma multiforme-derived cancer stem cells. J BUON 2010; 15:583-91.
14. Beier D, Hau P, Proescholdt M, et al. $CD133^+$ and $CD133^-$ glioblastoma-derived cancer stem cells show differential growth characteristics and molecular profiles. Cancer Res 2007; 67:4010-5.
15. Thon N, Damianoff K, Hegermann J, Grau S, Krebs B, Schnell O, Tonn JC, Goldbrunner R. Presence of pluripotent CD133+ cells correlates with malignancy of gliomas. Mol Cell Neurosci 2010; 243:51-9.
16. Brescia P, Ortensi B, Fornasari L, Levi D, Broggi G, Pelicci G. CD133 is essential for glioblastoma stem cell maintenance. Stem Cells 2013; 31:857-69.
17. Kar S, Deb M., Sengupta D, Shilpi A, Bhutia SK, Patran SK. Intricacies of hedgehog signaling pathways: A perspective in tumorigenesis. Exp Cell Res 2012; 318:1959-72.
18. Schaich M, Kestel L, Pfirrmann M. MDR1 (ABCB1) gene single nucleotide polymorphism predicts outcome of temozolomide treatment in glioblastoma patients. Ann Oncol 2009; 20:175-81.
19. Ulasov IV, Nandi S, Dey M, Sonabend AM, Lesniak MS. Inhibition of Sonic hedgehog and Notch pathways enhances sensitivity of CD133(+) glioma stem cells to temozolomide therapy. Mol Med 2011; 17:103-12.
20. Gadji M, Crous AM, Fortin D, Kreek J, Torchia M, Mai S, Drouin R, Klonisch T. EGF receptor inhibitors in the treatment of glioblastoma multiforme: old clinical allies and newly emerging therapeutic concepts. Eur J Pharmacol 2009; 625:23-30.
21. Li WQ, Li,YM, Tao BB, et al. Downregulation of ABCG2 expression in glioblastoma cancer stem cells with miRNA-328 may decrease their chemoresistance. Med Sci Monit 2010; 16:HY27-30.
22. Peñuelas S, Anido J, Prieto-Sanchez RM, et al. TGF-beta increases glioma-initiating cell self-renewal through the induction of LIF in human glioblastoma. Cancer Cell 2009; 15:315-27.
23. Ropolo M, Daga A, Griffero F, et al. Comparative analysis of DNA repair in stem and nonstem glioma cell cultures. Mol Cancer Res 2009; 7:383-92.
24. Moitra K, Lou H, Dean M. Multidrug efflux pumps and cancer stem cells: insights into multidrug resistance and therapeutic development. Clin Pharmacol Ther 2011; 89:491-502.
25. Tchorz JS, Tome M, Cloëtta D, et al. Constitutive Notch2 signaling in neural stem cells promotes tumorigenic features and astroglial lineage entry. Cell Death Dis 2012; 3,e325; doi:10.1038/cddis.2012.65 .
26. Cheng L, Wu Q, Huang Z, Guryanova OA, Huang Q, Shou W, Rich JN, Bao S. L1CAM regulates DNA damage checkpoint response of glioblastoma stem cells through NBS1. EMBO J 2011; 30:800-13.
27. Sunayama J, Sato A, Matsuda K, et al. Dual blocking of mTor and PI3K elicits a prodifferentiation effect on glioblastoma stem-like cells. Neuro-Oncology 2010; 12:1205-19.
28. Fang X, Yoon JG, Li L, et al. The SOX2 response program in glioblastoma multiforme: an integrated ChIP-seq, expression microarray, and microRNA analysis. BMC Genomics 2011; 12:11.
29. Kim KH, Seol HJ, Kim EH, et al. Wnt/β-catenin signaling is a key downstream mediator of MET signaling in glioblastoma stem cells. Neuro-Oncology 2013; 15:161-71.
30. Jin X, Jeon HY, Joo KM, et al. Frizzled 4 regulates stemness and invasiveness of migrating glioma cells established by serial intracranial transplantation. Cancer Res 2011; 71:3066-75.
31. Natsume A, Kato T, Kinjo S, et al. Girdin maintains the stemness of glioblastoma stem cells. Oncogene 2012; 31:2715-24.
32. Schulte A, Günther HS, Phillips HS, et al. A distinct

subset of glioma cell lines with stem cell-like properties reflects the transcriptional phenotype of glioblastomas and overexpresses CXCR4 as therapeutic target. Glia 2011; 59:590-602.
33. Martin-Castillo B, Vasquez-Martin A, Oliveras-Ferraros C, Menendez JA. Metformin and cancer. Doses, mechanisms and the dandelion and hormetic phenomena. Cell Cycle 2010; 9:1057-64.
34. Dilman VM, Anisimov VN. Effect of treatment with phenformin, diphenylhydantoin or L-dopa on life span and tumor incidence in C3H/Sn mice. Gerontology 1980; 26:241-6.
35. Rizos CV, Elisaf MS. Metformin and cancer. Eur J Pharmacol 2013; 705:96-108.
36. Soritau O, Tomuleasa C, Aldea M, et al. Metformin plus temozolomide-based chemotherapy as adjuvant treatment for WHO grade III and IV malignant gliomas. J BUON 2011; 16:282-9.
37. Ben Sahra I, Regazzetti C, Guillome R, et al. Metformin, independent of AMPK, induces mTOR inhibition and cell-cycle arrest through REDD1. Cancer Res 2011; 71:4366-72.
38. Aldea M, Tomuleasa C, Petrushev B, Susman S, Kacso GL, Irimie A, Florian IS, Soritau O. Antidiabetic pharmacology: a link between metabolic syndrome and neuro-oncology? J BUON 2011; 16:409-13.
39. Deng XS, Wang S, Deng A, Liu B, Edgerton SM, Lind SE, Wahdan-Alaswad R, Thor AD.Metformin targets Stat3 to inhibit cell growth and induce apoptosis in triple-negative breast cancers. Cell Cycle 2012; 11:367-76.
40. Sato A, Sunayama J, Okada M, et al. Glioma-initiating cell elimination by metformin activation of FOXO3 via AMPK. Stem Cells Transl Med 2012; 1:811-24.
41. Tomuleasa C, Soritau O, Fisher-Fodor E, et al. Arsenic trioxide plus cisplatin/interferon α. 2b/doxorubicin /capecitabine combination chemotherapy for unresectable hepatocellular carcinoma. Hematol Oncol Stem Cell Ther 2011; 4:60-6.
42. Zhen Y, Zhao S, Li Q, Kawamoto K. Arsenic trioxide-mediated Notch pathway inhibition depletes the cancer stem-like cell population in gliomas. Cancer Lett 2010; 292:64-72.
43. Villalva C, Martin-Lannerée S, Cortes U, et al. STAT3 is essential for the maintenance of neurosphere-initiating tumor cells in patients with glioblastomas: a potential for targeted therapy? Int J Cancer 2011; 128:826-38.
44. Wang H, Lathia JD, Wu Q, et al. Targeting interleukin 6 signaling suppresses glioma stem cell survival and tumor growth. Stem Cells 2009; 27:2393-404.
45. Sun H, Zhang S. Arsenic trioxide regulates the apoptosis of glioma cell and glioma stem cell via down-regulation of stem cell marker Sox2. Biochem Biophys Res Comm 2011; 410:692-7.
46. Liu Z, Hazan-Halevy I, Harris DM, Li P, Ferrajoli A, Faderl S, Keating MJ, Estrov Z. STAT-3 activates NFkB in chronic lymphocytic leukemia cells. Mol Cancer Res 2011; 9:507-15.
47. Chiu HW, Ho YS, Wang YJ. Arsenic trioxide induces autophagy and apoptosis in human glioma cells in vitro and in vivo through downregulation of survivin. J Mol Med 2011; 89:927-41.
48. Dizaji MZ, Malehmir M, Ghavamzadeh A, Alimoghaddam K, Ghaffari SH. Synergistic effects of arsenic trioxide and silibinin on apoptosis and invasion in human glioblastoma U87MG cell line. Neurochem Res 2012; 37:370-80.
49. Lampson LA. Monoclonal antibodies in neuro-oncology. Getting past the blood-brain barrier. mAbs 2011; 3(2):153-60.
50. Ryu S, Crocker I, Stieber V, Ye X, Fisher JD, Grossman SA. Perfusion and diffusion MRI in the assessment of the antivascular effect of arsenic trioxide combined with radiotherapy for glioblastoma multiforme: NABTTphase I study. J Clin Oncol 2005; 23:1538 (abstract).

EDITORIAL

INTERRELATIONSHIP BETWEEN IL-3 AND MAST CELLS

S.K. KRITAS[1], A. SAGGINI[2], G. CERULLI[3], A. CARAFFA[4], P. ANTINOLFI[4], A. PANTALONE[5], R. SAGGINI[6], S. FRYDAS[7], M. ROSATI[8], M. TEI[9], A. SPEZIALI[10], F. PANDOLFI[10] and P. CONTI[11]

[1]Department of Microbiology and Infectious Diseases, School of Veterinary Medicine, Aristotle University of Thessaloniki, Macedonia, Greece; [2]Department of Dermatology, University of Rome Tor Vergata, Rome, Italy; [3]Nicola's Foundation, Onlus, Arezzo, Italy; [4]Orthopedic Division, University of Perugia, Perugia, Italy; [5]Orthopedic Division, University of Chieti-Pescara, Chieti, Italy; [6]Department of Neurosciences and Imaging, Faculty of Medicine and Surgery, G. d'Annunzio University Chieti-Pescara, Chieti, Italy; [7]Department of Parasitology, School of Veterinary Medicine, University of Thessaloniki, Macedonia, Greece; [8]Gynecology Clinic, Pescara Hospital, Pescara, Italy; [9]Nicola's Foundation, Onlus, Arezzo, Italy; [10]Department of Internal Medicine, Catholic University of the Sacred Heart, Rome, Italy; [11]Immunology Division, Medical School, University of Chieti-Pescara, Chieti, Italy

Received November 20, 2013 – Accepted January 8, 2014

It is well established that mast cells, which are found in the tissues in the proximity of small blood vessels and post-capillary venules, play a key role in the early phase of IgE-mediated allergic reactions. A greatly expanded understanding of the biology of IL-3 has emerged since the early 1980s. IL-3 is a specific factor that stimulates the growth of hematopoietic stem and progenitor cells of a variety of lineages and can promote the proliferation of certain classes of lymphocytes distinct from those that are dependent on IL-2. IL-3 has been identified among the most important cytokines for regulation of mast cell growth and differentiation, migration and effector function activities of many hematopoietic cells. IL-3 termed multi colony-stimulating-factor (multi-CSF) or mast cell growth factor (MCGF) is a haematopoietic growth factor which stimulates the formation of colonies for erythroid, megakaryocytic, granulocytic and monocytic lineages. It is predominantly produced by activated T cells, natural killer (NK) cells and mast cells and supports the growth-promoting effects of SCF on mast cell precursors. IL-3 causes severe hypersensivity reactions and plays a pivotal role in exacerbating the inflammatory *response in vivo.* Here we report the interrelationship between IL-3 and mast cells.

Mast cells were first described in 1879 by Paul Ehrlich, and like basophils possess high-affinity immunoglobulin (Ig) E receptors (FcεRI) that are cross-linked upon engagement of receptor-bound IgE with corresponding antigens, resulting in the release of a number of mediators that are in part common for both cell types (1). Mast cells are present in the bone marrow as committed cell precursors and have been proposed to play an important role in the innate immune response to a variety of pathogens (2). Major participants in the development of an asthma phenotype include the

Key words: Interleukin-3, mast cells, inflammation

Mailing address: Spyridon K. Kritas, DVM, PhD, Dipl. ECPHM, Associate Professor,
Department of Microbiology and Infectious Diseases,
School of Veterinary Medicine, Aristotle University of Thessaloniki,
54124 Thessaloniki, Macedonia, Greece
Tel.: +30 2 310 999940 Fax: +30 2 310 999940
e-mail: skritas@vet.auth.gr

0393-974X (2014)

triggering stimuli such as the allergens themselves, cells such as T cells, epithelial cells and mast cells that produce a variety of cytokines including IL (interleukin)-5, granulocyte/macrophage-colony-stimulating factor (GM-CSF), IL-3, IL-4 and IL-13 and chemokines such as eotaxin (3). IL-3 has been identified among the most important cytokines for regulation of mast cell growth and differentiation, migration and effector function activities of many hematopoietic cells (4). This cytokine is involved in normal responses to infectious agents, bridging innate and adaptive immunity. However, in certain cases, the over-expression of IL-3 or its receptor can lead to excessive or aberrant initiation of signaling resulting in pathological conditions, with chronic inflammatory diseases. IL-3 is a relatively small monomeric protein of 133-aminoacids with a molecular weight of approximately 15 kD and has diverse biological effects on a variety of cells stimulated with a combination of phorbol ester, calcium ionophore, or substance P (5). IL-3 supports the growth-promotion effects of SCF on mast cell precursors and enhances the activity of IL-2 in the proliferation and differentiation of B lymphocytes (6). One of the most important ancd characteristic aspects is the ability of IL 3 to induce the differentiation of 20-alpha-SDH *in vitro* (7).

Human mast cells develop from committed precursors in the bone marrow expressing the differentiation marker CD34+ and distinct from the three other myeloid cells. Next, they migrate into a large variety of tissues where they locate perivascularly and mature, depending on microenviromental conditions. Due to their typical expression of the high affinity receptor for IgE, for many decades, mast cells have been regarded uniquely as effector cells in IgE-associated disorders. These cells, as well as basophils, monocytes, eosinophils, and neutrophils, are found in cord blood, peripheral blood, and bone marrow. Although mast cell progenitors have been documented as a separate lineage, e.g., characterized as $CD34^{+}/CD38^{+}$ or $CD34^{+}/c\text{-}kit^{+}/CD13^{+}$, most recently a new monoclonal antibody such as 97A6 has been described as specific for mature mast cells and their progenitors (8).

Allergen induces Th2 lymphocyte proliferation in individuals with allergies with the release of their characteristic combination of cytokines including IL-3, IL-4, IL-5, IL-9, IL-10, and IL-13.

Mast cells develop from bone marrow under the influence of both IL-3 and the c-kit ligand, also known as stem cell factor (SCF). In humans, the mast cell precursor is CD34+, FcεRI-. With time, mast cell precursors become less responsive to IL-3 and more responsive to SCF. Mast cell proliferation directed by SCF is enhanced by other cytokines including both IL-4 and IL-10. Mast cell precursors target tissues, and their survival may largely be dependent upon the local production of SCF. *In vitro*, withdrawal of IL-3 or SCF results in mast cell apoptosis (9).

The precursors of mast cells leave the bone marrow in a non-differentiated form as CD34+ cells. The presence of mast cell growth and differentiation factors control tissue maturation of different mast cells phenotypes. The main factors are the mast cell growth factor SCF, NGF (Nerve Growth Factor), and IL-3. T-cells are characterized by (simultaneous) production of IL-3, IL-4, IL-5 and others. These cytokines control the production of IgE by B cells and play a critical role in the activation and differentiation of effector cells of the allergic response (10).

As reported above, it has been recognized that mast cells themselves are the source of several cytokines, raising the possibility that they may enhance and sustain inflammatory reactions in an autocrine fashion. A large number of studies have shown that many cytokines can influence not only the proliferation but also the functional activity of human inflammatory cells. IL-3 represents a potent growth and differentiation factor for basophils and for mast cells. Th2-derived IL-3 and IL-4 are mast-cell growth factors that act in synergy, at least *in vitro*. Recent evidence indicates that allergen-specific Th2 cells are selectively enriched in tissues affected by allergic inflammation (11).

When mast cells are activated by cross-linking of their high affinity IgE receptors by the antigen and IgE antibodies, release of chemical mediators is followed by secretion of multiple pro-inflammatory cytokines such as GM-CSF, IL-9 and IL-13, IL-1, IL-6, IL-8 and TNF-α which are necessary for innate immunity. Moreover, IL-8 regulates recruitment and activation of leukocytes, as well as the expression of vascular adhesion molecules that permit leukocyte migration (12). Cytokines produce their cellular effects by activation of various transcription factors

Table I. *Biological effects of IL-3.*

- IL-3 is an haematopoietic growth factor
- It stimulates the formation of colonies for granulocytic, erythroid, and monocytic lineages
- It stimulates the renewal of pluripotent haematopoietic stem cells
- It is a multi colony-stimulating factor (multi-CSF) and mast cell growth factor (MCGF)
- It is a megakaryocyte growth factor and eosinophil CSF
- It has diverse biological effects on a variety of cells
- It is produced by activated T cells, natural killer (NK) cells and mast cells
- It acts on target cells types such as monocytes, eosinophils, basophils, and mast cells
- It acts on early stages of haematopoiesis,
- It acts in synergy with other cytokines to induce progenitors of various lineages
- Together with GMCSF or G-CSF it induces the granulocyte-macrophage lineages
- It synergizes with TNF for short-term proliferation of CD34 cells
- It causes the development of dendritic or Langerhans cells.
- It supports the growth-promoting effects of SCF on mast cell precursors
- It enhances the activity of IL-2 in the proliferation and differentiation of B lymphocytes
- It modulates the activity of a number of mature cell types
- It enhances histamine release from basophils
- It causes eosinophil activation
- It influences monocyte function
- It regulates macrophage cytotoxicity.
- IL-3 and GM-CSF induce monocyte adhesiveness by induction of the integrin CD18
- It stimulates the expression of human leucocyte antigen (HLA)-DR, CD14 and IL-1α
- IL-3 in combination with a growth factor elicits effects on thrombopoiesis.

such as AP-1 and NF-κB. Furthermore, the expression of many of these cytokines and their receptors are upregulated by these transcription factors. Ca2+ acts as a second messenger during cell activation.

An increase in the levels of intracellular Ca2+ has been proposed to act as an essential trigger for mast cell activation. It has also been reported that the release of intracellular Ca2+ from internal stores is required for MAPK activation. Recently, studies showed the involvement of MAPK and NF-κB activation by Ca2+, with increased Ca2+ levels inducing the release of biological mediators including TNF-α, IL-6 and IL-8 (13).

IL-3, IL-5, and GM-CSF promote mast cell maturation. IL-3, as well as IL-5, GM-CSF, and NGF have similar effects in respect to potentiating IgE-mediated mast cell histamine and LTC_4 releases, and they bind to receptors of the same subfamily but, of these, IL-3 is the most potent (14).

Pre-incubation or co-culture of mast cells with IL-3 causes significant enhancement of histamine and LTC_4 release to a number of immunologic and non-immunologic stimuli such as anti-IgE, C5a, C3a, and PAF (15). It has been also reported that IL-3, IL-5, and GM-CSF enhance mediator release following either IgE-dependent stimulation or activation. In addition, IL-3 in combination with C5a can cause mast cell mediator release independently of IgE-receptor cross-linking, suggesting a role for these cells in non-allergic inflammatory diseases caused by either bacterial infections or IgG (16). IL-3 treatment, in experimental animals caused severe hypersensitivity reactions including urticaria, vomiting, diarrhea, edema, arthritis, and stimulation of hemopoiesis. Given the above evidence, IL-3 and related hematopoietic growth factors potentially play a pivotal role in exacerbating the inflammatory response (17). In addition, cross-linking of high affinity IgE

receptors prevents apoptosis of mast cells by paracrine mechanisms, producing IL-3, IL-4 and GM-CSF (18). Moreover, mast cells generate inflammatory mediators including tryptase, histamine, leukotrienes, serotonin, and prostaglandin PGD2 which are elevated in allergic patients, and can cause widespread inflammation by stimulating protease-activated receptors (19). It has been reported that ERK activation is not sufficient in itself for leukotriene synthesis because IL-3, which strongly activates ERK in the absence of IgE-dependent stimulation, is almost ineffective in causing LTC_4 release (20). Despite this, in combination with anti-IgE, IL-3 leads to both a striking potentiation and prolongation of ERK phosphorylation compared with the effects of IL-3 or anti-IgE alone and leads to twice as much LTC_4 production than anti-IgE alone (20).

There is growing evidence that signals employed by priming factors such as IL-3 favor the production of IL-13 rather than IL-4. IL-3 potentiates the IgE-dependent release of both factors but, in addition to this, it has been shown that IL-3 stimulation alone is sufficient to give rise to IL-13 generation without a marked increase in IL-4 production (21).

However, despite the broad range of biological activities *in vitro*, the clinical utility of IL-3 has been elusive.

REFERENCES

1. Theoharides TC, Kempuraj D, Tagen M, Conti P, Kalogeromitros D. Differential release of mast cell mediators and the pathogenesis of inflammation. Immunol Rev 2007; 217:65-78.
2. Theoharides TC, Conti P. Mast cells: the Jekyll and Hyde of tumor growth. Trends Immunol 2004; 5(5):235-41.
3. Castellani ML, Shaik YB, Perrella A, et al. Expression and secretion of CXCL8 (IL-8), release of tryptase and transcription of histidine decarboxylase mRNA by anti-IgE-activated human umbilical cord blood-derived cultured mast cells. Neuroimmunomodulation 2007; 14(2):97-104.
4. Jamur MC, Oliver C. Origin, maturation and recruitment of mast cell precursors. Front Biosci Schol Ed 2011; 3:1390-406.
5. Adamus M. Substance P as a regulatory peptide of hematopoiesis and blood cell functions. Postepy Hig Med Dosw 2009; 63:106-13.
6. Wadhwa M, Thorpe R. Haematopoietic growth factors and their therapeutic use. Thromb Haemost 2008; 99(5):863-73.
7. Keller JR, Weinstein Y, Hursey M, Ihle JN. Interleukins 2 and 3 regulate the *in vitro* proliferation of two distinguishable populations of 20-alpha-hydroxysteroid dehydrogenase-positive cells. J Immunol 1985; 135(3):1864-71.
8. Kirshenbaum AS, Goff JP, Semere T, Foster B, Scott LM, Metcalfe DD. Demonstration that human mast cells arise from a progenitor cell population that is CD34(+), c-kit(+), and expresses aminopeptidase N (CD13). Blood. 1999 Oct 1; 94(7):2333-42.
9. Vande Walle L, Wirawan E, Lamkanfi M, et al. The mitochondrial serine protease HtrA2/Omi cleaves RIP1 during apoptosis of Ba/F3 cells induced by growth factor withdrawal. Cell Res 2010; 20(4):421-33.
10. T cells as orchestrators of the asthmatic response. Kay AB. Ciba Found Symp. 1997; 206:56-67.
11. Del Prete G. Human Th1 and Th2 lymphocytes: their role in the pathophysiology of atopy. Allergy 1992; 47(5):450-5.
12. Mirowska-Guzel DM, Kurowska K, Skierski J, Koronkiewicz M, Wicha W, Kruszewska J, Czlonkowski A, Czlonkowska A. High dose of intravenously given glucocorticosteroids decrease IL-8 production by monocytes in multiple sclerosis patients treated during relapse. J Neuroimmunol 2006; 176(1-2):134-40.
13. Sooryanarain H, Sapkal GN, Gore MM. Pathogenic and vaccine strains of Japanese encephalitis virus elicit different levels of human macrophage effector functions. Arch Virol 2012; 157(10):1905-18.
14. Marone G, Florio G, Petraroli A, Triggiani M, de Paulis A. Role of human FcepsilonRI+ cells in HIV-1 infection. Immunol Rev 2001; 179:128-38.
15. Columbo M, Horowitz EM, Botana LM, et al. The human recombinant c-kit receptor ligand, rhSCF, induces mediator release from human cutaneous mast cells and enhances IgE-dependent mediator release from both skin mast cells and peripheral blood basophils. J Immunol 1992; 149(2):599-608.
16. Knol EF, Mul FP, Lie WJ, Verhoeven AJ, Roos D. The role of basophils in allergic disease. Eur Respir J Suppl 1996; 22:126s-131s.
17. Allakhverdi Z, Allam M, Renzi PM. Inhibition

of antigen-induced eosinophilia and airway hyperresponsiveness by antisense oligonucleotides directed against the common beta chain of IL-3, IL-5, GM-CSF receptors in a rat model of allergic asthma. Am J Respir Crit Care Med 2002; 165(7):1015-21.

18. Yoshikawa H, Tasaka K. Suppression of mast cell activation by glucocorticoid. Arch Immunol Ther Exp 2000; 48(6):487-95.
19. Grzelewska-Rzymowska I, Grabski W, Kroczyńska-Bednarek J, Zieba M, Rozniecki J. Effect of nedocromil sodium on clinical course and histamine airway responsiveness in patients with pollen induced bronchial asthma. Pneumonol Alergol Pol 1995; 63(3-4):185-91.
20. Zhu Y, Bertics PJ. Chemoattractant-induced signaling via the Ras-ERK and PI3K-Akt networks, along with leukotriene C4 release, is dependent on the tyrosine kinase Lyn in IL-5- and IL-3-primed human blood eosinophils. J Immunol 2011; 186(1):516-26.
21. Poulsen LK, Hummelshoj L. Triggers of IgE class switching and allergy development. Ann Med 2007; 39(6):440-56.

CARBAMATE PESTICIDE-INDUCED APOPTOSIS AND NECROSIS IN HUMAN NATURAL KILLER CELLS

Q. LI, M. KOBAYASHI and T. KAWADA

Department of Hygiene and Public Health, Nippon Medical School, Tokyo, Japan

Received February 14, 2013 – Accepted January 10, 2014

We previously found that ziram, a carbamate fungicide, significantly induced apoptosis and necrosis in human NK-92MI, a natural killer cell line. To investigate whether other carbamate pesticides also induce apoptosis and necrosis in human natural killer cell, we conducted further experiments with NK-92CI, a human natural killer cell line using a more sensitive assay. NK-92CI cells were treated with ziram, thiram, maneb or carbaryl at 0.031-40 μM for 2-24 h in the present study. Apoptosis and necrosis were determined by FITC-Annexin-V/PI staining. To explore the mechanism of apoptosis, intracellular levels of active caspases 3 and mitochondrial cytochrome-c release were determined by flow cytometry. We found that ziram and thiram also induced apoptosis and necrosis in a time- and dose-dependent manner; however, maneb and carbaryl induced apoptosis and necrosis only at higher doses in NK-92CI cells. The strength of the apoptosis-inducing effect differed among the pesticides, and the order was as follows: thiram > ziram > maneb > carbaryl. NK-92CI was more sensitive to ziram than NK-92MI. Moreover, ziram and thiram significantly increased the intracellular level of active caspase 3 in NK-92CI and caspase inhibitor significantly inhibited the apoptosis. Ziram and thiram significantly caused mitochondrial cytochrome-c release in NK-92CI. These findings indicate that carbamate pesticides can induce apoptosis in natural killer cells, and the apoptosis is mediated by both the caspase-cascade and mitochondrial cytochrome-c pathways.

Carbamate pesticides are widely used throughout the world in agriculture as fungicides and insecticides (1-4). We previously reported that ziram, a carbamate fungicide, significantly inhibits natural killer (NK) activity (5). We have also found that ziram significantly induced apoptosis and necrosis in NK-92MI cell, a human natural killer cell line (6) and contributed to the inhibition of NK activity. However, it is not clear whether other carbamate pesticides have a similar ability to ziram and can induce apoptosis and necrosis in human natural killer cells. NK-92CI cell, another human natural killer cell line, was more sensitive to organophosphorus pesticides than NK-92MI cell line (7).

Thus, in the present study, we selected several carbamate pesticides such as carbaryl (insecticide), maneb (fungicide), thiram (fungicide) and ziram (fungicide) (1-4), which are used now in Japan as pesticides and investigated their cell death-inducing effect in human NK-92CI cells. Cell death can be divided into two basic forms, apoptosis and necrosis, based on the changes in morphology, enzymatic activity, and adjacent cellular effects (8, 9).

Apoptosis was originally proposed by Kerr

Key words: Annexin-V, apoptosis, carbamate pesticide, carbaryl, caspase, cytochrome-c, natural killer cell, maneb, thiram, ziram

Mailing address: Qing Li, MD, PhD,
Department of Hygiene and Public Health,
Nippon Medical School,
1-1-5 Sendagi, Bunkyo-ku,
Tokyo 113-8602, Japan
Tel.: +81 3 38222131 Fax: +81 3 56853065
e-mail: qing-li@nms.ac.jp

0393-974X (2014)

in 1972 as a form of programmed cell death in multicellular organisms, and involves a series of biochemical events leading to a characteristic cell morphology and death, including blebbing, changes to the cell membrane, such as loss of membrane asymmetry and attachment, cell shrinkage, nuclear fragmentation, chromatin condensation, and chromosomal DNA fragmentation (8, 10).

Apoptosis in the early stage can be detected by fluorescein isothiocynate (FITC)-Annexin-V staining and necrosis can be detected by propidium iodide (PI) staining using a flow cytometer (6, 7, 11-13).

The caspase family of cysteine proteases plays a key role in apoptosis. Caspase-3 is a key protease activated during the early stages of apoptosis and, like other members of the caspase family, is synthesized as an inactive proenzyme that is processed in cells undergoing apoptosis by self-proteolysis and/or cleavage by another protease such as caspase 8 or 9 (14, 15). Cytochrome-c initiates apoptosis through its release into the cytoplasm and binding of Apaf-1 which activates procaspase 9 (16). Goldstein (17) reported that the release of cytochrome-c from mitochondria was a very early event during apoptosis. Based on this background, we also investigated the effects of carbamate pesticides on caspases and cytochrome-c release to explore the mechanism of the apoptosis and necrosis.

MATERIALS AND METHODS

Reagents

Alpha minimum essential medium (α-MEM) without ribonucleosides and deoxyribonucleosides, inositol, 2-mercaptoethanol (2-ME), folic acid, glutamine, and propidium iodide (PI) were obtained from Sigma (St. Louis, MO). Fetal bovine serum (FBS) was purchased from JRH Biosciences (Lenexa, KS), and heat- inactivated at 56°C for 30 min prior to use.

Fluorescein isothiocynate (FITC)-anti human Annexin V and FITC-anti human active caspase-3, propidium iodide (PI), Z-VAD-FMK (a general caspase inhibitor), Z-FA-FMK (a negative control for Z-VAD-FMK), Cytofix/cytoperm solution were purchased from BD Pharmingen (San Diego, CA). Carbaryl, maneb, thiram and ziram were obtained from Wako Pure Chemical Industries (Osaka, Japan) and prepared as stock solutions in DMSO.

Cells

The NK-92CI cell line was obtained from ATCC (Manassas, VA) and was maintained in α-MEM without ribonucleosides and deoxyribonucleosides with 2 mM L-glutamine adjusted to contain 1.5 g/L sodium bicarbonate and supplemented with 0.2 mM inositol, 0.1 mM 2-ME, 0.02 mM folic acid, and 10% FBS at 37°C in a 5% CO_2 incubator. NK-92CI is an IL-2-independent NK cell line derived from NK-92 cells by transfection with human IL-2 cDNA (18).

Carbamate pesticides-induced apoptosis and necrosis in NK-92CI cells determined by FITC-Annexin V/PI staining

The NK-92CI cells at $1x10^5$/ml were treated with carbaryl, maneb, thiram or ziram at 0-40 μM for 2, 4, 8, 16 or 24 h at 37°C in a 5% CO_2 incubator. The treated cells were stained with FITC-Annexin-V/PI, and 10,000 cells were acquired and stored for analysis with a FACScan flow cytometer (Becton Dickinson, San Jose, CA) as described previously (6, 12, 13).

Determination of intracellular levels of active caspase-3 in NK-92CI by flow cytometry

NK-92CI cells at $1x10^5$ /ml were incubated with ziram and thiram at 0 (0.1% DMSO), 0.03125, 0.0625, 0.125, 0.25, 0.5, 1 or 2 μM for 16 h at 37°C in a 5% CO_2 incubator, harvested, and washed twice with PBS. The cells were fixed/permeablized with Cytofix/cytoperm solution for 20 min at 4°C, and active caspase-3 was stained with FITC- anti human active caspase-3 for 30 min at room temperature according to the manufacturer's instructions (BD PharMingen). Again, the flow cytometric analysis was performed with FACScan (10,000 cells per analysis) (6, 12, 13).

Protective effects of general caspase inhibitor on thiram- and ziram-induced apoptosis and necrosis in NK-92CI cells

NK-92CI cells at $1x10^5$/ml were preincubated with Z-VAD-FMK, a general caspase inhibitor, or Z-FA-FMK, a negative control for Z-VAD-FMK, at 20 μM for 30 min, treated with ziram or thiram at 0 (0.1% DMSO) or 1 μM for 16 h, harvested, and washed twice with PBS. The treated cells were stained with FITC-Annexin-V/PI. Flow cytometric analysis was performed with FACScan (10,000 cells for each analysis) (6, 12, 13).

Analysis of cytochrome-c release

NK-92CI cells at $1x10^5$ /ml were incubated with thiram or ziram at 0 (0.1% DMSO), 0.0625, 0.125, 0.25, 0.5, 1 or 2 μM for 16 h at 37°C in a 5% CO_2 incubator, harvested, and washed twice with PBS. The cells were fixed/permeablized with Cytofix/cytoperm solution for 20 min at 4°C, and the intracellular cytochrome-c was stained with FITC- anti human cytochrome-c (mouse

IgG1) or FITC- mouse IgG1 as an isotypic control for 30 min at 4°C according to the manufacturer's instructions (eBioscience, San Diego, CA). Flow cytometric analysis was performed with FACScan (10,000 cells per analysis) (6, 12, 13, 19).

Statistical analyses

The numbers of apoptotic cells, active caspase-positive cells and cytochrome-c-negative cells were used for statistical analyses. Statistical analyses were performed using one-way ANOVAs followed by a post hoc test, Tukey's test, with SPSS 16.0J software for Windows. Paired and unpaired t-tests were also conducted. The significance level for *p*-values was set at < 0.05.

RESULTS

Ziram-induced apoptosis and necrosis in NK-92CI cells

As shown in Fig. 1A and 1B, 28.7% of ziram-treated cells exhibited apoptosis (FITC-Annexin-V^+/PI^-) and 38.5% showed necrosis (FITC-Annexin-V^+/PI^+) (Fig. 1B), compared to only 12.2% and 9.7% of control cells, respectively (Fig. 1A). As shown in Fig. 1C and 1D, ziram induced apoptosis in a dose- and time-dependent manner. Similarly, as shown in Fig. 1E and 1F, ziram-induced necrosis also exhibited a dose- and time-dependent profile.

Difference in sensitivity to ziram between NK-92CI and NK-92MI cells

As shown in Fig. 2, ziram-induced higher apoptosis (2A) and necrosis (2B) in NK-92CI cells than NK-92MI cells, suggesting that NK-92CI cells are more sensitive to ziram than NK-92MI cells.

Thiram-induced apoptosis and necrosis in NK-92CI cells

As shown in Fig. 3, thiram induced cell death (apoptosis and necrosis) in a dose- and time-dependent manner in NK-92CI cells.

Maneb-induced apoptosis and necrosis in NK-92CI cells

As shown in Fig. 4, maneb induced cell death (apoptosis and necrosis) only at higher concentrations in NK-92CI cells and the concentrations were higher than for thiram and ziram. Cell death at 40 μM was higher for 24 h than 16 h.

Carbaryl-induced apoptosis and necrosis in NK-92CI cells

As shown in Fig. 5, carbaryl induced cell death (apoptosis and necrosis) only at higher concentrations in NK-92CI cells and the concentrations were higher than for thiram and ziram. Cell death at 40μM was higher for 16 h than 24 h.

Difference in the ability to induce cell death among the pesticides

As shown in Fig. 6, the strength of the cell death-inducing effect differed among these pesticides, the order was ziram > thiram > maneb > carbaryl with 16 h treatment; whereas, the order was thiram > ziram > maneb > carbaryl with 24 h treatment. However, the cell death induced by thiram at 24h was significantly stronger than ziram either at 16 h or 24h, indicating that ultimately thiram was stronger than ziram.

Detection of intracellular levels of active caspase-3 in apoptotic NK-92CI cells

To explore the mechanism of the apoptosis, we investigated whether ziram and thiram affected the intracellular level of active caspase-3. As shown in Fig. 7, both ziram and thiram induced a significant increase in active caspase-3 in a dose-dependent manner, suggesting that thiram induced apoptosis at least partially *via* the caspase-3 pathway.

Protective effects of a general caspase inhibitor on ziram- and thiram-induced apoptosis in NK-92CI cells

As shown in Fig. 8, a general inhibitor of caspases significantly protected against the apoptosis induced by ziram and thiram. The findings strongly suggest that ziram and thiram induced apoptosis *via* the caspase cascade pathway.

Detection of mitochondrial cytochrome-c release in apoptotic NK-92CI cells

To further explore the mechanism of ziram and thiram-induced apoptosis in NK-92CI cells, we investigated whether ziram and thiram induces mitochondrial cytochrome-c release. As shown in Fig. 9, both ziram and thiram induced a significant increase of cytochrome-c-negative cells in a dose-dependent manner, indicating that it induced mitochondrial cytochrome-c release.

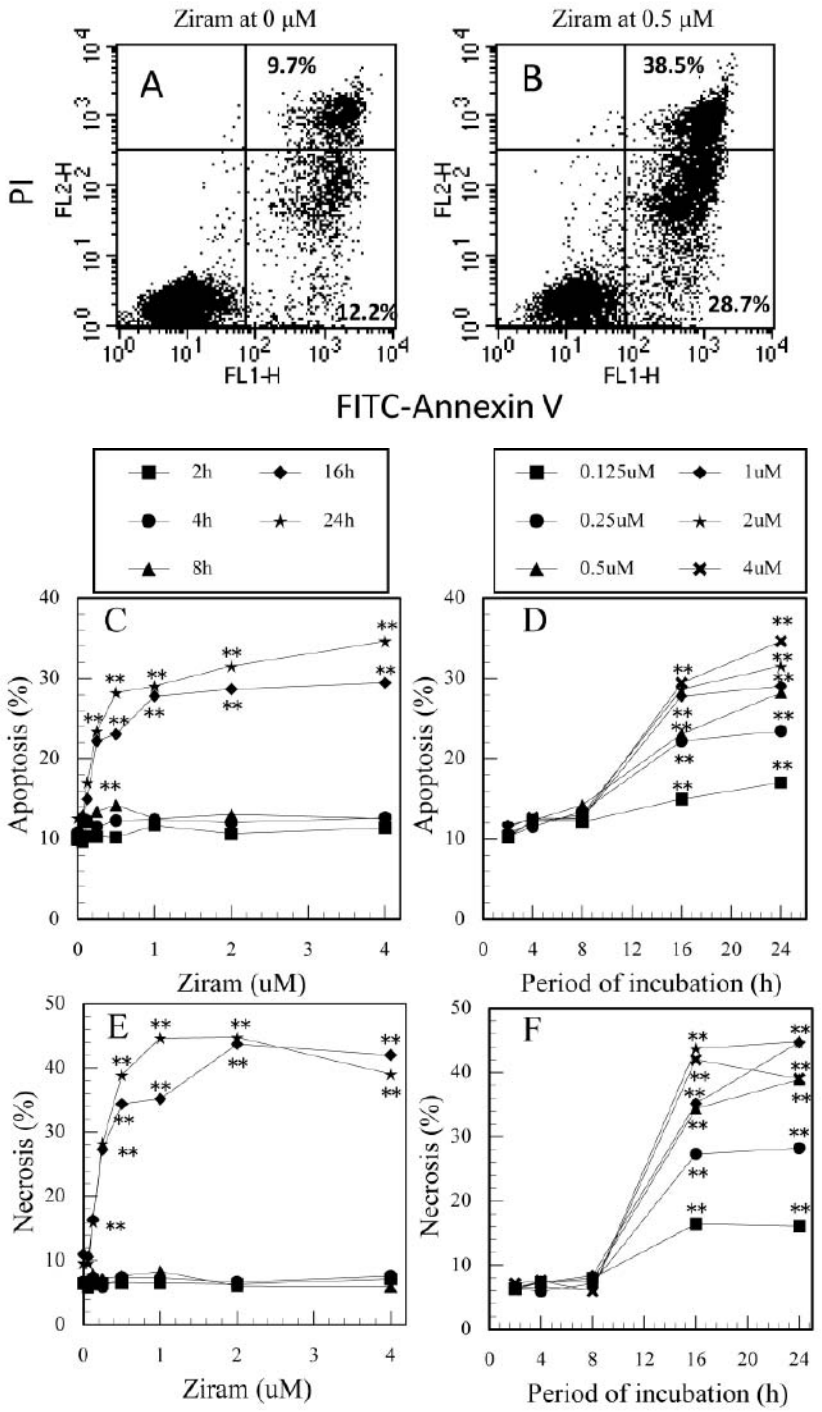

Fig. 1. *Ziram induced apoptosis in NK-92CI cells. (**A**): dot plot of FITC-Annexin V/PI in control cells, (**B**): dot plot of FITC-Annexin V/PI in ziram-treated cells, percentages in quadrants 2 and 3 show FITC-Annexin V^+/PI^+ (necrosis) and FITC-Annexin V^+/PI^- (apoptosis) cells, respectively. (**C**): dose-dependent increases in apoptotic cells in ziram-treated cultures, (**D**): time-dependent increases in apoptotic cells in ziram-treated cultures, (**E**): dose-dependent increases in necrotic cells in ziram-treated cultures, (**F**): time-dependent increases in necrotic cells in ziram-treated cultures. Data are presented as the mean (n=3). One-way ANOVA indicated that both the concentration of ziram and incubation period significantly affected apoptosis (all $p<0.01$) and necrosis ($p<0.01$ for 16 and 24 h). *: $p<0.05$; **: $p<0.01$; significantly different from 0 μM (Fig. 1C and 1E) or from 2 h (Fig. 1D and 1F) by Tukey's test.*

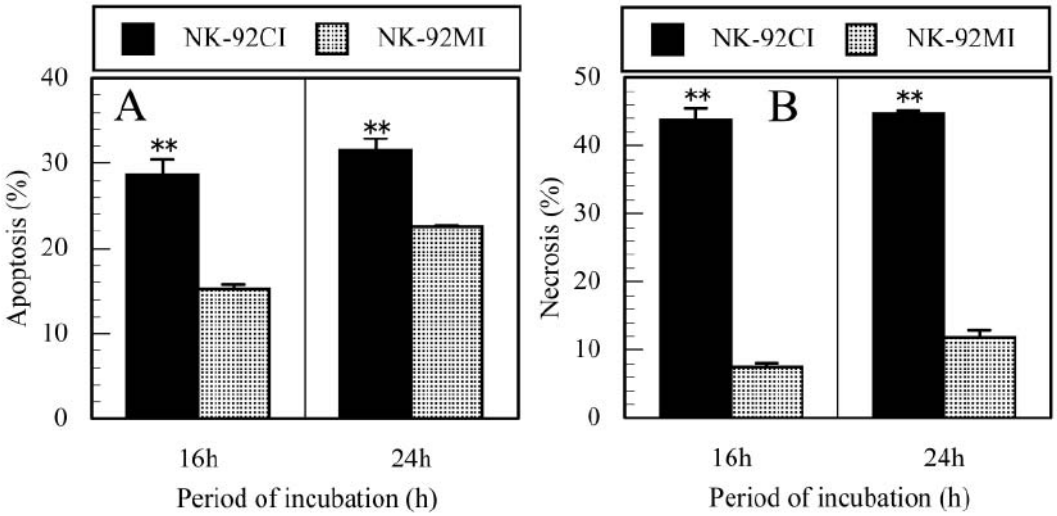

Fig. 2. *Difference in sensitivity to ziram between NK-92CI and NK-92MI in apoptosis and necrosis. NK-92CI and NK-92MI cells were treated with ziram at 2 μM for 16 and 24 h. **: p<0.01; significantly different from NK-92MI cells by t-test.*

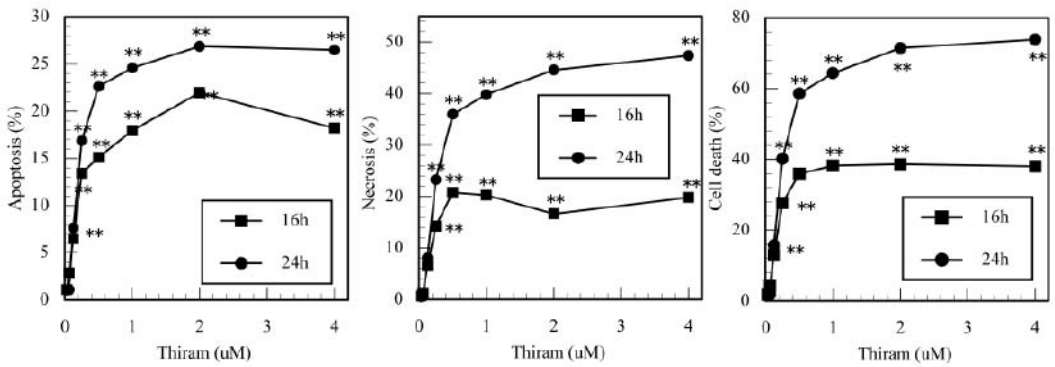

Fig. 3. *Thiram induced cell death (apoptosis and necrosis) in NK-92CI cells. Data are presented as the mean (n=3). One-way ANOVA indicated that both the concentration of thiram for 16 and 24 h significantly affected apoptosis and necrosis (all p<0.01). *: p<0.05; **: p<0.01; significantly different from 0 μM by Tukey's test. Cell death (apoptosis and necrosis) treated by 24 h was significantly greater than 16 h at 0.125-4 μM.*

DISCUSSION

Human exposure to carbamate pesticides may occur by coming into contact with latex rubber, ingesting treated crops, or via inhalation (20). In Japan, the residual standards for carbamate pesticides in rice and potato are 0.3 and 0.2 ppm, calculated as carbon disulfide, respectively (12).

Thus, 0.063-4 μM of thiram (approximately 0.015-0.96 ppm) and ziram (approximately 0.0195-1.25 ppm) were applied *in vitro* in the present study, which are reasonable related to the possible human exposure.

We previously reported that ziram, a carbamate pesticide significantly inhibits human NK activity (5). To explore the mechanism of this inhibition, we found that ziram significantly induces apoptosis/necrosis in human NK-92MI cell, a human NK cell line, which contributed to the inhibition of NK activity (6). We previously found that NK-92CI cell, another human natural killer cell line, was more sensitive to organophosphorus pesticides than NK-92MI cell line (7). Thus, in the present study, we investigated the effect of ziram on NK-92CI cells

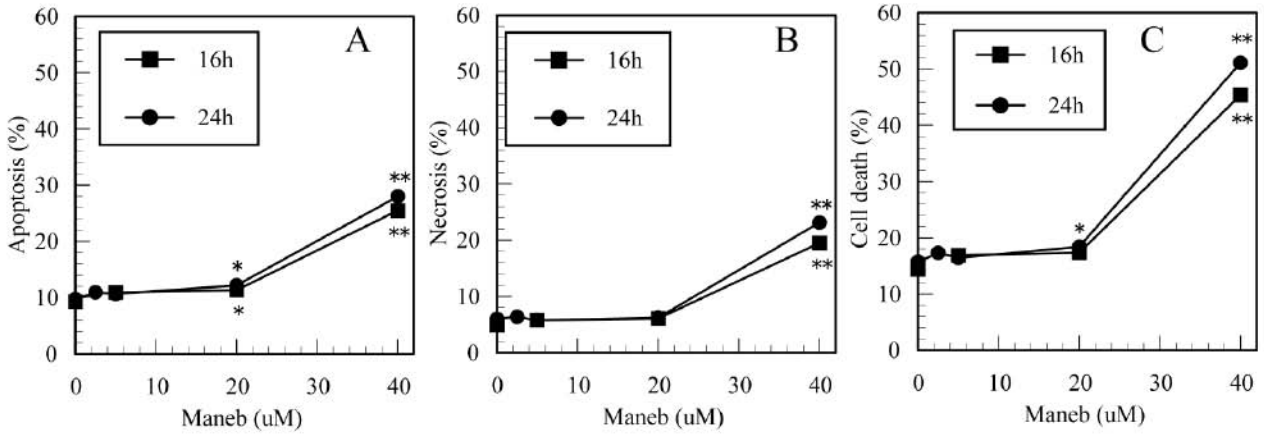

Fig. 4. *Maneb induced cell death (apoptosis and necrosis) in NK-92CI cells. Data are presented as the mean (n=3). One-way ANOVA indicated that the concentration of maneb for 16 and 24 h significantly affected apoptosis, necrosis and total cell death (all p<0.01). *: p<0.05; **: p<0.01; significantly different from 0 μM by Tukey's test. Cell death (apoptosis and necrosis) treated by 24 h was significantly greater than 16 h at 40 μM.*

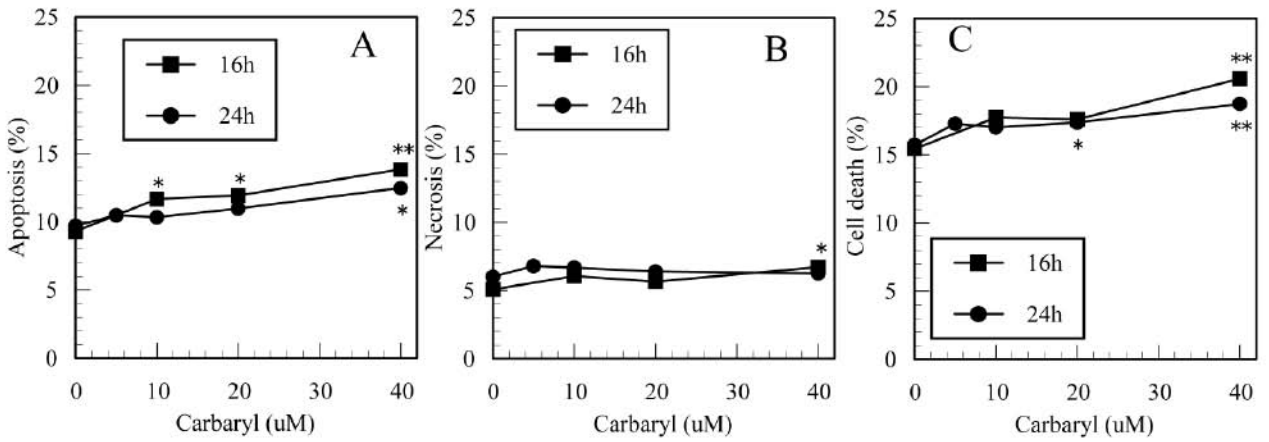

Fig. 5. *Carbaryl induced cell death (apoptosis and necrosis) in NK-92CI cells. Data are presented as the mean (n=3). One-way ANOVA indicated that both the concentration of carbaryl and incubation period significantly affected necrosis for 16 h, apoptosis and total cell death for both 16 and 24 h (all p<0.01). *: p<0.05; **: p<0.01; significantly different from 0 μM by Tukey's test.*

and found that ziram also significantly induced apoptosis in a dose- and time-dependent manner in human NK-92CI cells.

Moreover, NK-92CI cells are more sensitive to ziram than NK-92MI cells, which is similar to results induced by organophosphorus pesticides (7). On the other hand, it is not clear whether other carbamate pesticides also have the similar ability in apoptosis inducing in NK cells. Thus, in the present study, we further investigated several carbamate pesticides including carbaryl (insecticide), maneb (fungicide) and thiram (fungicide) (1-3) on apoptosis-inducing ability in human NK-92CI cells. Similar to ziram (6), thiram also induced apoptosis at a very low concentration (0.125μM) in a dose- and time-dependent manner in human NK-92CI cells. Moreover, we also found that maneb and carbaryl also induced apoptosis in a dose-dependent manner at higher concentrations in human NK-92CI cells.

However, the strength of the apoptosis-inducing

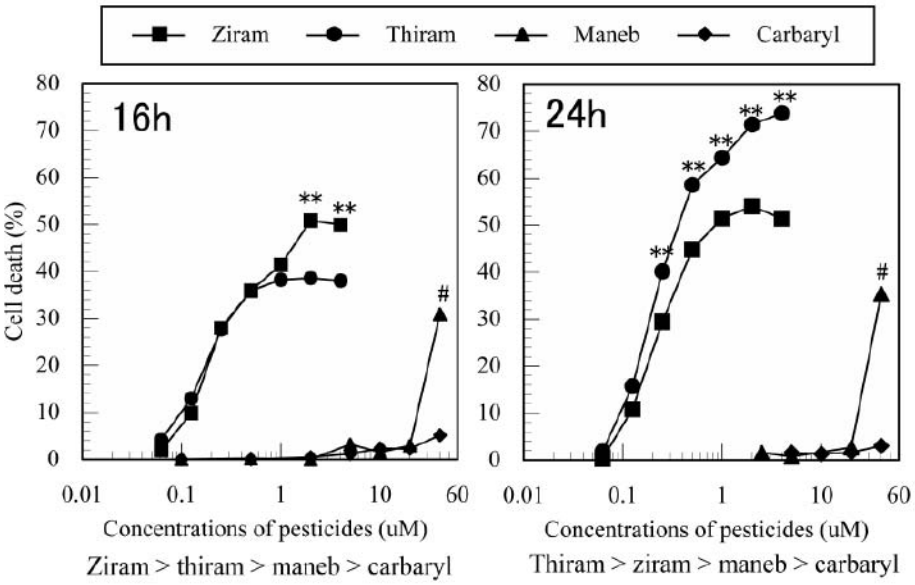

Fig. 6. *Different inducing ability in cell death among the pesticides. Data are presented as the mean (n=3). **: p<0.01; significant differences between ziram and thiram. #: p<0.01; significant differences between maneb and carbaryl by t-test.*

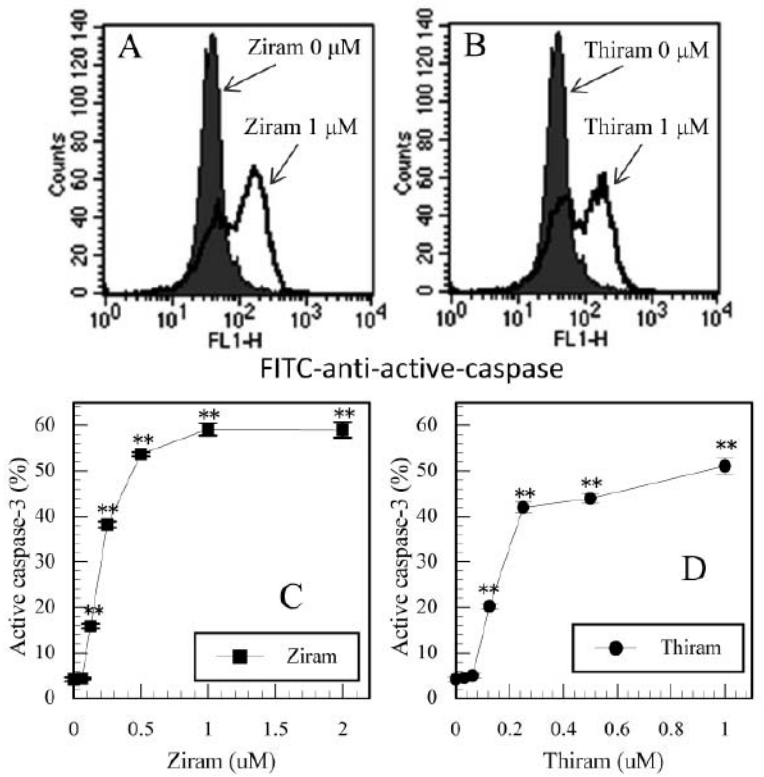

Fig. 7. *Ziram and thiram induced increases in active caspase-3-positive NK-92CI cells. **A**, **B**: the shaded histograms show the control cells (ziram or thiram at 0 μM) and the open histograms show the cells treated with ziram or thiram at 1 μM for 16 h and stained with FITC-rabbit anti-human active caspase 3. **C**, **D**: dose-dependent increases in active caspase-3-positive cells in ziram- and thiram-treated cultures. Data are presented as the mean ±SD (n=3). One-way ANOVA indicated that the concentration of ziram and thiram significantly affected the active caspase-3-positive cells (p<0.01). **: p<0.01; significantly different from 0 μM by Tukey's test.*

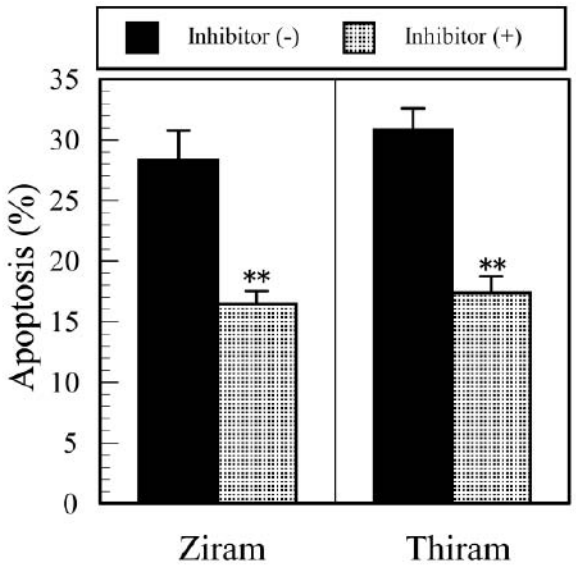

Fig. 8. *Protective effects of a general caspase inhibitor on ziram- and thiram-induced apoptosis. Inhibitor (-): cells pre-treated with Z-FA-FMK (a negative control) at 20 μM; Inhibitor (+): cells pre-treated with Z-VAD-FMK (a general caspase inhibitor) at 20 μM. Data are presented as the mean ±SD (n=3). **: p<0.01; significantly different from inhibitor (-) by paired t-test.*

ability differed among these pesticides, and the orders were ziram > thiram > maneb > carbaryl with 16 h treatment and thiram > ziram > maneb > carbaryl with 24 h treatment.

To explore the mechanism of ziram and thiram-induced apoptosis, we examined the active caspase-3 in ziram- and thiram-treated NK-92CI cells and found a significant increase in the intracellular levels. Moreover, a caspase inhibitor significantly blocked the ziram- and thiram-induced apoptosis indicating the involvement of all caspases (caspase cascade) in ziram- and thiram-induced apoptosis in NK-92CI cells. We previously found that ziram significantly activated the intracellular caspases 3/7, 8, 9 and pan-caspase in a dose-dependent manner and that caspase-3 and general caspase inhibitors significantly blocked the ziram-induced apoptosis in NK-92MI cells (6), suggesting that thiram has the similar mechanism with ziram in apoptosis inducing.

Cytochrome-c initiates apoptosis through its release into the cytoplasm and binding of Apaf-1 which activates procaspase 9 (16). Goldstein (17) reported that the release of cytochrome-c from mitochondria was a very early event during apoptosis. To explore whether this release mechanism was involved in the ziram- and thiram-induced apoptosis, we determined intracellular cytochome-c levels in NK-92CI cells. Ziram and thiram produced a significantly higher proportion of cells without cytochome-c in a dose-dependent manner, indicating that it induced the release of cytochrome-c from mitochondria. These findings also suggested that cytochrome-c was involved in the apoptosis. We previously found that ziram also significantly induced the release of cytochrome-c from mitochondria in NK-92MI cells (6), suggesting that thiram has the similar mechanism with ziram in apoptosis inducing.

Taken together, the above findings suggested that ziram and thiram affects both the caspase-cascade and the mitochondria/cytochrome-c pathways.

The strength of the apoptosis-inducing ability differed among these pesticides, and the orders were ziram > thiram > maneb > carbaryl with 16 h treatment and thiram > ziram > maneb > carbaryl with 24 h treatment. Why the strength of the apoptosis-inducing ability differed among these pesticides? We speculate that the different general toxicity of these chemicals may contribute to the difference in apoptosis inducing. We compare their ability to induce apoptosis to the respective LD50. The oral LD50s in rat of carbaryl, thiram, ziram and maneb are 250 mg/kg (21), 640 mg/kg (3), 1400 mg/kg (4) and 2600-5500 mg/kg (2), respectively. Carbaryl shows the strongest acute toxicity among these chemicals; however, carbaryl shows the weakest apoptosis inducing ability among these chemicals, suggesting that the apoptosis-inducing ability of those pesticides was not related to their acute toxicity.

Whether the different solubility in water contributes to the difference in apoptosis inducing? In fact, the solubility of carbaryl, thiram, ziram and maneb in water are 120 mg/l (120 ppm) (1), 30 mg/l (30 ppm) (3), 65 mg/l (65 ppm) (4) and 20 mg/l (20 ppm) (2), respectively. The highest concentrations of carbaryl, thiram, ziram and maneb used in the present study were 40 μM (8 ppm), 1 μM (0.24 ppm),1 μM (0.312 ppm) and 5 μM (1.327 ppm), indicating that all chemicals should be dissolved in the culture medium during the in vitro culture, suggesting

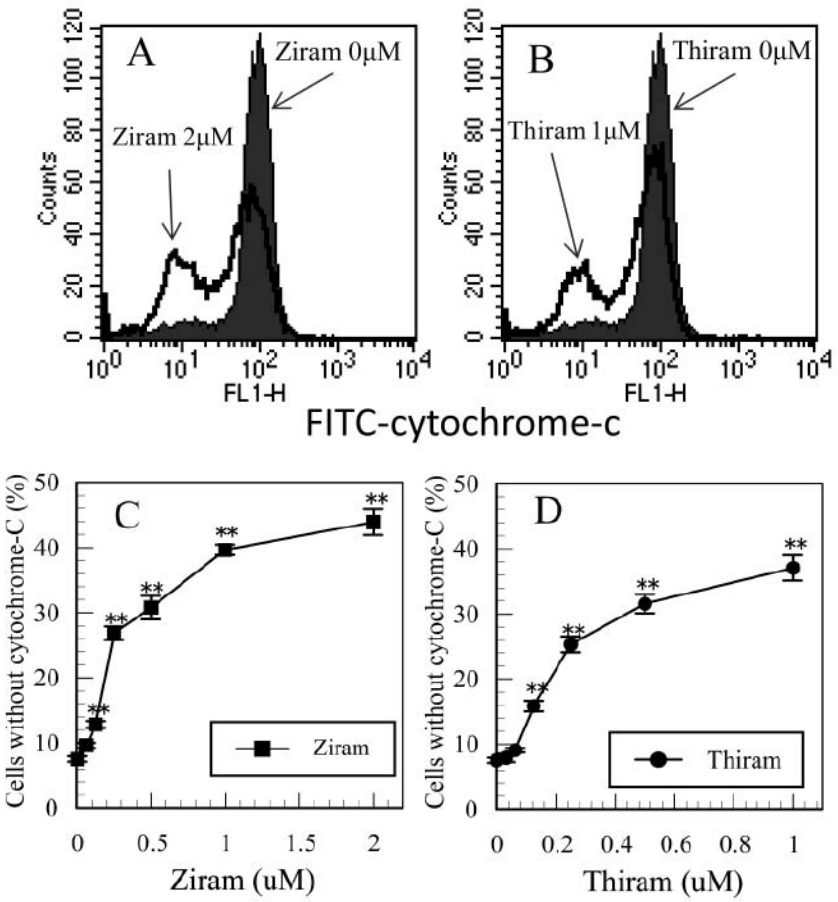

Fig. 9. *Detection of mitochondrial cytochrome-c release in apoptotic cells by flow cytometry.* ***A, B****: the shaded histograms show the control cells (ziram and thiram at 0 μM) and the open histograms show the cells treated with ziram at 2 μM (****A****) or thiram at 1 μM (B) for 16 h and stained with FITC-cytochrome-c.* ***C, D****: dose-dependent increases in the percentage of cells without cytochrome-c in ziram- (****C****) or thiram- (****D****) treated cultures. Data are presented as the mean ±SD (n=3). One-way ANOVA indicated that the concentrations of ziram and thiram significantly affected cytochrome-c release (p<0.01). **: p<0.01; significantly different from 0 μM by Tukey's test.*

that solubility in water would not contribute to the difference in apoptosis. The detailed mechanism should be explored in the future study.

Ziram was stronger than thiram in cell death with 16 h treatment; whereas thiram was stronger than ziram with 24 h treatment. There are almost the same levels at 16 and 24h in ziram-induced cell death, indicating that it has reached a peek at 16h; whereas thiram-induced cell death at 24h was significantly higher than that at 16h, suggesting that the toxic action of ziram more quick than thiram. However, the cell death induced by thiram at 24h was significantly stronger than ziram either at 16 h or 24h, indicating that ultimately thiram was stronger than ziram. Although these chemicals are rapidly metabolized within several days in animals (1-4) it is difficult to account for their metabolism in vitro because these chemicals may bind to the membrane of cells or enter the cells during the incubation.

Taken together, the present findings indicate that ziram, thiram, maneb and carbaryl can induce apoptosis in human NK-92CI cells, and the apoptosis is mediated by both the caspase-cascade and the mitochondria/cytochrome-c pathways. In addition, the strength of the apoptosis-inducing ability differed among these pesticides and the order was as follows:

thiram > ziram > maneb > carbaryl.

ACKNOWLEDGEMENTS

This work was supported by a grant from the Ministry of Education, Culture, Sports, Science and Technology of Japan. We are grateful to the staff at the Department of Hygiene and Public Health, Nippon Medical School for their assistance.

REFERENCES

1. Richardson ML. C62: Carbaryl. in: ML Richardson (Eds), The dictionary of substances and their effects, Vol. 2, The Royal Society of Chemistry, Cambridge 1993; 99-102.
2. Richardson ML. M19: Maneb. in: ML Richardson (Eds), The dictionary of substances and their effects, Vol. 5, The Royal Society of Chemistry, Cambridge 1993; 323-7.
3. Richardson ML. T130: Thiram. in: ML Richardson (Eds), The dictionary of substances and their effects, Vol. 7, The Royal Society of Chemistry, Cambridge 1993; 437-42.
4. Richardson ML. Z19: Ziram. in: ML Richardson (Eds), The dictionary of substances and their effects, Vol. 7, The Royal Society of Chemistry, Cambridge 1993; 908-11.
5. Li Q, Kobayashi M, Kawada T. Effect of ziram on natural killer, lymphokine-activated killer, and cytotoxic T lymphocyte activity. Arch Toxicol 2012; 86:475-81.
6. Li Q, Kobayashi M, Kawada T. Mechanism of ziram-induced apoptosis in human natural killer cells. Int J Immunopathol Pharmacol 2012; 25:883-91.
7. Li Q, Kobayashi M, Kawada T. Organophosphorus pesticides induce apoptosis in human NK cells. Toxicology 2007; 239:89-95.
8. Majno G, Joris I. Apoptosis, oncosis, and necrosis. An overview of cell death. Am J Pathol 1995; 146:3-15.
9. Levin S. Apoptosis, necrosis, or oncosis: what is your diagnosis? A report from the Cell Death Nomenclature Committee of the Society of Toxicologic Pathologists. Toxicol Sci 1998; 41:155-6.
10. Kerr JF, Wyllie AH, Currie AR. Apoptosis: a basic biological phenomenon with wide-ranging implications in tissue kinetics. Br J Cancer 1972; 26:239-57.
11. Nakadai A, Li Q, Kawada T. Chlorpyrifos induces apoptosis in human monocyte cell line U937. Toxicology 2006; 224:202-9.
12. Li Q, Kobayashi M, Kawada T. Ziram induces apoptosis and necrosis in human immune cells. Arch Toxicol 2011; 85:355-61.
13. Li Q, Kobayashi M, Kawada T. Mechanism of ziram-induced apoptosis in human T lymphocytes. Arch Toxicol 2012; 86:615-23.
14. Patel T, Gores GJ, Kaufmann SH. The role of proteases during apoptosis. FASEB J 1996; 10: 587-97.
15. Stennicke HR, Jürgensmeier JM, Shin H, et al. Pro-caspase-3 is a major physiologic target of caspase-8. J Biol Chem 1998; 273:27084-90.
16. Okada S, Li Q, Whitin JC, Clayberger C, Krensky AM. Intracellular mediators of granulysin-induced cell death. J Immunol 2003; 171: 2556-62.
17. Goldstein JC, Waterhouse NJ, Juin P, Evan GI, Green DR. The coordinate release of cytochrome C during apoptosis is rapid, complete and kinetically invariant. Nat Cell Biol 2000; 2: 156-62.
18. Tam YK, Maki G, Miyagawa B, Hennemann B, Tonn T, Klingemann HG. Characterization of genetically altered, interleukin 2-independent natural killer cell lines suitable for adoptive cellular immunotherapy. Hum Gene Ther 1999; 10:1359-73.
19. Stahnke K, Mohr A, Liu J, Meyer LH, Karawajew L, Debatin KM. Identification of deficient mitochondrial signaling in apoptosis resistant leukemia cells by flow cytometric analysis of intracellular cytochrome *c*, caspase-3 and apoptosis. Apoptosis 2004; 9:457-65.
20. Taylor TR, Whalen MM. Effects of ziram on tumor-cell-binding capacity, cell-surface marker expression, and ATP levels of human natural killer cells. Cell Biol Toxicol 1999; 25:447-55.
21. Vandekar M, Plestina R, Wilhelm K. Toxicity of carbamates for mammals. Bull World Health Organ 1971; 44:241-9.

THE INNATE IMMUNITY RECEPTOR TIR8/SIGIRR IS EXPRESSED IN THE EARLY DEVELOPMENTAL STAGES OF CHICKEN EMBRYOS

L. TURIN, G. MANAROLLA, T. RAMPIN and F. RIVA

Department of Veterinary Science and Public Health (DIVET), University of Milan, Milan, Italy

Received February 6, 2012 – Accepted February 6, 2014

The orphan receptor TIR8, also known as SIGIRR (Single Immunoglobulin IL-1R-Related molecule), belongs to the IL-1R/TLR (TIR) superfamily and plays an important role in the inflammatory responses. The signaling pathways of the receptors belonging to the TIR family are tightly regulated by both extracellular and intracellular mechanisms. TIR8 does not activate the transcription factors NFkB (nuclear factor kB) and IRF3 (interferon regulatory factor 3), although it negatively modulates the inflammatory responses. It acts as an antagonist for the IL-1 receptor family and triggers a negative pathway of the Toll-like/IL-1 receptor system, crucial for dampening inflammation stimuli in the gastrointestinal (GI) tract and in other organs (e.g. lung and kidney). The recent findings of TLRs expression in ovary and embryos of different species (mammals and chickens) are very important for an understanding of reproductive physiology and transovarian pathogen transmission. TIR8 was well characterized in mouse, humans and in other mammalian species, but it is still poorly characterized in the chicken. When *TIR8* expression was measured in selected organs of chicken embryos of both broiler and layer types at different time points a unique pattern of expression was observed. Interestingly, TIR8 was detected during the first stages of chicken development (day 1 of incubation), and reached a remarkable level of expression by day 10. We observed this receptor to be ubiquitously expressed in the kidney, GI tract, Bursa of Fabricius, with the highest expression levels in liver and kidney. This pattern was comparable to those observed in post-hatching chickens and in mammals examined to date. No expression differences were observed between the two different chicken breeds (layer- and broiler-type) in the first incubation period (8 days). Whereas in some organs starting from day 10, higher TIR8 expression was observed in broiler-type compared to layer-type. These are the first findings concerning *TIR8* expression in developmental stages and therefore they are of comparative value.

The orphan receptor TIR8 (Toll-like/interleukin-1 receptor-8), also known as SIGIRR (Single Immunoglobulin IL-1R-Related molecule), belongs to the TIR super-family (Toll-like/interleukin-1 receptors). Innate mechanisms of first-line defense against pathogens involve different members of the TIR superfamily, which includes Toll-like receptors (TLRs), IL-1Rs and adapter molecules, all sharing the intracellular TIR domain (1-3). TLR molecules are pattern recognition receptors, which sense specific microbial components (pathogen-associated molecular patterns, PAMPs) and activate signaling pathways leading to develop both innate and adaptive immune responses (4-5). The IL-1R subgroup includes receptors and accessory proteins involved in the inflammatory process (2, 3, 5).

Key words: Chicken, embryo, gene expression, IL-1 receptors, TIR8/SIGIRR, Toll-like receptors

Mailing address:
Prof. Lauretta Turin
via Celoria 10,
20133 Milan, Italy
Tel.: +39 02 50318090
Fax: +39 02 50318089
e-mail: lauretta.turin@unimi.it

0393-974X (2014)

Upon stimulation by their ligands, TLRs and IL-1Rs interact with specific adaptor proteins and initiate a signaling pathway leading to the synthesis of proinflammatory cytokines and chemokines. The signaling complexes also trigger a cascade of cell kinases, which finally activate transcription factors NFkB and IRF3 (6).

Signaling pathways of IL-1R/TLRs molecules are very complex and tightly regulated to ensure the appropriate modulation of the innate and inflammatory responses and limit deregulated activation that could cause severe local or systemic inflammation or autoimmunity (5, 7).

TIR8 acts as an intracellular inhibitor of IL-1R/TLRs signaling; it does not activate NFkB (nuclear factor kB) and IRF3 (interferon regulatory factor 3), therefore it behaves as an intracellular decoy for key components of the inflammatory pathways in the epithelial tissues and at mucosal sites, where it is highly expressed (8-11). Its regulatory activity is crucial for inhibiting immune response and controlling chronic inflammatory diseases due to Th1 cytokine toxicity (12-13). TIR8 is expressed ubiquitously, with the highest levels observed in the kidney and in the gastrointestinal (GI) tract (14). Many findings support TIR8 role in dampening excessive inflammatory responses: it is moderately downregulated upon LPS stimulation in various mouse tissues; TIR8-deficient mice were more susceptible to intestinal inflammation and to colitis-associated cancer in models of chronic colitis and colon carcinogenesis; finally, TIR8-knock-out mice were more susceptible to *Mycobacterium tuberculosis* infection than WT mice (2, 14-16).

Birds immune system is quite similar to the mammalian one in terms of overall organization and mechanisms of immunity. Bird TLR repertoire consists of 10 genes, most of which have orthologues in mammalian genomes, whereas three elements are unique to birds (17). Moreover, in chicken is present only IL-1R type I, whereas mammals show both IL-1Rs type I and II. Little is known about the other members of the TIR family.

TIR8 investigation has been mainly done in mouse and human models (2-3, 9, 11, 13, 14-15), and, more recently, also in other species (18-19). However, there is no information regarding embryonic expression of TIR8 in any species.

Chicken embryo has a long and distinguished history as a major model system for developmental studies in different fields, including genetic and immunology (20).

Chicken is a very powerful and advantageous experimental system available for investigations. Its eggs are a common and accessible source of embryos, which can be observed at different stages of incubation for progressive studies. The attractiveness of this animal model for gene expression studies is due to the availability of embryonated eggs and the absence of any technical and ethical limitation in the use of chicken embryos. Moreover chickens have been selected genetically either for improved feed conversion and rapid growth (broilers) or for production of eggs (egg-type). This selection for economically important production traits has led to two physiologically and phenotypically different types of chickens, which differ in body weight gain, productive lifespan and immunological responses (21). Meat-type chickens usually display a lower antibody and T-cell mediated immune response when compared under the same conditions to layer-type strains (22). Moreover, the first ones require higher doses of stimuli to develop immune responses comparable to the second ones (23).

Due to the importance of TIR8 molecule in innate immunity and in inflammation, its high level of evolutionary conservation and the lack of data on TIR8 expression during embryo development, we focused our study on the investigation of this receptor during incubation till hatching. TIR8 expression was examined both at the transcriptional level (mRNA) by mean of quantitative RT-Real-Time PCR and at the protein level by Western Blot and immunohistochemistry. Organs from two different chicken breeds (meat-type and egg-type) were compared at different time points. This is the first study on TIR8 receptor expression in embryos.

MATERIALS AND METHODS

Samples

Commercial embryonated eggs from broiler and layer breeders were incubated in laboratory incubators under standard conditions. The eggs were candled daily during incubation to check embryo development. At different time points embryo organs were collected as detailed in Table I.

The embryos were obtained at the beginning of the incubation (T1) (germinal disk), at 6 days (T2) the embryos (except the cephalic region) were taken from 5 eggs and at 8 days (T3) from 3 eggs. For the subsequent time points an average of 0.3 cm^3 pieces were collected from an adequate number of embryonated eggs. At day 10 of incubation (T4) kidney, liver, intestine, proventriculus and gizzard of the embryos were obtained and for the subsequent time points T5, T6, T7 and T8 (12, 14, 16 and 20 days of incubation respectively) kidney, liver, intestine, proventriculus and gizzard and Bursa of Fabricius were separately sampled.

The samples were immediately placed in sterile tubes containing 1.5 ml of RNA Later (Qiagen, Hilden, Germany) and stored at 4°C for 24 h.

The same organs from 4 extra eggs at day 14 (T6) of incubation were used for Western Blot analysis.

The experimental protocol was ethically approved by the Ethics Committee of the University of Milan (Protocol Number 121521500524).

RNA extraction

Total RNA was isolated from the samples by the guanidine isothiocyanate (4M) method with minor modifications. Briefly, the samples were homogenized in 1.5 ml of guanidine isothiocyanate using a rotor-stator system (Ultra Turrax T25 Ika-Werke, Staufen, Germany). The lysate was centrifuged overnight at 42,000 rpm at 18°C on a 5.7M cesium chloride layer (Optima TL ultracentrifuge, Beckman Instruments, Inc. Palo Alto, CA, USA). The pellet was dissolved in sterile water and the RNA was precipitated with absolute ethanol and sodium acetate 3M pH 5.4 in dry ice for 2 h. After centrifugation in a microcentrifuge (Eppendorf, Hamburg, Germany) at maximum speed for 30 min, the RNA pellet was dissolved in sterile water and stored at -20°C.

RNA determination and Reverse Transcription

The concentration of RNA was determined using a spectrophotometer (BioPhotometer, Eppendorf, Hamburg, Germany) at 260 nm wavelength. About 1 µg of total RNA from each sample was reverse transcribed to cDNA using the High Capacity cDNA Archive kit with random hexamers (Applied Biosystem, Foster City, CA, USA) and the resulting cDNA was stored at -20°C before Real-Time PCR assays.

Real-time PCR

The cDNA obtained from each sample was used as a template for Real-Time PCR in optimized 25 µl reaction volume in MicroAmp optical 96-well plates. Each plate contained duplicates of each cDNA sample diluted 1:100 (9 ml), 2X Power Syber Green PCR Master Mix (12.5 µl) (Applied Biosystem, Foster City, CA, USA) and primers 300 nM each (0.3 µl of 10 µM solution). The species-specific primer pairs were designed using as target the chicken sequence homologous to human and mouse *TIR8* available in the NCBI nucleotide sequences database (gi:118091084). Primers were custom synthesized by Invitrogen (Carlsbad, CA, USA); their sequences are listed in Table II.

To correct for variations of extracted mRNA amounts and cDNA synthesis efficacy in quantitative Real-Time PCR assays, primers for the detection of the chicken housekeeping gene beta-actin were designed as well by Primer Express on the sequence accession number gi:45382926 (NCBI). Their sequences also are listed in Table II.

In addition to the cDNA samples, duplicates of 10-fold serial dilutions of chicken kidney cDNA were used as templates to generate standard curves for estimation of the expression of the two genes. A duplicate no-template control (NTC) was also included in each plate.

Real-time quantitative PCR was carried out in the 7000 Sequence Detection System (Applied Biosystem, Foster City, CA, USA) at the following thermal cycle conditions, 10 min at 95°C followed by 40 cycles of 15 s at 95°C and 1 min at 60°C. Quantification was determined after application of an algorithm to the data analyzed by the software of the 7000 Detection System (Applied Biosystem, Foster City, CA, USA).

For each sample tested the expression level was calculated following the results of the calibrator of the same run. The chicken *TIR8* expression was normalized using the calculated beta-actin cDNA expression (mean) of the same sample and run.

Software

We used the free software BLAST available on PubMed web site. Primer Express software (Applied Biosystem, Foster City, CA, USA) was used for the specific primer design.

Protein extraction and Western Blot analysis

Samples of kidney, liver, proventriculus and gizzard, intestine and bursa of Fabricius were collected from 4 layer type chicken embryos at day 14 of incubation and immediately processed for the extraction of proteins. Each organ was mechanically homogenized in 1 ml of cold lysis buffer (50 mM Tris-HCl pH 7.6, 150 mM NaCl, 1% (v/v) NP40, 2% (v/v) TritonX100, 1% (w/v) Zwitterion, 1 mM EDTA) added with protease inhibitors cocktail and phenylmethanesulfonyl fluoride (Sigma-Aldrich, St. Louis, MO, USA) and incubated for 30 min on ice. After centrifugation for 10 min at 13,000 x g at 4°C, the supernatant was collected and protein

concentration was determined spectrophotometrically using the Bradford micromethod (BioRad Protein Assay, BioRad Laboratories, GmbH, Munich, Germany).

Aliquots of lysated organs, corresponding to 40 µg of total protein were loaded on 10% SDS-PAGE and Western blotted on nitrocellulose membrane. Immunodetection was carried out using a polyclonal goat anti-hSIGIRR Antibody (R&D Systems, Minneapolis, MN, USA) as the primary antibody at a concentration of 0.1 mg/ml (1:500 dilution from stock solution), overnight at 4°C. An HRP-conjugated anti-goat secondary antibody (Sigma-Aldrich, St. Louis, MO, USA) was used (1:2000 dilution, 1 h at room temperature). Positive bands were detected using chemiluminescent HRP substrate (Millipore, Molsheim, France).

Immunohistochemistry

Tissue samples (gizzard and proventriculus, kidneys, intestine, bursa of Fabricius) from a selection of 18-day embryos of the two breeds were fixed in 10% buffered formalin and routinely processed for histology. Four µm thick paraffin-wax sections were stained for demonstration of SIGIRR receptor using Avidin-Biotin-peroxidase Complex (ABC) immunohistochemistry (24). Additional sections were included as negative control. Briefly, after the quenching of endogenous peroxidase activity with 0.3% hydrogen peroxide in Phosphate Buffered Saline (PBS) pH 7.4 for 30 min, antigen retrieval was performed using microwave treatment at 750 W for 15 min (three cycles, 5 min each) in 10 mM citrate buffer (pH 6.0). After rinsing with PBS, 10% normal horse serum was applied for 30 min to block non-specific antibody binding. Subsequently, sections were incubated overnight at 4°C with the primary antibody (polyclonal goat anti-hSIGIRR Antibody, R&D Systems, Minneapolis, MN, USA) diluted 1:100. Biotinylated horse anti-goat antibody (Vector Laboratories Inc., Burlingame, California) was used as secondary antibody, followed by ABC Vectastain Elite kit (Vector Laboratories Inc., Burlingame, California). Peroxidase activity was revealed with 3-amino-9-ethylcarbazole (Vector Laboratories Inc., Burlingame, California).

Statistical analysis

Students' *t*-test was used to compare the expression level of TIR8 in the two chicken breed types at each time point. A P value <0.05 was considered statistically significant.

RESULTS

TIR8 mRNA expression analysis by Real-Time PCR

TIR8 expression was analyzed by mean of quantitative Real-Time PCR assays in meat-type and egg-type embryo samples at different time points of incubation. The panel of embryo organs tested for both chicken types is listed in Table I. Only at T4 (day 10 of incubation) and later it was possible to take biopsies from different organs in both the chicken types.

The complete mRNA sequence of chicken *TIR8* (gi:118091084) was selected to design specific primers spanning two adjacent exons. The primer pair with the highest score localized in the middle of the sequence was used in Real-Time PCR assays to amplify the cDNA from each sample (Table II).

All the sampled organs resulted positive to the presence of *TIR8* transcript, with different levels of expression. The results of Real-Time PCR quantification, expressed as ratio between each specimen and the adult kidney, which was chosen as experimental calibrator, are summarized in Fig. 1. In all the assays, the kidney cDNA from adult chicken was used as positive control besides calibrator.

The expression pattern of TIR8 in meat-type chicken embryos was similar qualitatively (for the type of organ) but different quantitatively (for the level of expression) to that found in egg-type layers chickens. Indeed, we observed a significant higher expression in the meat-type chicken organs compared to the layer-type ones.

Very low levels of expression were displayed until day 10 of incubation, corresponding to T4.

Liver and kidney were the organs showing the highest levels of TIR8 messenger RNA along all the embryonic development; intestine displayed a moderate level of the receptor transcript; stomachs and Bursa of Fabricius were also found positive, but expressed TIR8 at very low levels.

Interestingly, all the tested organs showed a progressive increase in TIR8 expression during the embryo growth, whereas, Bursa of Fabricius, after an initial increase from day 12 to day 14, maintained constant low expression levels of messenger RNA up to hatching.

TIR8 protein expression analysis by Western Blot

The expression of TIR8 protein in different layer-type chicken embryo organs collected at day 14 of incubation as well as the presence of possible organ-specific isoforms, was assessed by Western Blot.

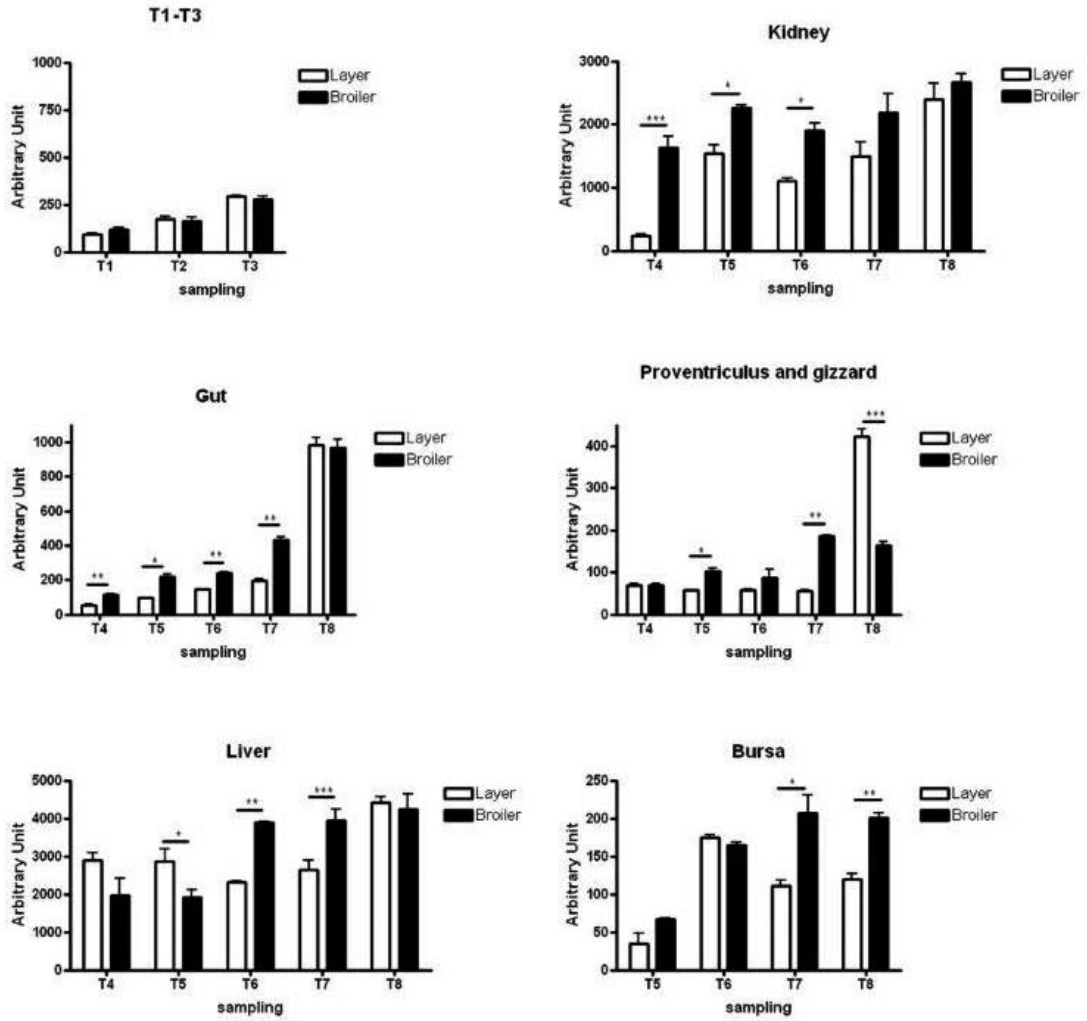

Fig. 1. *Summary of the quantitative Real-Time PCR analysis results of TIR8 mRNA expression in chicken embryo organs. The TIR8 expression level of each sample is quantified as folds of the expression of the same gene in the adult chicken kidney (calibrator) and reported as arbitrary units (folds of calibrator multiplied by 10000). Data were normalized to beta-actin expression in all the organs (multiple samples, repeatedly assayed samples and replicates were averaged). Stars indicate statistical significance between the two breeds (P value <0.05).*

A polyclonal goat anti-human TIR8 was used as primary antibody, after preliminary validation on chicken samples.

Results from Western Blot analysis presented in Fig. 2, showed TIR8 protein in all the organs examined.

A TIR8 form of about 45 kDa was observed in all the examined samples, very faint in Bursa of Fabricius. Some TIR8 bands, corresponding to different molecular weight, were also detected in some organs, such as kidney and liver. In these organs, the anti-human TIR8 antibody reacted with two proteins showing MW ranging from 20 to 30 kDa. Just the lowest molecular weight band of these two was detectable in the intestine and stomachs. In the liver the low molecular weight fraction (at about 25 kDa) appeared to be the major TIR8 component. Furthermore, Western Blot analysis also revealed specific heavier bands ranging from 75 to 100 kDa, which correspond to the expected molecular weight of the protein. TIR8 expression in Bursa of Fabricius went barely detectable by anti-TIR8 antibody.

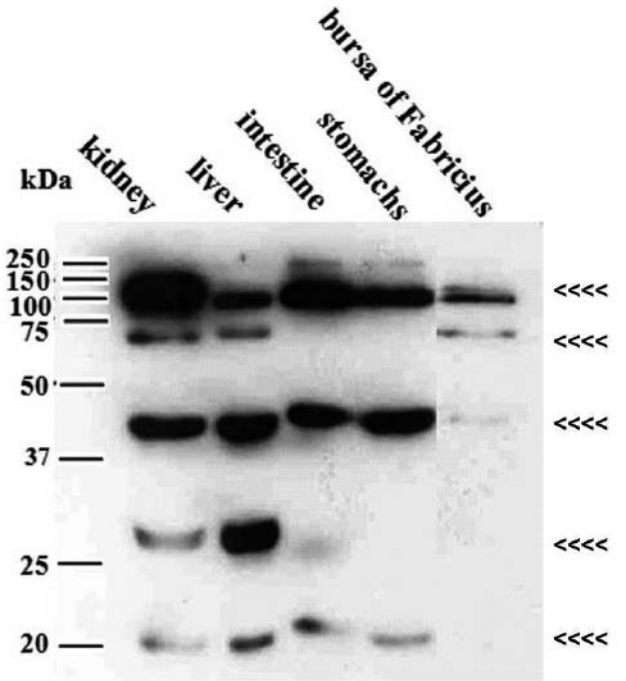

Fig. 2. *Western Blot analysis of TIR8 protein expression in different organs of chicken embryo. Homogenates of 40 μg of total protein extracted from each sample were loaded. Target protein was detected on the blots by staining with polyclonal goat anti-human SIGIRR antibody. A pool of 4 layer type embryos at day 14 of incubation (T6) was tested. Arrows indicate TIR8 specific bands.*

Table I. *Chicken embryo samples tested at different time points for both layer- and broiler-type.*

Time point days of incubation	**Samples**
T1 (germinal disk)	embryo
T2 (6 days)	embryo except cephalic region
T3 (8 days)	embryo except cephalic region
T4 (10 days)	kidney, liver, intestine, proventriculus and gizzard
T5 (12 days)	kidney, liver, intestine, proventriculus and gizzard, Bursa of Fabricius
T6 (14 days)	kidney, liver, intestine, proventriculus and gizzard, Bursa of Fabricius
T7 (16 days)	kidney, liver, intestine, proventriculus and gizzard, Bursa of Fabricius
T8 (20 days)	kidney, liver, intestine, proventriculus and gizzard, Bursa of Fabricius

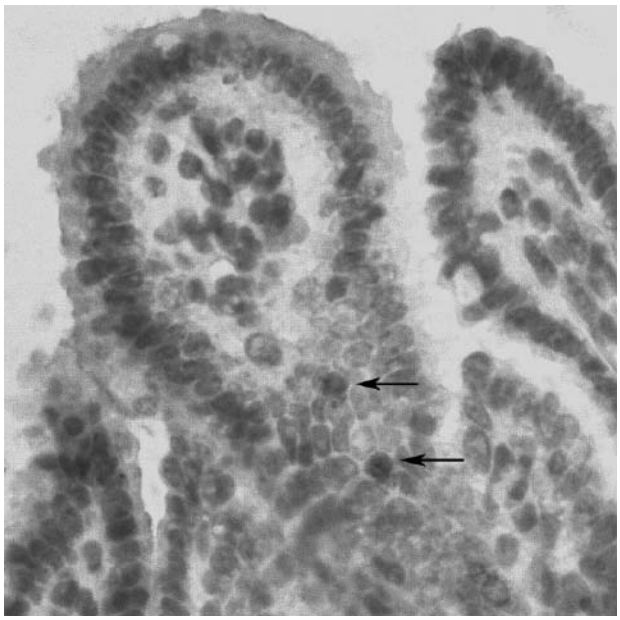

Fig. 3. *Section of intestine of 18-day old egg type embryo. Cytoplasm positive immunolabeling of TIR8 protein in few cells of intestinal villi. Anti-SIGRR immunohistochemistry, Mayer's Haematoxylin counterstain (arrows).*

Table II. *The following primer pairs were designed and used to quantify TIR8 expression in Real-Time PCR assays.*

Target gene	**Primers**
Chicken TIR8	5'-ACATTCCTGTCCGCAGTACCAG-3' (forward)
	5'-TCCCAGTGTTTGTCCAGTAGGC-3' (reverse)
Chicken □-actin	5'-CCCACCTGAGCGCAAGTACT-3' (forward)
	5'-GAGGCCAGGATAGAGCCTCC-3' (reverse)

Immunohistochemistry

The expression of TIR8 protein was assayed by immunohistochemistry with the same polyclonal anti-human TIR8 antibody used for Western Blot and validated for cross-reactivity with the chicken receptor.

Variably intense cytoplasm immunolabeling was observed only in scattered cells of the intestinal mucosa of the embryos of the two breeds (Fig. 3). The samples of kidney, liver, bursa of Fabricius, proventriculus and gizzard, and the negative controls showed no immunopositivity for TIR8 protein.

DISCUSSION

TIR8 mRNA was detected and quantified by Real-Time PCR in chicken embryos of two breeds (meat-type and egg-type) at 7 different developmental stages. In parallel, for practical reasons, TIR8 protein was identified by both Western Blot analysis and Immunohistochemistry at a single developmental time point. Interestingly, TIR8 mRNA was detected, at low levels, in very early embryos (T1), when the fertilized egg is at the blastodermal stage, characterized by thousands of undifferentiated cells forming the germinal disc (25). The levels of TIR8 mRNA increase at remarkable levels in most selected organs after day 10 of incubation (T4) (Fig. 1).

Remarkably, the highest expression of TIR8 was observed in liver and in kidney of chicken embryo; mRNA was also detected in the intestine, stomachs and Bursa of Fabricius, at lower levels. Embryonic TIR8 expression resembles the pattern observed in growing and adult chickens (18; data in publication). It is conceivable that the high level of expression in embryo liver and kidney could be typical of birds, as the result of a specific evolutionary pressure, due to the environment and the pathogens. Indeed, the rudimental lymphatic system of birds (lack of lymph nodes) and the presence of a renal portal system could account for the high TIR8 expression in avian liver and kidney.

TLRs signalling in embryos is tightly regulated as well as in post-hatching life (26-29). The well established increasing expression of TLRs during chicken embryo development could take part in a protection mechanism of embryos and newly hatched birds from pathogens, where TIR8 increases accordingly to the embryo development (28).

It is well known that chicken ovary is a preferential site of microbial infection (for example due to *Salmonella enteritidis*) that can be subsequently transmitted to the eggs and embryos (30). Different levels of TIR8 in different organs could suggest a complex regulatory mechanism for the receptor expression in response to microbial infections, particularly depending on their duration.

Since the embryo develops in a protected environment with few external stimulations of the immune system, the role of TIR8 in this context may be marginal or different than immune regulator. Indeed, recent studies showed the expression of TLRs in ovary during maturation and in embryos during development (28), suggesting a new role for TLRs both in fertility and in protection of reproductive organs, possibly as a further way to protect newly forming eggs from microbial infection.

In contrast with the results of the other tested organs, TIR8 mRNA expression in Bursa of Fabricius remains low during the embryo development.

In conclusion, an ubiquitous expression of TIR8 was demonstrated in embryos of both meat-type and layer-type chickens at both transcriptional (mRNA) and translational (protein) levels. The meat-type breeds are known to have a lower degree of immunocompetence compared to the egg-type breeds; indeed we observed a trend of higher TIR8 levels in the organs of meat-type chicken, that could partially reduce the immune response in the breed. Such higher expression of TIR8 in broiler chicken could be the result of selection and its biological significance could be irrelevant in egg incubation conditions highly controlled, but it could be a model for other species, such as wild birds, dairy cows, beef cattle, dog breeds.

Our findings document for the first time that TIR8 expression also occurs during the embryonic stages of chicken development and supports the aim at performing similar studies in other species embryos.

ACKNOWLEDGEMENTS

We wish to thank Dr. Silvia Russo for English editing. This work was supported by the FIRST and PUR Grants from the Italian Ministry of Education, Scientific Research and Health, Italy.

REFERENCES

1. Gangloff M, Weber ANR, Gibbard RJ, Gay NJ. Evolutionary relationships, but functional differences, between the *Drosophila* and human Toll-like receptor families. Biochem Soc Trans 2003; 31:659-63.
2. Mantovani A, Locati M, Polentarutti N, Vecchi A, Garlanda C. Extracellular and intracellular decoys in the tuning of inflammatory cytokines and Toll-like receptors: the new entry TIR8/SIGIRR. J Leukoc Biol 2004; 75:738-42.
3. Thomassen E, Renshaw BR, Sims JE. Identification

and characterization of SIGIRR, a molecule representing a novel subtype of the IL-1R superfamily. Cytokine 1999; 11:389-99.
4. Kaisho T, Akira S. Toll-like receptor function and signalling. J Allergy Clin Immunol 2006; 117:979-87.
5. O'Neill LA, Dinarello CA. The IL-1 receptor/toll-like receptor superfamily: crucial receptors for inflammation and host defense. Immunol Today 2000; 21:206-9.
6. Takeda K, Akira S. TLR signalling pathways. Semin Immunol 2004; 16:3-9.
7. Henson PM. Dampening inflammation. Nat Immunol 2005; 6:1179-81.
8. O'Neill LA. SIGIRR puts the brakes on Toll-like receptors. Nat Immunol 2003; 4:823-4.
9. Polentarutti N, Rol GP, Muzio M, et al. Unique pattern of expression and inhibition of IL-1 signaling by the IL-1 receptor family member TIR8/SIGIRR. Eur Cytokine Net 2003; 14:211-8.
10. Qin J, Qian Y, Yao J, Grace C, Li X. SIGIRR inhibits interleukin-1 receptor- and toll-like receptor 4-mediated signaling through different mechanisms. J Biol Chem 2005; 280:25233-41.
11. Wald D, Qin J, Zhao Z, et al. SIGIRR, a negative regulator of Toll-like receptor-interleukin 1 receptor signalling. Nat Immunol 2003; 4:920-7.
12. Huang X, Hazlett LD, Du W, Barrett RP. SIGIRR promotes resistance against Pseudomonas aeruginosa keratitis by down-regulating type-1 immunity and IL-1R1 and TLR4 signaling. J Immunol 2006; 177:548-56.
13. Lech M, Kulkarni OP, Pfeiffer S, Savarese E, Krug A, Garlanda C, Mantovani A, Anders HJ. Tir8/Sigirr prevents murine lupus by suppressing the immunostimulatory effects of lupus autoantigens. J Exp Med 2008; 205:1879-88.
14. Garlanda C, Riva F, Polentarutti N, et al. Intestinal inflammation in mice deficient in Tir8, an inhibitory member of the IL-1 receptor family. Proc Natl Acad Sci USA 2004; 101:3522-6.
15. Garlanda C, Di Liberto D, Vecchi A, et al. Damping excessive inflammation and tissue damage in Mycobacterium tuberculosis infection by Toll IL-1 receptor 8/single Ig IL-1-related receptor, a negative regulator of IL-1/TLR signaling. J Immunol 2007; 179:3119-25.
16. Xiao H, Gulen MF, Qin J, et al. The Toll–Interleukin-1 receptor member SIGIRR regulates colonic epithelial homeostasis, inflammation, and tumorigenesis. Immunity 2007; 26:461-75.
17. Temperley ND, Berlin S, Paton IR, Griffin DK, Burt DW. Evolution of the chicken Toll-like receptor gene family: a story of gene gain and gene loss. BMC Genomics 2008; 9:62.
18. Riva F, Polentarutti N, Tribbioli G, Mantovani A, Garlanda C, Turin L. The expression pattern of TIR8 is conserved among vertebrates. Vet Immunol Immunopathol 2009; 131:44-9.
19. Riva F, Rahman MM, Turin L, Ceciliani F, Russo S, Tribbioli G, Lecchi C. TIR8 receptor expression in bovine tissues. Vet Immunol Immunopathol 2010; 136:65-70.
20. Stern CD. The chick: a great model system becomes even greater. Dev Cell 2005; 8:9-17.
21. Praharaj NK, Dunnington EA, Siegel PB. Growth, immunoresponsiveness, and disease resistance of diverse stocks of chickens reared under two nutritional regimens. Poultry Sci 1995; 74:1721-9.
22. Koenen ME, Boonstra-Blom A, Jeurissen SHM. Immunological differences between layer- and broiler-type chickens. Vet Immunol Immunopathol 2002; 89:47-56.
23. Koenen ME, Kramer J, van der Hulst R, Heres L, Jeurissen SHM, Boersma WJA. Immunomodulation by probiotic lactobacilli in layer- and meat-type chickens. British Poultry Sci 2004; 45:355-66.
24. Hsu SM, Raine L, Fanger H. Use of avidin-biotin peroxidase complex (ABC) in immunoperoxidase techniques: a comparison between ABC and unlabeled antibody (PAP) procedures. J Hictochem Cytochem 1981; 29:577-80.
25. Eyal-Giladi H, Fabian BC. Axis determination in uterine chick blastodiscs under changing spatial positions during the sensitive period for polarity. Dev Biol 1980; 77:228-32.
26. Belderbos ME, van Bleek GM, Levy O, Blanken MO, Houben ML, Schuijff L, Kimpen JLL, Bont L. Skewed pattern of Toll-like receptor 4-mediated cytokine production in human neonatal blood: low LPS-induced IL-12p70 and high IL-10 persist throughout the first month of life. Clin Immunol 2009; 133:228-37.

27. Merkerova M, Vasikova A, Bruchova H, Libalova H, Topinka J, Balascak I, Sram RJ, Brdicka R. Differential gene expression in umbilical cord blood and maternal peripheral blood. Eur J Haematol 2009; 83:183-90.
28. Michailidis G, Theodoridis A, Avdi M. Transcriptional profiling of Toll-like receptors in chicken embryos and the ovary during sexual maturation and in response to Salmonella enteritidis infection. Anim Reprod Sci 2010; 122:294-302.
29. Yuan S, Huang S, Zhang W, et al. An amphioxus TLR with dynamic embryonic expression pattern responses to pathogens and activates NF-kB pathway via MyD88. Mol Immunol 2009; 46:2348-56.
30. Barua A, Yoshimura Y. Ovarian cell-mediated immune responde to Salmonella enteritidis infection in laying hens (gallus domesticus). Poult Sci 2004; 83:997-1002.

TOLL-LIKE RECEPTOR 4 PROMOTES CONTROL OF *LEISHMANIA INFANTUM* INFECTION THROUGH INDUCEMENT OF LEISHMANICIDAL ACTIVITY IN HOST MACROPHAGES: ROLE OF MITOGEN-ACTIVATED KINASES

M. AGALLOU[1], E. DOTSIKA[1], S. FRYDAS[2] and E. KARAGOUNI[1,]

[1]Laboratory of Cellular Immunology, Department of Microbiology, Hellenic Pasteur Institute, Athens, Greece; [2]Laboratory of Parasitology and Parasitic Diseases, School of Veterinary Medicine, Aristotle University of Thessaloniki, Thessaloniki, Greece

Received May 29, 2013 – Accepted February 17, 2014

Establishment of *Leishmania* infection inside macrophages requires deactivation of various signaling pathways that are dispensable for effective immune responses against the parasite. In the present study, we provide evidence that *Leishmania infantum* promastigotes attachment on the surface of peritoneal macrophages, internalization and transformation to amastigotes abrogated the activation of extracellular signal-regulated protein kinases (ERK) 1/2, p38 mitogen activated protein kinases (MAPK) and c-Jun NH_2-terminal kinases (JNK) and the production of pro-inflammatory cytokines IL-12 and TNFα. Subsequent macrophage stimulation with lipopolysaccharide (LPS) during the first hours of exposure to parasite or infection resulted in restoration of MAPK phosphorylation. However, LPS-mediated MAPK activation required parasite internalization (uptake) since cytochalasin-D pretreated macrophages did not responded to LPS stimulation. IL-12, TNFα, and NO production was positively regulated with MAPK phosphorylation in contrast to nuclear factor-kappaB (NF-κB) which was MAPK independent. Specifically, inhibition of MAPK activation with specific inhibitors revealed that IL-12 production required p38 MAPK activation, whereas TNFα and NO production required all three MAPK. The restoration of NO production resulted in decrease of infection rates. Hence, these results suggest that in contrast to phagocytosis of *L. infantum* promastigotes, establishment of infection does not desensitize macrophages to subsequent stimulation with LPS, resulting in parasite elimination through MAPK and NF-κB activation and partial restoration of IL-12, TNFα and NO synthesis.

Leishmaniasis comprises a group of diseases caused by protozoan parasites of the *Leishmania* genus and characterized by different clinical manifestations, which are dependent mainly on the infecting species. *Leishmania spp*. develop as flagellated motile promastigotes in the gut of blood-sucking female sand flies and as obligate intracellular non-motile amastigotes in the phagolysosomes of macrophages and dendritic cell lineage of the vertebrate hosts. Parasite persistence within host cell is determined by a balance between the ability of the immune response to activate infected macrophages versus the ability of the parasite to resist cytotoxic mechanisms of macrophage activation. Many studies have demonstrated that protective immunity against leishmaniasis is dependent on the induction of IL-12-driven $CD4^+$ Th1 response and IFN-γ production. Furthermore, IFN-γ-induced upregulation of

Key words: Leishmania, macrophage, MAPK, IL-12, TNFα, NO, LPS

Mailing address: Dr E. Karagouni,
Laboratory of Cellular Immunology,
Department of Microbiology,
Hellenic Pasteur Institute, 127 Vasilissis Sofias Ave.
115 21, Athens, Greece
Tel.: +30 210 6478826 Fax: +30 210 6423498
e-mail: ekaragouni@pasteur.gr

0393-974X (2014)

inducible nitric oxide synthase (iNOS) and subsequent nitric oxide (NO) production is important for leishmanicidal activity of macrophages, which is further enhanced by other cytokines, such as TNFα (1).

Until now, little is known about the mechanisms resulting in non-healing disease since the disparate survival phenotype of *Leishmania* parasite within genetically identical hosts may involve more than differences in the host T-cell response alone. Inhibition of macrophage activation is a consequent effect of specific targeting of host intracellular signaling pathways by parasite during infection. *Leishmania* impairs protein kinase C (PKC), mitogen activated protein kinases (MAPK) and nuclear factor-kappaB (NF-κB) activity resulting in inhibition of respiratory burst and suppression of other pro-inflammatory molecules (2). These signaling pathways may regulate the production of various effectors molecules such as cytokines and chemokines which will drive the activation of effectors mechanisms that could efficiently control the invading pathogen (3).

Recent reports have implicated Toll-like receptor 4 (TLR4) in the activation of immune response towards *Leishmania*. TLR4 contributes to the effective control of *L. major* and *L. donovani* infection by inducing the microbicidal activity of macrophages characterized by elevated TNFα and NO production in *in vivo* infections (4, 5, 6, 7). Gram-negative lipopolysaccharide (LPS), a ligand of TLR4, is a potent macrophage stimulus of the three major MAPK (extracellular regulated-kinase (ERK), p38 MAPK and c-Jun N-terminal kinase (JNK)) and leads to the production of pro-inflammatory cytokines, such as IL-12 and TNFα (8).

Considering these data in the present study, we explored the implication of *L. infantum*, the aetiological agent of zoonotic VL, on TLR4 pathway by stimulating peritoneal macrophages exposed to and infected with *L. infantum* promastigotes with LPS and analyzing MAPK and NF-κB activation and IL-12, TNFα and NO secretion.

MATERIALS AND METHODS

Antibodies

Affinity purified rabbit polyclonal antibodies, elicited against synthetic phospho-peptides corresponding to residues around Thr202/Tyr204 of human p44 MAP kinase (Cell Signaling, Cat. No. 9101), Thr180/Tyr182 of human p38 MAP kinase (Cell Signaling, Cat. No. 9211) and Thr183/Tyr185 of human SAPK/JNK (Cell Signaling, Cat. No. 9251), were used for the immunoblotting of phosphorylated forms of mouse ERK1/2, p38 and JNK MAPK, respectively. Total ERK1/2, p38 and JNK were detected with rabbit polyclonal antibodies obtained from Santa Cruz (Cat. No. sc-94) or Cell Signaling (Cat. No. 9212 and 9252), respectively. IκBα protein was also probed with rabbit polyclonal antibodies (Cell Signaling, Cat. No. 9242).

Animals

Female BALB/c mice (18-22 g), obtained from the breeding unit of the Department of Experimental Animal Models for Biomedical Research of the Hellenic Pasteur Institute (HPI; Athens, Greece), were used for the macrophage isolation as well as for the maintenance of parasite virulence. All experiments were carried out with prior approval by the Animal Bioethics Committee of the HPI regulating according to EC Directive 1986/609 and the National Law 1992/2015.

Leishmania cultivation - Preparation of soluble Leishmania antigen

L. infantum (MON-1, MCAN/PT/98/IMT 244 strain) was grown at 26°C in RPMI-1640 medium (Biochrom AG, Berlin, Germany) supplemented with 2 mM L-glutamine, 10 mM HEPES, 24 mM $NaHCO_3$, 0.05 mM β-mercaptoethanol, 100 U/ml penicillin, 100 μg/ml streptomycin and 10% (v/v) heat inactivated fetal bovine serum (FBS; Gibco, Paisley, UK). Parasite virulence was maintained by periodical passage of $1x10^7$ freshly transformed stationary phase promastigotes in BALB/c mice.

Soluble *Leishmania* antigen (SLA) was prepared from stationary phase promastigotes, as described previously (9). For the preparation of SLA, stationary phase promastigotes were washed in phosphate buffer saline (PBS) (1.37 M NaCl, 27 mM KCl, 43 mM Na_2HPO_4 in H_2O, pH 7.4) and adjusted to $1x10^9$ promastigotes/ml. Promastigotes were disrupted by repeated freezing/thawing cycles (liquid N_2/37°C) followed by 5 min incubation on ice. Lysed material were centrifuged at 8000 x g, for 30 min at 4°C and total protein concentration in the supernatant was determined using the Micro BCA Protein Assay Kit (Pierce, Rockford, IL). SLA was stored in aliquots at -80°C until used.

Isolation of peritoneal macrophages

Peritoneal macrophages (pMØ) were elicited by i.p. injection of 1.0 ml of sterile 4% (w/v) thioglycollate

medium, brewer modified (Becton-Dickinson France SA, Le Pont de Claix, France) into BALB/c mice. Seventy-two hours later, inflammatory exudate cells were harvested by washing off the peritoneal cavity with 5 ml of ice-cold PBS and plated in 10-cm culture dishes (Corning, NY, USA). pMØ were obtained by removing the non-adherent cells after 3 h of incubation at 37°C in 5% CO_2. A percentage of 95.93±1.4% of cells was confirmed to be $F4/80^+$ by specific staining using rat biotin-conjugated anti-F4/80 mAb (A3-1, Serotec Ltd, Oxford, UK) in conjunction with streptavidin PE-conjugated anti-rat IgG $F(ab)'_2$ (Pharmingen, Erembodegen, Belgium) and flow cytometry (FACS Calibur flow cytometer and CellQuest™ software; Becton-Dickinson Immunocytometry System, San Jose, CA, USA).

In vitro infection of macrophages

Isolated pMØ (1 x 10^6 cells/ml) were incubated for 18 h, at 37°C in 5% CO_2 at 24-well plates (Sarstedt, Newton, NC, USA) containing glass cover slips in each well in serum free RPMI-1640 medium in order to achieve a resting state. Subsequently, the medium was replaced with fresh medium supplemented with 10% (v/v) FBS and stationary phase promastigotes were added at a ratio of 1:10 (pMØ:parasites). At 6 h of incubation, non-phagocytosed parasites were removed by gentle washing with warm medium and pMØ were incubated until 48 h, at 37°C in 5% CO_2. At designated time points (0.5, 3, 6, 12, 24, 48 and 72 h) of exposure, triplicate cover slips were selected, fixed with methanol, stained with Giemsa and the parasitic load was determined microscopically.

Macrophage treatment and stimulations

pMØ were seeded at a density of 1 x 10^6 cells/ml at 24-well plates (cytokine and NO detection) or 10-cm culture dishes (Western blot) in RPMI-1640 supplemented with 10% FBS. For cytokine and NO detection, infection was done in the presence of LPS (1 μg/ml) (Sigma, St. Louis, MO, USA) for designated time points for each experiment, whereas pMØ stimulated only with LPS served as positive control.

For Western blot analyses, pMØ were exposed to promastigotes for 6 and 48 h and then were stimulated with LPS (1 μg/ml) for 5 or 10 min. pMØ stimulated with LPS served as positive control. Otherwise, pMØ were pretreated with cytochalasin-D (2.5 μg/ml) (Sigma) for 30 min prior to promastigotes exposure. Also, pMØ were stimulated with SLA (25 μg/ml) for 5, 15, 30 and 60 min.

For MAPK phosphorylation assays, pMØ were treated with MAPK inhibitors for 1 h prior their exposure to promastigotes and/or LPS stimulation. Specifically, MAPK signaling was impaired by the use of 50 μM PD98059 (MEK1/2 inhibitor, Calbiochem, San Diego, CA), 20 μM SB203580 (p38-MAPK inhibitor, Calbiochem) or 50 μM SP600125 (JNK inhibitor, Calbiochem). All inhibitors were prepared as 10 mM stock solutions in DMSO. The solvent alone had no effect on the MAPK phosphorylation under the conditions used.

Cytokine and NO detection assays

Cell-free supernatants from infected pMØ cultures were obtained at 6, 12, 24 and 48 h timepoints and analyzed for their content in IL-12 and TNFα by commercial solid phase sandwich enzyme linked immunosorbent assays (ELISAs) according to manufacturer's instructions (Invitrogen Co. Carlsbad, CA). Quantitation was performed using a standard dose-dependent curve and cytokine concentrations are presented as pg/ml. The detection limits of assays were 20 and 30 pg/ml for IL-12 and TNFα, respectively. Supernatants containing TNFα greater than 1250 pg/ml were further diluted and re-analysed.

NO was detected in cell free supernatants by Griess reaction at 6, 12, 24 and 48 h. Specifically, 100 μl of each supernatant and 50 μl of 1% (w/v) sulphanilamine (Sigma) and 0.1% (w/v) *N*-napthylethylene-diamine dihydrochloride (Sigma) in 1.25% (v/v) H_3PO_4 were placed in 96-well plates (Sarstedt, Newton, NC) for 10 min, at room temperature in the dark. Nitrite concentration in supernatants was determined by a standard curve of $NaNO_2$ (Sigma). Optical density was determined using a spectrophotometer (MRX, Dynatech Laboratories, Guernsey, UK) at 550 nm.

Western blot analysis

pMØ were washed with ice-cold PBS and homogenized in 150 μl of ice-cold cell lysis buffer (10 mM Tris-HCl pH 7.5, 2 mM EDTA, 10 mM benzamidine and 0.05% (v/v) Triton X-100) supplemented with protease and phosphatase inhibitors mixture consisted of 200 μM leupeptin, 10 μM E-64, 20 mM sodium fluoride (NaF), 5 mM dithiothreitol (DTT), 0.2 mM sodium orthovanadate (Na_3VO_4), 20 mM β-glycerophosphate and 300 μM phenylmethylsulfonyl fluoride (PMSF). After 30 min incubation on ice, lysates were centrifuged at 15000 x g, for 30 min at 4°C. Protein concentration was determined in the supernatants by the Micro BCA Protein Assay Kit. The supernatants were mixed proportionally with SDS loading buffer (300 mM Tris-HCl, pH 6.8, 13% (v/v) glycerol, 10% (w/v) SDS, 20% (v/v) β-mercaptoethanol and 0.2% (w/v) bromophenol blue), boiled for 5 min and resolved on 12% SDS-polyacrylamide electrophoresis gels. Approximately, 50 μg of cell lysate was loaded per well. Resolved proteins were semi-dry blotted to nitrocellulose membrane (GE Healthcare, Buckinghamshire, UK). After transfer, the membrane was blocked in TBS-T (Tris-buffered saline

containing 0.05% (v/v) Tween-20) containing 5% (w/v) non-fat milk for 1 h at room temperature and probed with Abs specific for phospho-p38, -ERK1/2, -JNK and total-p38, -JNK, -ERK1/2 and IKBa diluted 1:1000 in TBS-T containing 5% (w/v) bovine serum albumin at 4°C overnight. Then, membrane was washed three times with TBS-T and incubated for 1 h with HRP-conjugated anti-rabbit goat secondary antibody (Cell Signaling Technology) diluted 1:3000 in TBS-T containing 1% (w/v) non-fat milk at room temperature. Binding of secondary antibody was analyzed with the ECL reagent kit (GE Healthcare) according to the manufacturer's instructions and visualized at PhosphorImager (Storm 860 Gel and Blot Imaging System, GE Healthcare). Probed blots were quantified by scanning densitometry using the Image Quant software programme (Molecular Dynamics, CA).

Viability assay

To assess parasite killing and infected pMØ viability, pMØ were infected under conditions similar to those described above in the presence or absence of LPS (1 μg/ml). After 48 h, infected pMØ were subjected to acridine orange (100 μg/ml) - ethidium bromide (100 μg/ml; BD Biosciences, Mississauga, ON, Canada) staining for 5 min. Cover slips were mounted in a drop of PBS/glycerol (diluted 1:1 (v/v)) and examined immediately using a Leitz microscope equipped with standard epifluorescence filters. Only viable pMØ (stained green) were scored for parasite binding and the percentage of viable amastigotes was calculated by comparing pMØ containing dead (stained red) parasites with the total number of infected pMØ.

Statistical analysis

Where appropriate, data are expressed as means±SD. For comparison of the mean of two experimental groups, statistical significance was assessed by two-tailed Student's *t* test. The probability (*P*) of < 0.05 was considered to indicate statistical significance.

RESULTS

LPS stimulation partially restores NO, TNFα and IL-12 production in stably-infected macrophages

Regarding the fact that *L. infantum* presents intra-specific variability on its virulence (10), experiments were conducted for the assessment of the infective ability of MCAN/PT/98/IMT 244 strain, zymodeme MON-1. Firstly, it was assessed the high purity of macrophage population submitted to parasite infection. According to flow cytometry analysis, 95.93±1.4% of adherent peritoneal cell population was $F4/80^+$ cells and therefore they will be referred as peritoneal macrophages (pMØ). pMØ were exposed to stationary phase *L. infantum* promastigotes at a parasite/cell ratio of 10:1 for 6 hours. After this time point non-internalized or non-attached parasites were removed and macrophages remained in culture for 12, 24, 48 and 72 h. As shown in Fig. 1a, parasites attachment on pMØ surface was detected at 0.5 h of exposure (Fig. 1a) and parasite internalization (phagocytosis) started at 6 h, since at this time point a significant number of pMØ (85-90%) had parasites constantly attached on membrane (Fig. 1b). Amastigote transformation was observed at 12 h of incubation (data not shown) and the maximum infection level was detected at 48 h (Fig. 1d) where 68.25±12.4% of pMØ had been infected containing 234±32 amastigotes per 100 pMØ (Fig. 1e, f). In order to examine the effect of parasite infection on NO and cytokine (IL-12 and TNFα) production, pMØ culture supernatants analysis was performed until 48 h of infection. The results obtained revealed that neither promastigotes attachment (6 h), nor their internalization and transformation to amastigotes (12-48 h) induced NO release or TNFα and IL-12 production by pMØ above levels detected in control (medium) cells (Fig. 1g-i). This result was not an intrinsic defect of pMØ, since copious amounts of all three molecules were detected when cells were stimulated with LPS (Fig. 1g-i). Consequently, the ability of parasites to manipulate the LPS-induced activation of pMØ was tested. Promastigotes during attachment and internalization (6-12 h) suppressed LPS-induced IL-12 production (Fig. 1i) and NO release (Fig. 1g) to levels detected in control cells supernatants, whereas TNFα production was not affected compared to LPS-stimulated cells (Fig. 1h). In contrast, LPS stimulation of stably infected cells (24-48 h) resulted to 2-fold and 3.8-fold increase of IL-12 and NO production, respectively, relative to early infected cells that have been stimulated with LPS ($P < 0.05$), whereas LPS-induced TNFα production was 4.5-fold increased (Fig. 1G-I).

These observations confirmed the silent infection of pMØ by *L. infantum* promastigotes. However, establishment of amastigotes did not induce a state of tolerance in subsequent stimuli as confirmed by the increased IL-12, TNFα and NO production upon

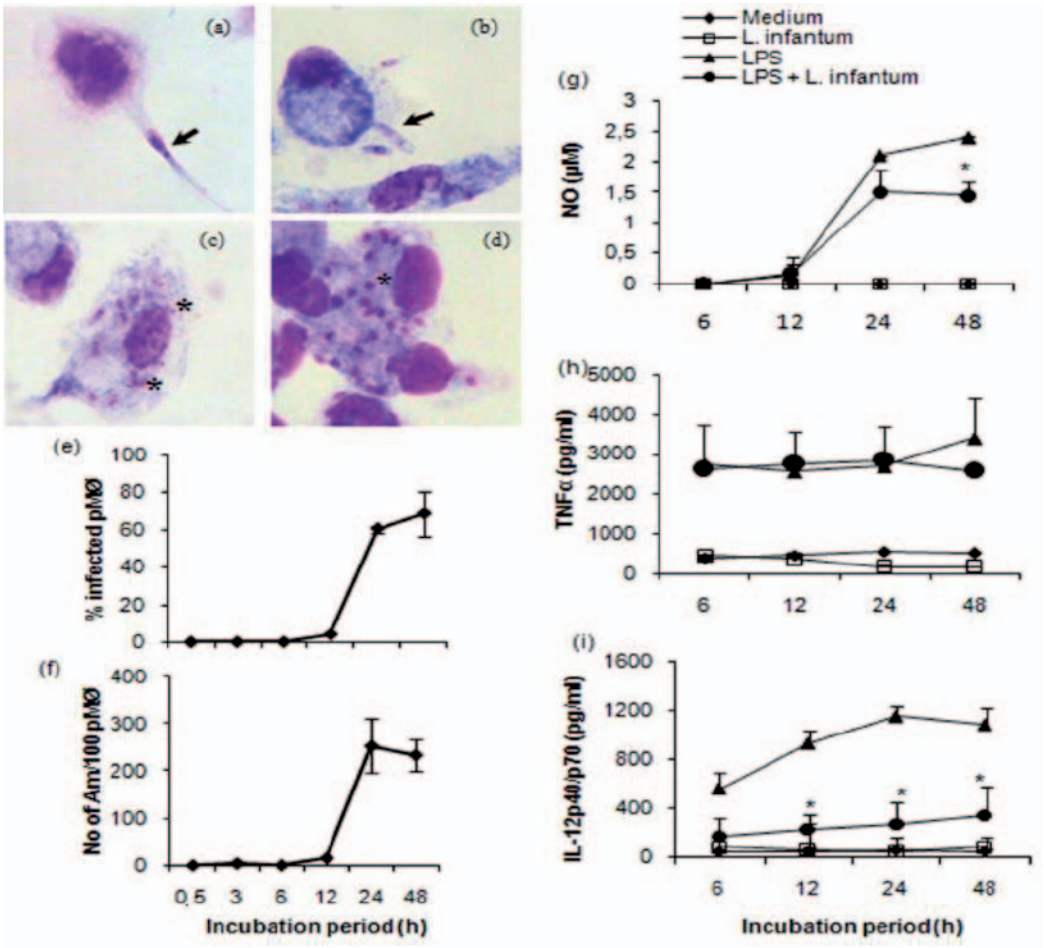

Fig. 1. *pMØ infection kinetics by L. infantum and its effect on NO, TNFα and IL-12 production. (a-d) Giemsa stain. pMØ were incubated with stationary phase promastigotes (macrophage:parasite ratio 1:10) for 0.5 (**a**), 6 (**b**), 24 (**c**) and 48 (**d**) hours. Arrows indicate bound promastigotes and asterisks indicate intracellular amastigotes. Magnification, x1000 (**e-f**). Percentages of infected pMØ and number of amastigotes (Am) per 100 pMØ were estimated by microscopic examination at the indicated time points. (g-i) pMØ were incubated with stationary phase promastigotes (macrophage:parasite ratio 1:10) for the time points indicated in the presence or absence of LPS (1 µg/ml) and NO, TNFα and IL-12 were assessed in culture supernatants. The results are the mean value from three independent experiments ± SD. Significant differences among LPS-stimulated infected and infected macrophages are indicated by * (P<0.05).*

subsequent LPS stimulation.

Promastigotes internalization abrogates LPS-induced MAPK activation which is restored in stably-infected cells

Then, activation of MAPK (ERK1/2, p38 and JNK1/2) pathways during pMØ infection was investigated. Specifically, detection of MAPK activation was performed at the times of promastigote attachment on macrophage surface (6 h) and establishment of amastigotes inside macrophages (48 h). As shown in Fig. 2, parasite alone did not induce phosphorylation of ERK1/2, p38 and JNK1/2 in pMØ in both time points selected compared to control cells. In contrast, stimulation of pMØ with LPS induced a 2-fold activation of all three MAPK studied (Fig. 2). Thus, it was investigated whether *L. infantum*-infected cells could undergo MAPK phosphorylation in response to subsequent LPS challenge. LPS-induced MAPK

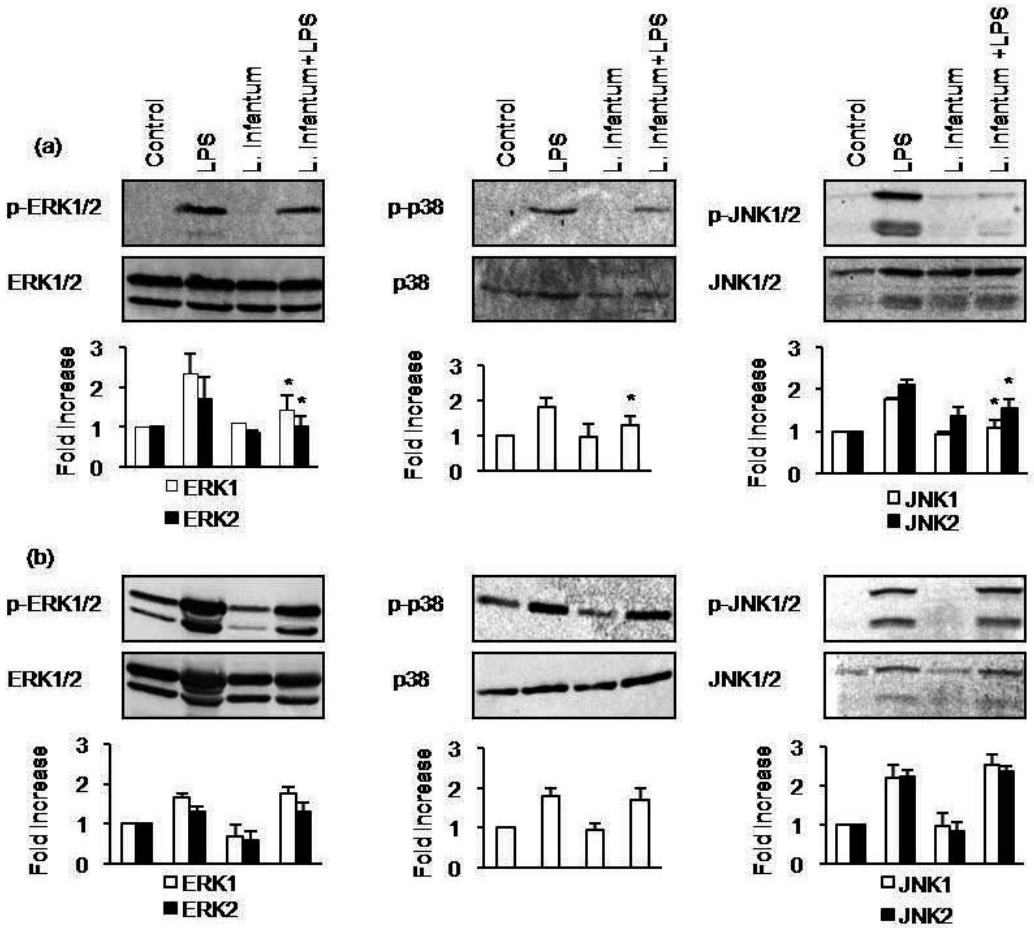

Fig. 2. *Effect of L. infantum on MAPK activation on LPS-stimulated pMØ. pMØ were infected with stationary phase promastigotes (macrophage:parasite ratio 1:10) for 6 (**a**) and 48 h (**b**). LPS (1 μg/ml) was added where indicated for 10 min prior to the lysis of cells. Cell lysates (50 μg) were subjected to immunoblotting with phospho (p)-ERK1/2, p-p38, p-JNK1/2 antibodies. The blots were reprobed with anti-ERK1/2, -p38 or –JNK1/2 antibodies to confirm equal protein loading. The blots shown are representative of three independent experiments. Densitometry values were normalized to ERK1/2, p38 or JNK1/2 and then to non-infected controls. Densitometry analysis for at least three independent experiments ± SD and representative blots are shown. Significant differences among LPS-stimulated and LPS-stimulated infected macrophages are indicated by * (P<0.05).*

activation was partially or fully inhibited during the first hours of interaction between parasite and host cell suggesting the establishment of a state of refractoriness to subsequent stimuli. Specifically, parasite significantly ($P < 0.05$) reduced LPS-induced ERK1/2 and p38 MAPK phosphorylation 1.6- and 1.5-fold, respectively, and completely blocked JNK1/2 activation (Fig. 2a). On the contrary, LPS stimulation of cells with established infection restored phosphorylation of all MAPK studied to levels similar to those detected in uninfected LPS-stimulated cells (Fig. 2b).

In order to elucidate whether inhibition of MAPK pathways detected during the first 6 h of macrophage co-incubation with parasite was a contact-dependent phenomenon, infection was also performed in pMØ pretreated with cytochalasin-D prior to promastigote exposure for the prevention of parasite phagocytosis. Whereas promastigote attachment due to cytochalasin D did not induce activation of MAPK pathways, it could not affect LPS-induced ERK1/2, p38 and JNK1/2 phosphorylation compared to

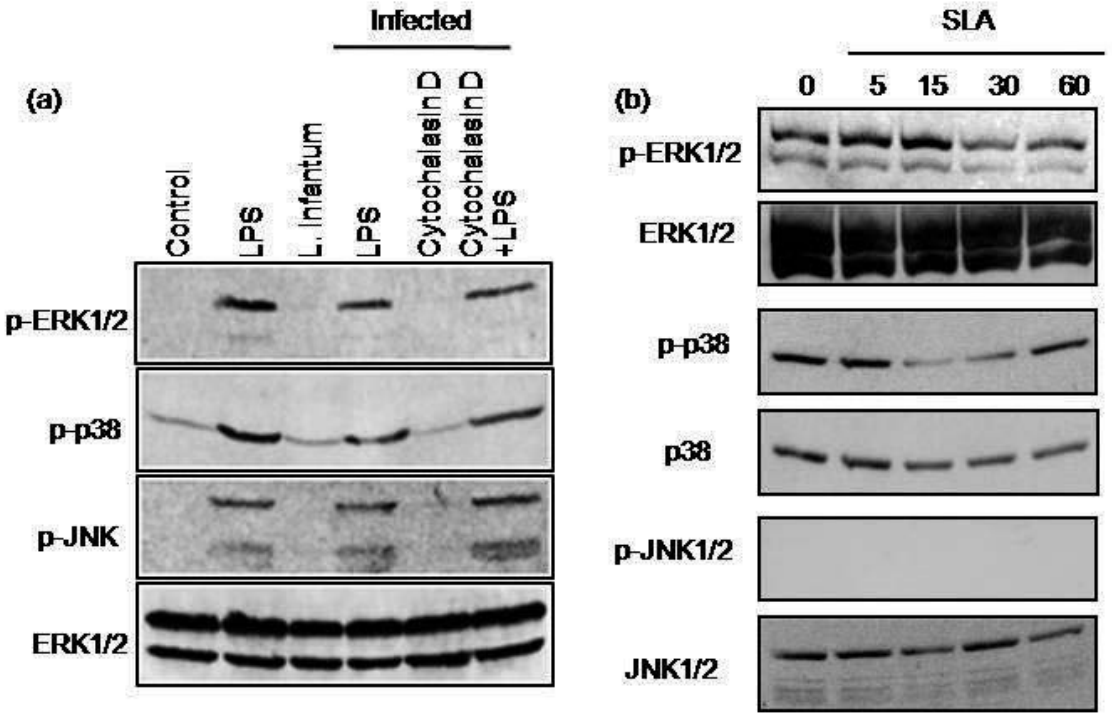

Fig. 3. *Effect of L. infantum attachment or its soluble antigen (SLA) on MAPK activation in pMØ (**a**). pMØ were incubated with cytochalasin-D and then were infected with stationary phase promastigotes (macrophage:parasite ratio 1:10) for 6 h. LPS (1 μg/ml) was added where indicated for 10 min prior to the lysis of cells (**b**). Also, pMØ were incubated with SLA (25 μg/ml) for 5, 15, 30, 60 min. Cell lysates (50 μg) were subjected to immunoblotting with phospho (p)-ERK1/2, p-p38, p-JNK1/2 antibodies. The blots were reprobed with anti-ERK1/2, -p38 or -JNK1/2 antibodies to confirm equal protein loading. The blots shown are representative of three independent experiments.*

phosphorylation detected in cells treated with LPS alone, indicating that parasite internalization was necessary for the desensitization of macrophages to subsequent LPS challenge during the first hours of infection (Fig. 3a).

It was further investigated whether MAPK inhibition detected was attributed to recognition of parasite fragments or antigens. For that reason, pMØ were stimulated with SLA for 5, 15, 30 and 60 min. Our results showed that stimulation of pMØ with SLA induced a rapid and transient phosphorylation of ERK1/2 within 5 min of incubation period, reaching the highest levels at 15 min and then dropped below the resting levels (0 min) at 30 min of incubation period (Fig. 3b). In contrast, SLA did not induce p38 MAPK and JNK1/2 activation compared to control cells (Fig. 3b).

The above combined data suggested that internalization of live *L. infantum* promastigotes into macrophages induced a state of tolerance which was subverted after establishment of infection.

LPS-induced NF-κB activation in stably-infected macrophages is independent of MAPK activation

The effect of parasite infection on NF-κB pathway was also examined. For that reason, IκBα degradation, a prerequisite for NF-κB activation, was detected in stably-infected cells. Whereas LPS induced a rapid degradation of IκBα, parasite abrogated NF-κB activation (Fig. 4). Interestingly, stably-infected cells were not refractory to subsequent LPS stimulation since IκBα degradation was detected. Eventually, it was examined if the detected NF-κB activation after LPS stimulation of stably-infected cells could be a downstream effect of LPS-induced MAPK activation. For that reason, pMØ were pretreated

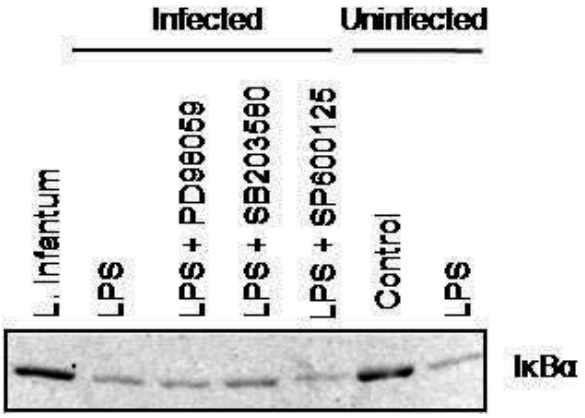

Fig. 4. *Role of LPS-induced MAPK on NF-κB activation in L. infantum-infected pMØ. pMØ were infected with stationary phase promastigotes (macrophage:parasite ratio 1:10) for 48 h. pMØ were pretreated with or without PD98059 (50 μM), SB203580 (20 μM) or SP600125 (50 μM) for 1 h and then LPS (1 μg/ml) was added where indicated for 5 min prior to the lysis of cells. Cell lysates (50 μg) were subjected to immunoblotting with anti-IκBα antibody. The blot shown is representative of three independent experiments.*

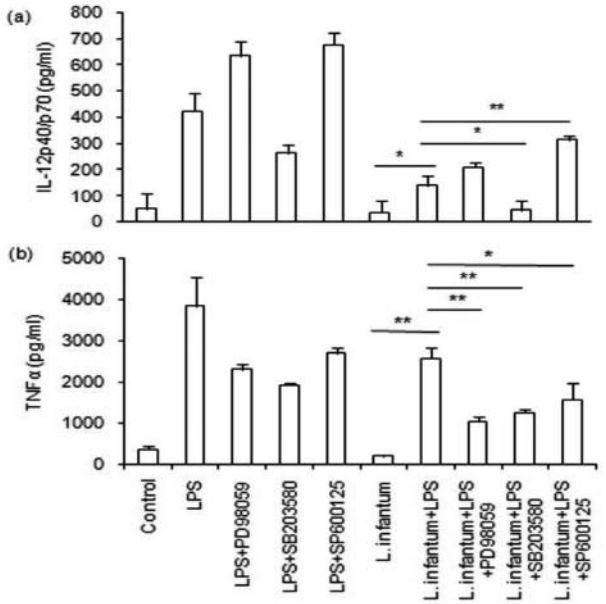

Fig. 5. *Effect of LPS-induced MAPK on IL-12 and TNFα production by L. infantum-infected pMØ. pMØ were pretreated with or without PD98059 (50 μM), SB203580 (20 μM) or SP600125 (50 μM) for 1 h before stimulation with LPS (1 μg/ml) in the presence or absence of L. infantum promastigotes (macrophage:parasite ratio 1:10) for 48 h. Cell culture supernatants were harvested for IL-12 (**a**) and TNFα (**b**) measurement. The results are the mean value from three independent experiments ± SD. Significant differences among groups are indicated by * ($P<0.05$) and ** ($P < 0.01$).*

with specific inhibitors of ERK1/2 (PD98059), p38 MAPK (SB203580) and JNK1/2 (SP600125) pathways before LPS stimulation. As shown in Fig. 4, pretreatment with the above inhibitors did not inhibit LPS-induced IκBα degradation, indicating that the induced MAPK activation could not account for the detected NF-κB activation.

According to the above results, stably-infected cells responded to LPS stimulation by activating, on a MAPK independent manner, the NF-κB transcription factor.

Role of LPS-induced MAPK on IL-12 and TNFα production in stably-infected macrophages

In order to investigate the role of LPS-induced MAPK activation to IL-12 and TNFα production in stably-infected pMØ, ERK1/2, p38 MAPK and JNK1/2 activation was inhibited with the use of specific inhibitors. Addition of PD98059 for ERK1/2 inhibition before stimulation with LPS of infected cells caused a slight, non-significant increase of IL-12 production (210.16±20 vs 139.22±37.1 pg/ml; $P = 0.177$) compared to untreated cells (Fig. 5a). Also, inhibition of JNK1/2 due to pretreatment with SP600125 resulted in significant increase of IL-12 production (316.02±15.86 vs 139.22±37.1 pg/ml, $P = 0.05$). In contrast, the presence of SB203580, inhibitor of p38 MAPK, marginally reduced IL-12 production (45.48±37.81 vs 139.22±37.1 pg/ml; $P = 0.03$) to levels detected in culture supernatants of infected pMØ (35.24±49.84 pg/ml). TNFα production in stably-infected cells was dependent on activation of all three MAPK, since pretreatment of pMØ with PD98059, SB203580 or SP600125 caused significant reduction of its production (PD98059: 1036±100.6 vs 2588.16±248.83 pg/ml; $P = 0.004$, SB203580: 1244.14±85.85 vs 2588.16±248.83 pg/ml; $P = 0.005$, SP600125: 1584.3±406.86 vs 2588.16±248.83 pg/ml; $P = 0.03$) (Fig. 5b). MAPK inhibitors affected cytokine production from

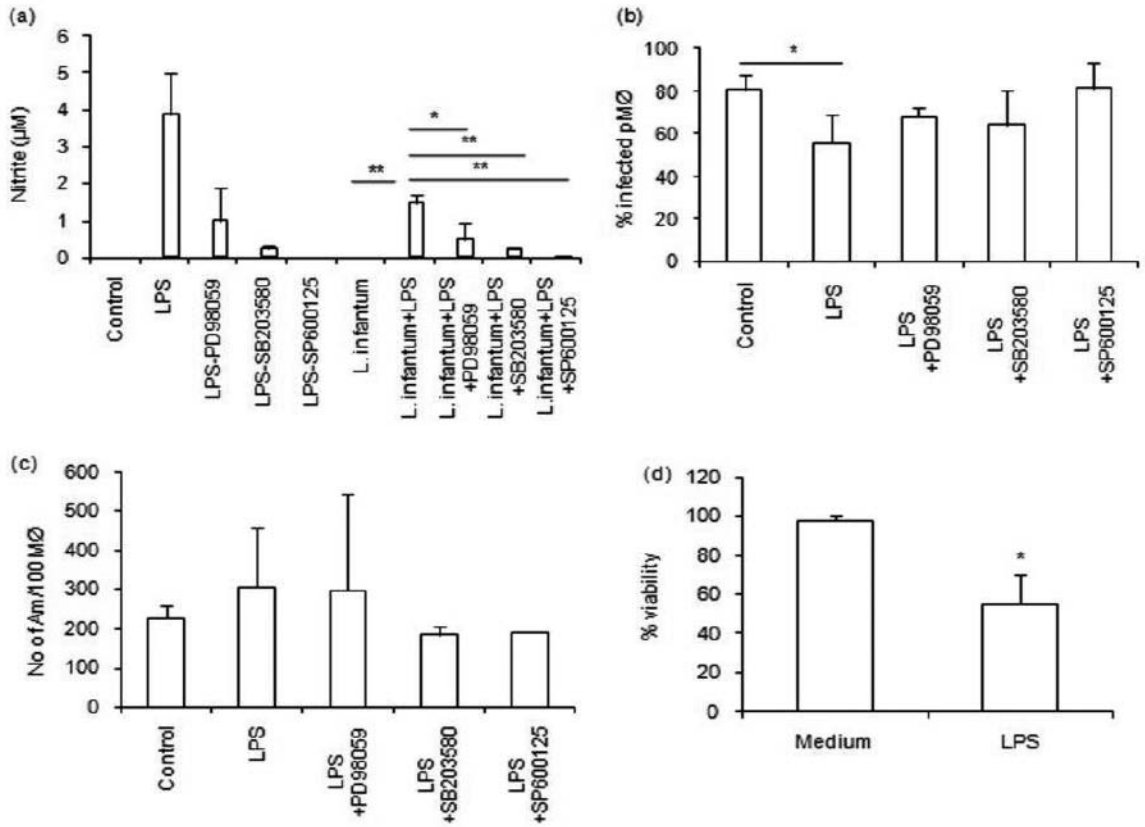

Fig. 6. *Effect of LPS-induced MAPK on NO production by L. infantum-infected pMØ and assessment of L. infantum amastigotes survival. pMØ were pretreated with or without PD98059 (50 μM), SB203580 (20 μM) or SP600125 (50 μM) for 1 h before stimulation with LPS (1 μg/ml) in the presence or absence of L. infantum promastigotes (macrophage:parasite ratio 1:10) for 48 h (**a**). Cell culture supernatants were harvested for NO. Cells were stained with Giemsa and percentages of infected pMØ (**b**) and number of amastigotes (Am) per 100 pMØ (**c**) were determined by microscopic examination. (**d**) Parasite viability was assessed by acridine orange-ethidium bromide staining. The results are the mean value from three independent experiments ± SD. Significant differences among groups are indicated by * ($P<0.05$) and ** ($P < 0.01$).*

uninfected LPS-stimulated cells the same way as in infected LPS-stimulated cells (Fig. 5). Consequently, the above combined data suggested that restoration of IL-12 and TNFα pro-inflammatory cytokines production due to LPS stimulation of stably-infected macrophages is differentially regulated by MAPK activation.

LPS stimulation abrogates parasite survival inside macrophage through induction of NO

Then, it was assessed the relevance of LPS-induced MAPK phosphorylation with elevated NO levels in stably-infected cells by using specific inhibitors of each pathway. As shown in Fig. 6a, inhibition of p38 MAPK and JNK1/2 pathway decreased NO production (SB203580: 0.24±0.02 vs 1.49±0.21 μM; $P = 0.009$, SP600125: 0.02±0.03 vs 1.49±0.21 μM; $P = 0.006$) to levels detected in supernatants from resting pMØ or infected pMØ cultures (Fig. 6a). Further, inhibition of ERK1/2 induced 3.1–fold reduction of NO production (0.47±0.48 vs 1.49±0.21 μM; $P = 0.04$) (Fig. 6a).

Therefore, it was examined the effect of increased NO secretion levels in parasite survival and multiplication by assessing the number of infected cells and the number of parasites per cell.

LPS stimulation caused 30% reduction of parasitized pMØ ($P < 0.05$; Fig. 6b). Pretreatment of pMØ with PD98059 and SB203580 inhibitors did not modulate infection levels. In contrast, JNK1/2 inhibition resulted to similar infection levels to non-stimulated cells. Despite infection levels decrease, it must be noted that the number of amastigotes did not change compared to control cells even in the presence of MAPK inhibitors (Fig. 6c). As a consequence, the viability of amastigotes in control and LPS-stimulated pMØ was determined by ethidium bromide-acridine orange staining. According to the results obtained from this assay, about 95±21% of the infected pMØ were viable independently of LPS stimulation. However, LPS-stimulated cells contained 40% less viable amastigotes compared to control ($P < 0.05$; Fig. 6d).

These data suggest collectively that LPS-induced MAPK activation enhances NO production resulting in parasite elimination.

DISCUSSION

Several reports show that establishment of pathogens to macrophages renders different modes of responsiveness to subsequent microbial stimuli (11, 12). Thus, in the present study we investigated the effect of LPS stimulation on activation status of macrophages exposed to and infected with *L. infantum* promastigotes.

We demonstrated that *L. infantum* promastigotes evaded ERK1/2, p38 MAPK and JNK1/2 phosphorylation accompanied by inhibition of IL-12, TNFα and NO production. Similarly, in previous study *L. donovani* promastigotes have shown to evade activation of MAPK during infection of naive macrophages resulting in defects on their parasiticidal mechanisms (13). However, in our study the evasion of MAPK phosphorylation required live parasites, since macrophages stimulation with whole parasite extracts resulted in rapid and transient activation of ERK1/2 during the first minutes of incubation.

Interestingly, promastigotes induced a state of tolerance against LPS stimulation only at the first hours of infection characterized by abrogation of cytokine and NO synthesis and silencing of MAPK pathways. The observed refractoriness required internalization of promastigotes, since treatment of macrophages with cytochalasin-D prior exposure to parasite did not inhibit LPS-induced MAPK activation. However, the state of refractoriness towards LPS was subverted after establishment of infection. These data contradict studies reporting that established infection of macrophages inhibits activation of MAPK in response to subsequent stimulation (14, 15) and might indicate a mechanism by which parasite keeps its host cell vital and functional in order to proliferate. Another study also supports that suppression of LPS-induced pro-inflammatory cytokines, such as IL-12, is parasite-specific, since *L. amazonensis* was more suppressive than *L. major* promastigotes (16). In agreement to our results, Ben-Ohtman et al reported that *L. major* stably-infected macrophages fail to suppress LPS- or PMA-induced MAPK activation and cytokine production (17, 18).

Using specific MAPK inhibitors, we showed that LPS-induced MAPK activation in stably-infected cells played a significant role in the restoration of cytokine and NO production. Whereas IL-12 production was positively regulated by p38 MAPK, significant or moderate increase of IL-12 production was detected after JNK1/2 and ERK1/2 inhibition, respectively. Differential activation of ERK1/2, JNK1/2 and p38 MAPK has been implicated in the suppression of IL-12 production in various studies (19-23). We also showed that in stably-infected macrophages TNFα production was dependent on LPS-induced MAPK activation. Studies investigating TNFα synthesis at transcriptional and translational level have shown that ERK1/2 and JNK1/2 play significant positive role (24-26). Furthermore, LPS-induced MAPK activation played a major role in NO production. This was demonstrated by showing significant down-regulation of NO release after inhibition of MAPK activation. Interestingly, MAPK inhibition resulted in elevation on rate of parasitized macrophages and this may be linked to the decreased NO levels produced by macrophages. This result is in agreement with previous studies showing that *Leishmania* reduces NO levels by inhibiting ERK1/2 activation and/or inducing JNK1/2 dephosphorylation (14, 27). In addition, the key role of p38 MAPK in macrophage parasiticidal action has been supported in anisomycin treated-human macrophages which managed to eliminate *L.*

donovani parasites (28).

Cytokine production is regulated not only through the activation of MAPK but also of NF-κB. We showed that parasite amastigotes inhibited NF-κB activation but not in the presence of LPS. However, these cells responded to LPS by activating NF-κB in a MAPK-independent manner. This strongly argues that NF-κB was regulated by other upstream signaling pathways as supported by various reports (29, 30) and in combination with our results support the notion that inflammatory cytokine regulation may require the complementary action of MAPK and NF-κB pathways.

Conclusively, the data presented here suggest that *L. infantum* promastigotes in the first hours of infection desensitize macrophages to a subsequent LPS challenge, whereas parasite establishment could not affect TLR4 pathway activation after LPS recognition. These data indicate that the two different forms of the parasite may differentially regulate the signaling molecules involved in the TLR4 pathway. Thus this report shows that activation of TLR4 pathway and consequently MAPK and NF-κB renders macrophages efficient to eliminate *Leishmania* parasites.

Further understanding of the role of ERK1/2, p38 MAPK and JNK1/2, interacting partners and their cross-talk will give significant information for the design of new therapeutic and preventive modalities against infection.

ACKNOWLEDGEMENTS

The work carried out in this paper was supported by a grant from Hellenic Pasteur Institute.

REFERENCES

1. Mansueto P, Vitale G, Di Lorenzo G, Rini GB, Mansueto S, Cillari E. Immunopathology of leishmaniasis: an update. Int J Immunopathol Pharmacol 2007; 20:435-45.
2. Olivier M, Gregory DJ, Forget G. Subversion mechanisms by which *Leishmania* parasites can escape the host immune response: a signaling point of view. Clin Microbiol Rev 2005; 18:293-305.
3. Zhang YL, Dong C. MAP kinases in immune responses. Cell Mol immunol 2005; 2:20-7.
4. Kropf P, Freudenberg MA, Modolell M, et al. Toll-like receptor 4 contributes to efficient control of infection with the protozoan parasite *Leishmania major*. Infect Immun 2004; 72:1920-8.
5. Kropf P, Freudenberg N, Kalis C, Modolell M., Herath S, Galanos C, Freudenberg M, Muller I. Infection of C57BL/10ScCr and C57BL/10ScNCr mice with Leishmania major reveals a role for Toll-like receptor 4 in the control of parasite replication. J Leukoc Biol 2004; 76:48-57.
6. Murray HW, Zhang Y, Zhang Y, Raman VS, Reed VS, Reed SG, Ma X. Regulatory actions of TLR2 and TLR4 in *Leishmania donovani* infection in the liver. Infect Immun 2013; 81(7):2318-26
7. Karmakar S, Bhaumik SK, Paul J, De T. TLR4 and NKT cell synergy in immunotherapy against visceral leishmaniasis. PLoS Pathog 2012; 8:e1002646.
8. Dobrovolskaia MA, Vogel SN. Toll receptors, CD14, and macrophage activation and deactivation by LPS. Microbes Infect 2002; 4:903-14.
9. Papadopoulou G, Karagouni E, Dotsika E. ISCOMs vaccine against experimental leishmaniasis. Vaccine 1998; 16:885-92.
10. Baptista-Fernandes T, Marques C, Roos Rodrigues O, Santos-Gomes GM. Intra-specific variability of virulence in *Leishmania infantum* zymodeme MON-1 strains. Comp Immunol Microbiol Infect Dis 2007; 30:41-53.
11. Kim L, Butcher BA, Denkers EY. *Toxoplasma gondii* interferes with lipopolysaccharide-induced mitogen-activated protein kinase activation by mechanisms distinct from endotoxin tolerance. J Immunol 2004; 172:3003-10.
12. Reiling N, Blumenthal A, Flad H-D, Ernst M, Ehlers S. Mycobacteria-induced TNF- and IL-10 formation by human macrophages is differentially regulated at the level of mitogen-activated protein kinase activity. J Immunol 2001; 167:3339-45.
13. Prive C, Descoteaux A. *Leishmania donovani* promastigotes evade the activation of mitogen-activated protein kinases p38, c-Jun N-terminal kinase, and extracellular signal-regulated kinase-1/2 during infection of naïve macrophages. Eur J Immunol 2000; 30:2235-44.
14. Ghosh S, Bhattacharyya S, Sirkar M, Sa GS, Das T, Majumdar D, Roy S, Majumdar S. *Leishmania*

donovani suppresses activated protein 1 and NF-kappaB activation in host macrophages via ceramide generation: involvement of extracellular signal-regulated kinase. Infect Immun 2002; 70:6828-38.

15. Nandan D, Lo R, Reiner NE. Activation of phosphotyrosine phosphatase activity attenuates mitogen-activated protein kinase signaling and inhibits c-FOS and nitric oxide synthase expression in macrophages infected with *Leishmania donovani*. Infect Immun 1999; 67:4055-63.
16. Lapara NJ 3rd, Kelly BL. Suppression of LPS-induced inflammatory responses in macrophages infected with *Leishmania*. J Inflamm (Lond) 2010; 7:8.
17. Ben-Ohtman R, Guizani-Tabbane L, Dellagi K. *Leishmania* initially activates but subsequently down-regulates intracellular mitogen-activated protein kinases and nuclear factor-kappaB signaling in macrophages. Mol Immunol 2008; 45:3222-9.
18. Ben-Ohtman R, Dellagi K, Guizani-Tabbane L. *Leishmania major* parasites induced macrophage tolerance: Implication of MAPK and NF-κB pathways. Mol Immunol 2009; 46:3438-44.
19. Feng GJ, Goodridge HS, Harnett MM, Wei XQ, Nikolaev AV, Higson AP, Liew FY. Extracellular signal-related kinase (ERK) and p38 mitogen-activated protein (MAP) kinases differentially regulate the lipopolysaccharide-mediated induction of inducible nitric oxide synthase and IL-12 in macrophages: *Leishmania* phosphoglycans subvert macrophage IL-12 production by targeting ERK MAP kinase. J Immunol 1999; 163:6403-12.
20. Piedrafita D, Proudfoot L, Nikolaev AV, Xu D, Sands W, Feng GJ, Thomas E, Brewer J, Ferguson MAJ, Alexander J, Liew FY. Regulation of macrophage IL-12 synthesis by *Leishmania* phosphoglycans. Eur J Immunol 1999; 29:235-44.
21. Lu HT, Yang DD, Wysk M, Gatti E, Mellman I, Davis RJ, Flavell RA. Defective IL-12 production in mitogen-activated protein (MAP) kinase kinase 3 (*Mkk3*)-deficient mice. EMBO J 1999; 18:1845-57.
22. Utsugi M,Dobashi K, Ishizuka T, Endou K, Hamuro J, Murata Y, Nakazawa T, Mori M. c-Jun N-terminal kinase negatively regulates lipopolysaccharide-induced IL-12 production in human macrophages: role of mitogen-activated protein kinase in glutathione redox regulation of IL-12 production. J Immunol 2003; 171:628-35.
23. la Sala A, Gadina M, Kelsall BL. G(i)-protein-dependent inhibition of IL-12 production is mediated by activation of the phosphatidylinositol 3-kinase-protein 3 kinase B/Akt pathway and JNK. J Immunol 2005; 175:2994-9.
24. Constant SL, Dong C, Yang DD, Wysk M, Davis RJ, Flavell RA. JNK1 is required for T cell-mediated immunity against *Leishmania major* infection. J Immunol 2000; 165:2671-6.
25. Geppert TD, Whitehurst CE, Thompson P, Beuler B. Lipopolysaccharide signals activation of tumour necrosis factor biosynthesis through the ras/Raf-1/MEK/MAPK pathway. Mol Med 1994; 1:93-103.
26. Swantek JL, Cobb MH, Geppert TD. Jun N-terminal kinase/stress-activated protein kinase (JNK/SAPK) is required for lipopolysaccharide stimulation of tumour necrosis factor alpha (TNF-α) translation: glucocorticoids inhibit TNF-α translation by blocking JNK/SAPK. Mol Cell Biol 1997; 17:6274-82.
27. Blanchette J, Abu-Dayyeh I, Hassani K, Whitcombe L, Olivier M. Regulation of macrophage nitric oxide production by the protein tyrosine phosphatase Src homology 2 domain phosphotyrosine phosphatase 1 (SHP-1). Immunology 2009; 127:123-33.
28. Junghae M, Raynes JG. Activation of p38 mitogen-activated protein kinase attenuates *Leishmania donovani* infection in macrophages. Infect Immun 2002; 70:5026-35.
29. Karaghiosoff M, Neubauer H, Lassnig C, et al. Partial impairment of cytokine responses in tyk2-deficient mice. Immunity 2000; 13:549-60.
30. Chakravortty D, Kato Y, Sugiyama T, Koide N, Mu MM, Yoshida T, Yokochi T. The inhibitory action of sodium arsenite on lipopolysaccharide-induced nitric oxide production in RAW264.7 macrophage cells: a role of Raf-1 in lipopolysaccharide signaling. J Immunol 2001; 166:2011-7.

IRON SUPPLEMENTATION IN YOUNG IRON-DEFICIENT FEMALES CAUSES GASTROINTESTINAL REDOX IMBALANCE: PROTECTIVE EFFECT OF A FERMENTED NUTRACEUTICAL

G. BERTUCCELLI[1], F. MAROTTA[1], N. ZERBINATI[2], A. CABECA[3], F. HE[4], S. JAIN[5], A. LORENZETTI[1], H. YADAV[2], M. MILAZZO[6], F. CALABRESE[6], C. TOMELLA[1] and R. CATANZARO[6]

[1]ReGenera Research Group for Aging Intervention, Milan, Italy; [2]CMP-Medical Center and Laboratories, Pavia, Italy; [3]Preventive and Functional Medicine Center Brunswick, GA, USA; [4]Department of Nutrition and Food Hygiene, West China School of Public Health, Sichuan University, Sichuan, China; [5]NIDDK, National Institute of Health, Bethesda, USA; [6]Dept of Internal Medicine, Gastroenterology Unit, University of Catania, Catania, Italy

Received January 24, 2013 – Accepted December 11, 2013

The aim of this study was to assess whether the concomitant supplementation of certified fermented papaya preparation (FPP, ORI, Gifu, Japan) together with iron supplementation could beneficially affect lipid peroxidation either systemically and at a intraluminal gut level in women with low iron stores. Treatment compliance and iron absorption was assessed as well. Fifty-two non-pregnant, fertile, non-smokers, healthy women with iron deficiency were recruited. The women were given iron supplements (100 mg Fe/d as ferrous sulfate) to be taken daily for 12 weeks (group A). Group B patients were also supplemented with 6g/day of a FPP. A detailed life style questionnaire was administered to all subjects. Iron, ferritin, transferrin receptors (Tf R) and malondialdehyde (MDA) in plasma were measured. The RBCs lysate was used for the estimation of superoxide dismutase (SOD) and glutathione peroxidase (GPx). The total and free iron concentration as well as analysis of oxidative stress in the feces was measured. FPP-supplemented subjects showed a significantly lower degree of gastrointestinal discomfort ($p<0.05$) and abolished the iron supplementation-induced increase of MDA ($p<0.001$) and the depletion of SOD and GPx ($p<0.01$). Moreover, the nutraceutical co-administration brought about a significant reduction of gut oxidative damage and lower fecal content of either total and free iron ($p<0.05$ *vs* group A). Overall, group B showed a better TfR/ferritin ratio response ($p<0.05$ *vs* group A). While iron supplementation maintains its clinical relevance considering the prevalence of iron deficiency among females, a careful clinical evaluation and a protective nutraceutical co-administration, as our data suggest with FPP, should be considered.

Iron is an essential nutrient, playing a central role in oxygen transport and cellular energy metabolism. The importance of ensuring adequate bioavailable dietary iron stems from the severe consequences associated with iron deficiency and anemia, including developmental delays and irreversible cognitive deficits in young children, reduced immune function and resistance to infection, impaired physical work

Key words: Fermented papaya preparation, iron supplementation, oxidative stress, young females

Mailing address: Prof. F. Marotta, MD, PhD, ReGenera, Research Group for Aging Intervention, Piazza Firenze, 12, 20154 Milano, Italy
Tel.: +39 02 4077243 Fax: +39 02 4077243
e-mail: fmarchimede@libero.it

0393-974X (2014)

performance and adverse pregnancy outcomes. Scholastically speaking, iron deficiency anemia (IDA) is a consequence of depletion of body iron stores due to decreased iron uptake or increased iron loss/use. Body iron content is imposed by controlling its entrance into the body through the gastrointestinal system rather than by controlling its excretion.

Indeed, the International Anemia Consultative Group (1) recommends a daily supplementation of 60 to 120 mg during pregnancy depending also on the prevalence of anemia among women of childbearing age in different geographical areas and such recommendations exceed the iron RDA for pregnant women by 2- to 3-fold (2). Iron stores can be replenished through oral and parenteral therapy. In asymptomatic and mildly symptomatic patients with IDA, oral iron replacement therapy has been the mainstay therapy. Oral supplemental iron therapy is less expensive and demanding than the parenteral route, does not have potential severe side effects and is more easily available for most patients. Various iron salts have been used, ferrous sulfate being the most common but the use of oral iron is primarily limited by its gastrointestinal side effects that are mediated by non-absorbed iron.

Although newer preparations have been claimed to have less side effects, ferrous sulfate is still the most commonly used oral iron preparation. Accordingly, no difference in efficacy and side effect profile were found among ferrous sulfate, ferrous gluconate, and ferrous fumarate in a randomized, double blind study (3). On the other hand, it is recognized that ''free iron'' stimulates lipid peroxidation which leads to cell and tissue damage (4) and this has also been shown in *in vivo* animal studies (5, 6). Moreover, only a few studies have been conducted to investigate the effect of iron supplementation on oxidative stress in humans and, despite some contradictory reports (7), most available clinical data suggest a detrimental role of uncontrolled iron supplementation (8, 9).
Recently, it has been shown that recommended doses of iron effective for improving Hb cause an increase of lipid peroxidation end products when used by non-anemic women with marginal iron status deficiency (10). A certified fermented papaya-based nutraceutical (FPP, Immun-Age®, ORI, Gifu, Japan, made under ISO 9001 and ISO 14001 obtained from a patented biofermentation process of non-OGM carica papaya) has been shown to possess effective redox-modulating properties either in *in vitro*, experimental and in clinical setting, as summarized in a recent review and with stronger antioxidant properties as compared to vitamin E and commercially available multivitamin preparations (11). In particular, as far as this study concerns, it has been shown by authoritative haematological and molecular biology research groups that it could effectively exert iron-chelating properties (12, 13). The aim of this study was to determine whether the concomitant supplementation of FPP together with iron supplementation in women with low iron stores for 12 weeks could mitigate systemic lipid peroxidation and intraluminal gut production of reactive oxygen species in human feces while testing treatment compliance and iron absorption as well.

MATERIALS AND METHODS

Subjects

Fifty-two non-pregnant women, aged 24-37, participated in the study. They were non-smokers, generally healthy, with regular weights for height, with blood hemoglobin >10.0 g/dL, and plasma ferritin <12 µg/dL at screening. All participants were not taking any drugs or supplements. At the checkup, before entering the study, those with diabetes mellitus (fasting blood sugar >126 mg/dl), hypercholesterolemia (fasting total cholesterol >220 mg/dl, low-density lipoprotein cholesterol >140 mg/dl, high-density lipoprotein cholesterol <40 mg/dl or triglycerides >150 mg/dl) or arterial hypertension (>140 mmHg systolic or >90 mmHg diastolic blood pressure) based on National Heart Lung and Blood Institute clinical guidelines were excluded from the study.

Subjects served as their own controls as pre-supplementation (baseline) results were compared with values measured during and at the end of supplementation. Written approval was obtained from all subjects before the study which conformed to the ethical guidelines of the 1975 Declaration of Helsinki.

Study design - diet and lifestyle questionnaire

A detailed lifestyle questionnaire was administered to all subjects who were instructed to refrain from intense physical exercise. Moreover, the web-based version of the National Institutes of Health Diet History Questionnaire (NIH DHQ) was used to assess diet history over the past month and along the study period. The NIH DHQ is a food frequency questionnaire (FFQ) consisting of 124 food items including also portion sizes. Data indicate that

this instrument provides reasonable nutrient estimates and sufficient reliability and validity. Patients were advised not to use any vitamin supplement, fortified food or tea while maintaining their usual diet and, in particular, keeping unmodified their intake of fibres and carbohydrates.

Patients were also instructed not to take any gastric acid inhibitory agent or over the counter antacid, unless specifically prescribed by their physician and to report this to the investigators team.

Supplementation regimen

The subjects were given iron supplements (100 mg Fe/d as ferrous sulfate) to be taken daily for 12 weeks, in the afternoon 2 h after lunch (group A). Group B patients were supplemented for 4 months also with 6g/day of FPP. The supplement, in the amount of 3g/sachet, was given in the morning before breakfast and in the afternoon. Venous blood was obtained on day 1 prior to supplementation (basal values) and repeated after 6 and 12 weeks of supplementation. However, the transferrin receptors (Tf R)/serum ferritin ratio was also checked at 8 weeks. Moreover, each volunteer was asked to collect 3 fecal samples at baseline, 6 and 12 weeks according to normal bowel habit for the below mentioned analysis.

Sample collection

Six milliliters of venous blood were drawn into trace metal-free polypropylene syringes from each subject at the time of recruitment and at scheduled observation period. Plasma was obtained by centrifugation, transferred into polyethylene tubes, divided into three aliquots and stored at -70°C until analysis. Four milliliters of whole blood were also transferred into heparin containing tube and then centrifuged at 3000 rpm for 15 min. The serum was separated and used to estimate iron and total iron binding capacity by a colorimetric assay using bathophenanthroline sulfonate and magnesium carbonate, whereas ferritin was tested by electrochemiluminescent immunoassay with a cobas 6000 (Roche Diagnostics), soluble transferrin receptor (sTfR) by sandwich ELISA (R&D Systems, UK) and malondialdehyde (MDA) by gas chromatography- mass spectrometry using the method of Yeo et al. (14). The red blood cells (RBCs) were lysed by mixing chilled water and RBC lysate was used for the evaluation of antioxidant enzymes namely superoxide dismutase (SOD) and glutathione peroxidase (GPx) by spectrophotometry.

Quantification of the total and free iron concentration in stool

The total iron concentration of the feces was measured after the feces collections were freeze-dried and then ashed in silica vessels at 480°C for 48 h. Afterwards, the ash was dissolved in concentrated hydrochloric acid and the solution diluted to an appropriate volume with distilled water.

Free iron, i.e. weakly bound iron, in feces was assessed by using a slightly modified method described by Simpson et al. (15). A pre-weighed sample of fecal homogenate containing 5 g feces (wet weight) was mixed with a measured volume of water to reach a final volume of 15 mL. This sample was centrifuged for 30 min at room temperature at 6000×*g* and the supernatant was retrieved. The pellet was then washed with a 10 mL water and centrifuged while the two supernatants were pooled and the total volume documented. The iron and free iron content of the resultant solutions were assessed by atomic absorption spectrophotometry and was expressed in micrograms per gram of native stool. This allowed to examine the relationship between free radical production in feces and the iron content in the intestinal lumen.

Analysis of oxidative stress in the feces

To determine the *in vitro* production of reactive oxygen species in the morning feces, the method based on dimethyl sulfoxide-methanesulfinic acid reaction was applied with slight modification (16). Each fecal sample (1-2 g) was incubated for 5 h at 37°C in tris-buffered saline (pH 7.0) containing 5% dimethyl sulfoxide, used as a scavenger for hydroxyl radicals (0.7 mol/L), glucose (0.1%), and Na_2EDTA (50 mmol/L) at 37°C. The sample was then centrifuged at 900 × *g* for 10 min at room temperature, the supernatant removed, and the protein removed as a precipitate by lowering the pH to 1.0 for 10 min by adding 12 mol HCl/L. The pH was then returned to 7.4, the sample was centrifuged at 900 × *g* for 10 min at room temperature and the supernatant was stored at −20°C before batch analysis of the methanesulfinic acid content. Standards were prepared before each assay, using 0-75 mmol methanesulfinic acid/L in the incubation medium. The control sample contained deferoxamin at the beginning of the incubation period to prevent the catalytical conversion of superoxide to the hydroxyl radical. After the reaction was halted with 500 µL deferoxamin (15 mmol/L), methane sulfinic acid was extracted and analyzed by straight phase HPLC to determine methane sulfinic acid. All samples were measured in triplicate.

Statistical Analysis

Normality of distribution was tested with the Kolmogorov-Smirnov test. Whenever distribution was not normal, data were log-transformed prior to analysis. Data are expressed as the mean±standard error of the mean (S.E.M.) of multiple determinations from an experiment. Statistical significance was determined by Student's *t*-test when two data sets were analyzed or, alternatively, by

ANOVA followed by the appropriate post hoc test for multiple data sets with the statistical software StatView (Abacus Concepts, Calabasus, CA, USA). Non-parametric methods were used to test for differences in proportions. *p*-values of <0.05 were considered statistically significant.

RESULTS

No subject was anemic at baseline and their hemoglobin and mean cell volume values were in the lower part of normal limits. At the entry, plasma iron, transferrin saturation and plasma ferritin were low (Table I). The dietary analysis did not reveal any excesses in the intakes of antioxidants or iron that might have influenced the antioxidant status of the participants (data not shown). No significant correlations was observed between estimated dietary intake of micronutrients and indicators of iron status and of baseline lipid peroxidation. After pooling together gastrointestinal complaints (nausea, constipation, abdominal cramps, diarrhea) it appeared that compared to group A, FPP-supplemented subjects showed a significantly lower degree of discomfort (Fig. 1, p<0.05). Although no drop out occurred, 19% (4/21) of group A subjects had to be shifted to iron administration during meals so to better tolerate the treatment and 9.5 % (2/21) were put on alternative days administration whereas no such events occurred in FPP-supplemented group (not statistically significant due to the limitation of data).

Starting from 6 weeks of supplementation, hemoglobin, mean cell volume and indices of iron status (serum iron, plasma transferrin saturation and serum ferritin) showed a statistically significant improvement which peaked at 12-week observation (p<0.001 *vs* baseline, Table I). There was no difference among the two groups although iron level in group B showed a not significant trend benefit as compared with group A.

As for group A, two subjects after 6 weeks and one subject after 8 weeks of supplementation were still slightly iron depleted whereas none of the above abnormalities appeared in FPP-supplemented group (group B) (data not shown, not statistically significant). Iron supplementation caused a significant decrease of TfR (p<0.05 *vs* baseline)

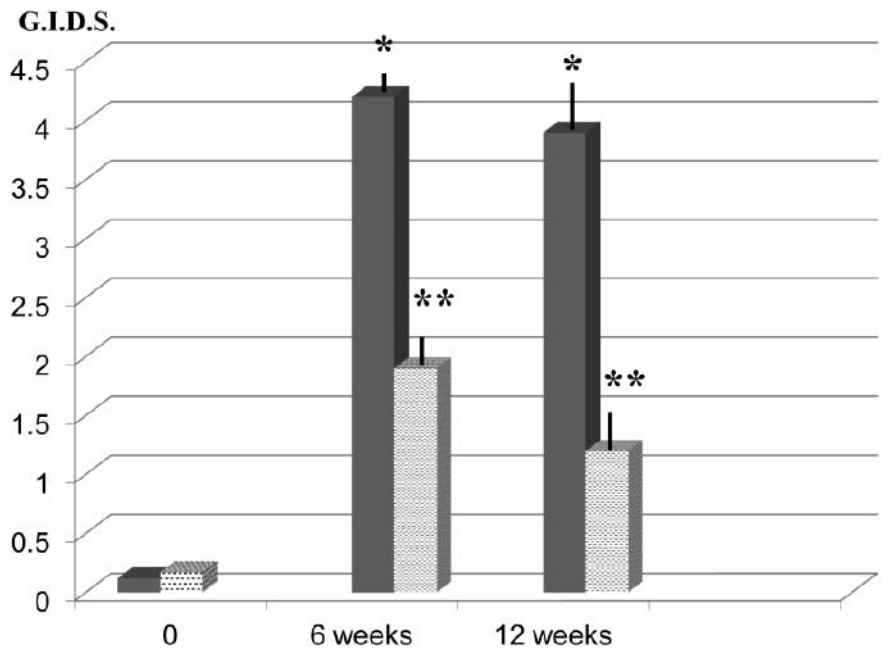

Fig. 1. *Gastointestinal discomfort during iron therapy: effect of nutraceutical supplementation with FPP. Black bars: iron supplemented subjects (group A); Dotted bars: subjects supplemented with iron and FPP (group B). G.I.D.S. (gastroin-testinal discomfort score) based on nausea, diarrhea, constipation, abdominal cramps, each graded 0 to 3 (1: light, 2: mild-moderate; 3: severe) *p<0.05.*

Table I. *Baseline values of relevant biochemistry examinations: effect of iron and iron plus FPP supplementation.*

	Group A		Group B	
	baseline	12 weeks	baseline	12 weeks
Hemoglobin (g/dL)	11.3 ± 0.3	12.6 ± 0.4	11.7 ± 0.6	13.4 ± 0.7
Mean red cell volume (*fL*)	74.8 ± 0.6	89.8 ± 0.7*	77.5 ± 0.5	92.3 ± 0.4*
Plasma Iron (µg/dL)	66.8 ± 12,3	104.8 ± 17.8*	71.2 ± 10.6	126.6 ± 21.3*
TIBC (µg/dL)	354 ± 73	394 ± 62	377 ± 56	389 ± 48
Ferritin (µg/dl)	9.8 ± 2.6	18.9 ± 3.7*	9.2 ± 4.3	21.6 ± 3.8*
sTfR(µg/ml)	3.8 ± 0.9	3.4 ± 1.1*	3.9 ± 0.8	3.3 ± 0.7*
Tr Saturation (%)	16.4 ± 2.7	26.9 ± 3.4*	15.7 ± 3.6	28.1 ± 3.4*
RBC SOD (U/L)	23.3 ± 4.4	16.1 ± 3,5*	21,9 ± 2,8	20.6 ± 4.2**
RBC GPx (U/g Hb)	34.7 ± 8,1	21.2 ± 4,4*	36.1 ± 7,3	31.3 ± 8,1**

*TIBP: plasma total iron-binding capacity; sTfR: Plasma transferrin receptors; Tr Saturation: plasma transferrin saturation; RBC: red blood cells. *p<0.01 vs baseline value; **p<0.05 vs group A.*

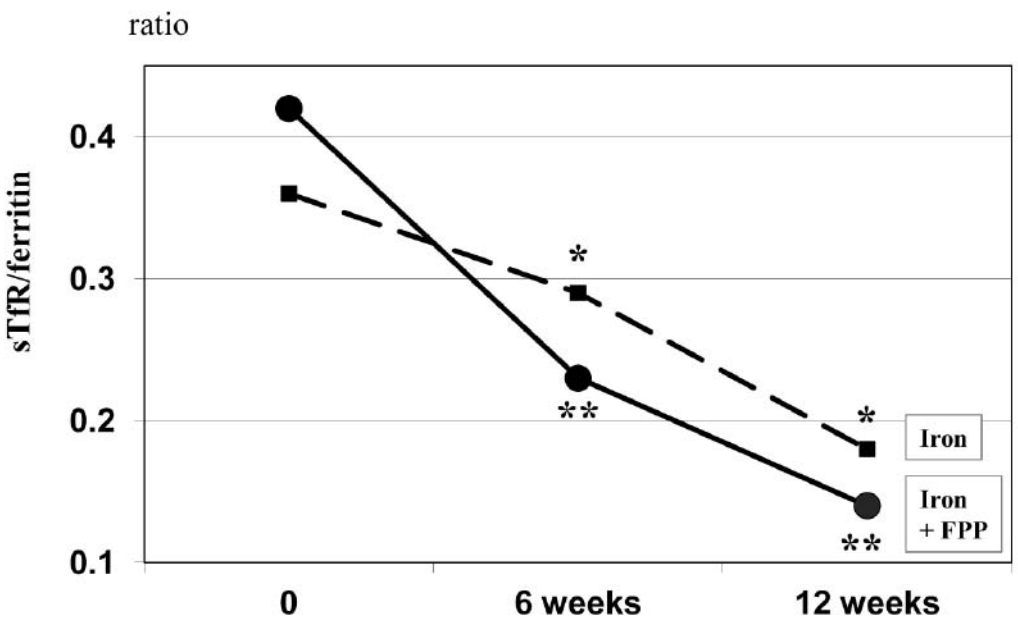

Fig. 2. *Time-course variation of sTfR/ferritin ratio during iron supplementation: effect of concomitant administration of FPP Squared indicators: iron supplemented subjects (group A); Round indicators: subjects supplemented with iron and FPP (group B). sTfR: soluble transferrin receptor. *p<0.01 vs baseline value; **p<0.05 vs group A.*

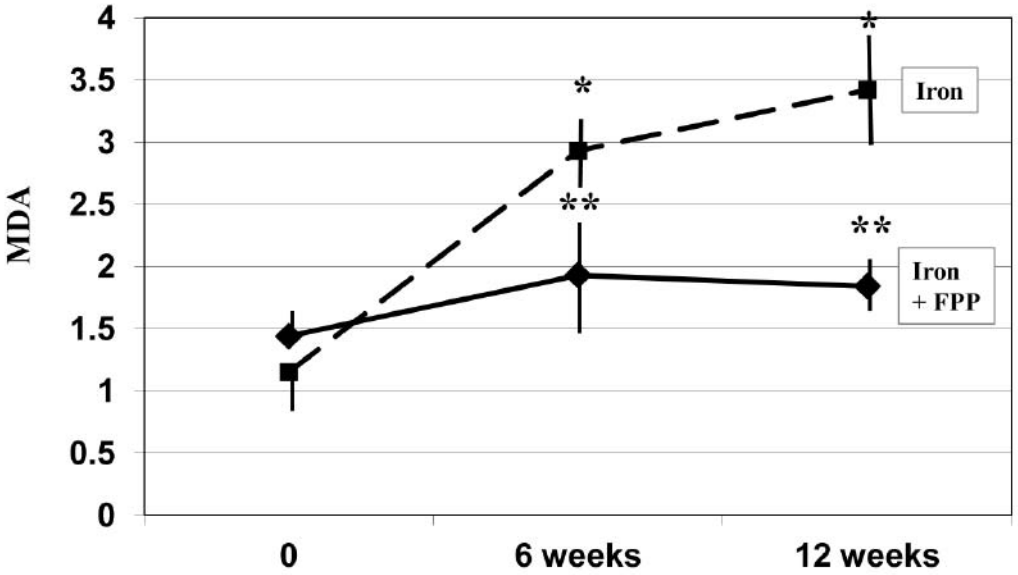

Fig. 3. *Plasma time-course MDA level in subjects administered iron therapy: effect of iron and iron plus FPP supplementation Squared indicators: iron supplemented subjects (group A); Round indicators: subjects supplemented with iron and FPP (group B). MDA: malondialdehyde. *p<0.001 vs baseline value; **p<0.01 vs group A.*

ranging from 10 % to 12% and without significant differences between the two groups. However, when looking at the Tfr/ferritin ratio, although both groups followed a comparable dietary intake, it appeared that the decrease of plasma TfR was more significant in group B ($p<0.05$ *vs* group A, Fig. 2). These data showed a significant inverse correlation with MDA (r: 0.73, $p<0.05$).

The study of systemic oxidative stress status revealed that iron supplementation brought about an increasing imbalance or redox status with a significant time-course increase of MDA ($p<0.001$ *vs* baseline values, Fig. 3) and depletion of SOD and GPx ($p<0.01$ *vs* baseline values, Table I). This phenomenon significantly appeared already at 6 weeks and displayed a further increase at 12 weeks observation. The co-administration of FPP totally abolished such phenomena ($p<0.01$ *vs* group A).

Fecal Iron Concentration

Total fecal non-heme iron in stool samples collected prior to iron supplementation was ranging from 280 to 324 mg/g dry weight and this value significantly changed during supplementation ($p<0.001$, Fig. 4a). However, under nutraceutical co-administration it appeared a partial but significant decrease ($p<0.05$ *vs* group A). The same pattern occurred also when testing the free iron concentration (Fig. 4b) where the concomitant administration of nutraceutical confirmed to yield a significant reduction of this parameter ($p<0.05$ *vs* group A).

In vitro assay of fecal oxidative stress

The reactive oxygen species (ROS) generation in fecal samples following iron supplementation is shown in Figure 5. ROS generated in stools during iron supplementation were significantly elevated when compared to baseline values ($p<0.001$). This phenomenon occurred already starting from the 6 weeks observation period and gradually increased with time with a 12-week value further enhanced ($p<0.05$ *vs* 6-week supplementation period). Such increased generation was significantly blunted in the group co-administered FPP (group B) where values

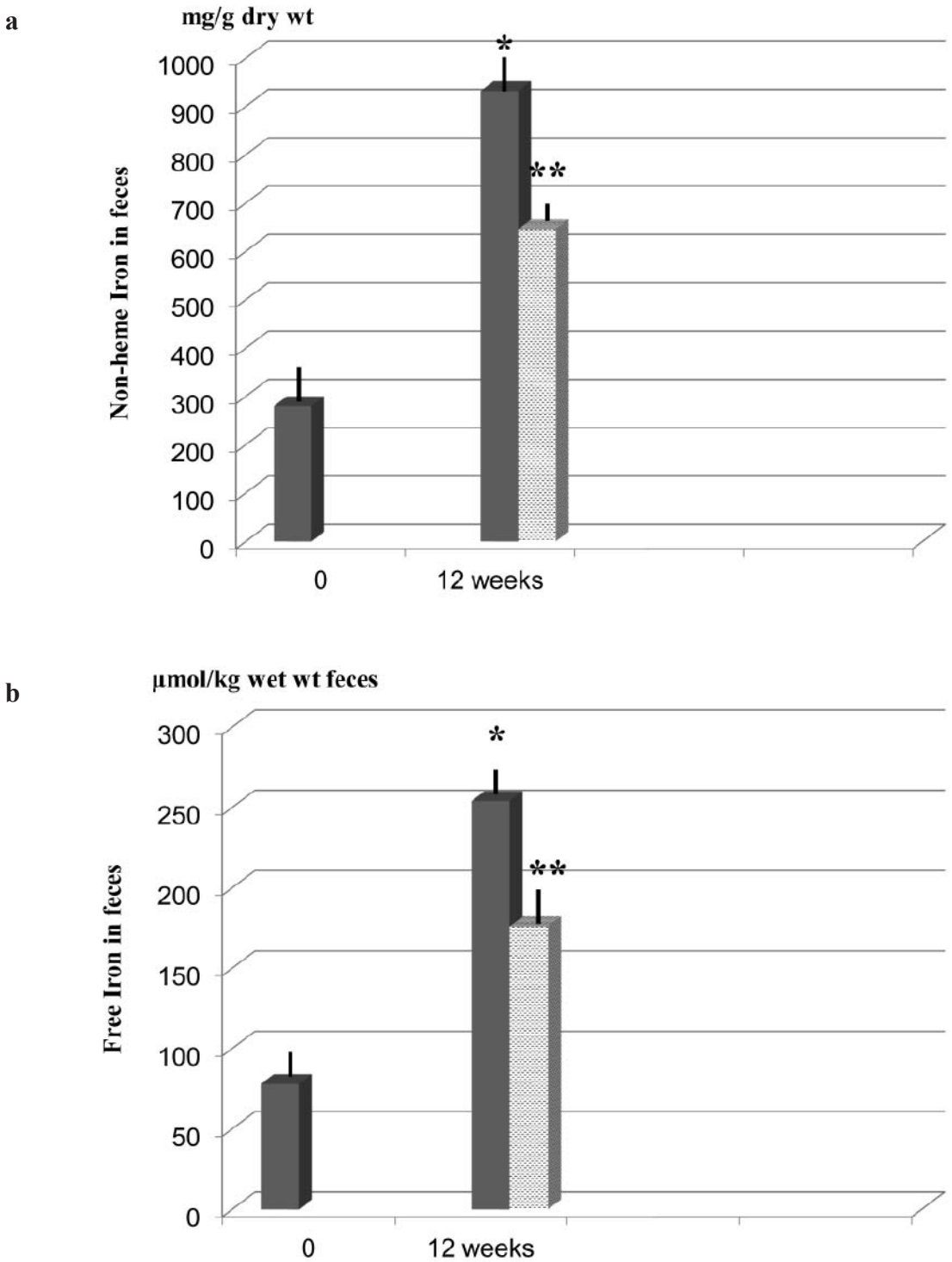

Fig. 4. *Level of non-heme iron and free iron in feces of hyposideremic females: effect of iron and iron plus FPP supplementation. Estimation of fecal level of non-heme iron (**a**) and of free iron (**b**). Black bars: iron supplemented subjects (group A); Dotted bars: subjects supplemented with iron and FPP (group B). *p<0.01 vs baseline value; **p<0.05 vs group A.*

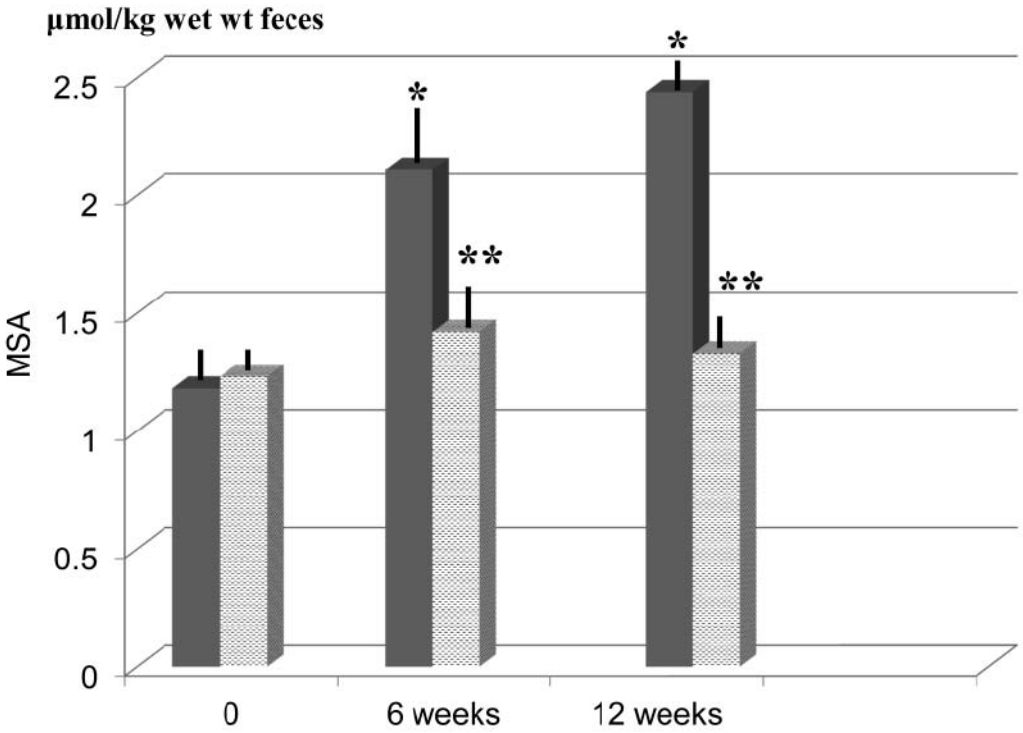

Fig. 5. *Time-course variation of in vitro Assay of Free Radical Production from feces in subjects administered iron therapy: effect of iron and iron plus FPP supplementation Black bars: iron supplemented subjects (group A); Dotted bars: subjects supplemented with iron and FPP (group B). MSA: methanesulfinic acid. *p<0.001 vs baseline value; **p<0.01 vs group A. The time-course increase of MSA level noted in A group didn't reach a statistical significance. Values for B group recorded at 6 and 12 weeks were not statistically different from baseline.*

showed a slight not-significant trend increase.

DISCUSSION

Daily iron supplementation has been traditionally a standard practice for preventing and treating anaemia and, for instance, iron supplements are generally recommended to pregnant women in most countries at doses ranging from 30-120 mg/day (1). However, its long term use may be limited by its associated adverse side effects. A large Cochrane survey has concluded that intermittent iron supplementation in menstruating women is a feasible intervention in settings where daily supplementation is not amenable for a number of reasons (17). However, in comparison with daily supplementation, the intermittent provision of iron supplements has been found to be less effective in preventing or controlling anaemia. Moreover, besides the clinically overt and easily recognizable side effects, one has also to consider possible subtly detrimental actions whose short-term impact is not known as yet but which deserves special attention in the long term. Indeed, it is known that unabsorbed dietary iron enters the colon and by interacting with intraluminal bacteria may become available for Haber-Weiss and Fenton-type reactions that generate hydrogen peroxide and hydroxyl radicals at the mucosal surface (8). Such phenomena at a mucosal level may be associated also to increased production of carcinogens and very recent epidemiological evidence supports the hypothesis that heme iron present in meat promotes colorectal cancer through either a catalytic effect on the endogenous formation of carcinogenic N-nitroso compounds and/or the formation of cytotoxic and genotoxic aldehydes by lipoperoxidation (18).

Overall, consumption of 100 mg of daily iron as ferrous sulfate improved the iron status of women with low iron stores and at the end of the study, plasma ferritin increased by 92-117%, plasma transferrin saturation by 39-44%, hemoglobin by 10-12% and plasma level of iron normalized too. At baseline, all women were chosen to be iron deficient and as a group, these women exhibited normal levels of MDA and regular intake of dietary antioxidants and minerals. A substantial increase in markers of lipid peroxidation occurred during iron supplementation suggesting an ongoing oxidative stress. These data are consistent with previous studies in animals and humans. Although some controversies exist (7) probably explained by different iron dosages, duration of treatment and/or markers of oxidative stress used, a recent study has clearly demonstrated that supplemental oral iron intake at usual recommended doses for correcting iron deficiency may turn to be excessive as judged by elevated generation of lipid peroxidation products (19).

Indeed, supplementation with only 19 mg of iron per day as ferrous sulfate for 2 weeks has been shown to be capable to increase the concentration of weakly bound iron and the production of free-radicals in feces of adult men and women (8). It is then very likely that the repeated administration of supplemental ferrous sulfate brought about an increased free radicals formation with a vicious cycle of oxidative stress, lipid peroxidation and gut inflammation explaining why plasma MDA levels exhibited a time-course increase along the study. This finding further implies that no adaptation to the damage being caused by the daily intake of normally prescribed dosages of iron occurred. Moreover, MDA showed a significant inverse correlation with the efficiency of iron stores deposition, as judged by TfR/ferritin ration. Plasma ferritin is an acute phase protein and thus its value may not accurately reflect the iron status in the presence of infection or inflammation. It comes that the about 100% increase we observed in plasma ferritin during the study may be partly an epiphenomenon consequent to gut mucosal free radical generation with unabsorbed iron (7) and/or the systemic oxidative stress. Moreover, serum ferritin is limited in its use as a measure of the magnitude of an iron depletion because, unlike sTfR concentration, values maintain a stable level once the iron stores are exhausted (20).

The sTfR concentration is increased because more TfRs are expressed on the surfaces of cells that require additional iron. Interestingly, nutraceutical co-administration proved to yield a more significant iron stores when evaluated as TfR/ferritin ration, as compared to iron supplementation alone. Indeed, sTfR:SF ratio has been proposed as a specific evaluation of the complete distribution of iron-status and it has been found to have a good agreement between the estimated prevalence of iron deficiency and the previously described multiple indicator index in preschool children and women of childbearing age by using samples from the US NHANES 2003-2006 (21). Thus the slightly higher concentration of iron status parameters in this group, although some values didn't reach a statistical significance, together with the significantly reduced concentration of fecal iron may be tentatively interpreted as the result of a better absorption and/or transport of iron. In conclusion, supplementation with 100 mg iron per day increased indicators of lipid peroxidation in non-anemic, iron-depleted women.

Therefore, this regimen of supplemental iron as such may provide excessive amounts of iron and appears to increase the risk of oxidative stress and this equally applies to the different iron oral formulations tested (22) while the intravenous route may elicit an acute endothelial dysfunction (23). On the other hand, we have shown that the co-administration of FPP significantly mitigated these phenomena while allowing a better compliance and iron absorption. This holds of interest when considering that the association of vitamin C to enhance the bioavailability of supplemental iron has been shown to result in uncontrolled lipid peroxidation with potential adverse effects for the mother and the fetus. (24).

Although we didn't address the psychological stress factor in the present study, it is worth mentioning that very recent experimental work has shown that iron supplements further aggravated iron deposition and oxidative stress injury to the liver induced by the stress exposure. Moreover, during stress exposure, glucose-related stress hormones are negatively affected by iron supplementation which, on its turn further worsens iron deposition and oxidative stress in the liver and brain while impairing stress adaptative mechanisms (25). Interestingly, we have recently shown that FPP might

significantly mitigate psychological stress-induced redox imbalance (30). While dietary and supplemental iron remain important interventions considering that prevalence of iron deficiency among female adolescents (26), recreational athletes (27) and military recruits (28), a judicious clinical evaluation (29) and possibly a supportive nutraceutical co-administration, as our data suggest, should be carefully considered. Finally, although we didn't investigate heme-iron absorption, we have also to consider that a large number of proteins are involved and, among them, heme-iron which is taken up by heme carrier protein and its internalisation in the cytoplasm is partly linked to heme-oxygenase. The iron released from heme passes to the basal cytoplasm and is transported across the basal membrane by ferroportin, oxidized to ferric-iron and transported in the plasma by transferrin. Given that we have shown in clinics the beneficial HO-modulating properties of FPP (30), this might represent a further positive mechanism triggered by FPP to be ascertained while broader application in gastrointestinal diseases may warrants further investigations. This is also considering that over 30% of the world's population are anaemic and in developing countries every second pregnant woman and about 40% of preschool children are estimated to be anaemic.

However, it is difficult to gather precise estimations but, regarding pregnant women, for example, the prevalence is roughly 73%, 50%, 42%, 35% and 25% in South-East Asia, Africa, Western Pacific, Americas and Europe, respectively (WHO report 1998, http://www.who.int/topics/anaemia/en/). Indeed, future trial with this nutraceutical should be specifically directed to pregnant women who carry a higher risk of miscarriage when anaemic. Gut flora investigation could provide further information in the understanding of iron absorption and interaction with nutraceutical interventions. Finally, although we didn't compare the nutraceutical intervention against higher antioxidant-rich food intake, it is unlikely that the latter, besides its questionable feasibility, is unlikely to exhibit a better performance and significant epigenomic effect (31) as shown by the nutraceutical employed (11).

REFERENCES

1. CDC. Recommendations to prevent and control iron deficiency in the United States. Center for Disease Control and Prevention. Morb Mortal Wkly Rep 1998; 47:1-29.
2. Institute of Medicine, Dietary Reference Intakes. The Essential Guide to Nutrient Requirements. Washington, DC: National Academy Press 2006.
3. Hallberg L, Ryttinger L, Sölvell L. Side-effects of oral iron therapy. A double-blind study of different iron compounds in tablet form. Acta Med Scand Suppl 1966; 459:3-10.
4. Lu N, Li X, Li J, Xu W, Li H, Gao Z. Nitrative and oxidative modifications of enolase are associated with iron in iron-overload rats and in vitro. J Biol Inorg Chem 2011; 16:481-90.
5. Younes M, Eberhardt I, Lemoine R. Effect of iron overload on spontaneous and xenobiotic-induced lipid peroxidation in vivo. J Appl Toxicol 1989; 9:103-8.
6. Zhang Y, Huang Y, Deng X, Xu Y, Gao Z, Li H. Iron overload-induced rat liver injury: Involvement of protein tyrosine nitration and the effect of baicalin. Eur J Pharmacol. 2012; 680:95-101.
7. Binkoski AE, Kris-Etherton PM, Beard JL. Iron supplementation does not affect the susceptibility of LDL to oxidative modification in women with low iron status. J Nutr 2004; 134:99-103.
8. Lund EK, Wharf SG, Fairweather-Tait SJ, Johnson IT. Oral ferrous sulfate supplements increase the free-radical-generating capacity of feces from healthy volunteers. Am J Clin Nutr 1999; 69:250-5.
9. Proteggente AR, England TG, Rice-Evans CA, Halliwell B. Iron supplementation and oxidative damage to DNA in healthy individuals with high plasma ascorbate. Biochem Biophys Res Comm 2001; 288:245-51.
10. Tiwari AK, Mahdi AA, Chandyan S, Zahra F, Godbole MM, Jaiswar SP, Srivastava VK, Negi MP. Oral iron supplementation leads to oxidative imbalance in anemic women: a prospective study. Clin Nutr 2011; 30:188-93.
11. Marotta F, Catanzaro R, Yadav H, Jain S, Tomella C, Polimeni A, Mantello P. Functional foods in genomic medicine: a review of fermented papaya preparation research progress. Acta Biomed. 2012; 83:21-9.
12. Prus E, Fibach E. The antioxidant effect of fermented papaya preparation involves iron chelation. J Biol

Regul Homeost Agents 2012; 26:203-10.
13. Fibach E, Tan ES, Jamuar S, Ng I, Amer J, Rachmilewitz EA. Amelioration of oxidative stress in red blood cells from patients with beta-thalassemia major and intermedia and E-beta-thalassemia following administration of a fermented papaya preparation. Phytother Res 2010; 24:1334-8.
14. Yeo HC, Helbock HJ, Chyu DW, Ames BN. Assay of malondialdehyde in biological fluids by gas chromatography-mass spectrometry. Anal Biochem 1994; 220:391-6.
15. Simpson RS, Sidhar S, Peters TJ. Application of selective extraction to the study of iron species present in diet and rat gastrointestinal tract contents. Br J Nutr 1992; 67:437-44.
16. Steiner MG, Babbs CF. Quantitation of the hydroxyl radical by reaction with dimethyl sulfoxide. Arch Biochem Biophys 1990; 278:478-81.
17. Fernández-Gaxiola AC, De-Regil LM. Intermittent iron supplementation for reducing anaemia and its associated impairments in menstruating women Cochrane Database Syst Rev. 2011; 12:CD009218.
18. Bastide NM, Pierre FH, Corpet DE. Heme iron from meat and risk of colorectal cancer: a meta-analysis and a review of the mechanisms involved. Cancer Prev Res Phila 2011; 4:177-84.
19. Orozco MN, Solomons NW, Schümann K, Friel JK Response of urinary biomarkers of systemic oxidation to oral iron supplementation in healthy men. Food Nutr Bull 2012; 33:53-62.
20. Skikne BS, Flowers CH, Cook JD. Serum transferrin receptor: a quantitative measure of tissue iron deficiency. Blood 1990;75:1870-6.
21. Cogswell ME, Looker AC, Pfeiffer CM. Assessment of iron deficiency in US preschool children and nonpregnant females of childbearing age: National Health and Nutrition Examination Survey 2003-2006. Am J Clin Nutr 2009; 89:1334-42.
22. Orozco MN, Arriaga C, Solomons NW, Schümann K. Equivalent effects on fecal reactive oxygen species generation with oral supplementation of three iron compounds: ferrous sulfate, sodium iron EDTA and iron polymaltose. Ann Nutr Metab 2012; 60:108-14.
23. Rooyakkers TM, Stroes ES, Kooistra MP, van Faassen EE, Hider RC, Rabelink TJ, Marx JJ. Ferric saccharate induces oxygen radical stress and endothelial dysfunction in vivo. Eur J Clin Invest 2002; 32(S)1:9-16.
24. Lachili B, Hininger I, Faure H, Arnaud J, Richard MJ, Favier A, Roussel AM. Increased lipid peroxidation in pregnant women after iron and vitamin C supplementation. Biol Trace Elem Res 2001; 83:103-10.
25. Feng Y, Qi R, Xu M, Shen Z, Li M. Dietary iron supplements may affect stress adaptation and aggravate stress hyperglycemia in a rat model of psychological stress. Nutrition 2012; 28:691-7.
26. Marotta F, Naito Y, Padrini F, et al. Redox balance signalling in occupational stress: modification by nutraceutical intervention. J Biol Regul Homeost Agents 2011; 25:221-9.
27. Cooper MJ, Cockell KA, L'Abbé MR. The iron status of Canadian adolescents and adults: current knowledge and practical implications. Can J Diet Pract Res 2006; 67:130-8.
28. Di Santolo M, Stel G, Banfi G, Gonano F, Cauci S. Anemia and iron status in young fertile non-professional female athletes. Eur J Appl Physiol 2008; 102:703-9.
29. Israeli E, Merkel D, Constantini N, Yanovich R, Evans RK, Shahar D, Moran DS. Iron deficiency and the role of nutrition among female military recruits. Med Sci Sports Exerc 2008; 40(11):685-90.
30. Schümann K, Ettle T, Szegner B, Elsenhans B, Solomons NW. On risks and benefits of iron supplementation recommendations for iron intake revisited. J Trace Elem Med Biol 2007; 21:147-68.
31. Møller P, Vogel U, Pedersen A, Dragsted LO, Sandström B, Loft S. No effect of 600 grams fruit and vegetables per day on oxidative DNA damage and repair in healthy nonsmokers. Cancer Epidemiol Biomarkers Prev 2003; 12:1016-22.

THE USE OF ENGINEERED BIOMATERIAL BONE PLEXUR M® IN BENIGN EPIPHYSEAL TUMORS: OUR EXPERIENCE AT 20 MONTHS OF FOLLOW-UP

C. ZOCCALI, V. ANELLI, G. CHICHIERCHIA, F. ERBA and R. BIAGINI

Regina Elena National Cancer Institute, Rome, Italy

Received February 14, 2013 – Accepted February 14, 2014

The objective is to reconstruct the subchondral bone after curettage of benign tumors located in the epiphysis, a relevant topic in oncological orthopedics. Several bones substituted are commercially available, yet none of these are suitably moldable to repair or be placed in the bone defect; although autologous bone for little defects and homologous for bigger defects are still considered the standard in reconstruction, we verify the ability to adapt and support articular cartilage through the application of Plexur M®, a newly engineered biomaterial bone. In the present study, we enrolled the first ten consecutive cases referred to our department, where patients were affected by a benign epiphyseal tumor destroying the subchondral bone through to the articular cartilage. Every patient underwent curettage of the disease, apposition of a newly engineered biomaterial bone and filling with homologous morselized bone. The quality of reconstruction was evaluated by two surgeons and by a radiologist based on the achievement of surgical objectives and comparing pre and postoperative imaging. In seven out of eight cases of lesions located in the lower limbs the quality of reconstruction was considered good, restoring an adequate support to the articular cartilage. The quality of the remaining case was considered poor probably due to the extent of the spread of the disease, which destroyed the entire proximal tibial epiphysis. In the two cases where the disease was located in the upper limbs, the Plexur M® application restored support to the articular cartilage sufficiently well. However, in the case of a giant cell tumor of the distal radial epiphysis there was a slight reabsorption of the morselized homologous bone. Our series suggest that Plexur M® should be considered a valid option for orthopedic surgeons in restoring adequate mechanical support to the articular cartilage; nevertheless, considering its high cost, its use might be reserved to selected cases until further studies can verify the integration process, the effects on the survival of the articular cartilage and on the prevention of premature osteoarthritis.

Several benign bone tumors arise near the joint surface, probably due to higher levels of meta-epiphysis biological activity. Often tumors are diagnosed when the subchondral bone is damaged and the cartilage is the only layer opposing joint invasion.

Usual treatment consists in curettage of the lesion and filling of the residual cavity with autologous bone for little gaps and with homologous bone or cement for bigger ones (1, 2).

The bone graft can be morselized, making the filling of the bone gap easier especially in complex shaped defects. To assure mechanical stability, autologous or homologous cortical struts can be placed under the cartilage but, unfortunately, in some cases, they are not suitable to adapt to the defect

Key words: subchondral bone reconstruction, curettage, giant cell tumor, Plexur M, bone substitute, benign bone tumor

Mailing address: Dr. Carmine Zoccali,
IFO - Regina Elena National Cancer Institute,
Via Elio Chianesi, 53, 00144, Rome Italy;
University of L'Aquila, Surgical Science Department
Via ospedale S. Salvatore 6, 67100 L'Aquila, Italy
Tel.: +39 338 6355040 Fax: +39 06 52662778
e-mail: carminezoccali@libero.it

0393-974X (2014)

or restore support to the articular cartilage, and probably biological support to the cartilage is also limited (3). In addition, even if the cement presents local adjuvant activity, it reduces segment resistance so that stabilization is often necessary (4, 5).

In this paper, we present preliminary findings in 10 cases, at 20 months of follow-up proposing the use of Plexur M® (PM), an engineered biomaterial bone which is moldable when heated and particularly suitable in restoring complex bone gaps and maintaining the articular cartilage when the subchondral bone is destroyed by the tumor.

MATERIALS AND METHODS

In this retrospective observational study, we enrolled the first ten consecutive cases that were referred to the Oncological Orthopedic Department of Regina Elena National Cancer Institute of Rome from September 2010 to September 2012. Patients were affected by a benign epiphyseal tumor destroying the subchondral bone. In these cases, PM was applied to sustain articular cartilage after curettage. Morselized homologous bone and at times cortical struts were used to fill the curetted area.

The group was composed of 8 males and 2 females, with a median age of 17 years (12-44). Six cases were diagnosed with Giant Cell Tumor (GCT), 4 with primary tumors (of which 2 in the proximal epiphysis of the tibia, 1 in the distal radius epiphysis, 1 in the proximal humeral epiphysis) and 2 had local relapses (proximal tibial epiphysis), 3 cases had chondroblastoma, in the proximal and distal femur and in the proximal tibia, 1 case presented an Aneurismal Bone Cyst (ABC) of the pelvis (Table I).

Pre-operative radiological evaluations by means of X-ray, MRI and CT scan were carried out for each patient; biopsies were performed in all cases before surgery to confirm any possible clinical suspicions. Curettage, followed by the local application of phenol as local adjuvant treatment was carried out in all cases. Reconstruction was performed with PM placed beneath the cartilage and homologous morselized bone in 7 out 10 cases. In the other 3 cases, bone struts were necessary to provide mechanical stability to the reconstruction. In one case, which presented a GCT recurrence of the proximal tibia, resorbable bone cement consisting of a resinous biomaterial, was added to restore the tibial anatomy that was totally destroyed.

After meticulous curettage of the disease, the bone defect was regulated with a high power drill followed by the application of phenol as a local adjuvant treatment to increase margins (Fig. 1A). Reconstruction was performed in every case by applying the PM (Fig. 1B) and the morselized bone graft (Fig. 1C). In 8 out of 10 cases 10cc. of PM was sufficient to restore the subchondral bone. In the case of the giant ABC of the Pelvis 20 cc was necessary; in the case of the distal femur chondroblastoma 5 cc was sufficient. The PM was heated for 6 min and then modeled to restore normal anatomy under articular cartilage. The morselized bone was then used to fill the entire residual defect. In some cases another segment of the PM was used to close the medullary canal or the cavity access, in an attempt to reduce spillage into the diaphysis and into soft tissue, respectively (Fig. 2D).

Weight bearing was forbidden for approximately 6-8 months because the PM could go through the remodeling phase at four months from surgery. An X-ray was performed in post-operative days, at 3, 6, 9, 12, 18 and 24 months.

MRIs and CT scans were alternately performed every 3 months for the first 12 months, in order to verify osteo-integration and any possible inflammatory reaction. Successively MRI was performed at 18 months and CT at 24 months of follow-up. The average follow-up was 20 months.

The results of the reconstruction were based on the findings of the two orthopedic surgeons who performed the procedure and of on expert radiologist evaluating pre and post-operative imaging.

The quality of reconstruction was considered good if every one of the following objectives was reached: complete filling of subchondral defect, complete restoring of the joint aspect, total respect of ligaments and tendons insertions, considered sufficient if only 1 of the above objectives was not achieved, poor in the other cases.

After 1 year of caring for the tenth patient, our cohort was reviewed in order to verify whether our indications could be suitable in evaluating the preliminary results. The procedures performed were in accordance with the ethical standards of the committee responsible for experiments involving humans (institutional and national) and with the 1975 Helsinki Declaration, revised in 2000.

RESULTS

Eight out of 10 cases were affected by a lesion located in the lower limbs. In 7 out of 8 cases adequate support to the cartilage surface was restored. Total consensus was reached by all 3 judges. In the eighth case, the result was reputed poor by all 3 experts. This poor result may be due to the fact that the patient had a very aggressive local recurrence of GCT of the proximal tibia with subtotal destruction. At 6 months follow-up the patient had a further local relapse and is taking Denosumab which caused a

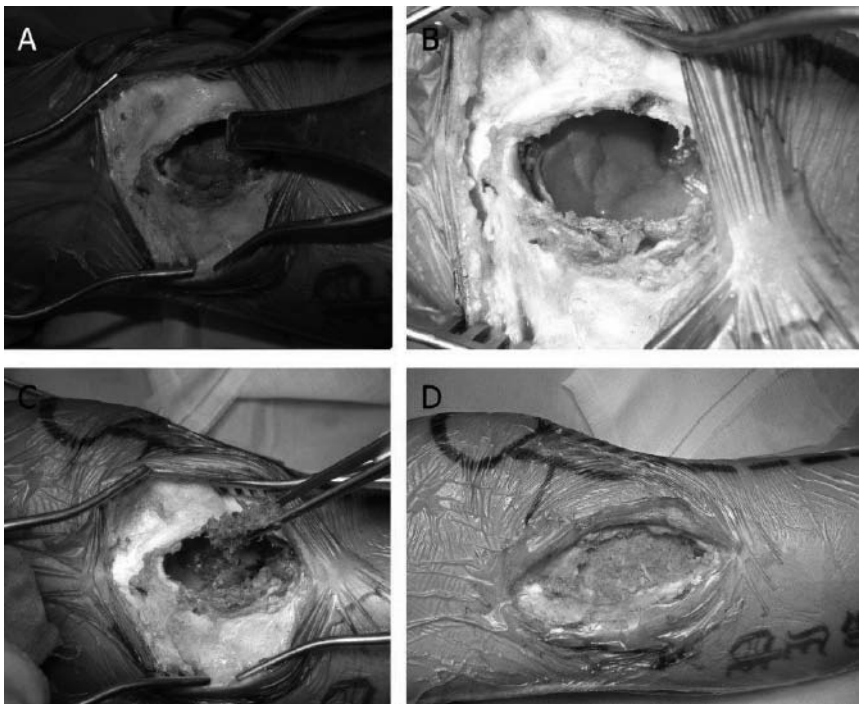

Fig. 1. ***A)****: intraoperative picture showing the inferior aspect of the tibial cartilage after meticulous curettage of a GCT;* ***B)****: the reconstruction of subchondral bone with PM;* ***C)****: application of morselized homologous bone;* ***D)****: the cavity fully filled.*

calcification and regression of the disease and allows weight bearing without pain, postponing the decision to undergo a proximal tibial replacement in case of a future no response. In one out of 7 cases, where the joint surface was successfully restored in a 12-year old patient who was affected by a chondroblastoma of the distal femoral epiphysis, bore weight too early. The patient had a slight collapse which was evident at an MRI scan performed at three months of follow-up without causing any clinical effects. In the case of chondroblastoma of proximal femoral epiphysis at 5 months of follow-up, a hip synovitis was reported with intense local pain increased by motion resolved with systemic steroid therapy. In one case of GCT of the proximal tibia, a spot recurrence was detected at 12 months of follow-up and treated with radiofrequency thermoablation. At 3 months of follow-up from this procedure the patient is asymptomatic and total weight bearing.

Two out of 10 cases were affected by a lesion in the upper limbs. In the case of GCT of the distal radius, partial bone chip reabsorption was observed but no clinical problems were noted. This may possibly be associated to an inflammatory reaction. In the second case of a GCT of the distal humerus, reconstruction was good, albeit the patient actually had a limited ROM also because pre and post surgical immobilization postponed the kinesitherapy, causing a slow recovery.

Figure II shows preoperative and postoperative X-rays in 4 patients. These results evidence the possibility in guaranteeing a successful reconstruction.

DISCUSSION

Osteoarthritis is the most prevalent of joint disease; its pathology is characterized by the degeneration of articular cartilage, sclerosis of subchondral bone and osteophyte formation. Several authors turned their attention to the mechanical and biological role of subchondral bone in developing osteoarthritis, even if it is unknown today whether the “primum movens” is in the cartilage or in the

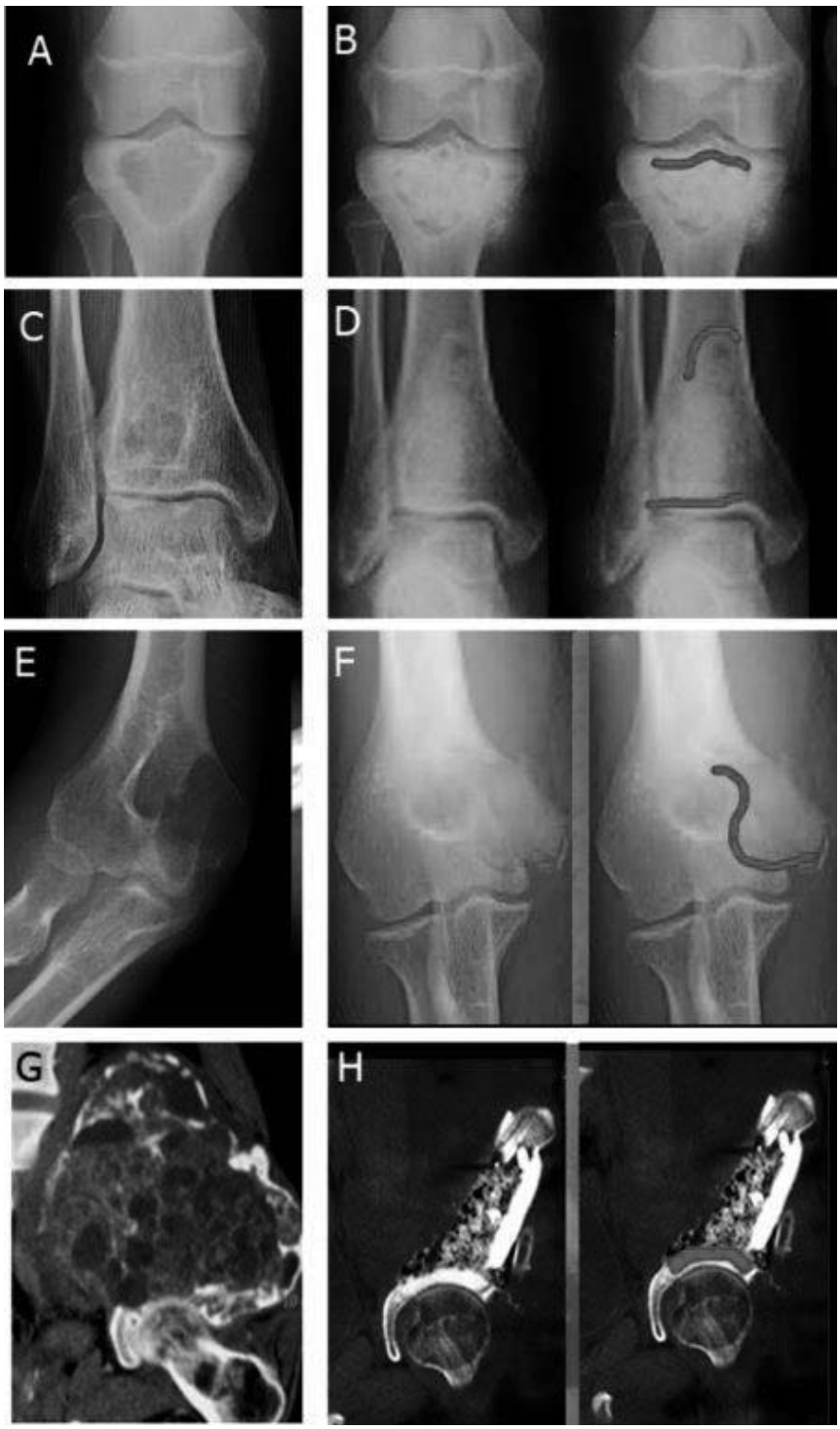

Fig. 2. ***A)****: X-ray showing chondroblastoma of proximal tibial epiphysis;* ***C)****: X-ray showing a local relapse of a GCT of distal epiphysis of tibia;* ***E)****: X-ray showing a GCT of distal humeral epiphysis;* ***B-D-F)****: post-operative X-ray showing the filled cavity and the position of PM in red;* ***G)****: CT-scan showing an ABC of the left hemipelvis;* ***H)****: post-operative CT-scan showing the reconstruction of the acetabular roof with PM in red, morselized homologous bone and cortical struts.*

Table I. *The epidemiological clinical characteristics and follow-up of the patients.*

PZ	Age	Sex	Diagnosis	Site	Surgery	Complications	Follow-up	Results
1	16	M	ABC	Left hemipelvis	Curettage/ Intralesional resection, phenol, reconstruction with morselized homologous bone, sticks, PM and screws		34	Total weight baring, asymptomatic
2	17	M	Chondroblastoma	Left femur proximal epiphysis	Curettage, phenol, reconstruction with morselized homologous bone and PM	Synovitis at 5 months from surgery	23	Total weight baring, asymptomatic
3	44	F	GCT (relapse)	Right tibia distal epiphysis	Curettage, phenol, reconstruction with morselized homologous bone and PM		23	Total weight baring, asymptomatic
4	21	M	GCT	Left radius distal epiphysis	Curettage, phenol, reconstruction with morselized homologous bone and PM		20	Total range of motion, no pain
5	12	M	Chondroblastoma	Left femour distal epiphysis	Curettage, phenol, reconstruction with morselized homologous bone and PM	Collapse at 3 months from surgery	19	total weight baring, asympthomatic
6	12	F	Chondroblastoma	Right tibia proximal epiphysis	Curettage, phenol, reconstruction with morselized homologous bone and PM		19	Total weight baing, meniscal degeneration
7	17	M	GCT (relapse)	Right tibia proximal epiphysis	Curettage, phenol, reconstruction with morselized homologous bone, struts, PM and Kryptonite™	Recurrence at 6 months	19	total weight baring, asympthomatic, under medical therapy with Denosumab
8	37	M	GCT	Right humerus distal epiphysis	Curettage, phenol, reconstruction with morselized homologous bone and PM		17	ROM decreased; under kinesitherapy, no pain
9	36	M	GCT	Right tibia proximal epiphysis	Curettage, phenol, reconstruction with morselized homologous bone and PM	Recurrence at 12 months treated by	15	total weight baring, asympthomatic
10	34	M	GCT	Left tibia proximal epiphysis	Curettage, phenol, reconstruction with morselized homologous bone, struts and PM		15	Total weight baring, asymptomatic

subchondral bone (6-8).

The role of the subchondral bone is also evident in a recent paper published by Xu et al. which reports how the percentage of developing osteoarthritis after curettage of giant cell bone tumor is higher in patients where reconstruction was done with cement than in those where reconstruction was done with bone grafting (9).

Considering the mechanical and trophic role of the subchondral bone, its restoration is essential for a good outcome after curettage of tumors located in the epiphysis.

Even if morselized bone probably presents a better metabolic activity and allows to completely fill the bone gap, it has no primary mechanical stability. Alternatively, cortical strut allograft is used to assure mechanical support even if it probably has an insufficient biological activity.

Autologous bone graft from iliac crest or other segments, is still the gold standard for filling bone defects because of its osteoinductive and osteoconductive properties but it can present problems related to pain and complications of donor site and to the amount of tissue available. Homologous graft doesn't have this problem and it can be used to fill big defects and associated to major resorption and lesser osteoinductive and osteoconductive properties (1, 2, 10).

Several bone substitutes are commercially available to fill bone defect, but unfortunately sufficient data isn't available at present in literature to draw conclusions, especially long-term results. (11).

PM is a uniquely flexible biomaterial composed of human mineralized cortical fibers bound in a resorbable polymer. The primary constituent is poly, (DL lactide-co-glycolide) known as PLGA, a scaffold already used in other bone substitutes where it is mixed mainly with calcium phosphate (12). When heated, this biocomposite becomes moldable and it can be used to restore complex bone loss. After cooling, it becomes hard and it is possible to drill or to fix with screws. PM fully remodels into the new host bone via creeping substitution, from the periphery of the graft inward. Moreover, it can be used in trauma reconstruction. In benign bone tumors, it can be used to fill bone loss after curettage. Despite its high cost, it is largely used in correcting small defects.

Benign tumors often occur in the epiphysis and when they are diagnosed the subchondral bone is already damaged. Today, to fill the bone defect, autologous bone for small defects and homologous bone for bigger defects are considered the gold standard.

To maintain the articular surface, bone cortical struts were used, but often these did not adapt to the complex anatomy so that premature osteoarthritis is the natural consequence. PM should overcome this problem by completely restoring support to the articular cartilage. Moreover, bone cortical struts can be placed vertically under PM to increase the axial resistance without damaging the cartilage. Other bone graft substitutes that are commercially available, are not moldable and do not completely replace the host bone (11).

PM can also be used to obstruct the intramedullary canal consequently reducing the risk of an insufficient filling for intramedullary bone migration (Fig. 2D). In addition, we closed the surgical opening performed in the bone segment to assess disease for curettage, decreasing the risk of soft tissue migration and related pain.

Unfortunately, PM does not have primary stability so weight bearing is forbidden for almost 4 months, even if we preferred to prolong this period to 8 months in order to reducing the risk of mechanical failure caused by PM remodeling process. In our case series, a 12-year-old patient affected by chondroblastoma of the posterior aspect of the distal epiphysis suffered a slight structural collapse without clinical evidence due to bearing weight 3 months after surgery.

Another 16-year-old male patient, affected by an enormous aneurismal bone cyst of the left hemipelvis, presented a totally damaged acetabular roof (Fig. 2G). By using 20cc. of PM the local anatomy was restored (Fig. 2H) and the patient was able to partially and fully bear weight at eight and twelve months, without limp, respectively.

Our study suggests that PM can be considered as a valid alternative to homologous bone chips in restoring the anatomy of subchondral bone when destroyed by the disease.

Nevertheless, considering its high cost, its use could be reserved to selected cases. Further studies are necessary to confirm our hypothesis and to clarify the bone graft replacement process and support to

the articular cartilage and above all, whether this technique is capable of preventing the onset of premature osteoarthritis.

ACKNOWLEDGEMENTS

We thank Tania Merlino for reviewing the English language.

REFERENCES

1. Arrington ED, Smith WJ, Chambers HG, Bucknell AL, Davino NA. Complications of iliac crest bone graft harvesting. Clin Orthop Relat Res1996; 329:300-9.
2. St John TA, Vaccaro AR, Sah AP, Schaefer M, Berta SC, Albert T, Hilibrand A. Physical and monetary costs associated with autogenous bone graft harvesting. Am J Orthop 2003; 32(1):18-23.
3. Buecker PJ, Gebhardt MC. Are fibula strut allografts a reliable alternative for periarticular reconstruction after curettage for bone tumors? Clin Orthop Relat Res 2007; 461:170-4.
4. Errani C, Ruggieri P, Asenzio MA, et al. Giant cell tumor of the extremity: A review of 349 cases from a single institution. Cancer Treat Rev 2010; 36(1):1-7.
5. Fraquet N, Faizon G, Rosset P, Phillipeau JM, Waast D, Gouin F. Long bones giant cells tumors: treatment by curretage and cavity filling cementation. Orthop Traumatol Surg Res 2009; 95(6):402-6.
6. Pastoureau PC, Chomel AC, Bonnet J. Evidence of early subchondral bone changes in the meniscectomized guinea pig. A densitometric study using dual-energy X-ray absorptiometry subregional analysis. Osteoarthritis Cartilage 1999; 7(5):466-73.
7. Yamada K, Healey R, Amiel D, Lotz M, Coutts R. Subchondral bone of the human knee joint in aging and osteoarthritis. Osteoarthritis Cartilage 2002; 10(5):360-9.
8. Hayami T, Pickarski M, Wesolowski GA, et al. The role of subchondral bone remodeling in osteoarthritis: reduction of cartilage degeneration and prevention of osteophyte formation by alendronate in the rat anterior cruciate ligament transection model. Arthritis Rheum 2004; 50(4):1193-206.
9. Xu HR, Niu XH, Zhang Q, Hao L, Ding Y, Li Y. Subchondral bone grafting reduces degenerative change of knee joint in patients of giant cell tumor of bone. Chin Med J (Engl) 2013; 126(16):3053-6.
10. Johansson B, Grepe A, Wannfors K, Hirsch JM. A clinical study of changes in the volume of bone grafts in the atrophic maxilla. Dentomaxillofac Radiol 2001; 30(3):157-61.
11. Dinopoulos H, Dimitriou R, Giannoudis PV. Bone graft substitutes: What are the options? Surgeon 2012; 10(4):230-9.
12. Kuzyk PR, Schemitsch EH, Davies JE. A biodegradable scaffold for the treatment of a diaphyseal bone defect of the tibia. J Orthop Res 2010; 28(4):474-80.

CATHELICIDIN LL-37 IN BRONCHOALVEOLAR LAVAGE AND EPITHELIAL LINING FLUIDS FROM HEALTHY INDIVIDUALS AND SARCOIDOSIS PATIENTS

M. GOLEC[1], C. REICHEL[2], M. LEMIESZEK[1], J. BUCZKOWSKI[3], B.MACKIEWICZ[3], C. SKÓRSKA[1], J.DUTKIEWICZ[1], A. GÓRA[1], R.ZIESCHE[4] and J. MILANOWSKI[1,3]

[1]Institute of Rural Health, Lublin, Poland; [2]Austrian Institute of Technology, Seibersdorf Laboratories, Seibersdorf, Austria; [3]Department of Pneumonology, Oncology and Allergology, Medical University of Lublin, Lublin, Poland; [4]Department of Internal Medicine II, Clinical Division of Pulmonary Medicine, Medical University of Vienna, Vienna, Austria

Received March 20, 2013 – Accepted December 3, 2014

Sarcoidosis is a granulomatous disease of unknown etiology most often characterized by pulmonary manifestations. Changes in an innate immune system, involving antimicrobial peptides, have been noted during the course of pulmonary sarcoidosis. This study focuses on the level of LL-37 peptide, the only human cathelicidin, additionally characterized by a wide range of pleiotropic activities, in pulmonary sarcoidosis. A cross-sectional study was conducted in groups of 32 patients with sarcoidosis and 12 healthy individuals. Bronchoalveolar lavage fluid (BALF) sampling, followed by LL-37 measurements by mass spectrometry combined with previous immunoaffinity purification, was performed. Based on urea levels, concentrations of LL-37 in epithelial lining fluid (ELF) were calculated. The levels of LL-37 peptide in BALF samples derived from patients with pulmonary sarcoidosis (median: 17.45 pg/ml, 25th–75th percentile: 8.05-28.33 pg/ml) were significantly higher compared to the healthy group (median: 6.38 pg/ml, 25th–75th percentile: 4.90-11.55 pg/ml) (U Mann-Whitney test, p=0.04). Assessment of LL-37 in ELF confirmed the differences across the groups that were observed in BALF. The level of LL-37 in patients with sarcoidosis (median: 2.25 ng/ml, 25th–75th percentile: 1.03-5.06 ng/ml) was again higher compared to healthy individuals (median: 0.62 ng/ml, 25th-75th percentile: 0.43-2.17 ng/ml) (p=0.06, Mann-Whitney U test). The results of this study demonstrate that the level of LL-37 peptide is elevated in pulmonary compartment affected by sarcoidosis. This might have a meaning in the pathomechanism of the disease, especially taking into consideration versatile activity of human cathelicidin revealed in numerous experimental studies during the last years.

Sarcoidosis is a granulomatous disease of unknown etiology which may affect multiple organs. However, it is most often characterized by pulmonary manifestations (1). Pulmonary sarcoidosis exerts an excessive immune response with overproduction of proinflammatory mediators, such as IFN-gamma or TNF-alpha (2, 3). Changes in an immune system during the course of sarcoidosis have been noted as similar to those occurring during pathogenic microorganisms infections, especially regarding *Mycobacterium tuberculosis* (3, 4). As a consequence, the role of microbial factors in the pathological mechanism of sarcoidosis has been postulated (5).

It is thus no surprise that pathological changes

Key words: Cathelicidin, LL-37, sarcoidosis, BALF, ELF, antimicrobial peptide

Mailing address: Dr Marcin Golec,
Unit of Fibroproliferative Diseases,
Institute of Rural Health,
Jaczewskiego 2,
20-950 Lublin, Poland
Tel.: +48 501 472942
e-mail: msgolec@yahoo.com

0393-974X (2014)

in sarcoidosis affect also the immune system, the first line of defense of multicellular organisms against microorganisms, and its most prominent effector molecules: antimicrobial peptides (3, 6). Antimicrobial peptides provide an immediate response of the respiratory system against infections caused by bacteria, actinomycetes and fungi – with no exception of *M. tuberculosis* (7).

Besides their bactericidal activity, antimicrobial peptides are also pleiotropic mediators, which take part in a whole variety of processes in human lungs and bronchial tree and thus are critical to preserving homeostasis in the respiratory system (8). Such versatile activity is especially characteristic for the LL-37 peptide, the only member of the cathelicidins proteins family described in humans (9). It exerts a number of activities, beginning from antimicrobial and LPS-neutralizing effects, through acceleration of epithelium repair, stimulation of angiogenesis, induction of cell migration and cytokine release to necrosis of human cells (10).

However, although a large number of studies may be found concerning *in vitro* experiments with LL-37 peptide (10), only few of them have addressed a role of cathelicidin in clinical conditions in humans. Moreover, participation of human cathelicidin in few respiratory diseases have been already suggested during last year's (11). This is also the case regarding sarcoidosis: the results of Agerberth et al. and Barna et al. studies have shown alterations of LL-37 levels in pulmonary manifestations of this disease (2, 12).

The aim of this work was to study changes of LL-37 cathelicidin level in airways in pulmonary sarcoidosis by measuring concentrations of this peptide in bronchoalveolar lavage fluid (BALF) samples and epithelial lining fluid (ELF) collected from patients suffering from the disease, in comparison to healthy individuals.

MATERIALS AND METHODS

Examined population

We compared 12 healthy individuals with 32 patients with stage II pulmonary sarcoidosis. The diagnosis of sarcoidosis was based on clinical characteristics and radiological findings. Twelve healthy persons: 3 women and 9 men, average age 30.4±6.4 years. The sarcoidosis group consisted of 17 women and 15 men, average age 39.0±9.8 years. None of the patients was under treatment with corticosteroids or other immunomodulating agents, no patient had infections. All subjects gave formal consent to participate in the study. The Ethics Committees of the Institute of Rural Health in Lublin and Medical University in Vienna approved the study protocols.

BALF Sampling

Bronchoscopies were performed with Olympus BFP30 (Olympus, Tokyo, Japan) and Pentax EB-1970K (Shinjuku-tu, Tokyo, Japan) bronchoscopes. Bronchoalveolar lavage fluid (BALF) was obtained by reaching the wedge position by bronchoscope (usually mid lobe segment 4 – 5 right side) and injecting 5 times 20 ml 0.9% NaCl at body temperature into the bronchoalveolar compartment. Obtaining at least 80% recovery was required. The supernatant was obtained by centrifugation for 10 min at 1500 rpm at 4˚C. The obtained supernatant was stored frozen in -80ºC.

Quantification of LL-37 in BALF

The determination of LL-37 levels in BALF was done as described earlier (11) using a three-step strategy, namely solid-phase extraction (SPE), immunoaffinity purification, and quantitation by mass spectrometry. (1) Solid-phase extraction: BALF-peptides were extracted as described by Agerberth et al. (12) and Sabounchi-Schütt et al. (13), respectively. Briefly, the samples (typically 10 to 20 mL) were centrifuged at 1000 rpm/4°C for 10 min in order to remove insoluble particles. The supernatants were then collected and acidified with trifluoroacetic acid (TFA; 0.1% (v/v) final concentration). SPE-cartridges (Oasis HLB, 60 mg; Waters; Hertfordshire, UK) were preconditioned with 50% acetonitrile (ACN) containing 0.1% TFA and then equilibrated with MQ-water. Then the supernatants were applied on the SPE cartridges and after a washing step (MQ-water / 0.1% TFA) the bound peptides were eluted with 1.2 ml 80% ACN / 0.1% TFA. Subsequently, the eluates were dried in a vacuum centrifuge (SpeedVac) at 40°C for 90 min and then re-dissolved in 50 µl of 2% acetic acid.

Stable isotope labelled LL-37 was used as an internal standard and was added to all samples before SPE extraction. (2) Immunoaffinity purification: the re-dissolved SPE-extracts were neutralized with phosphate-buffered saline (PBS) and immunoprecipitated using a polyclonal rabbit anti-LL-37 antibody (Innovagen; Lund, Sweden) and protein-A coated magnetic beads (Dynabeads; Invitrogen, Carlsbad, CA). After overnight incubation, bound LL-37 was eluted with 20 µl of 0.1% TFA. (3) Quantitation by mass spectrometry (Fig. 1) using the absolute quantitation (AQUA) technique: the eluates obtained after immunoprecipitation were separated on a Dionex Ultimate 3000 dual gradient nano-HPLC system

(Dionex; Sunnyvale, CA) in online pre-concentration mode. The analytical column was a 75 µm i.d. × 15 cm capillary column packed with C18 particles (3 µm particle size, 100 Å pore size; C18 PepMap100 (Dionex, Sunnyvale, CA)) and was operated at a flow rate of 300 nl/min. Solvent A was 2% ACN containing 0.1% formic acid (FA), solvent B was 90% ACN with 0.1% FA. A linear gradient starting at 0% B and ending at 80% B after 60 min was used. The eluting peptides were measured on-line in an LTQ-Orbitrap FT mass spectrometer (Thermo Electron; Bremen, Germany). The ratio between the peak area of the sample and the isotope labeled LL-37 internal standard was used for accurate quantization of LL-37 in the BALF samples. Only this method takes losses into account which might occur during sample preparation.

Calculation of LL-37 Level in Epithelial Lining Fluid – ELF

As urea is a substance freely diffusible through most body compartments including lungs we used BALF urea concentration to quantify the volume of ELF (epithelial lining fluid) recovered by bronchoalveolar lavage. Earlier studies have shown that urea concentrations in ELF and in plasma are identical (14). As a result, ELF volume can be calculated based on the ratio of dilution of urea (15, 16, 17, 18).

Urea concentration in BALF and plasma was determined using a commercial kit (Fluitest UREA UV, Biocon Diagnostic) assessing the urea concentration by hydrolyzing urea in the presence of urease to CO_2 and NH_4^+. Ammonia reacts with 2-oxoglutarate and NADH in presence of GLDH (glutamate dehydrogenase) to yield water, glutamate and NAD^+. Oxidation of NADH to NAD^+ was measured by decrease in optical density at 340 nm wavelength, which is directly proportional to the urea concentration in the sample. The change of light absorbance (ΔA) was done after 30 sec (A_1) and 90 sec (A_2). Absorbance was determined using the NanoDrop ND-1000 spectrophotometer. Distilled water was used for zero adjustment. Working reagent was prepared by mixing 1000 µl working solution with 10 µl sample or standard (urea 50 mg/dl). Working solution was prepared by mixing 5 volumes enzyme reagent R1 (containing: Tris buffer pH 8.0 (50 mmol/l), 2-oxoglutarate (15 mmol/l), urease (≥ 1000 U/l) and GLDH in concentration ≥ 6000 U/l) with one volume starting buffer R2 (containing: NADH in concentration 0.18 mmol/l). Urea concentration in BALF was then calculated as follows: urea concentration (mg/dl) = (ΔA sample/ΔA standard) * standard concentration.

The volume of ELF in BALF was then finally calculated by the method of Rennard et al. (15) (volume ELF (ml) = total amount of urea in BALF (mg)/serum urea concentration (mg/ml)).

LL-37 concentration in ELF was calculated by dividing the total amount of LL-37 in BALF (ng) by the volume of ELF (ml).

Statistical analysis

Statistical analysis was conducted with the use of the Mann-Whitney U test for analysis of the differences between two groups. Spearman test was used for analysis of correlation. The $p<0.05$ level was considered

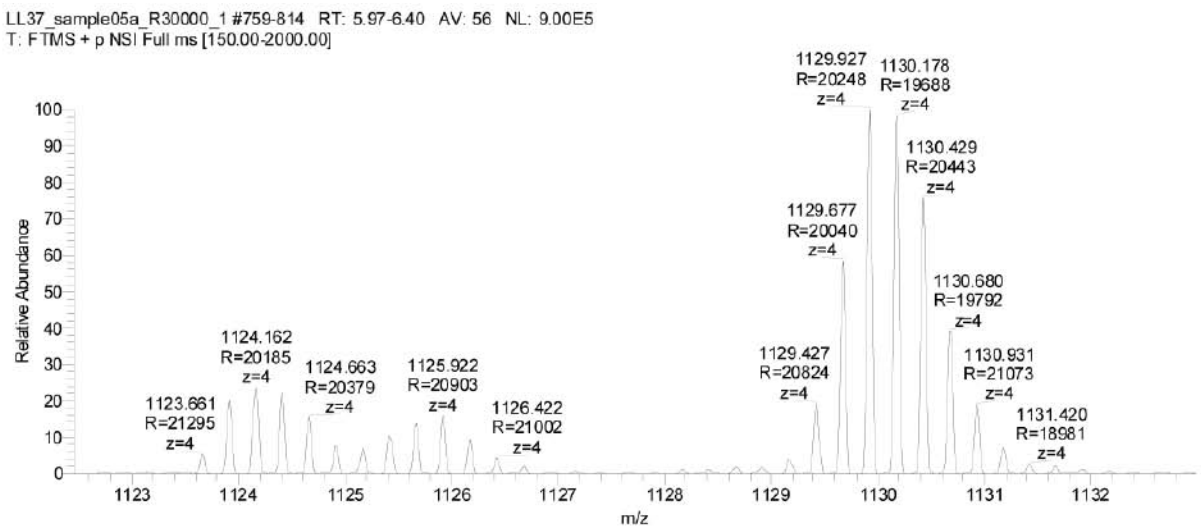

Fig. 1. *Quantification of LL-37 by mass spectrometry using a stable isotope labeled internal LL-37 standard. Shown is the fourfold protonated endogenous peptide (M) and its labeled counterpart (M*). The ratio between both forms enables absolute quantitation of LL-37 in samples.*

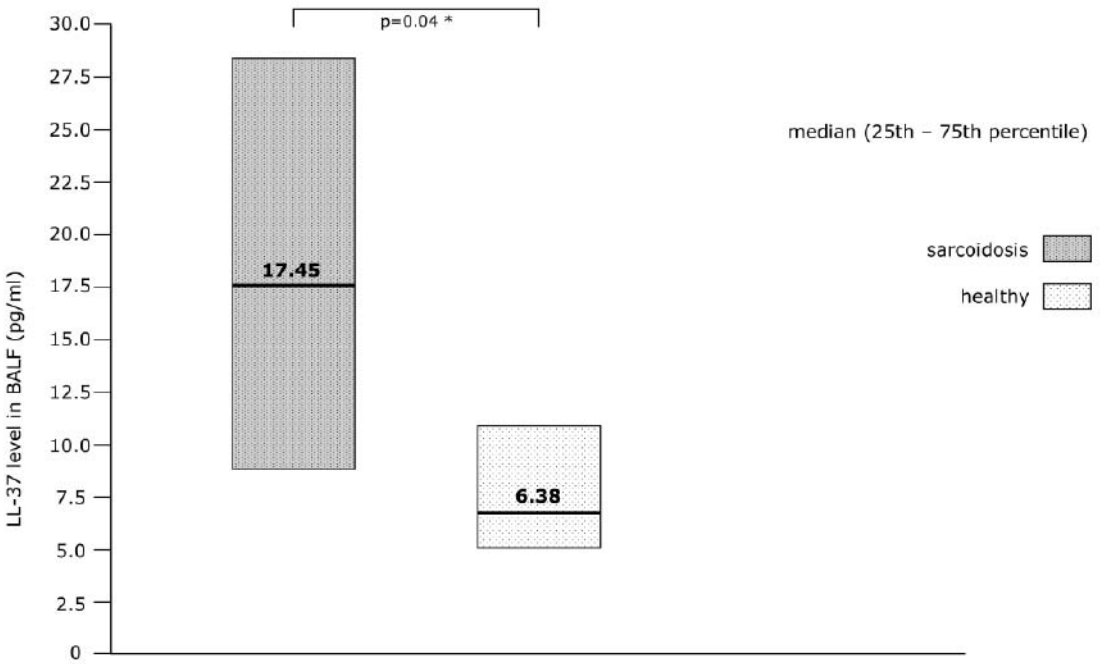

Fig. 2. *LL-37 levels in BALF samples from patients with sarcoidosis and healthy controls. * - significant differences between groups, U Mann-Whitney test, p=0.04.*

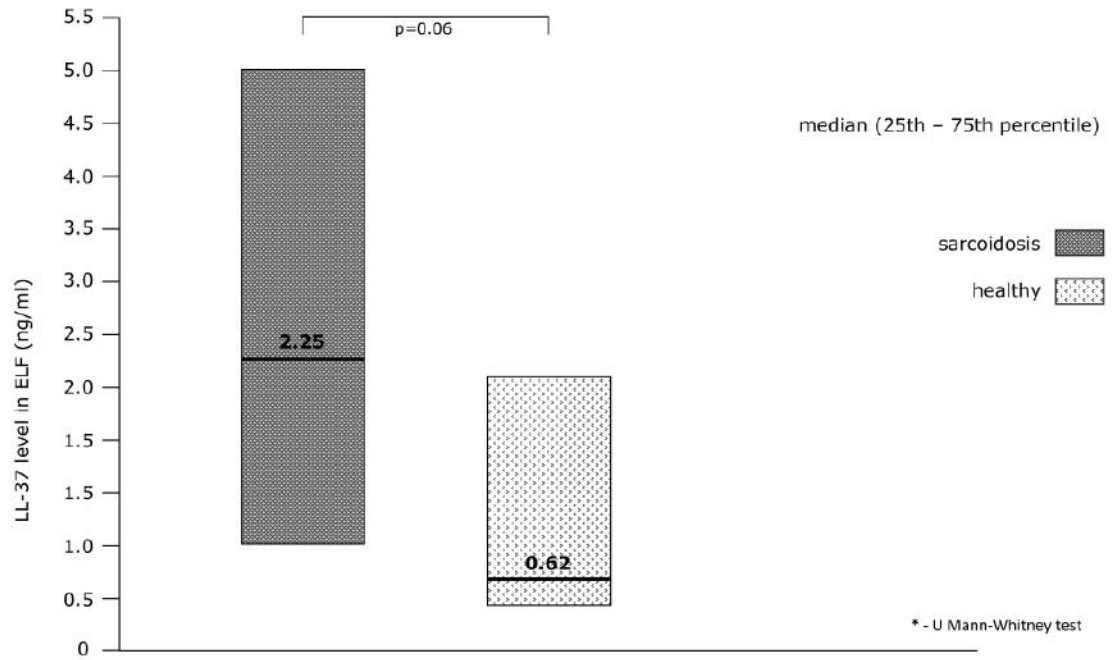

Fig. 3. *LL-37 levels in **ELF** from patients with sarcoidosis and healthy controls. U Mann-Whitney test, p=0.06).*

significant. The statistical analysis was carried out with the use of the Statistica version 8.0 package (Statsoft Inc., Tulsa, OK, USA).

RESULTS

LL-37 levels in BALF

The levels of LL-37 peptide in BALF samples derived from patients with pulmonary sarcoidosis (median: 17.45 pg/ml, 25th-75th percentile: 8.05-28.33 pg/ml) were significantly higher compared to the healthy group (median: 6.38 pg/ml, 25th–75th percentile: 4.90-11.55 pg/ml) (U Mann-Whitney test, p=0.04). The results are presented in Fig. 2.

LL-37 levels in ELF

Assessment of LL-37 in epithelial lining fluid (ELF) confirmed the differences across the groups that were observed in BALF (Fig. 3). The level of LL-37 in ELF in patients with sarcoidosis (median: 2.25 ng/ml, 25th–75th percentile: 1.03-5.06 ng/ml) was considerably higher compared to healthy individuals, though the difference did not attain the significance level (median: 0.62 ng/ml, 25th–75th percentile: 0.43-2.17 ng/ml) (p=0.06, Mann-Whitney U test).

No statistical differences in LL-37 levels were noted regarding genders. No correlation was seen between LL-37 concentration and age. This was true both for BALF and ELF.

DISCUSSION

LL-37 is a potent and versatile mediator helping to sustain homeostasis in the pulmonary compartment (10). However, in contrary to a number of experimental investigations, studies trying to address the role of LL-37 clinical conditions are rare. According to our best knowledge only two studies have been published up to now regarding the role of cathelicidin in pulmonary sarcoidosis in a clinical setting (2, 12).

The results of the presented work reveal significantly elevated levels of LL-37 in BALF in patients with pulmonary sarcoidosis, compared to healthy individuals (Fig. 1). Similar results were obtained for epithelial lining fluid, however the differences were not statistically significant in this case. According to our best knowledge this study examines the highest number of BALF samples from sarcoidosis patients ever (n=32). Additionally, this is the only case where the concentration of LL-37 in ELF in sarcoidosis was assessed.

The results of the presented work are in line with the outcomes obtained by Agerberth et al. (n=12) (12). However, Barna et al. have shown decrease of LL-37 expression in alveolar macrophages and bronchial epithelial cells, mainly in four patients with severe sarcoidosis, compared to healthy individuals. Though, depletion observed in the advance phases of a disease may be a result of profound dysfunction caused by a long term pathology, rather than phenomenon which mirrors the pathological mechanism of a disease. Similar situation of a marked LL-37 decrease was observed by Golec *et al*. in final stages of COPD (despite significantly increased LL-37 concentration in early stages of COPD) (11).

One of the main functions of LL-37 is neutralization of bacterial lipopolysaccharide (LPS) during septic shock caused by Gram-negative bacteria or exposure to organic dust. Elevated levels of other elements of immune system which role is to interact with LPS and bacterial contamination were noted in sarcoidosis. Striz et al. described an augmented concentration of both soluble CD14 and alveolar macrophage membrane-bound CD14, antigen which is a receptor for LPS structures (18). Also the levels of other antimicrobial peptides, defensins, seem to be augmented in pulmonary sarcoidosis (6). The role of pattern recognition receptors such as toll-like receptors (TLR), in the pathological mechanism of sarcoidosis has been indicated several times (19). Increased levels of LPS in BALF from sarcoidosis patients were reported and, last but not least, participation of Gram-negative bacteria in the development of sarcoidosis has also been proposed (20).

Granulomatous inflammation in sarcoidosis leads to overproduction and elevated level of vitamin D (especially regarding its active form, 1, 25-dihydroxyvitamin D) (21). In the light of the last discoveries, vitamin D is more and more often seen as an immunomodulating hormone, among other activities causing also Th-1 cells proliferation and cytokine release (reaction so characteristic also for sarcoidosis) (2, 21). Last years brought evidence

concerning influence of vitamin D on release of LL-37 peptide (22). Vitamin D appeared to be one of strong stimulators of LL-37 release (23).

The results of this study demonstrate that the level of LL-37 peptide is elevated in pulmonary compartment affected by sarcoidosis. Two potential explanations of this finding may be given; 1): stimulation of the innate immunity by bacteria and their products (like LPS); 2): nonspecific activation of innate immune system in the course of the disease, affecting also LL-37.

While the mechanisms in which LL-37 is elevated in a pulmonary compartment in sarcoidosis require further studies, the consequence of the increased cathelicidin concentration may be hypothesized based on activities exerting by LL-37 in *in vitro* studies: gearing up inflammation, leukocytes chemotaxis, cytokines release. This might add to the pathological mechanism of the disease.

ACKNOWLEDGEMENTS

This study was supported by the Polish Ministry of Science and Higher Education (Grant No. 402 056 32/1659). We are obliged to the personnel of both the Laboratories for Molecular Pneumology and Lung Function of the Department of Pulmonary Medicine in Vienna, Austria and Unit of Fibroproliferative Diseases in Lublin, Poland for their outstanding and professional technical support, as well as to Prof. L.H. Block for his permission to utilize the facilities.

REFERENCES

1. Lynch JP 3rd, Ma YL, Koss MN, White ES. Pulmonary sarcoidosis. Semin Respir Crit Care Med 2007; 28:53-74.
2. Barna BP, Culver DA, Kanchwala A, et al. Alveolar macrophage cathelicidin deficiency in severe sarcoidosis. J Innate Immun 2012; 4(5-6):569-78.
3. Chen ES, White ES. Innate pathways shape sarcoidosis signaling: from bugs to drugs. Am J Respir Crit Care Med 2011; 183(4):425-7.
4. Gupta D, Agarwal R, Aggarwal AN, Jindal SK. Molecular evidence for the role of mycobacteria in sarcoidosis: a meta-analysis. Eur Respir J 2007; 30:508-16.
5. Ukena SN, Koenecke C, Geffers R, Fuehner T, Welte T, Ganser A, Buer J, Franzke A. T helper type 2 differentiation is associated with induction of antibacterial defense mechanisms in blood lymphocytes of patients with sarcoidosis. Immunol Invest 2009; 38:49-66.
6. Ashitani J, Matsumoto N, Nakazato M. Elevated alpha-defensin levels in plasma of patients with pulmonary sarcoidosis. Respirology 2007; 12(3):339-45.
7. Méndez-Samperio P. The human cathelicidin hCAP18/LL-37: a multifunctional peptide involved in mycobacterial infections. Peptides 2010; 31:1791-8.
8. Diamond G, Legarda D, Ryan LK: The innate immune response of the respiratory epithelium. Immunol Rev 2000; 173:27-38.
9. Pütsep K, Carlsson G, Boman HG, Andersson M. Deficiency of antibacterial peptides in patients with morbus Kostmann: an observation study. Lancet 2002; 360:1144-9.
10. Shaykhiev R, Beisswenger C, Kandler K, Senske J, Puchner A, Damm T, Behr J, Bals R: Human endogenous antibiotic LL-37 stimulates airway epithelial cell proliferation and wound closure. Am J Physiol Lung Cell Mol Physiol 2005; 289:842-8.
11. Golec M, Reichel C, Lemieszek M, et al. Cathelicidin LL-37 in bronchoalveolar lavage and epithelial lining fluids from COPD patients and healthy individuals. J Biol Regul Homeost Agents 2012; 26:617-25.
12. Agerberth B, Grunewald J, Castaños-Velez E, Olsson B, Jörnvall H, Wigzell H, Eklund A, Gudmundsson GH: Antibacterial components in bronchoalveolar lavage fluid from healthy individuals and sarcoidosis patients. Am J Respir Crit Care Med 1999; 160:283-90.
13. Sabounchi-Schütt F, Aström J, Hellman U, Eklund A, Grunewald J: Changes in bronchoalveolar lavage fluid proteins in sarcoidosis: a proteomics approach. Eur Respir J 2003; 21:414-20.
14. Adams FH, Moss AJ, Fagan L. The tracheal fluid in the fetal lamb. Biol Neonat 1963; 5:151-8.
15. Rennard S, Basset G, Lecossier D et al. Estimation of volume of epithelial lining fluid recovered by lavage using urea as a marker of dilution. J Appl Physiol 1986; 60:532-8.
16. Taylor AE, Guyton AC, Bishop VS. Permeability

of the alveolar membrane to solutes. Circ Res 1965; 16:353-62.
17. Theodore J, Robin ED, Gaudio R, Acevedo J. Transalveolar transport of large polar solutes (sucrose, insulin, and dextran). Am J Physiol 1975; 229:989-96.
18. Striz I, Zheng L, Wang YM, Pokorná H, Bauer PC, Costabel U. Soluble CD14 is increased in bronchoalveolar lavage of active sarcoidosis and correlates with alveolar macrophage membrane-bound CD14. Am J Respir Crit Care Med 1995; 151:544-7.
19. Pabst S, Bradler O, Gillissen A, Nickenig G, Skowasch D, Grohe C. Toll-like receptor-9 polymorphisms in sarcoidosis and chronic obstructive pulmonary disease. Adv Exp Med Biol 2013; 756:239-45.
20. Kelly DM, Greene CM, Meachery G, O'Mahony M, Gallagher PM, Taggart CC, O'Neill SJ, McElvaney NG. Endotoxin up-regulates interleukin-18: potential role for gram-negative colonization in sarcoidosis. Am J Respir Crit Care Med 2005; 172:1299-307.
21. Burke RR, Rybicki BA, Rao DS. Calcium and vitamin D in sarcoidosis: how to assess and manage. Semin Respir Crit Care Med 2010; 31:474-84.
22. Liu MC, Xiao HQ, Brown AJ, Ritter CS, Schroeder J. Association of vitamin D and antimicrobial peptide production during late-phase allergic responses in the lung. Clin Exp Allergy 2012; 42:383-91.
23. Gombart AF, O'Kelly J, Saito T, Koeffler HP. Regulation of the CAMP gene by 1,25(OH)2D3 in various tissues. J Steroid Biochem Mol Biol 2007; 103:552-7.

EFFICACY AND SAFETY OF γδ T CELL-BASED TUMOR IMMUNOTHERAPY: A META-ANALYSIS

S. BUCCHERI[1,2], G. GUGGINO[1,2], N. CACCAMO[1,2], P. LI DONNI[3] and F. DIELI [1,2]

[1]Dipartimento di Biopatologia e Biotecnologie Mediche e Forensi, Università di Palermo, Palermo, Italy; [2]Biomedical Research Centre, Università di Palermo, Palermo, Italy; [3]Dipartimento di Scienze Economiche, Aziendali e Finanziarie, Università di Palermo, Palermo, Italy

Received July 24, 2013 – Accepted January 15, 2014

S.B. and G.G. share first authorship for this work.
P.L.D. and F.D. share last authorship for this work.

Vγ9Vδ2 T cells are important effector cells that may play a role in the anti-tumor immune response. Their capability to exert MHC-nonrestricted lytic activity against different tumor cells *in vitro* and their detection among tumor infiltrating lymphocytes in a variety of human cancers have supported the development of Vγ9Vδ2 T cell-based immunotherapy in the context of novel treatment against cancer. Accordingly, promising reports from recent clinical trials support the use of Vγ9Vδ2 T cells as immunotherapeutic agents, either via adoptive transfer of *ex-vivo* expanded Vγ9Vδ2 T cells or *in vivo* activation of Vγ9Vδ2 T cells with compounds such as phosphoantigens or aminobisphosphonates. In this study we have performed a meta-analysis to assess the objective efficacy and safety of Vγ9Vδ2 T cell-based immunotherapy. Database including Pubmed, Web of Science and SCOPUS were investigated to identify relevant studies. Thirteen clinical trials involving patients with advanced or metastatic cancer were selected. In order to estimate the strength of association between Vγ9Vδ2 T cell-based immunotherapy and favorable clinical effect or toxicity grade we used event rate (ER) with 95% confidence interval (CI). The total effective rate provided significant results (ER = 0.407; *P* <0.014) while no correlation was found between serious adverse effects and Vγ9Vδ2 T cell-based therapy. This meta-analysis demonstrates that Vγ9Vδ2 T cell-based immunotherapy improves overall survival and, in view of its low toxicity grade, provides a proof of principle for its utilization as adjuvant to conventional therapies for resistant/refractory patients care.

Human γδ T lymphocytes comprise two main subsets defined by the T cell receptor (TCR): one subset expresses the Vδ1 chain paired to any Vγ chain and is localized in peripheral tissues, while the other subset expresses the Vδ2 chain preferentially paired to the Vγ9 chain (here and after referred to as Vγ9Vδ2 T cells) and predominate in lymphoid organs and peripheral blood (1-2).

Vγ9Vδ2 T cell activation is achieved by recognition, in non-major histocompatibility complex (MHC)-restricted fashion, of non-peptidic phosphorylated molecules, known as phosphoantigens (PAgs), produced through the isoprenoid biosynthesis pathways (3-5). PAgs are

Key words: Vγ9Vδ2 T cells, tumor, meta-analysis, efficacy, safety

Mailing address: Francesco Dieli, MD, PhD,
Dipartimento di Biopatologia e
Biotecnologie Mediche e Forensi, Università di Palermo,
Corso Tukory 211, Palermo 90134 Italy
Tel.: +39 091 6555916
Fax: +39 091 6555924
e-mail: francesco.dieli@unipa.it

0393-974X (2014)

not stimulatory at physiologic levels, but tumor and infected cells, produce elevated levels of PAgs that are able to activate Vγ9Vδ2 T cells (6-8). Vγ9Vδ2T cells can also be activated, through an indirect mechanism, by aminobisphosphonates (N-BPs), a class of drugs used to treat bone metastases, that inhibit farnesyl pyrophosphate synthase and cause accumulation of endogenous upstream PAgs.

There are several direct and indirect evidences which support the clinical use of Vγ9Vδ2 T cells in cancer immunotherapy; a): Vγ9Vδ2 T cells perform non-MHC restricted cytotoxic activity against a broad variety of cancer cells and produce cytokines with known anti-tumor activity (9, 10); b): the localization of γδ T cells within epithelia and their capacity to infiltrate tumors suggest that these cells may contribute to the surveillance of malignancies (1, 2, 9); c): tumor-infiltrating Vγ9Vδ2 T cells have been found in a broad spectrum of malignancies although their prognostic value is controversial (11-14). Moreover, when autologous radiolabeled Vγ9Vδ2 T cells were injected into patients with advanced solid tumors, they localized predominantly in the lungs, liver, spleen and to sites of metastasis (15).

Altogether, these findings have clearly shown that Vγ9Vδ2 T cells constitute an important component of immune responses against tumors. Accordingly, several small clinical trials involving patients with advanced disease, refractory to conventional treatments, have been performed to assay the safety and efficacy of Vγ9Vδ2 T cells activated *in vivo* with PAgs/IL-2 or N-BPs/IL-2 and of the adoptive transfer of *ex vivo* preactivated autologous Vγ9Vδ2 T lymphocytes (15-27). However, the heterogeneity of therapeutic algorithms, non standardized cellular products and the lack of established criteria for clinical responses have made it impossible to draw valid conclusions from single clinical trials.

In this study, we used a meta-analysis based on data from pooled patient samples to obtain a more powerful estimate of the objective efficacy and side effects of Vγ9Vδ2 T cell-based immunotherapy in patients with advanced or metastatic chemotherapy-resistant tumors.

MATERIALS AND METHODS

Literature search strategy

Cancer clinical trials involving Vγ9Vδ2 T lymphocytes and performed from January 2000 to October 2012, were identified through a search on PubMed, Web of Science, and SCOPUS using the following keywords: ‘‘gammadelta T cell’’ or ‘‘gamma delta T cell’’ and ‘‘cancer immunotherapy’’ or “tumor immunotherapy”. The search was performed in accordance to the relevant criteria from the PRISMA (Preferred Reporting Items for Systematic Reviews and Meta-Analyses) statement. All references cited in these studies and published reviews were examined in order to identify additional works. To avoid duplication of data the body of each publication and the names of all authors were examined. The selection criteria used for the search included: 1): studies written in the English language and limited to human trials; 2): removal of case reports, reviews, comparative studies, opinion, pharmacologic and methodological articles etc; 3); studies adopting randomized and non-randomized groups including patients in advanced or metastatic stage.

Data extraction

Data extraction was carried out by one reviewer (SB) and independently checked for accuracy by a second reviewer (GG). When any discrepancy occurred the consensus was reached by discussion among the investigators. For each study, the following data were extracted: first author’s surname, year of publication, clinical study phase, diagnosis criterion, stage of patients, number of patients, treatment design, dosage and toxicity.

The clinical outcomes used to evaluate effectiveness and safety of Vγ9Vδ2 T cell-based immunotherapy in advanced or metastatic tumors were progression disease (PD), stable disease (SD), partial response (PR) and complete response (CR), defined based on Response Evaluation Criteria in Solid Tumors (RECIST), with the exception of the antitumor effects reported by Kobayashi et al. (22), which were analyzed according to tumor-doubling time (DT). We assessed the objective immunotherapeutic response as event rate (SD+PR+CR/N. of patients).

All clinical studies included in this meta-analysis presented different adverse side effects (AEs) which were graded using the National Cancer Institute Common Toxicity Criteria, version 2.0 and 3.0 (31) except AEs reported by Wilhelm et al. (16), that instead were analyzed using the World Health Organization (WHO) criteria. We evaluated toxicity by classifying side effects into three groups: 1): mild; 2): moderate; 3); severe; and considering adverse events described in the works as follows: grade 1 plus 2 belonging to the first group, grade 3 to the second and grade 4 to the third one.

Statistical analysis

The meta-analysis was performed by using Comprehensive Meta Analysis V2. We used as effect sizes the event rate reported in each studies measured as

the number of patients showing a response to the therapy over the total number of treated patients. Testing the homogeneity of the effect sizes is an important issue when meta-analysis are performed since if the effect sizes are heterogeneous, the calculated Standard Errors (SEs) could be underestimated. In this context a simple approach relies on t^2 indicating the variability on the effect sizes which is larger than the sampling error. Despite t^2 cannot be interpreted directly, Higgins and Thompson (28) proposed several indices to quantify the degree of heterogeneity. One of them is the I^2 index. I^2 statistics is interpreted as the proportion of total variation contributed by between-study variation. If there was no statistical heterogeneity among the studies (I^2 <50% and P >0.05), the event rate and 95% confidence interval (CI) would be estimated for each study in a fixed-effects model. Otherwise, a random-effect model should be employed. In our analysis we exploited the I^2 statistics to test heterogeneity among studies. In sensitivity analysis, relative influence of each study on the pooled estimate was assessed by omitting one study at a time. Funnel plots were used to evaluate publication and/or bias. Forest plots were supplemented with the overall Mantel-Haenszel estimate (fixed effect). All P-values were two-tailed.

RESULTS

Characteristic of articles in our meta-analysis

A total of 165 studies were identified by the searches. By scanning titles and abstracts, redundant publications, reviews, letters, opinion articles and control or case reports were excluded. After referring to full texts, we removed 152 studies that did not meet the selection criteria. As a result, 13 studies that included a total of 204 patients were selected

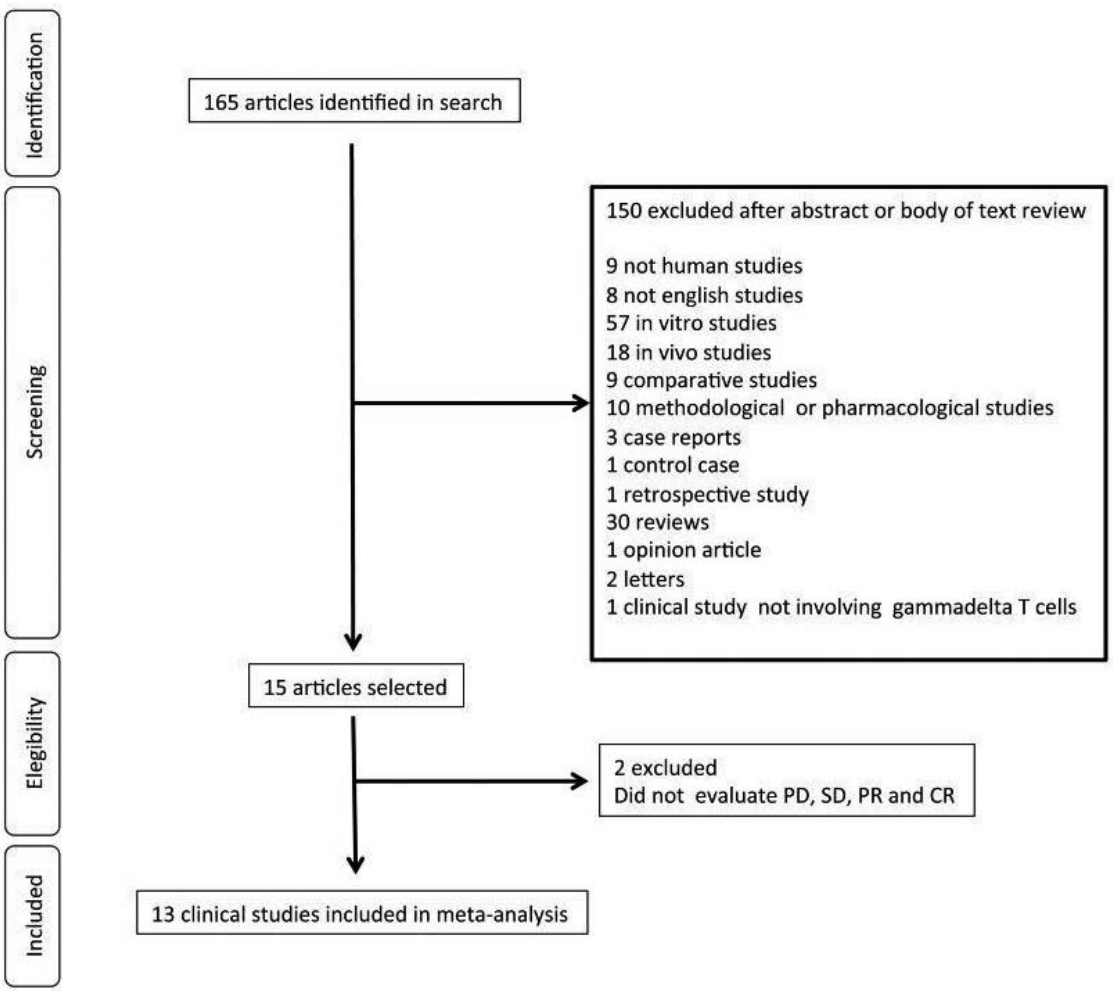

Fig. 1. *Flowchart showing record identification, record screening, full text article eligibility and study inclusion process.*

Table I. *Overview of 13 studies included in the meta-analysis (N=204).*

Source (Reference)	Trial Phase	Diagnosis	Stage of patients	Treatment design	Dosage	No. of patients	% of events/No. of patients				No. of patients with AEs		
							PD	SD	PR	CR	Mild	Moderate	Severe
Bennouna J. et al. 2008	Phase-I	RCC	metastatic	Autologous γδ T cells (Innacell gammadelta TM) + IL-2	1,4,8 and 12X10^9 cells/every 21 days/2X10^6 IU/m2/2 times for day /day 21 to day 28- day 42 to day 48	10	40	60			6	3	1
Bennouna J. et al. 2010	Phase-I	solid tumors	advanced or metastatic	BrHPP (IPH1101)+IL-2	200mg/m2 for1 time in 21 days/ 600, 1200, 1800 and 2400 mg/m2/every 21 days/day 1-7/IL-2 1X10^6 IU/m2/day	28		42,8			26	2	
Dieli F. et al. 2007 (A)	Phase-I	HRPC	metastatic	Zoledronate + IL-2	4 mg/every 21 days/IL-2 0,6X10^6IU/ every 21 days/for 1 year	9	33,3	44,5	22,2		6		
(B)	Phase-I	HRPC	metastatic	Zoledronate	4 mg/every 21 days/for 1 year	9	78	11	11		2		
Kobayashi H. et al. 2007	Pilot	RCC	metastatic or recurrent	Autologous γδ T cells + IL-2	0,7 x10^6 cells/day1/ IL-2/week	7			42,8		7		
Kobayashi H. et al. 2011	Phase I/II	RCC	metastatic	Zoledronate+ autologous γδ T cells+ IL-2	4 mg/cells/IL-2 1,4X10^6 UI/day/day1-5/6 times once every 4 weeks	11	45,4	45,4		9,2	10		
Kunzmann V. et al. 2012	Phase I/II	RCC, MM or AML	advanced or metastatic	Zoledronate +IL-2	4mg/day1 every 28 days/ IL-2 1X10^6U/m2/day/day 1-6/ up to a total of 6 cycles	21	57,1	28,6	9,5		21	2	
Lang J.M. et al. 2011 (A)	Pilot	RCC	metastatic	Zoledronate + IL-2	4mg/day1 every 28 days/ IL-2 7X10^6U/m2/day/day 1-5, weekly in week 1 through 3 of each cycle	9	11,1	44,4			7	3	3
(B)	Pilot	RCC	metastatic	Zoledronate + IL-2	4mg/day1 every 21 days/ IL-2 1X10^6U/m2/day/day 1-5, weekly in week 1 through 3 of each cycle	3		100			3	1	
Meraviglia S. et al. 2010	Phase-I	BC	metastatic	Zoledronate + IL-2	4 mg/every 21 days/IL-2 10^6IU/ every 21 days	10	70	20	10		6		
Nakajima J. et al. 2010	Phase-I	NSCLC	advanced	Autologous γδ T cells	from 1X10^7 cells up to a maximum 1x10^9 cells/dose/biweekly/for 6 times	10	40	40			3	2	
Nicol A.J. et al. 2011 (A)	Phase-I	solid tumors	metastatic	Zoledronate + Autologous γδ T cells	1mg/24h before/1mg/day1/0,04X10^9 to 2,8X10^9 cells/for 8 times	6	66,7	33,3			2		
(B)	Phase-I	solid tumors	metastatic	Zoledronate + Autologous γδ T cells	1mg/24h before/1mg/day1/average of 0,9X10^9 cells/for 6-8 times	9	77,8	11,1			3		
(C)	Phase-I	solid tumors	metastatic	Zoledronate+ Autologous γδ T cells + other therapies	1mg/24h before/1mg/day1/average of 1,2X10^9 cells/for 7-8 times	3			66,7	33,3	2		
Noguchi A. et al. 2011 (A)	Phase-II	solid tumors	metastatic	Autologous γδ T cells	average 2,55x10^9 cells/for three times every 2-weeks	5	40	40					
(B)	Phase-II	solid tumors	metastatic	Autologous γδ T cells + other therapies	average 2,55x10^9 cells/for three times every 2-weeks	20	30	5	15		2		
Sakamoto M. et al. 2011	Phase-I	NSCLC	metastatic or recurrent	Autologous γδ T cells	from 1,1X10^7 to 1,1X10^9 cells/biweekly/for 6 times	15	40	40			2	3	
Wilhelm M. et al. 2003 (A)	Pilot	NHL,MM, CLL,MZL,IC, FCL	advanced III/IV	Pamidronate + IL-2	90mg/3h on day1/IL-2 0,25 to 3x10^6IU/m2/day3 to day8	10	80	10			8	2	
(B)	Pilot	NHL,MM, CLL,MZL,IC,FCL	advanced III/IV	Pamidronate + IL-2	90mg/3h on day1/IL-2 0,25 to 2x10^6 IU/m2 /day1 to day6	9	44,5	22,2	33,3		8		

Abbreviations: PD: progression disease; SD: stable disease; PR: partial remission CR: complete remission RCC: renal carcinoma cancer; HRPC: hormone-refractory prostate cancer; MM: multiple myeloma; AML: acute myeloid leukemia; BC: breast cancer; NSCLC: non-small-cell lung carcinoma; NHL: non-Hodgkin lymphoma; CLL: chronic lymphocytic leukemia; MZL: mantle zone lymphoma; IC: immunocytome ; FCL: follicle center lymphoma.

for meta-analysis. The details for the study searching process are shown in Fig. 1 and the comprehensive characteristics of the 13 clinical studies included are shown in Table I.

Efficacy of Vγ9Vδ2 T cell-based immunotherapy

Fig. 2 lists the results of the meta-analysis and heterogeneity test: it shows that the objective anti-tumor response conferred by Vγ9Vδ2 T cell-based

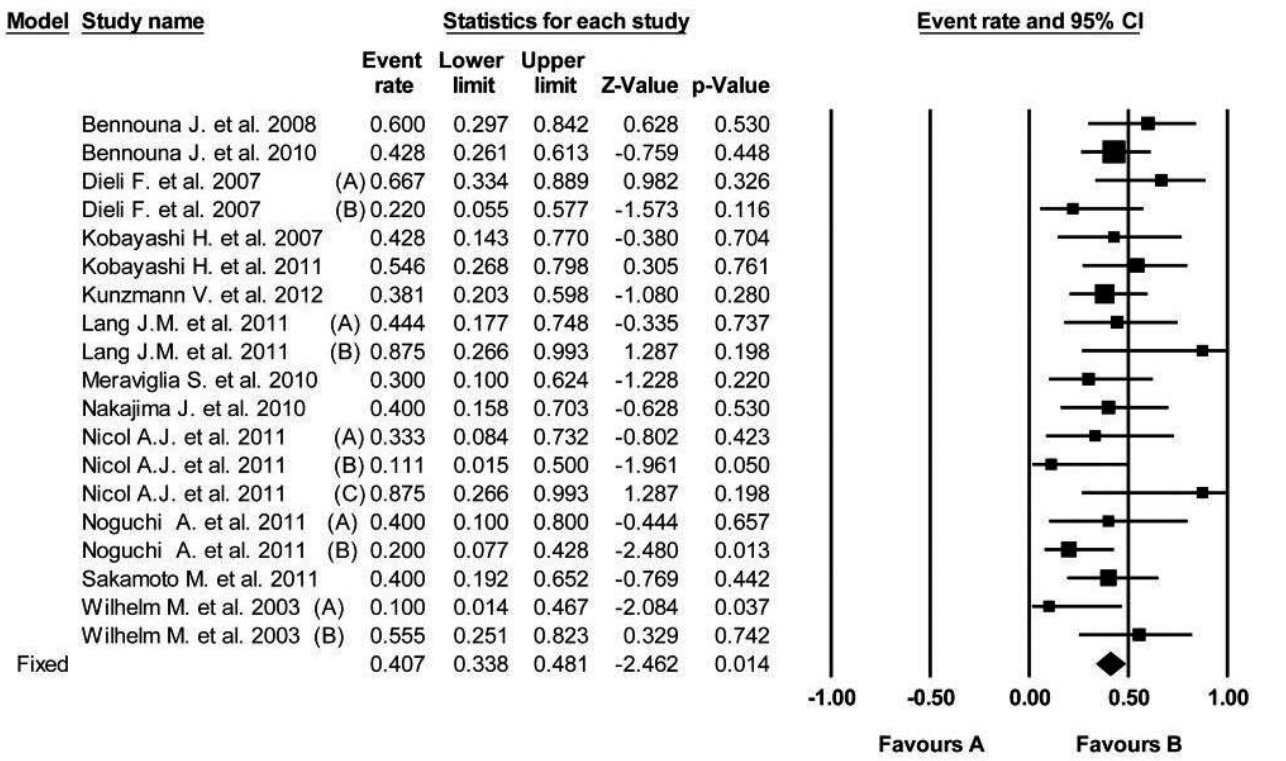

Fig. 2. *Forest plot of comparison of Vγ9Vδ2 T cell-based immunotherapy and clinical response is displayed. The size of the squares is proportional to the sample size. Horizontal lines denote 95% CI for single studies, the diamond the 95% CI for the overall Mantel-Haenszel estimate (fixed effect).*

immunotherapy in the overall 13 studies and groups reaches a significant difference. There was no evidence of heterogeneity among the overall studies (I^2 = 14.12%), suggesting that fixed effect model is appropriate. The estimated event rate was 0.407 (*P*-value = 0.014) for patients with SD or PR or CR.

To further strengthen the confidence for the results, we conducted a sensitivity analysis. First we computed the Begg's Funnel plot and Egger's test to access the publication bias of the studies. The shape of the Funnel plots was symmetrical, suggesting there is no evidence of publication bias among the studies (Fig. 3). The Egger's regression intercept was 0.24 (*P*-value>0.10) demonstrating no evidence for publication bias. Therefore, this sensitivity analysis confirmed the stability of the association between Vγ9Vδ2 T cell-based immunotherapy and the lack of disease progression.

We then measured the relative influence of each study on the pooled estimate by excluding a single study from analysis (data not shown). Together with the above reported results, this meta-analysis showed significant association between Vγ9Vδ2 T cell-based immunotherapy and the progression free survival.

Two different immunotherapy protocols have been used in the 13 selected studies (15-27): Vγ9Vδ2 T cells activated *in vivo* with PAgs/IL-2 or N-BPs/IL-2 and of the adoptive transfer of *ex vivo* preactivated autologous Vγ9Vδ2 T lymphocytes. We then compared patients treated with P-Ags or N-BPs plus IL-2 *in vivo* (16-22), with patients treated with adaptive transfer of *ex vivo*-expanded Vγ9Vδ2 T cells (22-26) and patients who received

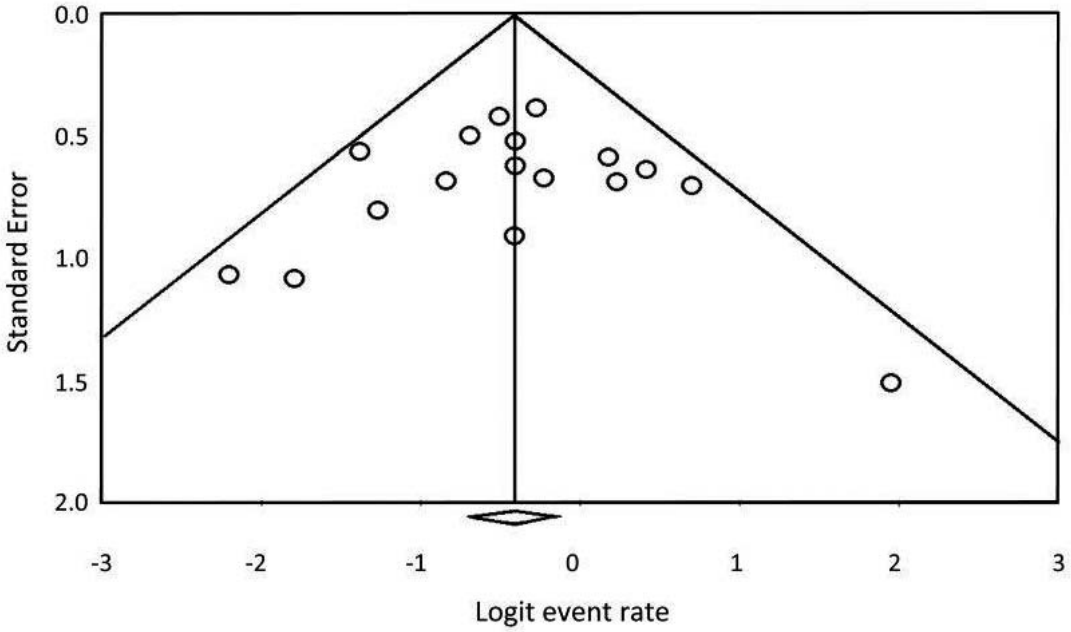

Fig. 3. *Funnel plot showing the association between Standard Errors (SEs) and logit event rate for individual studies.*

Model	Group by Study Type	Study name	Event rate	Lower limit	Upper limit	Z-Value	p-Value
	A	Bennouna J. et al. 2008	0.600	0.297	0.842	0.628	0.530
	A	Kobayashi H. et al. 2007	0.428	0.143	0.770	-0.380	0.704
	A	Nakajima J. et al. 2010	0.400	0.158	0.703	-0.628	0.530
	A	Noguchi A. et al. 2011 (A)	0.400	0.100	0.800	-0.444	0.657
	A	Noguchi A. et al. 2011 (B)	0.200	0.077	0.428	-2.480	0.013
	A	Sakamoto M. et al. 2011	0.400	0.192	0.652	-0.769	0.442
Fixed	A		0.384	0.271	0.510	-1.806	0.071
	B	Bennouna J. et al. 2010	0.428	0.261	0.613	-0.759	0.448
	B	Dieli F. et al. 2007 (A)	0.667	0.334	0.889	0.982	0.326
	B	Dieli F. et al. 2007 (B)	0.220	0.055	0.577	-1.573	0.116
	B	Kunzmann V. et al. 2012	0.381	0.203	0.598	-1.080	0.280
	B	Lang J.M. et al. 2011 (A)	0.444	0.177	0.748	-0.335	0.737
	B	Lang J.M. et al. 2011 (B)	0.875	0.266	0.993	1.287	0.198
	B	Meraviglia S. et al. 2010	0.300	0.100	0.624	-1.228	0.220
	B	Wilhelm M. et al. 2003 (A)	0.100	0.014	0.467	-2.084	0.037
	B	Wilhelm M. et al. 2003 (B)	0.555	0.251	0.823	0.329	0.742
Fixed	B		0.416	0.322	0.517	-1.633	0.102
	C	Kobayashi H. et al. 2011	0.546	0.268	0.798	0.305	0.761
	C	Nicol A.J. et al. 2011 (A)	0.333	0.084	0.732	-0.802	0.423
	C	Nicol A.J. et al. 2011 (B)	0.111	0.015	0.500	-1.961	0.050
	C	Nicol A.J. et al. 2011 (C)	0.875	0.266	0.993	1.287	0.198
Fixed	C		0.434	0.248	0.641	-0.612	0.541
Fixed	Overall		0.407	0.338	0.481	-2.462	0.014

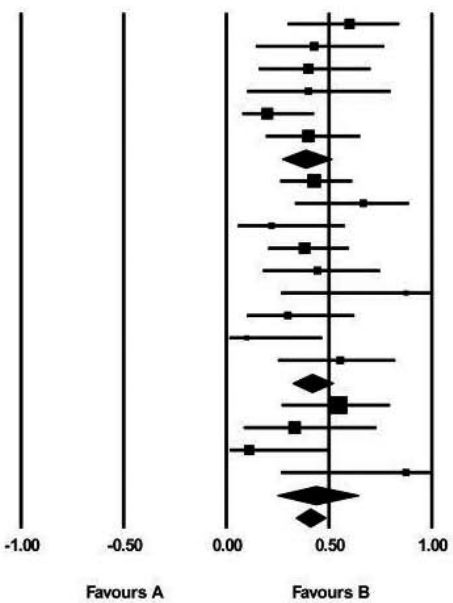

Fig. 4. *Forest plot of comparison of three different Vγ9Vδ2 T cell-based protocols and clinical response is displayed. The size of the squares is proportional to the sample size. Horizontal lines denote 95% CI for single studies, the diamond the 95% CI for the overall Mantel-Haenszel estimate (fixed effect).*

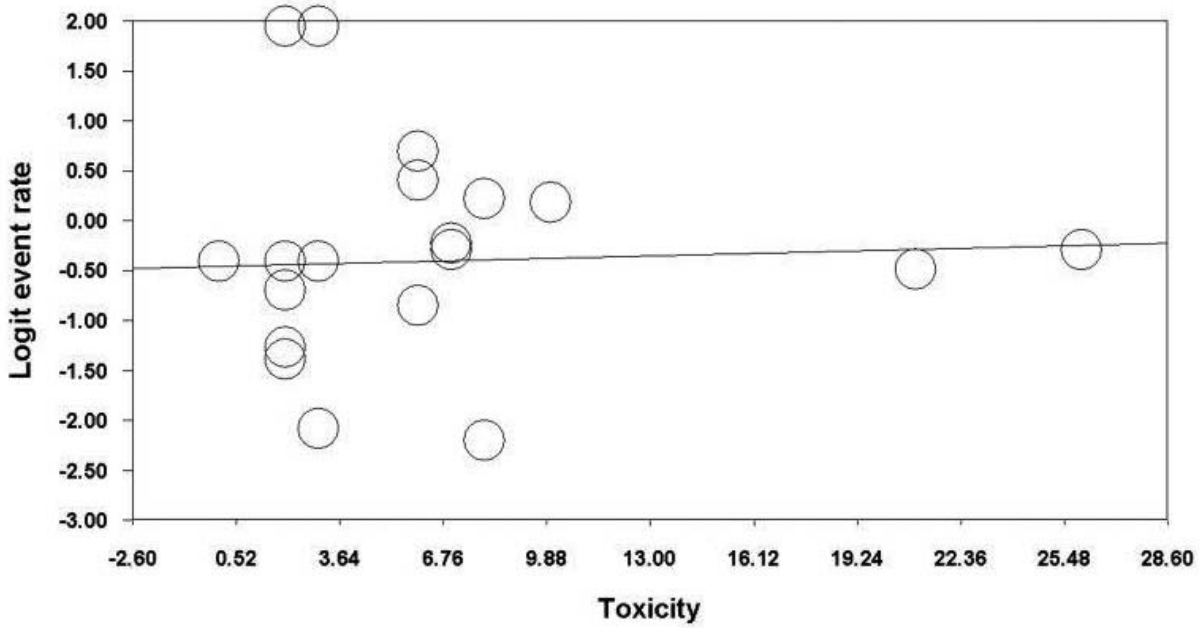

Fig. 5. *Forest plot of comparison of Vγ9Vδ2 T cell-based immunotherapy and adverse effects is displayed. The size of the squares is proportional to the sample size. Horizontal lines denote 95% CI for single studies, the diamond the 95% CI for the overall Mantel-Haenszel estimate (fixed effect)*

both treatments (15, 27). As shown in Fig. 4, there were not significant differences between the three tested groups (*P*-value > 0.05).

Vγ9Vδ2 T cell treatment-related toxicity

Safety analysis was based on the AEs detected by clinical and laboratory examination in the 13 trials (15-27). Only two studies have reported severe side effects: Bennouna et al. (23) reported one instance of disseminated intravascular coagulation, while Lang et al. (20) reported 3 instances of severe effects, elevation in creatinine levels, hyperglycemia and myocardial infarction, but this last was believed unrelated to study medication.

Among the reviewed 13 studies, most AEs were mild or moderate, and included typically flu-like syndrome, injection-site reaction, gastrointestinal disorders (abdominal pain, diarrhea) and hypotension.

To investigate the potential determinants of these AEs we then run a simple meta- regression of the logit event rate on the toxicity. Results (Fig. 5) show no association between Vγ9Vδ2 T cell treatment-related AEs and the immunotherapy efficacy (*P*-value > 0.05) indicating that Vγ9Vδ2 T-cell based immunotherapy does not correlate with AEs and, in turn, AEs do not influence or affect Vγ9Vδ2 T cell-based immunotherapy

DISCUSSION

A growing body of evidence indicates that gd T lymphocytes, and in particular their Vγ9Vδ2 subset, are important effector cells of the immune system that may play a role in the anti-tumor surveillance in peripheral tissues (1, 9, 10). Accordingly, several clinical trials involving patients with different advanced disease, resistant to conventional treatments, have been peformed to assay the safety and efficacy of Vγ9Vδ2 T cell-based immunotherapy (15-27). However, the heterogeneity of therapy algorithms, non standardized cellular products and the lack of established criteria for clinical responses have made it impossible to draw valid conclusions from single clinical trials. This has also been due to the design of clinical trials conducted so far, most being small phase I/II or pilot studies with conventional end points of feasibility. Therefore, the objective of this meta-analysis was to determine

whether efficacy and side effects of Vγ9Vδ2 T cell-based immunotherapy could be detected. The established criteria for the articles selection have allowed the recruitment just a few Vγ9Vδ2 T cell-based immunotherapy clinical trials presenting high variability linked to cancer type, treatment type, concomitant therapy, duration of follow-up period and general patient demographics.

The 13 selected clinical studies included in this meta-analysis have adopted two different types of Vγ9Vδ2 T cell-based immunotherapy: the *in vivo* activation of Vγ9Vδ2 T with PAgs/IL-2 or N-BPs/IL-2 or the adoptive transfer of *ex vivo* preactivated autologous Vγ9Vδ2 T lymphocytes. Nevertheless, the different therapeutic approaches show the same final goal, the expansion and activation of Vγ9Vδ2 T cells against cancer.

The patients were affected by several hematological and solid tumors (e.g. multiple myeloma, acute myeloid leukemia, non-Hodgkin lymphoma, hormone resistant prostate cancer, renal cell carcinoma, breast adenocarcinoma and others) in advanced or metastatic stage (15-27), with wide range of age and different demographical origin.

The variability of the different immunotherapy studies with respect to treatment modality (adoptive cell transfer *vs* PAgs or N-BPs and IL-2), number of treatments (single, repeated), cancer type (solid, haematological), concomitant therapy, general patient demographics and length of follow-up period, and the limitations of the study, should not technically allow for a meta-analysis to assess treatment outcomes across such diverse trials. However, this is a general problem that applies to all rare diseases and small-scale trials where it is impossible to reach sufficient statistical power.

Nonetheless, we pooled in this meta-analysis studies including different types cancers, our results showed no evidence of overall heterogeneity. Moreover, no significant publication bias existed. To avoid bias in the identification and selection of studies, as many non-randomized and randomized controlled trials as possible were included to improve the statistical reliability. The literature search strategy was designed to ensure that all important published trials were supervised. Finally, estimation of event rate demonstrated that no statistical inconsistency existed between the results from each of the original studies and those of subgroup analyzed, suggesting that the results of this meta-analysis are valid.

Vγ9Vδ2 T cell-based immunotherapy *vs* clinical outcome was evaluated. In all overlooked clinical studies, cancer immunotherapeutic approach was always applied after standard treatment modalities. However, we also included in the analysis patient groups in which immunotherapy was combined with conventional therapy after failure of it alone or very early relapse from its administration.

The results of the overall meta-analysis showed that immunotherapy is significantly associated with better clinical outcome, with an estimated event rate (SD + PR + CR/N. of patients) of 0.407 and a *P*-value of 0.014, providing statistically significant evidence that Vγ9Vδ2 T cell-based immunotherapy may give clinical benefit to patients with advanced/metastatic or drug-resistant tumors who have failed conventional therapies.

In the selected trials two kinds of immunotherapy were administrated: *in vivo* activation of Vγ9Vδ2 T with PAgs/IL-2 or N-BPs/IL-2 or the adoptive transfer of *ex vivo* preactivated autologous Vγ9Vδ2 T lymphocytes. As the PR rate was higher in the subgroup of patients receiving *in vivo* PAgs or N-BPs and IL-2 (Table I), we also evaluated if differences existed between patients undergoing the two kinds of immunotherapeutic regimens; comparison also included 2 clinical studies (15, 27) in which patients received both treatments. As shown in Fig. 4, our meta-analysis did not highlight any statistically significant difference between the three analyzed groups.

Vg9Vd2 T cell-based immunotherapy induced treatment-related AEs. Occurrence of a total of 4 severe side effects were reported by two studies (20, 23) (but one of such AEs was believed unrelated to study medication (20), while the great majority of AEs were mild or moderate: approximately 40% of patients treated with i.v. N-BPs manifested an acute-phase response after the first administration of the drug (29). This is characterized by a flu-like syndrome, with fever, fatigue, malaise and myalgia, arthralgia, and bone pain (29). It is benign and self-limited and is consequent to the immune response induced by the N-BP, caused by the release of cytokines by Vγ9Vδ2 T cells and macrophages (29). It has been speculated that the occurrence of the flu-like syndrome, reflecting overall Vγ9Vδ2 T

cell responsiveness, should be predictive of further clinical response *in vivo*: however, results of this meta-analysis demonstrate that AEs do not influence the efficacy of Vγ9Vδ2 T cell-based immunotherapy and *v.v*.

Vg9Vd2 T cell-based clinical trials have defined conditions for the safe use of P-Ags and N-BPs for the activation of these cells in patients *in vivo*; similarly, immunotherapy based on the adoptive transfer of *ex vivo* preactivated, autologous Vγ9Vδ2 T lymphocytes is now feasible and safe but technically more demanding than the former (30). Clearly, advantages of the adoptive therapy are the ability to control cell expansion and to modify the growing cells throughout the culture process, for example by supplementation of the cultures with selected cytokines. Moreover, this method makes it possible to additionally treat patients who cannot or have failed to respond to injection of PAgs or N-BPs and IL-2. Furthermore, the lack of MHC restriction theoretically opens the possibility of expanding *ex vivo* allogeneic Vγ9Vδ2 T lymphocytes, to produce batches of several billion Vγ9Vδ2 T lymphocytes to re-inject into patients Protocols aimed to combine chemotherapy and therapeutic monoclonal antibodies are now rapidly progressing through phase I-III trials, and some clinical successes seem to emerge (30). Therefore, novel regimens that combine such drugs with Vγ9Vδ2 T cell-based strategies, should be taken into consideration.

In conclusion, gd T cell-based immunotherapy shows a statistically significant advantage for SD, PR and CR in patients with hematological and solid malignancies and it also produces a low-grade toxicity. The results of this meta-analysis, despite its limitation, confirm that alone or in combination regimens gd T cell-based immunotherapy can be used in all patients affected by metastatic resistant/ refractory cancer. Further investigation in phase III randomized trials are required to finally demonstrate the clinical benefit of Vγ9Vδ2 T cell -based immunotherapy.

ACKNOWLEDGEMENTS

We thank Giorgio Stassi, Matilde Todaro, Serena Meraviglia and Giuseppe Cicero for helpful discussion and criticism. This work has been supported by grants from the Italian Ministry for Instruction, University and Research (Contract No. 2008L57JXW to FD), the Italian Ministry of Health (Progetto Ricerca Finalizzata 2007 "Stem cells in different pathological conditions: innovative therapeutical approches" to FD) and the University of Palermo. The funders had no role in study design, data collection and analysis, decision to publish, or preparation of the manuscript.

REFERENCES

1. Hayday AC. gd T cells and the lymphoid stress-surveillance response. Immunity 2009; 31:184-96.
2. Bonneville M, O'Brien RL, Born WK. gd T cell effector functions: a blend of innate programming and acquired plasticity. Nat Rev Immunol 2010; 10:467-78.
3. Constant P, Davodeau F, Peyrat MA, Poquet Y, Puzo G, Bonneville M, Fournié JJ. Stimulation of human gd T cells by nonpeptidic mycobacterial ligands. Science 1994; 264:267-70.
4. Eberl M, Hintz M, Reichenberg A, Kollas AK, Wiesner J, Jomaa H. Microbial isoprenoid biosynthesis and human gd T cell activation. FEBS Lett 2003; 544:4-10.
5. Tanaka Y, Morita CT, Nieves E, Brenner MB, Bloom BR. Natural and synthetic non-peptide antigens recognized by human gd T cells. Nature 1995; 375:155-8.
6. Gober HJ, Kistowska M, Angman L, Jeno P, Mori L, De Libero G. Human T cell receptor gd cells recognize endogenous mevalonate metabolites in tumor cells. J Exp Med 2003; 197:163-8.
7. Kistowska M, Rossy E, Sansano S, Gober HJ, Landmann R, Mori L, De Libero G. Dysregulation of the host mevalonate pathway during early bacterial infection activates human gd TCR cells. Eur J Immunol 2008; 38:2200-20.
8. Sireci G, Espinosa E, Di Sano C, Dieli F, Fournié JJ, Salerno A. Differential activation of human gd T cells by nonpeptide phosphoantigens. Eur J Immunol 2001; 31:1628-34.
9. Vantourout P, Hayday A. Six-of-the-best: unique contributions of gd T cells to immunology. Nat Rev Immunol 2013; 13:88-100.
10. Hannani D, Ma Y, Yamazaki T, Dechanet-Merville

J, Kroemer G, Zitvogel L. Harnessing gd T cells in anticancer immunotherapy. Trends Immunol 2012; 33:199-206.

11. Viey E, Lucas C, Romagne F, Escudier B, Chouaib S, Caignard A. Chemokine receptors expression and migration potential of tumor-infiltrating and peripheral-expanded Vγ9Vδ2 T cells from renal cell carcinoma patients. J Immunother 2008; 31: 313-23.
12. Inman BA, Frigola X, Harris KJ, Kuntz SM, Lohse CM, Leibovich BC, Kwon ED. Questionable relevance of gd T lymphocytes in renal cell carcinoma. J Immunol 2008; 180:3578-84.
13. Ma C, Zhang Q, Ye J, et al. Tumor-Infiltrating gd T lymphocytes predict clinical outcome in human breast cancer. J Immunol 2012; 189:5029-36.
14. Cordova A, Toia F, La Mendola C, et al. Characterization of human gd T lymphocytes infiltrating primary malignant melanomas. PLoS One 2012; 7:e49878.
15. Nicol AJ, Tokuyama H, Mattarollo SR, Hagi T, Suzuki K. Clinical evaluation of autologous gd T cell-based immunotherapy for metastatic solid tumours. Br J Cancer 2011; 105:778-86.
16. Wilhelm M, Kunzmann V, Eckstein S, Reimer P, Weissinger F, Ruediger T, Tony HP. gd T cells for immune therapy of patients with lymphoid malignancies. Blood 2003; 102:200-6.
17. Dieli F, Vermijlen D, Fulfaro F, et al. Targeting human gd T cells with zoledronate and interleukin-2 for immunotherapy of hormone-refractory prostate cancer. Cancer Res 2007; 67:7450-7.
18. Bennouna J, Levy V, Sicard H, et al. Phase I study of bromohydrin pyrophosphate (BrHPP, IPH 1101), a Vγ9Vδ2 T lymphocyte agonist in patients with solid tumors. Cancer Immunol Immunother 2010; 59:1521-30.
19. Meraviglia S, Eberl M, Vermijlen D, et al. In vivo manipulation of Vγ9Vδ2 T cells with zoledronate and low-dose interleukin-2 for immunotherapy of advanced breast cancer patients. Clin Exp Immunol 2010; 161:290-7.
20. Lang JM, Kaikobad MR, Wallace M, et al. Pilot trial of interleukin-2 and zoledronic acid to augment gd T cells as treatment for patients with refractory renal cell carcinoma. Cancer Immunol Immunother 2011; 60:1447-60.
21. Kunzmann V, Smetak M, Kimmel B, et al. Tumor-promoting versus tumor-antagonizing roles of gdT cells in cancer immunotherapy: results from a prospective phase I/II trial. J Immunother 2012; 35:205-13.
22. Kobayashi H, Tanaka Y, Yagi J, Osaka Y, Nakazawa H, Uchiyama T, Minato N, Toma H. Safety profile and anti-tumor effects of adoptive immunotherapy using gd T cells against advanced renal cell carcinoma: a pilot study. Cancer Immunol Immunother 2007; 56:469-76.
23. Bennouna J, Bompas E, Neidhardt EM, et al. Phase-I study of Innacell gd, an autologous cell-therapy product highly enriched in gd g9d2 T lymphocytes, in combination with IL-2, in patients with metastatic renal cell carcinoma. Cancer Immunol Immunother 2008; 57:1599-609.
24. Nakajima J, Murakawa T, Fukami T, Goto S, Kaneko T, Yoshida Y, Takamoto S, Kakimi K. A phase I study of adoptive immunotherapy for recurrent non-small-cell lung cancer patients with autologous gd T cells. Eur J Cardiothorac Surg 2010; 37:1191-7.
25. Noguchi A, Kaneko T, Kamigaki T, Fujimoto K, Ozawa M, Saito M, Ariyoshi N, Goto S. Zoledronate-activated Vg9 gd T cell-based immunotherapy is feasible and restores the impairment of gd T cells in patients with solid tumors. Cytotherapy 2011; 13:92-7.
26. Sakamoto M, Nakajima J, Murakawa T, et al. Adoptive immunotherapy for advanced non-small cell lung cancer using zoledronate-expanded gd T cells: a phase I clinical study. J Immunother 2011; 34:202-11.
27. Kobayashi H, Tanaka Y, Yagi J, Minato N, Tanabe K. Phase I/II study of adoptive transfer of gd T cells in combination with zoledronic acid and IL-2 to patients with advanced renal cell carcinoma. Cancer Immunol Immunother 2011; 60:1075-84.
28. Higgins J, and Thompson S. Quantifying heterogeneity in a meta-analysis. Stat Med 2002; 21:1539-58.
29. Thompson K, Roelofs AJ, Jauhiainen M, Mönkkönen H, Mönkkönen J, Rogers MJ Activation of gd T cells by bisphosphonates. Adv Exp Med Biol 2010; 658:11-20.
30. Zitvogel L, Kepp O, Kroemer G. Immune parameters affecting the efficacy of chemotherapeutic regimens. Nat Rev Clin Oncol 2011; 8:151-60.

BASOPHILS ARE RAPIDLY MOBILIZED FOLLOWING INITIAL AEROALLERGEN ENCOUNTER IN NAÏVE MICE AND PROVIDE A PRIMING SOURCE OF IL-4 IN ADAPTIVE IMMUNE RESPONSES

D. PODDIGHE[1,2,3], C.B. MATHIAS[1], E.J. FREYSCHMIDT[1], D. KOMBE[1], B. CAPLAN[1], G.L. MARSEGLIA[2] and H.C. OETTGEN[1]

[1]Department of Medicine, Division of Immunology, Children's Hospital, Harvard Medical School, Boston, Massachusetts, USA; [2]Dipartimento di Scienze Pediatriche, Universita' degli Studi di Pavia, Italy; [3]Dipartimento di Pediatria, Azienda Ospedaliera di Melegnano (MI), Italy

Received October 8, 2013 – Accepted February 12, 2014

Chronic aeroallergen inhalation elicits the expansion of IL-4-producing Th2 cells and the production of IgE antibodies. In sensitized subjects, who have established IgE and Th2 responses, re-exposure to allergen leads to rapid recruitment of basophils, which are thought to be important effectors of late phase allergic reactions. Several investigations of responses to parasites and injected antigens have identified an additional role for basophils as innate immune effectors during initial antigen encounter in immunologically naïve hosts. These cells constitutively express IL-4 and promote Th2 polarized adaptive responses to such antigens. Their early recruitment and modulation of cellular immune responses to natural inhaled allergens in the airways has been scarcely investigated. In this study, basophils were enumerated in lung tissue, blood and spleen from BALB/c mice in the first days after inhalation of an aqueous extract of the allergen, *Aspergillus fumigatus* (*Af*). *Af* inhalation induced rapid increases in basophil numbers in the lung, blood and spleen. This was Rag-1-, MyD88- and IL-3-independent. The basophils expressed abundant IL-4. Their depletion during *Af* sensitization resulted in an attenuated induction of both IL-4 producing Th lymphocytes and specific IgE and IgG1 responses to an inhaled protein antigen, ovalbumin, which was co-administered. Our results suggest that basophils are rapidly recruited to the airways of naïve mice following initial fungal allergen exposure, produce IL-4 and influence the development of the adaptive immune response.

Asthma is a chronic inflammatory process triggered by inhalation of a wide range of ubiquitous environmental substances including fungi (1). The airway immune response of asthma is characterized by expansion of Th2-polarized $CD4^+$ T cells: they produce some cytokines (IL-4, IL-5 and IL-13), which orchestrate the main features of the disease, including generation of IgE antibodies (2-3). A murine model of bronchial hypersensitivity to natural fungal allergens, induced by intranasal (*i.n.*) instillation of an aqueous extract of *Aspergillus fumigatus* (*Af*), was initially described by Kurup *et al.* (4, 5). *Af* extract contains both protein antigen targets of adaptive immune responses and a range of immune stimulants, including proteases as well as ligands for receptors of the innate immune system. The *Af* model has been extensively characterized by our group. Mice repeatedly subjected to *Af* inhalation

Key words: Basophils, Th2 cells, Allergic inflammation, Aspergillus fumigatus, Interleukin-4

Mailing address: Dimitri Poddighe, M.D.,
Dipartimento di Pediatria,
Azienda Ospedaliera di Melegnano,
Via Pandina 1,
20070 Vizzolo Predabissi MI, Italy
Tel.: +39 347 7241851 Fax: +39 02 9805
e-mail: dimimedpv@yahoo.it

0393-974X (2014)

over weeks gradually develop intense eosinophil dominant airway inflammation and markedly elevated IgE levels (6, 7).

The cellular signals inciting Th2 differentiation early in the induction of immune responses to allergens have not been fully defined. IL-4, the critical growth factor for expanding antigen-specific Th2 clones, is produced neither by airway epithelium nor by resident dendritic cells (DC). Identification of its initial cellular sources in the respiratory mucosa is therefore of great interest (8,9). Basophils have been identified as key participants in late phase reactions in the airways of subjects with airway allergy and pre-existing allergen-specific IgE antibodies. In such sensitized individuals basophils are rapidly recruited and produce abundant IL-4 following allergen challenge and they likely play important effector functions in late phase allergic responses (10-12). While such studies identify basophils as key IL-4 producing effectors in established allergic airway disease, their recruitment and function in immunologically naïve hosts subjected to aeroallergen inhalation has not been extensively studied.

Direct analyses of basophil contributions to mechanisms of immune sensitization and influences on Th polarity would optimally be carried out in a mouse model. However, questions have been raised for long time regarding the existence of a murine equivalent to the human basophil. Recent advances in flow cytometric identification have clearly established the presence in mice of a FceRI^{+} c-kit^{-} circulating cell population whose immunophenotype has extensive overlap with that of the human basophil (12-14). Although this murine cell does not appear to be as granulated as its human counterpart (15), it is also a robust IL-4 producer and is mobilized in settings of allergen exposure. These features strongly suggest biologically relevant functional overlap between the human and murine "basophils." Mouse basophils drive Th2 differentiation in culture (16, 17). Sokol and colleagues have shown that the Th2-dominated immune response of mice to the cysteine protease, papain, following injection into the foot-pads, is preceded by recruitment of IL-4-producing basophils to the draining lymph nodes (18, 19). Similarly, antibody responses to intraperitoneally injected antigens with innate immune system stimulating adjuvants are augmented by basophils, as are B cell memory responses (16, 19-21).

Despite these recent advances in mouse basophil biology, little is known about their role in initiation of responses to natural aeroallergens following first encounter in the airway mucosa of a naïve host. We hypothesized that, as constitutive IL-4 producers implicated in Th2 responses in other experimental systems, basophils might be rapidly mobilized and provide an early source of IL-4 following natural allergen inhalation. We tested this hypothesis by examining the basophil response in the first few days following allergen inhalation in a mouse model of *Af*-driven airway inflammation. We observed a very rapid recruitment of basophils, both locally and systemically. The basophils constitutively expressed IL-4. The basophil response to *Af* remained intact in mice with targeted deletions of the *Rag-1, Myd88* or *Il-3* genes indicating that adaptive immune function, IL-1/TLR signaling and IL-3 are not critical in this response. Moreover, mice repeatedly exposed to *Af* over three weeks exhibited a gradual accrual of IL-4^{+} Th cells. Both the increase in lung and spleen Th2 cells and the *in vivo* production of specific IgG1 and IgE antibody responses to co-inhaled OVA were attenuated if basophils were depleted at the time of *Af* exposure. Our findings implicate basophils as rapidly mobilized IL-4 producers following natural fungal allergen exposure in the respiratory mucosa and provide evidence that these cells may play a role in emerging Th2 responses.

MATERIALS and METHODS

Reagents and mice

A sterile aqueous extract of *Aspergillus fumigatus* (1:10 w/v at 87.000 PNU/ml) was obtained from Greer Laboratories. OVA was purchased from Sigma. BALB/c mice were purchased from Taconic Farms. RAG1$^{-/-}$ (BALB/c background) and *4get* mice were from Jackson Laboratories. IL-3$^{-/-}$ mice (BALB/c background) were obtained from Taconic with the kind permission of Dr. Glen Dranoff. MyD88$^{-/-}$ (BALB/c background) mice were provided to us by Dr. S. Umetsu (Research Institute for Microbial Diseases, Osaka University, Japan). Mice were housed in a specific pathogen-free environment and were 8-10 wk old. All experiments were conducted in accordance with the Institutional Animal Care and Use Committee policies and procedures of Children's Hospital

Boston.

Sensitization of mice

Mice were lightly anesthetized by isoflurane and 50 µl of *Aspergillus fumigatus* extract (*Af*) or sterile saline was applied to the nares. In the short sensitization protocol (3 days), mice were immunized with daily doses over three consecutive days. Mice were studied 18 hrs after the final dose, unless specified otherwise. In the chronic sensitization protocol (3 weeks), three daily sensitizations were performed weekly for 3 weeks and mice were studied 16-24 hrs. after the final dose, unless specified otherwise. In experiments including OVA sensitization, 50 µl (1.5 µg/µl) was administered intra-nasally (*i.n.*) along with *Af*.

Collection of specimens

For bronchoalveolar lavage (BAL), 1 ml of PBS was infused into the trachea and then retrieved. To obtain lung cell suspensions for flow cytometry, after lavage, whole lungs were minced, treated with 1.3 mM EDTA and digested with 100U/ml collagenase (Gibco) in staining medium (SM) consisting of HBBS supplemented with 10 mM HEPES buffer (pH 7.2.) and 2% newborn calf serum, at 37ºC for 30 min. Lung cells were collected by mashing the tissue through a cell strainer (BD Biosciences); erythrocytes were lysed using ammonium chloride (8.3 g/l) in 0.01M Tris-HCl buffer (Sigma) and lung cells were resuspended in SM.

Spleens were excised and gently mashed and cells were collected in SM after lysing red blood cells (RBC) and cell filtration. Blood was collected by cardiac puncture. Peripheral mononuclear blood cells (PMBC) were obtained by sedimentation of red blood cells in Dextran 2% solution for 60 min. at 4ºC and eventually by two treatments with Sigma RBC lysis buffer.

BAL cytology

BAL fluid was cytocentrifuged onto slides and differential cellular analysis was performed by light microscopy after staining with Wright-Giemsa (Richard-Allan Scientific). Total cells were enumerated by light microscopy and viability was assessed by trypan blue exclusion.

Flow cytometry

Mononuclear cells from lung, BAL, spleen and blood were analyzed by flow cytometry. Basophils and mast cells were incubated with Fc block (anti-CD16/CD32) for 20 min on ice. Cells to be stained with anti-IgE were preincubated with 10µg/ml anti-DNP mouse IgE for 45 min at 4ºC. Cells were washed and then incubated with various combinations of fluorochrome (FITC, PE, PECy7, APC) conjugated monoclonal antibodies (mAbs), specific for IgE, CD49 (DX5), c-Kit, IL-3R (CD123), CD3, CD4, Gr-1 and NKp46 for 30 min at 4ºC. mAbs were purchased from eBioscience, BD Biosciences and R&D Systems. Finally, cells were washed and resuspended in SM containing propidium iodide (PI) to differentiate between live and dead cells.

In order to evaluate cellular IL-4 expression, IL-4 reporter knock-in mice (*4get*), expressing enhanced green fluorescent protein (eGFP), were used or intra-cellular cytokine staining was performed. In the latter case, after completing surface marker staining, cells were incubated with brefeldin A for 5 hr at 37ºC. Cells were then washed, permeabilized and fixed using Cytofix/Cytoperm kit (BD Bioscience) and, finally, stained with IL-4/FITC mAb or the appropriate FITC conjugated isotype control Ab (eBioscience). Samples were analyzed using FACS Calibur and FACS Canto flow cytometers; acquired data were processed using FlowJo software (Tree Star).

Basophil depletion

Mice were depleted of basophils by using MAR-1 purified anti-FceRI mAb (eBioscience). MAR-1 has recently been used by a number of groups to effectively reduce basophil numbers without significantly affecting mast cells (20, 22, 24). Mice were administered 10 µg/day *i.p.* for 3 days a week, as recently described, and every week for the length of the protocol. Appropriate controls were performed to establish that flow cytometric basophil detection was not impaired by MAR-1 treatment (as has also been confirmed by others) (16). Alternatively, basophils could be also identified as CD49b $(DX5)^+$, IL-$3R^+$ and c-kit^- cells (22).

Splenocyte stimulation assay

Spleen cells were suspended (2 x 10^6/ml) in RPMI 1640 (Sigma) containing fetal calf serum (10%, Sigma), penicillin-streptomycin combination (1%, Gibco), L-glutamine (1%, Sigma), sodium pyruvate (1%, Sigma), minimal non-essential amino acids (1%, Gibco), HEPES buffer (1%, Sigma) and 55mM beta-mercapto-ethanol (0.1%, Sigma) and cultured on plates pre-coated overnight at 4ºC with either 1 ml of OVA (50 mg/100 ml, Sigma) or anti-CD3 mAb (0.2 µg/ml, BD Pharmigen). Anti-CD28 mAb (BD Pharmigen) was added to anti-CD3 coated wells at a final concentration of 0.2 µg/ml. OVA (at a final concentration of 50 mg/100 ml) was added to the OVA coated wells. Plates were incubated at 37ºC for 48 hrs and cytokine levels in supernatants were analyzed in duplicate.

ELISAs

ELISAs for OVA-specific IgG1, OVA-specific IgE and IL-4 were performed as we have previously described

(23). IFN-γ on supernatants was quantified using a sandwich ELISA (DuoSet ELISA, R&D Systems).

Statistical analyses

Differences in values between experimental groups were examined for significance with GraphPad Prism® software using the unpaired Student's *t* test. Values are presented as means ± standard error of the mean (SEM).

RESULTS

Af allergen inhalation elicits a rapid pulmonary cellular infiltrate dominated by neutrophils

The Th2-driven eosinophil-dominated chronic allergic inflammatory response that evolves in mice after repeated intranasal *(i.n.)* instillation of *Af* extract in mice over three weeks has previously been extensively characterized (4-7). The objective of the current study was to examine *early* events in *Af* sensitization. For this purpose, BALB/c mice were analyzed after only three days of *i.n. Af* exposure. A modest influx of inflammatory cells into the lungs was already evident by BAL cytology at this early time point. The cell count was 280±29.7 x10^3/ml *vs* 52.5±8.5 x10^3/ml in saline control mice (Fig. 1A). This increased to significantly higher levels when mice were subjected to *i.n. Af* according to 3 weeks protocol (650±71.34 x10^3/ml, Fig. 1A). Whereas the cellular influx into the airways after chronic *Af* exposure was dominated by eosinophils (243.6±28.9x10^3/ml, Fig. 1D), neutrophils represented the major infiltrating cell at the 3 days time point (162.5±23.5 x10^3/ml, Fig. 1C). In naïve controls, almost all cells recovered were monocytes/ macrophages (Fig. 1B).

Af treatment for three days elicits an early basophil response, both locally and systemically

Since basophils have been implicated as IL-4 producing Th2-inducers in other experimental systems, we sought to determine whether they were mobilized following allergen inhalation. Basophils were enumerated by flow cytometry (FCS^{lo} SSC^{lo}, IgE^{high}, CD49b $(DX5)^+$) in blood, lungs and spleens of mice treated with *Af* for three days. We confirmed that cells with this immunophenotype were uniformly $CD3^-B220^-Gr1^-NKp46^-IL3R^+$and $c\text{-}Kit^-$. Significant increases in basophil numbers were detected in lung, blood and spleen of mice treated with *Af* for three days, with approximately 2-fold increases from baseline observed in each tissue (Fig. 2). No basophils were detected in BAL (not shown). The systemic response had a very rapid onset, with the

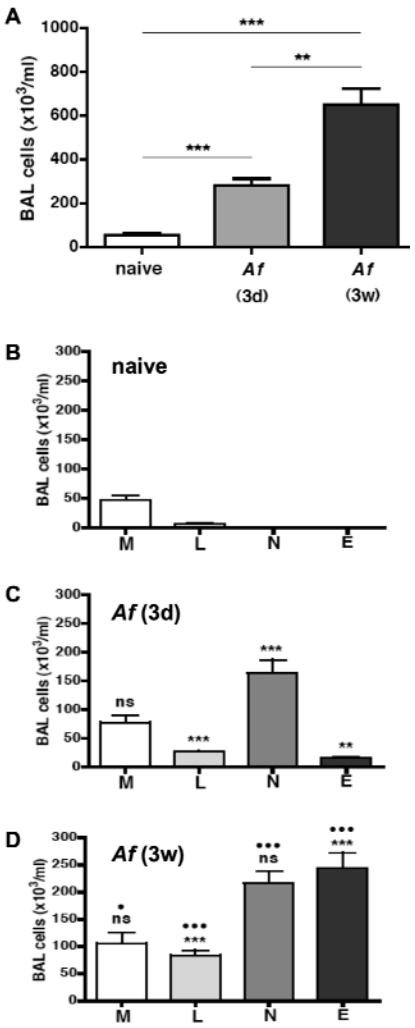

Fig. 1. *Cell recruitment to the airways after acute or chronic Af allergen inhalation. Mice were subjected to daily instillation i.n. of an aqueous extract of Af for 3 days (**3d**) or three days each week over three weeks (**3w**). (**A**) Total BAL total cell counts. Differential cell counts were performed on Wright-Giemsa stained cytocentrifuged BAL specimens from (**B**) naïve mice, (**C**) mice treated for three days and (**D**) mice treated for 3 weeks. Numbers of macrophages (**M**), lymphocytes (**L**), neutrophils (**N**) and eosinophils (**E**) are shown. n=5 mice per group. ns, not significant; *, p<0.05; **, p<0.01; ***, p<0.001 (compared to naïve mice). ·, p<0.05; ···, p<0.001 (compared to 3d Af mice).*

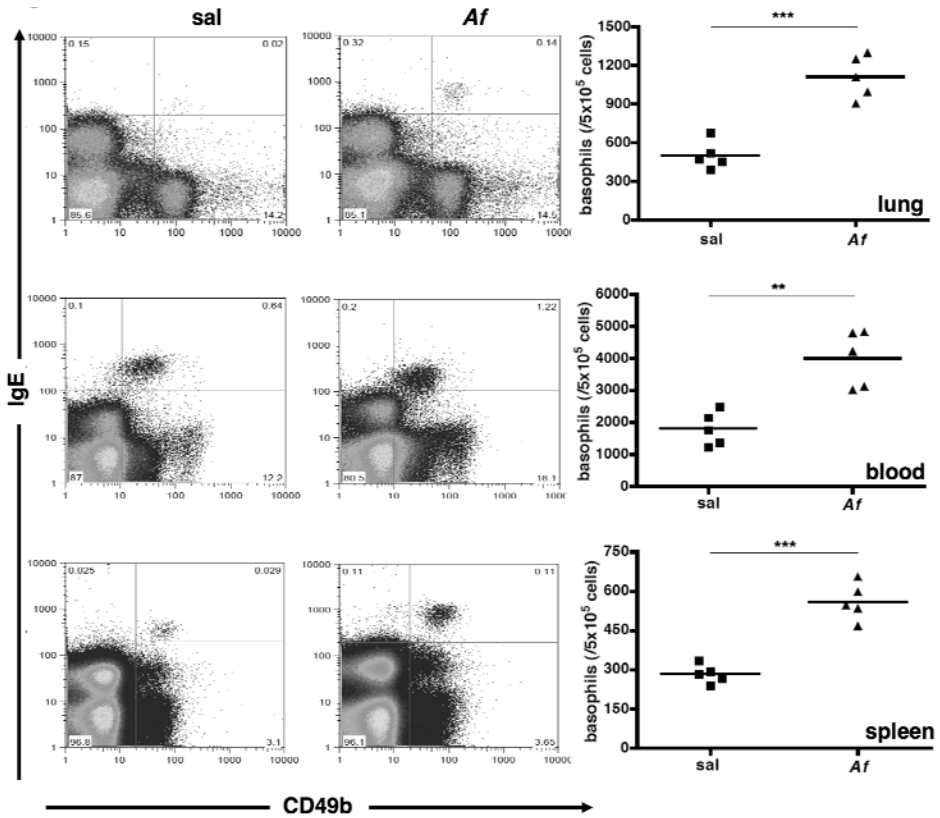

Fig. 2. *Basophil induction early after allergen inhalation. Basophils were enumerated by flow cytometry, in lung, blood and spleen of BALB/c mice treated for three days with saline* ***(sal)*** *or Af. Mice were euthanized 18 h after the final Af dose. Cells were stained for CD49b (DX5) and IgE. Representative plots for each group (n=5/group) as well as summary total cell counts are shown. **, p<0.01; ***, p<0.001.*

trend towards increasing basophil numbers evident in spleen and blood even after only a single inhalation of *Af* extract (Fig. 3). Upon cessation of *Af* treatment, basophil counts rapidly declined.

The systemic basophil response to Af inhalation arises independently of adaptive immune function, MyD88 signaling and IL-3

The rapid induction of basophils by *Af* strongly suggested that innate immune mechanisms rather than antigen-specific adaptive pathways trigger this response. Consistent with this hypothesis, basophil induction was comparable in *Af*-treated Rag-1$^{-/-}$ and control animals (106,600±20,620 basophils/spleen in WT *vs* 90,510±4,916 in Rag-1$^{-/-}$, Fig. 4A).

Natural fungal allergens are rich in ligands for Toll-like receptors (TLR), most of which signal via receptor-associated MyD88. We anticipated that TLR function might be important in sensing fungal factors in a naïve host, playing a potential role in the early basophil response. Actually, basophil numbers after *Af* treatment were equivalent in control and MyD88$^{-/-}$ animals, both on the BALB/c background (843.2±65.4/5x10^5 PI$^-$ cells in WT *vs* 729.4±70/5x10^5 PI$^-$ cells in MyD88$^{-/-}$, Fig. 4B). This finding suggests that other innate immune sensors are critical in this specific setting.

Basophils arise in the bone marrow from pluripotent progenitors under the influence of a number of hematopoietic growth factors, including IL-3. Although IL-3$^{-/-}$ mice have previously been shown to have normal basophil numbers, indicating the existence of IL-3-independent pathways of basophil differentiation (24), we hypothesized that the

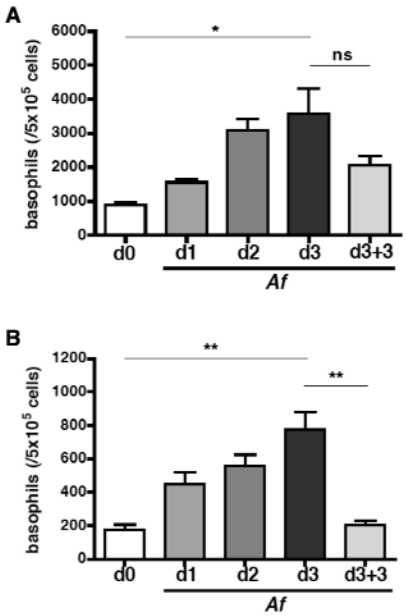

Fig. 3. *Kinetics of induction and resolution of the early basophil response to allergen inhalation. Basophil numbers in the (**A**) blood and (**B**) spleen of naïve mice (**d0**), mice subjected to daily (**d1-3**) i.n. Af instillation and Af treated mice after 72 h. wash-out (**d3+3**). Basophils were counted 18 hrs after receiving the last Af dose. n=4 mice per group. ns, not significant; *, p<0.05; **, p<0.01.*

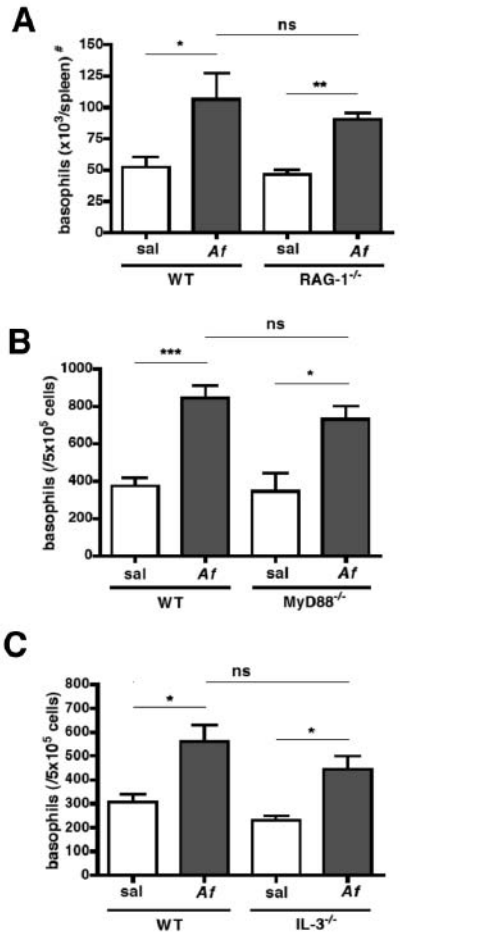

Fig. 4. *Basophil responses in mice lacking normal function of Rag-1, Myd88 or Il-3 genes. Basophils were enumerated in spleens of (**A**) RAG-1$^{-/-}$, (**B**) MyD88$^{-/-}$ and (**C**) IL-3$^{-/-}$ mice following 3 days i.n. Af. n=3-5 mice per group. Basophil numbers per 5 x 105 splenocytes are represented with the exception of the RAG-1$^{-/-}$ mice experiment in which (because of the absence of lymphocytes) basophils are expressed as total number per spleen, to permit comparison with controls (#). ns, not significant; *, p<0.05; **, p<0.01; ***, p<0.001.*

cytokine might exert an effect in allergen-mediated basophil recruitment as has been shown to be the case in parasite-related basophil responses. Using IL-3$^{-/-}$ animals, however, we observed that basophils were effectively induced by *i.n. Af*, (561±67.1/5x10^5 PI$^-$ cells in WT *vs* 445±52.7/5x10^5 PI$^-$ cells, Fig. 4C). Taken together, these findings suggest that basophil mobilization following allergen inhalation arises independently of adaptive immune function, MyD88 signaling and IL-3.

Aeroallergen-induced basophils but not mast cells rapidly produce IL-4 in vivo

Given the known capacity of basophils to produce IL-4 in the settings of parasite infestation and parenteral allergen injection, we considered that activated basophils in response to aeroallergen inhalation might provide a source of IL-4. In order to evaluate this hypothesis, we took advantage of IL-4 reporter *4get* mice expressing enhanced green fluorescent protein (eGFP) under the control of the IL-4 promoter (25). Mast cell responses and IL-4 production were evaluated in the same experimental system, as mast cells constitute another potential innate immune cellular source of IL-4 and as we have recently reported that chronic *Af* administration drives an expansion in airway mast cell numbers (7).

Following 3 days of *Af* inhalation, *4get* mice, as expected, exhibited basophil induction (476.8±29.4

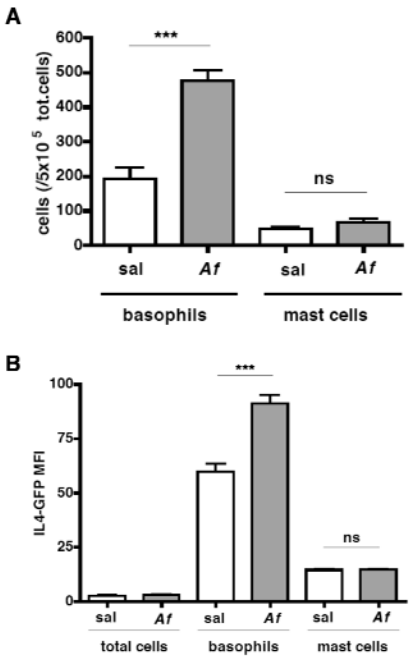

Fig. 5. *Reporter mouse analysis of IL-4 expression in basophils of Af treated animals. GFP expression was determined in mast cells (IgE$^+$ DX5$^-$ c-kit$^+$) and basophils (IgE$^+$ DX5$^+$ c-kit$^-$) from 4get mice following allergen inhalation. (**A**) Splenic basophil and mast cell counts following 3 days of i.n. Af [or saline (**sal**) control] treatment.(**B**) GFP MFI of total splenocytes, basophils and mast cells from 4get mice. n=5 mice per group; ns: not significant; ***, p<0.001.*

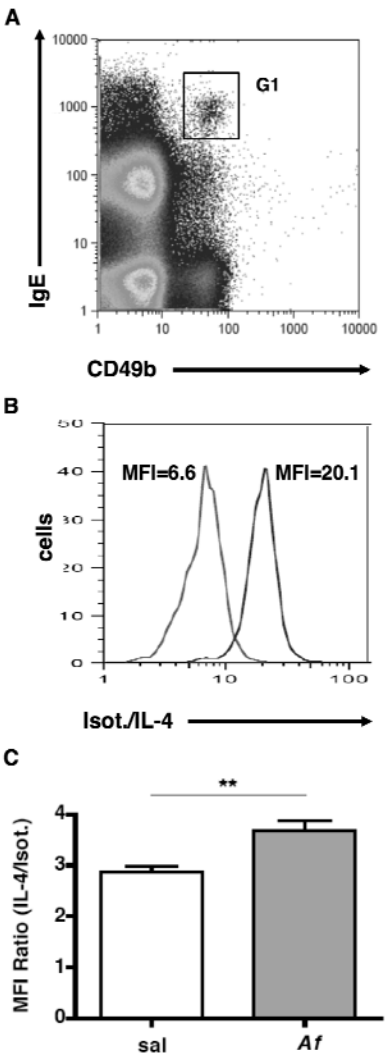

Fig. 6. *Intracellular IL-4 staining in basophils from Af-treated mice. Splenic basophils from mice treated with Af or saline for 3 days were subjected to intracellular IL-4 staining. (**A**) Basophils (gate **G1**) were identified on the basis of CD49b (DX5) and IgE expression and (**B**) a representative IL-4 fluorescence histogram (right curve) is presented, alongside the isotype control (left curve). (**C**) Relative levels of IL-4 staining in basophils from animals treated with Af, compared to those from saline treated mice, are expressed as MFI ratios (IL-4:isotype control).*

vs 193.4±31,7/5x10^5 PI$^-$ cells in saline-treated mice Fig. 5A). No significant increase in splenic mast cells was induced during this period, suggesting that chronic allergen exposure is required to affect mast cell homeostasis (67.8±9.5 *vs* 47.8±6.4/5x10^5 PI$^-$ cells in saline-treated mice, Fig. 5A). Compared to total splenocytes, both mast cells and basophils exhibited some basal eGFP signal indicative of IL-4 transcription. However the eGFP MFI was markedly higher in basophils than in mast cells (MFI: 14.46±0.72 in mast cells vs. 59.88±3.47 in basophils, Fig. 5B). Furthermore, an additional incremental increase in eGFP expression of about 30% was observed in basophils (MFI: 91.12±3.99, Fig. 5B) from *Af*-treated *4get* animals, indicating that allergen exposure increases not only basophil numbers but also enhances IL-4 gene expression.

Although the *4get* reporter model provides a reliable representation of cell lineage commitments to produce IL-4, we corroborated our observations in the reporter mice using direct intracellular cytokine staining in BALB/c mice (Fig. 6). As in the *4get* animals, we observed constitutive strong

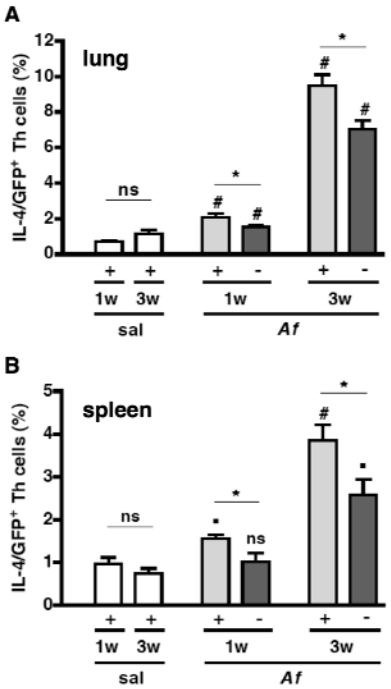

Fig. 7. *Basophil-enhanced Th2 cell expansion following Af exposure. GFP⁺ T lymphocytes were enumerated in the (**A**) lungs and (**B**) spleens of 4get IL-4 reporter mice, after acute (**3d**) and chronic (**3w**) Af inhalation. Starting one day before the first allergen dose, mice received three daily i.p. injections of either purified MAR-1 (-), in order to specifically deplete basophils, or isotype control (+). Mice were euthanized 72 h after the Af final dose and GFP⁺ T helper cells were enumerated and are represented as a percentage of total CD3⁺CD4⁺ cells. n=5 mice per group. ns: not significant; *, p<0.05. # indicates p<0.001 and ▪ indicates p<0.01 (relative to baseline value in the appropriate saline treated group).*

IL-4 expression in splenic basophils. Basophils from both control and *Af*-treated mice were more uniformly IL-4 bright. Basophils from *Af*-treated mice exhibited a significantly, though modestly, increased MFI ratio (IL-4:isotype control, 3.68±0.19 in *Af*-treated mice *vs* 2.86±0.11 in saline controls, Fig. 6C). This finding, consistent with our observations regarding eGFP expression in basophils from naïve vs. *Af*-treated *4get* mice, indicates that basophils, while constitutively strongly IL-4 positive, can be induced to further enhancement of IL-4 expression in the presence of *Af* allergens.

Basophils facilitate Th2 development after Af exposure

Af-treated *4get* mice were used to track the induction of IL-4 committed (Th2) T cells over the course of three weeks of *Af* exposure. A significant accrual of eGFP-positive T cells was evident in both spleen and lung (4-fold increase in spleen and 14-fold increase in lung, Fig. 7). As Th2 cells are absolutely dependent on IL-4 for their expansion, we hypothesized that the IL-4⁺ basophils induced early in the *Af* response might have provided a priming source of IL-4, driving the Th2 expansion. In order to test this hypothesis, basophil depletion was performed using MAR-1, an anti-FceRI mAb, which has been well characterized by several groups as an effective agent for basophil depletion without effects on mast cells (14, 16, 18). MAR-1 treatment completely eliminated basophils (not shown) and resulted in significant attenuations in eGFP⁺ T cell expansion in both the spleen (33% reduction) and lungs (26% reduction) of *Af*-exposed animals (Fig. 7). In order to assess the effects of basophil depletion on antigen-specific Th2 responses, some mice were given the T-dependent marker antigen ovalbumin (OVA) *i.n.* along with *Af*. Splenocytes from animals receiving OVA together with *Af* exhibited significant IL-4 production in response to *in vitro* antigen stimulation. In contrast, the antigen-induced IL-4 production by splenocytes from mice subjected to basophil depletion was significantly suppressed (Fig. 8A). There was a striking inverse effect on the IFN-γ response (Fig. 8 B). OVA-specific IgE and IgG1 responses were induced in both isotype-control and MAR-1-treated animals. However levels of both of these Th2-dependent isotypes were markedly lower in the basophil depleted animals (IgG1: 212.9±21.67 *vs* 84.84±18.20 mU/ml; IgE: 2.565±0.719 *vs* 0.793±0.213 mU/ml, Fig. 8C-D). These findings indicate that the basophil response of naïve allergen-exposed mice enhances developing Th2 responses to aeroallergens.

DISCUSSION

Although basophils have long been implicated as potential effector cells in late phase reactions to

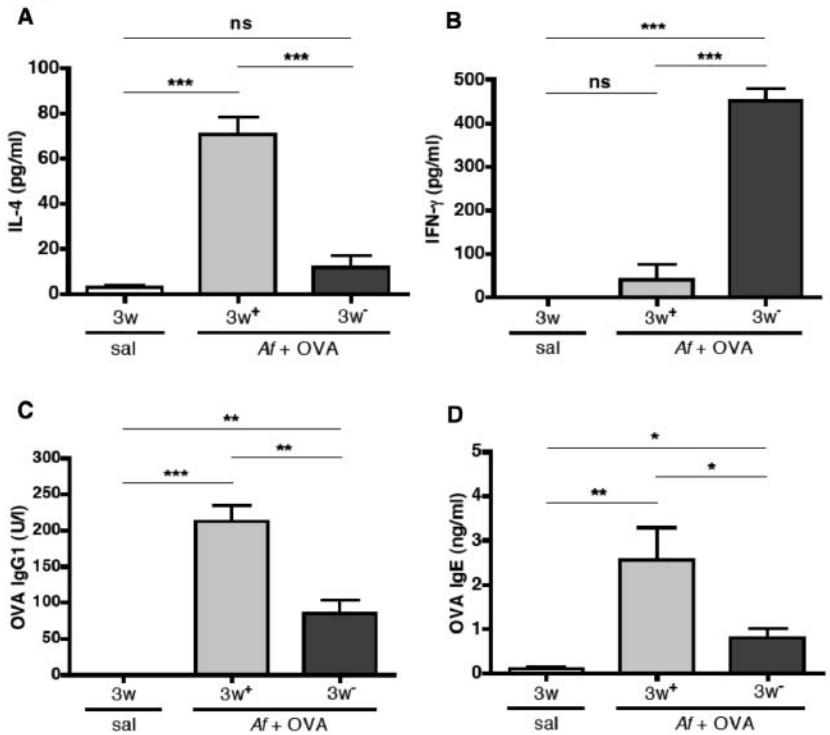

Fig. 8. *Basophil effects on antigen-specific cellular and humoral Th2 responses. The marker antigen ovalbumin (**OVA**) was intranasally administered concomitantly with Af for 3 weeks to mice depleted of basophils (**3w$^-$**, dark grey column) or treated with isotype control (**3w$^+$**, light grey column). Spleen cells from these mice were re-stimulated in vitro with OVA for 48 h and culture supernatants were assayed for the presence of (**A**) IL-4 or (**B**) IFN-γ. (**C**) Anti-OVA IgG1 and (**D**) anti-OVA IgE serum levels were determined by ELISA. n=5 mice per group. Ns: not significant; *, p<0.05; **, p<0.01; ***, p<0.001.*

allergens in subjects with established IgE and Th2 responses, one of the most interesting emerging roles of these cells is their potential function as innate early responders modulating the differentiation program of CD4$^+$ T cells following parenteral immunization with protein antigens in naive hosts (14, 19, 21, 26-27). Human basophils have long been known as rapid IL-4 producers following immunologic activation (27, 28). In individuals with established IgE-mediated sensitivity to allergens these cells are rapidly recruited and produce IL-4 following bronchial challenge, indicating important roles in the effector mechanisms of allergic airway diseases (10-12). Neither the early recruitment of these cells in the immunologically naïve host exposed to natural aeroallergens nor their role in the genesis of subsequent Th2 responses has been amenable to examination in human subjects. Therefore, in the current study, we applied a murine model of natural aeroallergen responses to test the hypothesis that basophils might serve as instigators or amplifiers of Th2 responses to inhaled allergens.

The *Af* model of chronic allergen administration had previously been well characterized by our group and others (4-7). In this investigation, however, we shifted the focus of analysis to an *early* time window, the first 3 days of allergen encounter. We observed that inflammatory cell recruitment to the airways, initially dominated by neutrophils, had begun within that time frame, while the eosinophil infiltrate (which is characteristic of the chronic *Af* response) was not yet evident (Fig. 1). This early response was characterized by lung and systemic induction of basophils (Fig. 2-5). Miyoshi-Higashino et al. recently reported systemic basophil responses following chronic exposure to cedar pollen extract

(29).

A number of recent reports have brought basophils into focus as potential early sensors of proteases and other allergens/adjuvants and as producers of Th2-inducing cytokines including IL-4 and TSLP (16, 18-20). Chronic *Af* inhalation results in the eventual induction of a Th2 response. We tracked the induction of this response by monitoring the systemic accrual of GFP^+CD4^+ cells in IL-4 reporter *4get* mice, the production of IL-4 by antigen-stimulated splenocytes and the production of the Th2-dependent antibody isotypes, IgE and IgG1. All of these responses were attenuated in mice depleted of basophils during *Af* exposure and IFN-γ production was, conversely, increased (Fig. 6-8), suggesting a role for these cells in Th2 priming in respiratory allergy. Previously, Metcalfe's group used a protein-based model of pulmonary inflammation initiated by *i.p.* sensitization in the presence of alum and the authors described IgE^+ $c\text{-}kit^-$ myeloid cells as early IL-4 sources following *i.p.* priming (30). Our findings provide novel information, showing that basophils are recruited and appear to modulate Th2 immune responses to natural respiratory allergens in an experimental system free of antigen injection or adjuvant administration.

Given the rapidity of the basophil response to inhaled *Af*, we hypothesized that their recruitment was mediated by innate immune mechanisms and likely independent of adaptive immune function. However, we considered the possibility that T cells might be important in basophil differentiation and homeostasis, as is the case for mucosal mast cells (31). Moreover, Corry *et al.* reported that $CD4^+$ T cells are required for the development of airway inflammation following chronic *Af* exposure (32). In order to examine this issue we took advantage of RAG-$1^{-/-}$ mice on the BALB/c background and observed a completely intact basophil response to *Af* (Fig. 4A). This finding is most consistent with innate immune mechanisms as instigators of basophil mobilization following fungal allergen recruitment and that, in contrast to mucosal mast cells, basophils are not T cell dependent for their survival.

Fungi express a plethora of innate immune recognition ligands, including structures recognized by several TLR. We therefore considered that this receptor family might link *Af* allergen exposure in the respiratory mucosa to the rapid local and systemic mobilization of basophils. It has long been known that TLR contribute to host defense against fungal infections, including *Af*, and that early protective responses to respiratory infections to *Af* are mediated at least in part by MyD88-dependent signaling pathways. Recently, it has been reported that basophils themselves can be activated by TLR in a MyD88-dependent pathway and that bacterial products can deviate Th2 immune response to fungal antigens via MyD88 signaling (33). However, in our murine model, the basophil response of MyD88$^{-/-}$ mice was indistinguishable from that of control animals also on a BALB/c strain background (Fig. 4B), implicating either MyD88-independent TLR signaling as can be mediated by the TRIF pathway or completely TLR-independent signaling pathways activated by fungal components via other pattern recognition receptors such as Dectin-1.

The cytokine IL-3 is known to provide activating signals to basophils and it has been implicated in basophil differentiation and homeostasis. Although IL-$3^{-/-}$ animals have normal basophil numbers, indicating that it is not required for baseline basophil production, the same mice exhibit a failure to further mobilize basophils after nematode infection as do normal mice (24). Moreover, these knock-out mice seem to also have an impaired basophil IL-4 production *in vitro* and *in vivo* (22). In contrast, in our experimental model, we found that systemic basophil mobilization in IL-$3^{-/-}$ mice spleen following fungal allergen inhalation does not seem to require normal IL-3 levels (Fig. 4C). We conclude that requirements for IL-3 in regulation of basophil responses may be complex and vary depending on the type of immunization and on the timing.

The concept of mouse basophils as rapid IL-4 producers was introduced 20 years ago when Paul and colleagues first described spleen non-B non-T cells producing IL-4 after cross-linking of FceRI *in vitro* (34). Since that time additional non-Th2 IL-4 producers have been identified including mast cells, NKT cells and eosinophils (17, 35). However, both the rapidity of induction and the abundance of IL-4 produced per cell distinguish basophils from the other potential sources and became most evident when production of this cytokine could be easily studied *in vivo* using *4get* or *G4* reporter mice

expressing GFP under control of the IL-4 promoter. In such animals infected with Th2-inducing parasites, basophils appear to be the predominant, if not sole, IL-4 producing non lymphocytic cells (13, 36). Further evidence for a role of basophils as a source of IL-4 early in Th2 responses is provided by animal model systems in which basophils are over-produced. For instance, IRF-$2^{-/-}$ mice, which harbor increased basophils, also exhibit enhanced generation of Th2 cells (37). Rivera's group recently described basophilia and enhanced basophil IL-4 expression in $Lyn^{-/-}$ mice, which develop rapid and dysregulated Th2 responses as a consequence (38).

Against the background of this emerging role for basophils in driving Th2 responses, we hypothesized that the basophils induced early following inhalation of aeroallergens like *Af* might also impact developing T cell responses. We tested this hypothesis by comparing the responses of mice with intact basophil mobilization following inhalation of allergen to those of mice in which basophils were ablated. Denzel and others have described the use of the anti-FceRI mAb, MAR-1, without altering mast cell homeostasis (14, 16, 18). We found that MAR-1 depletion in the course of *Af* inhalation led to an effective clearance of basophils from spleen and bone marrow. The accumulation of circulating $CD4^+$ IL-4/GFP^+ cells over several weeks of *Af* treatment, which is a characteristic marker of Th2 induction for the chronic model, was significantly attenuated following MAR-1 basophil depletion (Fig. 6) as were *ex vivo* IL-4 production, but not IFN-γ, by antigen-stimulated splenocytes and *in vivo* IgE and IgG1 specific responses to the co-administered marker antigen, OVA (Fig. 7-8). Interestingly, we did not observe a parallel reduction of pulmonary inflammation in basophil depleted *Af*-treated mice as assessed by BAL cytology (not shown). This suggests that the inflammatory response to *Af* arises in large part via innate mechanisms and redundant pathways independent of basophil-derived IL-4. However, these findings provide support for a role of basophils in determining the polarity of T cell responses following allergen exposure in the airway.

In conclusion, we have characterized early responses to fungal aeroallergen inhalation in an animal model. Our observation of a rapid mobilization of IL-4 producing basophils both in lungs and systemically suggests that these cells might prime evolving Th2 responses to inhaled allergens and might have an important role in promoting respiratory allergies, as it is emerging from other recent studies (39-40). This is an important and physiologically relevant extension of previous work in the basophil field, so far focused mainly on responses following nematode parasite infestation or protein antigen injection.

ACKNOWLEDGEMENTS

This project was supported by National Institutes of Health grant NIAID R01-AI054471. D.P. received support from the Centro per la Comunicazione e la Ricerca of Collegio Ghislieri of Pavia, Italy.

REFERENCES

1. Simon-Nobbe B, Denk U, Poll V, Rid R, Breitenbach M. The spectrum of fungal allergy. Int Arch Allergy Immunol 2008; 145:58-86.
2. Umetsu DT, Dekruyff RH. Immune dysregulation in asthma. Curr Opin Immunol 2006; 18:727-32.
3. Akdis CA. New insights into mechanisms of immunoregulation in 2007. J Allergy Clin Immunol 2008; 122:700-9.
4. Kurup VP, Choi H, Murali PS, Resnick A, Fink JN, Coffman RL. Role of particulate antigens of Aspergillus in murine eosinophilia. Int Arch Allergy Immunol 1997; 112:270-8.
5. Kurup VP, Seymour BW, Choi H, Coffman RL. Particulate Aspergillus fumigatus antigens elicit a TH2 response in BALB/c mice. J Allergy Clin Immunol 1994; 93:1013-20.
6. Mathias CB, Freyschmidt EJ, Caplan B. IgE influences the number and function of mature mast cells, but not progenitor recruitment in allergic pulmonary inflammation. J Immunol 2009; 182:2416-24.
7. Mehlhop PD,van de Rijn M, Goldberg AB, Brewer JP, Kurup VP, MartinTR, Oettgen HC.Allergen-induced bronchial hyperreactivity and eosinophilic inflammation occur in the absence of IgE in a mouse model of asthma. Proc Natl Acad Sci U S A 1997; 94:1344-9.

8. Swain SL, Weinberg AD, English M, Huston G. 1990. IL-4 directs the development of Th2-like helper effectors. J Immunol 1990; 145:3796-806.
9. Brusselle GG, Kips JC, Tavernier JH, van der Heyden JG, Cuvelier CA, Pauwels RA, Bluethmann H. Attenuation of allergic airway inflammation in IL-4 deficient mice. Clin Exp Allergy 1994; 24:73-80.
10. Lichtenstein LM, Bochner BS. The role of basophils in asthma. Ann N Y Acad Sci 1991; 629:48-61.
11. Guo CB, Liu MC, Galli SJ, Bochner BS, Kagey-Sobotka A, Lichtenstein LM. Identification of IgE-bearing cells in the late-phase response to antigen in the lung as basophils. Am J Respir Cell Mol Biol 1994; 10:384-90.
12. Schroeder JT. Basophils beyond effector cells of allergic inflammation. Adv Immunol 2009; 101:123-61.
13. Min B. Basophils: what they 'can do' versus what they 'actually do'. Nat Immunol 2008; 9:1333-9.
14. Karasuyama H, Mukai K, Tsujimura Y, Obata K. Newly discovered roles for basophils: a neglected minority gains new respect. Nat Rev Immunol 2009; 9:9-13.
15. Lee JJ, McGarry MP. When is a mouse basophil not a basophil? Blood 2007; 109:859-61.
16. Denzel A, Maus UA, Rodriguez Gomez M, et al. Basophils enhance immunological memory responses. Nat Immunol 2008; 9:733-42.
17. Gessner A, Mohrs K, Mohrs M. Mast cells, basophils, and eosinophils acquire constitutive IL-4 and IL-13 transcripts during lineage differentiation that are sufficient for rapid cytokine production. J Immunol 2005; 174:1063-72.
18. Sokol CL, Barton GM, Farr AG, Medzhitov R. A mechanism for the initiation of allergen-induced T helper type 2 responses. Nat Immunol 2008; 9:310-8.
19. Sokol CL, Chu NQ, Yu S, Nish SA, Laufer TM, Medzhitov R. Basophils function as antigen-presenting cells for an allergen-induced T helper type 2 response. Nat Immunol 2009; 10:713-20.
20. Yoshimoto T, Yasuda K, Tanaka H, Nakahira M, Imai Y, Fujimori Y, Nakanishi K. Basophils contribute to T(H)2-IgE responses *in vivo* via IL-4 production and presentation of peptide-MHC class II complexes to CD4+ T cells. Nat Immunol 2009; 10:706-12.
21. Kim S, Shen T, Min B. Basophils can directly present or cross-present antigen to CD8 lymphocytes and alter CD8 T cell differentiation into IL-10-producing phenotypes. J Immunol 2009; 183:3033-9.
22. Hida S, Yamasaki S, Sakamoto Y, et al. Fc receptor gamma-chain, a constitutive component of the IL-3 receptor, is required for IL-3-induced IL-4 production in basophils. Nat Immunol 2009; 10:214-22.
23. Bryce P. Geha J, Oettgen HC. Desloratadine inhibits allergen-induced airway inflammation and bronchial hyperresponsiveness and alters T-cell responses in murine models of asthma. J Allergy Clin Immunol 2003; 112:149-58.
24. Lantz CS, Boesiger J, Song CH. Role for interleukin-3 in mast-cell and basophil development and in immunity to parasites. Nature 1998; 392:90-3.
25. Shinkai K, Mohrs M, Locksley RM. Helper T cells regulate type-2 innate immunity *in vivo*. Nature 2002; 420:825-9.
26. Min B, Paul WE. Basophils and type 2 immunity. Curr Opin Hematol 2008; 15:59-63.
27. PerrigouJG, Saenz SA, Siracusa MC, et al. MHC class II-dependent basophil-CD4+ T cell interactions promote T(H)2 cytokine-dependent immunity. Nat Immunol 2009; 10:697-705.
28. Schroeder JT, MacGlashan jr DW, Lichtenstein LM. Human basophils: mediator release and cytokine production. Adv Immunol 2001; 77:93-122.
29. Miyoshi-Higashino M, Hirano M, Ogita-Nakanishi H, et al. IL-4-dependent induction of IgE basophils in peripheral blood and IgE B cells in spleen as respective indicators of allergen sensitization and a precursor of cells secreting allergen-specific IgE antibody. Microbiol Immunol 2009; 53:30-40.
30. Luccioli S, Brody DT, Hasan S, Keane-Myers A, Prussin C, Metcalfe DD. IgE(+), Kit(-), I-A/I-E(-) myeloid cells are the initial source of Il-4 after antigen challenge in a mouse model of allergic pulmonary inflammation. J Allergy Clin Immunol 2002; 110:117-24.
31. Urban JF, Schopf Jr L, Morris SC, et al. Stat6 signaling promotes protective immunity against Trichinella spiralis through a mast cell- and T cell-dependent mechanism. J Immunol 2000; 164:2046-52.
32. Corry DB, Grunig G, Hadeiba G, Kurup VP, Warnock ML, Sheppard D, Rennick DM, Locksley

RM. Requirements for allergen-induced airway hyperreactivity in T and B cell-deficient mice. Mol Med 1998; 4:344-55.
33. Allard JB, Rinaldi L, Wargo MJ, et al. Th2 allergic immune response to inhaled fungal antigens is modulated by TLR-4-independent bacterial products. Eur J Immunol 2009; 39:776-88.
34. Ben-Sasson SZ, Le Gros G, Conrad DH, Finkelman FD, Paul WE. Cross-linking Fc receptors stimulate splenic non-B, non-T cells to secrete interleukin 4 and other lymphokines. Proc Natl Acad Sci U S A 1990; 87:1421-5.
35. Voehringer D, Shinkai K, Locksley RM. Type 2 immunity reflects orchestrated recruitment of cells committed to IL-4 production. Immunity 2004; 20:267-77.
36. Min B, Prout M, Hu-Li J, et al. Basophils produce IL-4 and accumulate in tissues after infection with a Th2-inducing parasite. J Exp Med 2004; 200:507-17.
37. Hida S, Tadachi M, Saito T, Taki S. Negative control of basophil expansion by IRF-2 critical for the regulation of Th1/Th2 balance. Blood 2005; 106:2011-7.
38. Charles N, Watford WT, Ramos HL. Lyn kinase controls basophil GATA-3 transcription factor expression and induction of Th2 cell differentiation. Immunity 2009; 30:533-43.
39. Wakahara K, Van VQ, Baba N, Begin P, Rubio M, Delespesse G, Sarfati M. Basophils are recruited to inflamed lungs and exacerbate memory Th2 responses in mice and humans. Allergy 2013; 68(2):180-9.
40. Sawaguchi M, Tanaka S, Nakatani Y, et al. Role of mast cells and basophils in IgE responses and in allergic airway hyperresponsiveness. J Immunol 2012; 188(4): 1809-18.

OLEA EUROPEA-DERIVED PHENOLIC PRODUCTS ATTENUATE ANTINOCICEPTIVE MORPHINE TOLERANCE: AN INNOVATIVE STRATEGIC APPROACH TO TREAT CANCER PAIN

C. MUSCOLI[1,2,3], F. LAURO[1,2,3], C. DAGOSTINO[1,2,3], S. ILARI[1,2,3], L.A. GIANCOTTI[1,2,3], M. GLIOZZI[1,2], N. COSTA[1], C. CARRESI[1,2], V. MUSOLINO[1,2], F. CASALE[1], D. VENTRICE[4], M. OLIVERIO[1], E. PALMA[1], S. NISTICÒ[1], A. PROCOPIO[1] and V. MOLLACE[1,2,3]

[1]Department of Health Sciences, University "Magna Graecia", Germaneto, Catanzaro, Italy; [2]Interregional Research Center for Food Safety and Health (IRC-FSH), Germaneto, Catanzaro, Italy; [3]Drug Center, IRCCS San Raffaele Pisana, Roma, Italy; [4]CETA, ArpaCal, Catanzaro, Italy

Received December 13, 2013 – Accepted January 27, 2014

Morphine and related opioid drugs are currently the major drugs for severe pain. Their clinical utility is limited in the management of severe cancer pain due to the rapid development of tolerance. Restoring opioid efficacy is therefore of great clinical importance. A great body of evidence suggests the key role of free radicals and posttranslational modulation in the development of tolerance to the analgesic activity of morphine. Epidemiological studies have shown a relationship between the Mediterranean diet and a reduced incidence of pathologies such as coronary heart disease and cancer. A central hallmark of this diet is the high consumption of virgin olive oil as the main source of fat which contains antioxidant components in the non-saponifiable fraction, including phenolic compounds absent in seed oils. Here, we show that in a rodent model of opiate tolerance, removal of the free radicals with phenolic compounds of olive oil such as hydroxytyrosol and oleuropein re-instates the analgesic action of morphine. Chronic injection of morphine in mice led to the development of tolerance and this was associated with increased nitrotyrosin and malondialdehyde (MDA) formation together with nitration and deactivation of MnSOD in the spinal cord. Removal of free radicals by hydroxytyrosol and oleuropein blocked morphine tolerance by inhibiting nitration and MDA formation and replacing the MnSOD activity. The phenolic fraction of virgin olive oil exerts antioxidant activities *in vivo* and free radicals generation occurring during chronic morphine administration play a crucial role in the development of opioid tolerance. Our data suggest novel therapeutic approach in the management of chronic cancer pain, in particular for those patients who require long-term opioid treatment for pain relief without development of tolerance.

For many oncological patients, pain is the first sign of cancer, and 30-50% of all cancer patients will experience moderate to severe pain. Cancer can cause pain at any time during the course of the disease, but the frequency and intensity of pain tend to increase during the advanced stages. In fact, 75-95% of patients with metastatic or advanced-stage cancer will experience significant amounts of cancer induced pain (1).

According to the ''analgesic ladder'' approach by

Key words: Cancer pain, oxidative stress, morphine

Mailing address: Prof. Steven Nistico,
Dermatologist, Associate Professor of Dermatology,
University Magna Graecia,
Viale Europa, Germaneto,
88100 Catanzaro, Italy
Tel.: +39 0961 3694001 Fax: +39 0961 3694001
e-mail: steven.nistico@gmail.com

0393-974X (2014)

the World Health Organisation (WHO), morphine is still recommended as the standard ''step 3'' therapy.

Unlikely, prolonged treatment with these drugs leads to the induction of side effects such as hyperalgesia and antinociceptive tolerance (2, 3). The mechanisms leading to these side effects are poorly understood but increasing evidence suggests that are associated with nitroxidative stress (2-5).

Our studies revealed that development of antinociceptive tolerance and hyperalgesia to repeated doses of morphine in mice was consistently associated with overproduction of nitroxidative species as peroxynitrite (PN), the reaction product between superoxide (SO) and nitric oxide (NO) (5). The morphine induced hyperalgesia is also accompanied by production of several proinflammatory cytokines, oxidative DNA damage and activation of the nuclear factor poly(ADPribose) polymerase (4-6). Furthermore, we have, recently, demonstrated that central sensitization is associated with the appearance of several tyrosine-nitrated proteins in the dorsal horn of the spinal cord, including the mitochondrial isoform of superoxide ($O_2^{\bullet-}$) dismutase, the glutamate transporter GLT-1, the enzyme glutamine synthase (GS) and NMDAR subunits, GluN1 and GluN2B (7) leading to the impairment of glutamate turnover. PN is a signaling mediator in this setting, in fact pointing it's production by inhibition of NO synthesis or removal of SO lead to a reinstate of morphine analgesic action. The co-administration of morphine with the PN decomposition catalyst, Fe(III)5,10,15,20-tetrakis(N-methylpyridinium-4-yl)porphyrin^{5+} (FeMTPyP^{5+}) blocks protein nitration, attenuating the observed biochemical changes, and preventing the development of tolerance in a dose-dependent manner (2, 4).

The olive is the fruit of *Oleaeuropaea,* a tree native to the coastal Mediterranean region which produces 98% of the world total (approximately 11 million tons), and lends important economic and dietetic benefits to the people of that region (8). Oleuropein and its hydrolysis product hydroxytyrosol are the main phenolic constituents of olive leaves, and thought to be responsible for their pharmacological effects (9) being the most potent olive oil antioxidants. The antioxidant action of olive oil *in vitro* has been highly documented and linked to chemoprotection, anti-inflammatory, hypoglycemic, antihypertensive and antimicrobial action, and prevention of atherosclerotic plaque formation (8). Indeed, several studies demonstrated that oleuropein dose-dependently inhibits copper sulphate-induced oxidation and the lipid peroxidation of low-density lipoproteins (LDL) (10,11). Oleuropein has also a direct antioxidant and protective action on chronic UVB-induced skin damage through a reduction in COX-2 levels, and during aging decreases the intracellular levels of reactive oxygen species (ROS), reduces the amount of oxidized proteins through increased proteasome-mediated degradation rates and retains proteasome function during replicative senescence (8). Therefore, the present study was designed to test the hypothesis that chief antioxidant olive extracts could exert their antioxidant effects against the development of tolerance to the antinociceptive effect of morphine in mice.

MATERIALS AND METHODS

Male CD-1 mice (24-30 g; Charles River Laboratory) were housed and cared for in accordance with the guidelines of the Institutional Animal Care and Use Committee (IACUC) of the Saint Louis University Health Science Center and in accordance with the NIH Guidelines on Laboratory Animal Welfare and the in compliance with Italian regulations on protection of animals used for experimental and other scientific purposes (D.M. 116192) as well as with European Economic Community regulations. The IACUC and the University of Catanzaro "Magna Graecia" approved all studies. Mice were housed 5-7 per cage and maintained under identical conditions of temperature (21±1°C) and humidity (60%±5%) with a 12-h light/12-h dark cycle and allowed food *ad libitum*. Natural antioxidants OLEA and HT were extracted at the University of Catanzaro "Magna Graecia", in the laboratories of Faculty of Pharmacy. All others drugs were purchased from Sigma and dissolved in saline (sodium chloride 0,9%). The following experimental groups were used:

1. Acute morphine groups: Mice received a single s.c. injection of morphine (1, 3, 6 mg/kg, n=15 each dose). Behavioral tests have been carried out after 30, 45, 60 min from the treatment;
2. Naive group: In this group, mice (n=15) were injected twice a day with an i.p. injection of saline (vehicle used to deliver the drugs to the other groups over 4 days) and a s.c. injection of saline (vehicle used to deliver morphine to the other groups over 4 days). On day 5 mice received an i.p. injection of saline followed 15 minutes later by a s.c. injection of morphine (3 mg/kg);
3. Morphine group: In this group, mice (n=15)

were injected twice a day for 4 days with an i.p. injection of saline and a s.c. injection of morphine (20 mg/kg). On day 5 mice received an i.p. injection of saline followed 15 minutes later by a s.c. dose of acute morphine (3 mg/kg).

Morphine plus drug groups

In this group, mice were injected twice a day for 4 days with an i.p. injection of MnTBaP^{3-} L-NAME(10 mg/kg; n=15),or different doses of OLEA (3 mg/kg; 10 mg/kg; 30mg/kg; for each dose n=15) or HT (1 mg/kg; 3 mg/kg; 10 mg/kg; for each dose n=15) followed by s.c. injection of morphine (20 mg/kg/d; n=15). On day 5 mice received an i.p. dose of drugs, followed 15 minlater by the s.c. dose of acute morphine (3 mg/kg). All doses were given in a 0.1ml volume at approximately 7 am and 4 pm.

On day 5 and after the behavioral tests, carried out after 60 min from the treatment, spinal cord tissues from the lumbar enlargement segment of the spinal cord (L4–L5) were removed and tissues stored at -80°C for subsequent analysis.

Hot plate test

Nociceptive thresholds were determined by measuring latencies (in seconds) of mice placed in a transparent glass cylinder on a hot plate (Ugo Basile) maintained at 52°C. Determination of antinociception was assessed between 7:00 am and 10:00 am. Responses indicative of nociception included intermittent lifting and/or licking of the hind paws or escape behavior. Hot plate latencies were taken in mice from all groups on day 5 before (baseline latency) and 60 min after an acute dose of morphine (3 mg/kg). Results are expressed as percentage of maximum possible antinociceptive effect, which was calculated as follows: (response latency−baseline latency)/(cut-off latency−baseline latency)×100. A cut-off latency of 20 s was employed to prevent tissue damage. 15 mice per group were used, and all experiments were conducted with the experimenters blinded to treatment conditions.

Immunohistochemical detection of nitrated proteins in the spinal cord

The lumbar portion of the spinal cord (L4-L6) were fixed and processed for immunostaining as described (12). Monoclonal anti-nitrotyrosine antibody (1:100 in 10% normal horse serum, Calbiochem) were used as a primary antibody. The processed samples were visualized for immunolabeling by using secondary antibody, A/B complex, and diaminobenzidine accordingly to the manufacturer's instructions (Vector ABC Elite Kit, Vector Laboratories).

Immunoprecipitation and Western blot analyses

Dorsal half of the spinal cord lumbar region enlargement (L4-L5) were obtained as described previously (12-14). The resulting lysates samples were stored immediately at -80°C and immunoprecipitation of tyrosine nitrated protein followed by Western blot analysis performed as previously described (12, 13). For immunoprecipitation of nitrated proteins, a well-characterized affinity-purified anti-nitrotyrosine monoclonal antibody conjugated to agarose beads from Upstate Biotechnology was used according to the manufacturer's instructions. To determine whether MnSOD was nitrated, Western blot analysis of i.p. protein complex and total lysates were performed using antibodies specific to these proteins. Briefly, the immunoprecipitated proteins were resolved in 10% SDS-PAGE mini and proteins transferred to nitrocellulose membranes. Membranes were blocked for 2 h at room temperature with 5% BSA in TBST 0.1%, followed by overnight incubation with monoclonal antibody for MnSOD (1:1000; Cayman Chemical). Membranes were then washed with TBS/T and incubated secondary antibodies conjugated to peroxidase for 1 h at room temperature. After washes, protein bands were visualized by enhanced chemiluminescence (Amersham Biosciences). After stripping, total lysates membranes were reprobed with either monoclonal anti β-actin antibody (1:2000; Sigma-Aldrich) as a loading control. The relative expression of the protein levels as the band density for MnSOD (29 kDa) and β-actin (45kDa) were quantified by scanning of the X-ray films with MSF-300G and a computer program.

Measurement of MnSOD activity

Dorsal half of the spinal cord lumbar region enlargement (L4-L5) were homogenized with 10 mM PBS (pH 7.4) in a Polytron homogenizer and then sonicated on ice for 1 min (3 times, 20 s each time). The sonicated samples were subsequently centrifuged at 1,100 g for 10 min and SOD activity was measured in the supernatants. In brief, a competitive inhibition assay was performed that used xanthine-xanthine oxidase-generated $O_2^{\bullet-}$ to reduce nitroblue tetrazolium (NBT) to blue tetrazolium salt. The reaction was performed in sodium carbonate buffer (50 mM, pH 10.1) containing EDTA (0.1 mM), nitroblue tetrazolium (25 μM), and xanthine and xanthine oxidase (0.1 mM and 2 nM, respectively; Boehringer). The rate of NBT reduction was monitored spectrophotometrically (Perkin Elmer Lambda 5 Spectrophotometer) at 560 nm. The amount of protein required to inhibit the rate of NTB reduction by 50% was defined as 1 unit of enzyme activity. Enzymatic activity was expressed in units per milligram of protein (12).

Malonylaldehyde detection

The solid-phase extraction procedure was applied to isolate 2,4-dinitrophenylhydrazone from biological

samples. Tissue samples were suspended in phosphate buffer (0.01 M, pH 7.0), sonicated and then centrifuged at 5000×g for 5 min. The supernatant was collected and stored at -80°C for further analysis.

For the derivative process, MDA standard was prepared by hydrolysis of 1,1,3,3-tetraethoxypropane (TEP). The reaction of MDA with 2,4-dinitrophenylhydrazine (DNPH) was carried for 30 min at room temperature. The 2,4-dinitrophenylhydrazone was filtered, purified and used for the study of accuracy and precision, extraction recovery and stability.

Conditioned cartridge, based on a polymeric matrix with a high hydrophilic–lipophilic balance HLB (Oasis SPE 1 mL, 30 mg; Waters-Milford, MA), provided with a LiChrolut extraction unit (Merck), was chosen to isolate MDA-derived from biological samples. After washing samples with 2 mL of water containing 5% methanol, the analytes were eluted twice with 2 mL of methanol. For all dry steps the pressure was maintained at 39.9 kPa for 3 min. The eluate was dried under a nitrogen stream at 45°C and the residue was dissolved in 200 mL of mobile phase before HPLC analysis.

Quantitative analysis of MDA was performed on Jasco PU 1580 pump and LG 1580-02 ternary unit (Tokyo, Japan) using a 100 mL loop injection valve. The chromatographic system was associated to a diode-array Jasco MD-1510 detector (Tokyo, Japan); methanolic solution of hydrazone and acid solution of DNPH were injected into the column and identified by their relative retention times determining the maximum wavelength of absorption of the hydrazone at 310 nm. Data were processed using Borwin chromatography software (version 1.21) from Jasco (Tokyo, Japan). A mixture of H2O acidified by CF3COOH (pH=2,20) and acetonitrile (ACN), in ratio of 45:55 (*vv*) was used as mobile phase. It was delivered at a flow rate of 1.0 mL/min through a Nucleosil 100-5 RP/18 (25 cm×4.6 cm, 4 μm) reverse phase column (Agilent), with a relative guard column (4.5 cm×0.46 cm). A block heater Gastorr GF 103 (Jones Chromatography, CO) was utilized to maintain the analytical column at 25°C.

Statistical analysis

Results are given as mean ± SEM. Statistical analysis was performed using ANOVA followed by Student-Newman-Keuls. $P<0.05$ was considered statistically significant.

RESULTS

Inhibition of oxidative stress blocks morphine antinociceptive tolerance

Acute administration of different morphine doses demonstrated dose-dependent analgesic effects of this opioid. We tested 3 different doses 1mg/kg, 3 mg/kg and 6 mg/kg and examined their analgesic pharmacological effect after 30 min, 45 min and 60 min (Fig. 1). 3 mg/kg was identified as the most efficacious acute dose and was choice for the following experiments.

After repeated administration of morphine (20 mg/kg/d) for 5 days, a significant tolerance to its antinociceptive effect appeared, and it is highlighted by a significant (p <0.001) reduction in hot plate latency(s) after an acute dose of morphine challenge (3 mg/kg) in mice receiving repeated morphine administration over 5 days compared to mice receiving repeated saline injection (Fig. 2). Pretreatment, 15 min before morphine, with different doses of major phenolic compound of olive oil oleoeuropein (OLEA, 3 mg/kg, 10 mg/kg, 30 mg/kg) or hydroxytyrosol (HT; 1 mg/kg, 3 mg/kg, 10 mg/kg), prevented the development of tolerance to the antinociceptive effect of morphine in a dose-dependent manner (Fig. 2A-B). In particular, in animals that received morphine together with OLEA (30 mg/kg) or HT (10 mg/kg), tolerance did not develop during the experiment. In contrast, 3 or 10mg/kg OLEA or 1 and 3 mg/kg HT did not completely prevent the development of tolerance to the antinociceptive effect of morphine. However, concomitant treatment of saline with morphine had no antitolerant effect (Fig. 2A-B). The inhibitory effects of OLEA or HT were not attributable to acute antinociceptive interactions between this natural antioxidants and acute morphine doses, since the response to acute morphine in animals treated with higher OLEA or HT dose (30 and 10 mg/kg respectively) or their vehicle over 4 days was statistically insignificant (Fig. 2A-B).

Therefore, we show for the first time that natural antioxidants play a critical role in the inhibition of morphine-induced antinociceptive tolerance.

In addition, we compared intraperitoneal administration of higher and more efficacy dose of natural antioxidants OLEA (30 mg/kg) and HT (10 mg/kg) to synthetic antioxidants as the nonselective NOS inhibitor N-nitro-L-arginine methyl ester (L-NAME, 10 mg/kg) (15) and with the nonselective $O_2^{\bullet-}$ scavenging agent $MnTBAP^{3-}$ (10 mg/kg) (Mn(III) 5, 10, 15, 20-tetrakis(4-carboxylatophenyl)

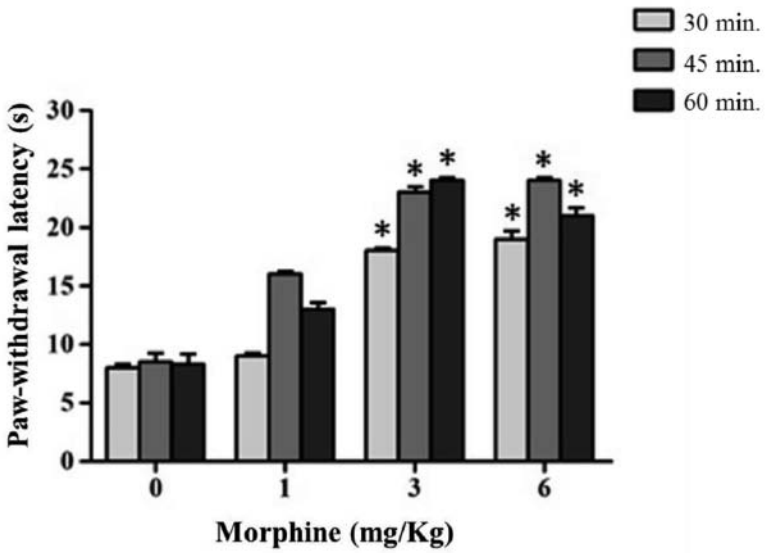

Fig. 1. *Morphine dose-response curve analysis. Acute injection of morphine (3 mg/kg) in normal mice produced a significant near-maximal antinociceptive response [percentage maximal possible antinociceptive effect (%MPE), ranging from 90–95% until 60 minutes]. Results are expressed as mean ± SEM for 15 rats;*P<0.001 vs morphine 0 mg/kg.*

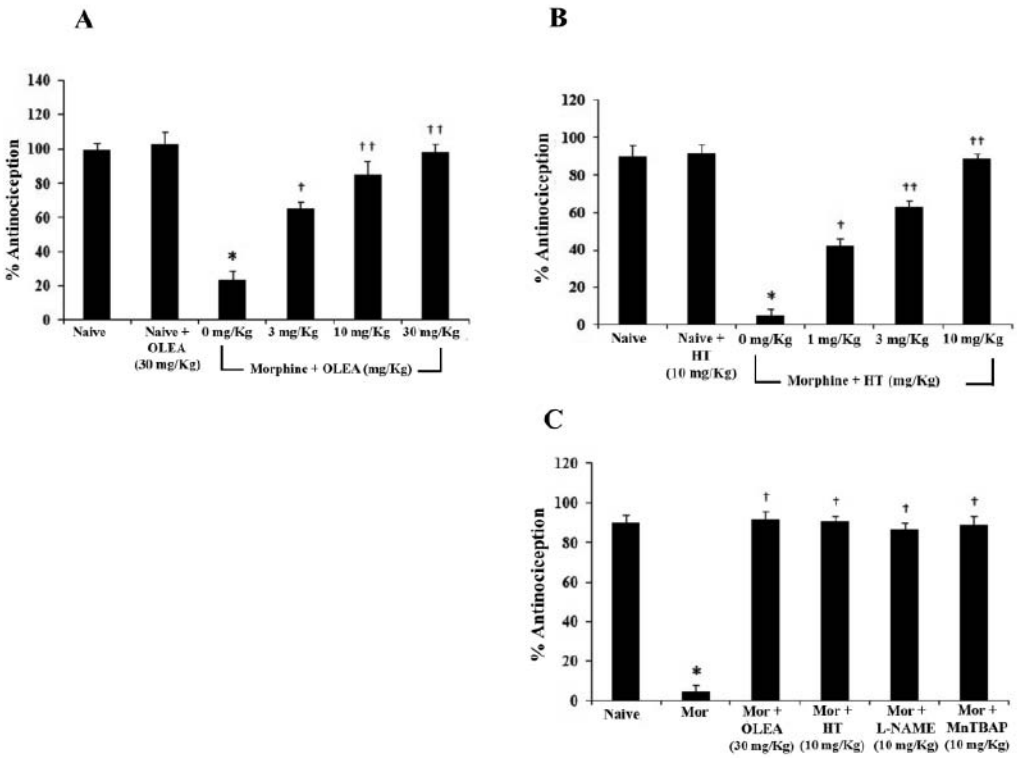

Fig. 2. *Antioxidants inhibited development of morphine antinociceptive tolerance. A significant loss to the antinociceptive effect of the acute injection of morphine was observed in animals that received repeated administration of morphine over 4 days. Co-administration of morphine over 4 days with (**A**) OLEA (3–30 mg/Kg) or (**B**) HT (1-10 mg/kg), inhibited the development of tolerance in a dose-dependent manner and their higher dose effect **(C)** was comparable to synthetic antioxidants L-NAME (10 mg/kg/d) and MnTBAP[3] (10 mg/kg/d). (**A-B**) Tested alone at the highest dose, neither OLEA (30 mg/kg) nor HT (10 mg/kg) demonstrated antinociceptive effects. Results are expressed as mean ± SEM for 15 rats. *P<0.001 vs Naive; †P<0.01 vs morphine; ††P<0.001 vs morphine.*

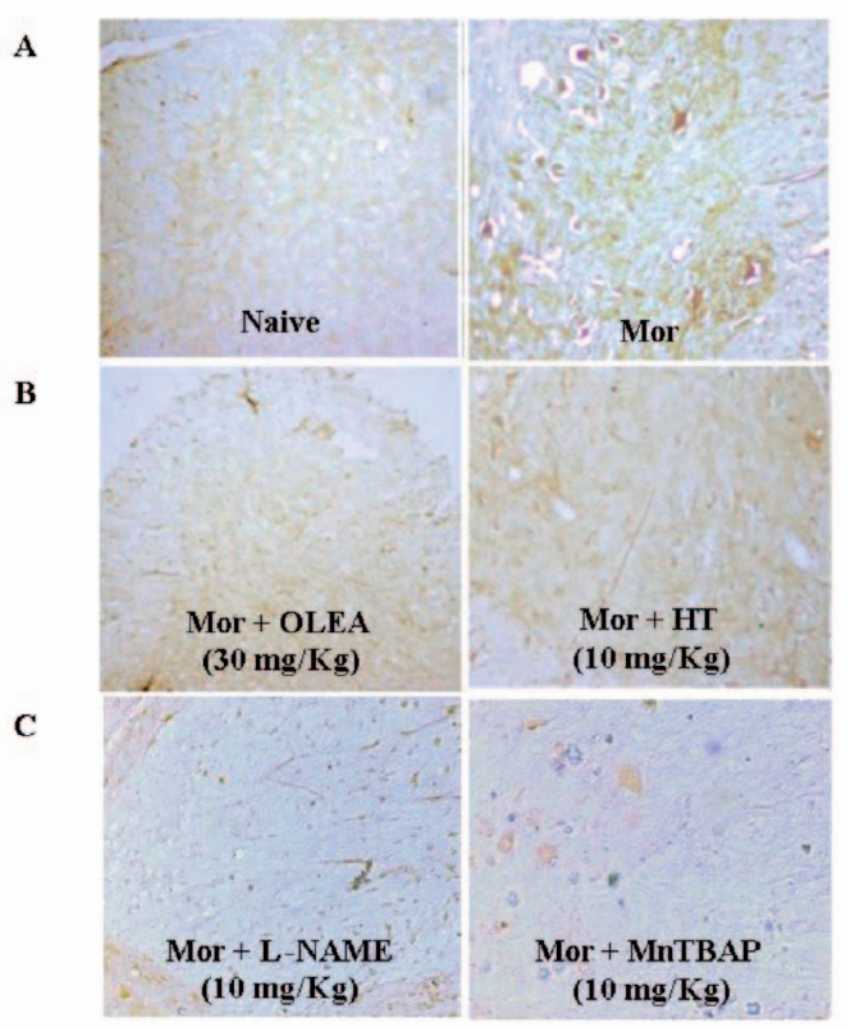

Fig. 3. *Oleuropein and hydroxytyrosol inhibited nitrotyrosine formation in the L4-L5 portion of spinal cord during chronic morphine administration. (**A**) On day 5 acute injection of morphine (3 mg/kg) did not lead to the appearance of nitrotyrosine staining in the superficial layers of the dorsal horn of naive mice. On the other hand, repeated administration of morphine led to significant protein nitration in the superficial layers of the dorsal horn. (**B-C**) Coadministration of morphine with OLEA (30 mg/Kg), HT (10 mg/Kg), L-NAME (10 mg/kg/d) or MnTBAP^{3-} (10 mg/kg/d) blocked nitrotyrosine formation. Original magnification, ×10. Micrographs are representative of at least 6 experiments from 3 different animals performed on different days.*

porphyrin) (16, 17).

The effects of the tested antioxidants were similar and no significant difference have been observed in the capacity of inhibition the development of morphine tolerance antinociceptive.

The development of morphine-induced tolerance is associated with protein tyrosine nitration and this is inhibited by both synthetic and natural antioxidants

The development of morphine-induced tolerance observed following chronic administration was associated with a significant increased protein tyrosine nitration, as detected by immunohistochemistry, in the superficial layers of the spinal cord from the lumbar enlargement (L4-L5) when compared with non-tolerant animals.

Co-administration of morphine with daily injections of the antioxidant OLEA (30 mg/kg), HT (10 mg/kg), L-NAME (10 mg/kg) or MnTBAP^{3-}(10 mg/kg) blocked the increased formation of protein

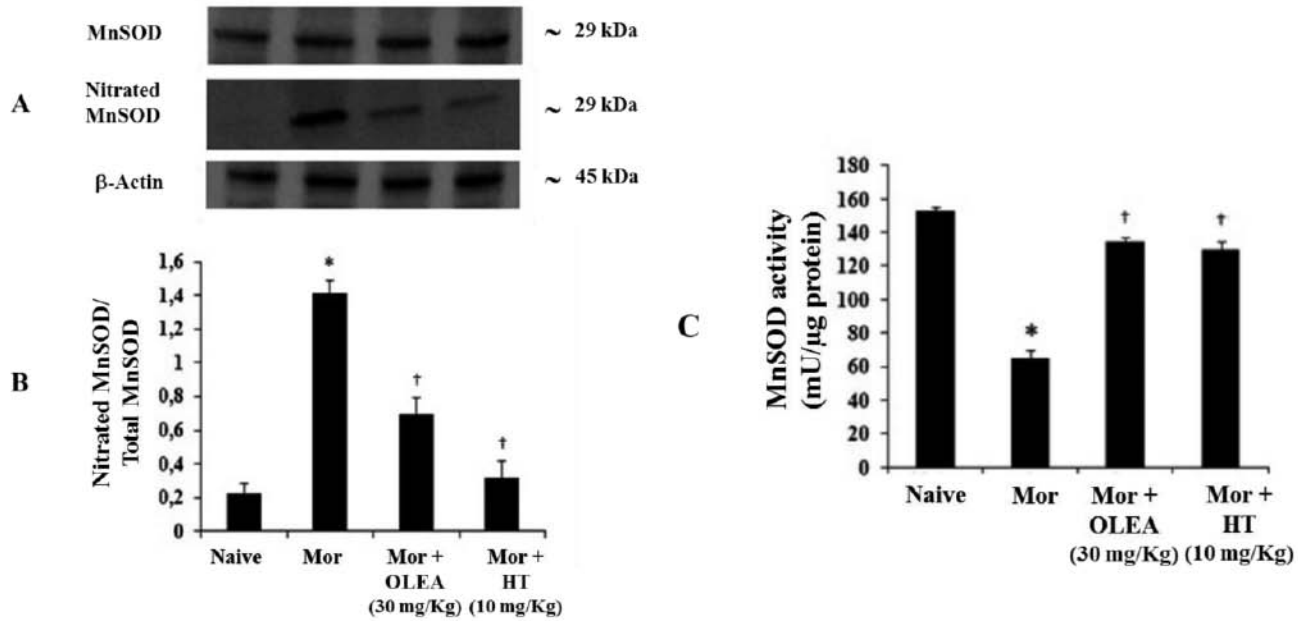

Fig. 4. *Morphine antinociceptive tolerance is associated with nitroxidative stress which is blocked by OLEA and HT.* ***(A)*** *When compared with naive mice, morphine group lead to significant nitration of MnSOD in spinal cord tissues as measured by immunoprecipitation. Coadministration of morphine over 4 days with OLEA (30 mg/kg) or HT (10 mg/kg) prevented MnSOD nitration. Total protein levels don't change among groups as measured by Western blotting analysis. Gels shown are representative of at least 6 experiments from 4 different animals performed on different days.* ***(B)*** *Bar graph in B represents quantification by densitometric analysis.* ***(C)*** *Posttranslational nitration of MnSOD led to functional enzymatic inactivation as evidenced by measurement of MnSOD activity. Co-administration of morphine with OLEA (30 mg/kg) or HT (10 mg/kg) prevented nitration and restored the enzymatic activity of MnSOD. Activity results are expressed as mean ± SEM of 4 mice; *P<0.001 vs Naive; †P<0.001 vs morphine.*

nitration (Fig. 3B-C) and the development of the associated antinociceptive tolerance (Fig. 2). Previously, we have shown that synthetic antioxidant as L-NAME or $MnTBAP^{3-}$ effectively block the production of tyrosine nitration in the spinal cord in morphine-tolerant mice (2), but now we demonstrated for the first time that also natural antioxidants are able to prevent the development of morphine-induced antinociceptive tolerance blocking the nitrotyrosine formation.

Oleuropein and hydroxytyrosol are able to inhibit MnSOD tyrosine nitration appeared during development of morphine-tolerance

We show that the development of morphine tolerance is associated with nitration tyrosine of different proteins with central importance in glutamate homeostasis as glutamate transporter GLT-1 and GS (2). We also demonstrated nitration of mitochondrial manganese $O_2^{\bullet-}$ dismutase (MnSOD), the enzyme that normally keeps concentrations of $O_2^{\bullet-}$ under tight control (2). Posttranslational nitration of this protein led to enzymatic modulation and irreversible neuronal damage (18). Inhibition of antinociceptive tolerance by synthetic antioxidant as L-NAME or $MnTBAP^{3-}$ was associated with a reduction in nitrotyrosine staining in the superficial layers of the dorsal horn (2). We now demonstrate that also natural antioxidants as OLEA (30 mg/kg) and HT (10 mg/kg) are able to reduce nitrotyrosine formation and posttranslational modulation. Chronic administration of morphine for 5 days led to MnSOD tyrosine nitration, as detected by immunoprecipitation analysis shown in figure 4A-B, accompanied by loss of its catalytic activity to dismutate SO (Fig. 4C). In contrast, the enzymatic activity of MnSOD was not affected in non-tolerant animals receiving OLEA (30 mg/kg) before

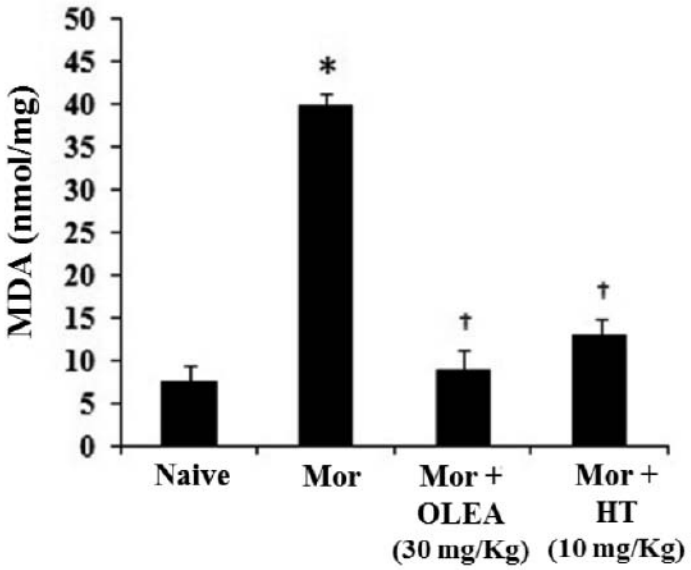

Fig. 5. *OLEA and HT prevent lipid peroxidation associated to morphine antinociceptive tolerance. HPLC analysis revealed a specific formation of MDA in mice treated chronically with morphine but not in naive and in OLEA or HT pretreated mice. Results are expressed as mean ± SEM of 4 mice; *P<0.001 vs Naive; † P<0.001 vs morphine.*

morphine administration. Protection of the enzymatic inactivation of MnSOD (Fig. 4C) was associated to attenuation of posttranslational nitration of MnSOD (Fig. 4A-B), and suggests that inhibition of tolerance by OLEA and HT is secondary, at least in part, to inhibition of posttranslational nitration of MnSOD.

Lipid peroxidation is induced during chronic morphine administration in mice

To confirm the role of oxidative stress during morphine tolerance we quantified the malondialdehyde (MDA), a highly reactive three carbon dialdehyde produced as a byproduct of polyunsaturated fatty acid peroxidation and arachidonic acid metabolism. Then, MDA is one of the most frequently used biomarkers providing an indication of the overall lipid peroxidation levels. Employing an HPLC analysis, we demonstrated that prolonged morphine treatment produced a conspicuous increase of MDA (Fig. 5). In OLEA (30 mg/kg) or HT (10 mg/kg) pretreated mice, HPLC analysis revealed no specific formation of MDA (Fig. 5). Thus, these results indicate that after morphine chronic treatment there are high levels of lipid peroxidation in the spinal cord of tolerant mice and that, treatment with OLEA or HT, two natural phenols with strong antioxidant activity, are able to inhibit this effect.

DISCUSSION

Pain is the most disruptive influence on the quality of life of cancer patients, and although significant advances have been made in cancer treatment and diagnosis, the basic neurobiology of cancer pain is poorly understood.

Cancer is made up of many cell types other than cancer cells, including immune-system cells such as macrophages, neutrophils and T cells. These secrete various factors that sensitize or directly excite primary afferent neurons, and include prostaglandins, tumour necrosis factor-α (TNF-α), endothelins, interleukin-1 and -6, epidermal growth factor, transforming growth factor-β and platelet derived growth factor. Receptors for many of these factors are expressed by primary afferent neurons (1).

Furthermore, there are several mechanisms

by which cancer could cause a decrease in pH. As inflammatory cells invade the neoplastic tissue, they release protons that generate local acidosis. The large amount of apoptosis that occurs in the tumor environment also contributes to acidosis, as apoptotic cells release intracellular ions to create an acidic environment. This drop in pH can activate signaling by acid-sensing channels that are expressed by nociceptors. Finally, rapid cancer growth frequently entraps and injures nerves, causing mechanical injury, compression, ischaemia or direct proteolysis (19). Proteolytic enzymes that are produced by cancer cells can also cause injury to sensory and sympathetic fibres, causing neuropathic pain. So, cancer pain induces, and is at least partially maintained by, a state of central sensitization, in which neurochemical changes in the spinal cord and forebrain promote an increased transmission of nociceptive information (1).

The World Federation of Societies of Anaesthesiologists (WFSA) and The International Association for the Study of Pain (IASP), in collaboration with WHO, are developing a manual for basic, low-tech pain relief. The most important part of the WHO method, and the reason for its success, is the efficient use of oral opioids for moderate to severe pain. Morphine is the opioid of first choice for moderate to severe cancer pain (20, 21). Prolonged morphine treatment leads to numerous and debilitating side effects that diminish patient's quality of life.

Antinociceptive tolerance to morphine is one of the most debilitating side effects and still poorly contrasted since it is caused by complex and interrelated processes such as free radical generation, nitroxidative stress, lipid peroxidation, neuroinflammation and neuronal apoptosis.

Our study focused on the role of oxidative stress during the development of morphine tolerance and demonstrated a substantial role for nitroxidative stress and lipid peroxidation. Superoxide ($O_2^{\bullet-}$) and its downstream signaling mediator, peroxynitrite ($ONOO^-$, PN), have emerged as powerful pronociceptive reactive oxygen and nitrogen species (22, 23). Indeed, their involvement in central sensitization has been reported during the development of thermal hyperalgesia associated with acute and chronic inflammation (6, 12, 24) in response to spinal activation of the N-methyl-d-aspartate receptor (NMDAR) (7, 13) in the development of opiate-induced hyperalgesia and antinociceptive tolerance (2, 25, 26).

Immunohistochemical analysis of L4 L5 superficial dorsal horn of spinal cord, revealed high level of tyrosine residues nitrated in mice treated chronically with injection of morphine compared to naive group (Fig. 3). Peroxynitrite produced in response to an oxidative stress condition, is the reactive species mainly responsible for the nitration of tyrosine residues, so we tested the action of phenolic compounds with antioxidant action an extracted from olive oil, OLEA and HT, and we demonstrated that as L-NAME and $MnTBAP^{3-}$ also these substances are able to decrease the levels of tyrosines nitration together with morphine tolerance (Fig. 3).

In particular, we have shown nitration of endogenous scavenger MnSOD, a well-know mitochondrial enzyme that keeps under control oxidative stress level. We have reported that nitration and inactivation of spinal mitochondrial superoxide dismutase provides a critical source of reactive oxygen and nitrogen species during morphine tolerance (2, 5, 27). Nitrated enzyme results deactivated and this event lead to the increase of oxidative stress. Indeed, tolerant animals show higher levels of oxidative stress and higher levels of nitration that ultimately causes an alteration in the animals behaviour, lowering nociceptive threshold as measured by the hot plate test in mice.

We report that pretreatment of animals with OLEA or HT, prevents the nitration of tyrosines, maintains the activity of mitochondrial MnSOD and the normal pain threshold, emphasizing the protective role of OLEA and HT against damage caused by oxidative stress.

Recent findings demonstrated that OLEA, possesses different pharmacological and healing properties suggesting that their beneficial effects could be linked to its antioxidant characteristics (28). In this regard, some studies have shown that OLEA scavenges a various of endogenous and exogenous free radicals and oxidants, including those generated by hypochlorus acid, xanthine/xanthin oxidases, and hydrogen peroxide. Several mechanisms may account for the antioxidant activity of OLEA such as

chelating of metal ions, inhibition of inflammatory enzyme, and providing of hydroxyl group for quenching and neutralization of free radicals (29). Lipid peroxidation is an important pathological event involved in different neurodegenerative diseases and are accumulating evidence that dietary virgin olive oil and its phenolics have neuroprotective effects both *in vitro* and *in vivo*. One of the neuroprotective mechanisms of dietary virgin olive oil and its phenolics oleuropein and hydroxytyrosol (30) on brain slices damage after hypoxia-reoxygenation, and tyrosol (31) on transient focal cerebral ischemia in rats may be due, in part, to its effects on free radical-induced lipid peroxidation. Olive oil reduced tissue lipid peroxidation by 20.3% in brain in hyperlipemic rabbits. Furthermore, recent study demonstrated neuroprotective effects of oleuropein in an experimental spinal cord injury (SCI) model, and showed that the administration of OLEA after SCI significantly attenuated the level of the marker of lipid peroxidation MDA (29). We highlighted similar effects in our model of tolerance induced by morphine, in fact, OLEA or HT administrated 15 min before morphine injection, are able to maintain low levels of MDA in the spinal cord tissue of tolerant mice, thus inhibiting the onset of a condition of oxidative stress, preventing lipid peroxidation and thus MDA formation.

Results of our study indicate that repeated administration of morphine for several consecutive days to mice resulted in development of oxidative stress in spinal cord tissue being this event associated with the loss of the morphine analgesic action. This effect was indicated by a progressive increase in MDA level and decrease in spinal cord of enzymatic antioxidant activity, following tyrosine nitration.

We also demonstrated the ability of natural products to inhibit these phenomena, maintaining the antinociceptive action of morphine during chronic administration.

In conclusion, our study confirms the hypothesis that an antioxidant of natural origin could be able to reinstate the analgesic effect of morphine. This finding is crucial for the treatment of oncological or inflammatory disease (32-37) affected patients that receive repeated administration of morphine and could benefit of the protective effects of extracts of olive oil.

ACKNOWLEDGEMENTS

This work was supported by Grants from “Investiamo nel vostro futuro”, PON a3-00359, and GR-2010-2318370. The authors would like to thank Mr. Giovanni Politi for technical assistance.

REFERENCES

1. Mantyh PW, Clohisy DR, Koltzenburg M & Hunt SP. Molecular mechanism of cancer pain. Nature Review Cancer 2002; 2:201-9.
2. Muscoli C, Cuzzocrea S, Ndengele MM, et al. Therapeutic manipulation of peroxynitrite attenuates the development of opiate-induced antinociceptive tolerance in mice. The J Clin Invest 2007; 117(11):3530-9.
3. Muscoli C, Doyle T, Dagostino C, et al. Counter-regulation of opioid analgesia by glial-derived bioactive sphingolipids. J Neurosci 2010; 30(46):15400-8.
4. Doyle T, Bryant L, Muscoli C, Cuzzocrea S, Esposito E, Chen Z, Salvemini D. Spinal NADPH oxidase is a source of superoxide in the development of morphine-induced hyperalgesia and antinociceptive tolerance. Neurosci Lett 2010; 483:85-9.
5. Salvemini D, Little JW, Doyle T, Neumman WL. Roles of reactive oxygen and nitrogen species in pain. Free Radic Biol Med 2011; 51(5):951-66.
6. Chen Z, Muscoli C, Doyle T, et al. NMDA-receptor activation and nitroxidative regulation of the glutamatergic pathway during nociceptive processing. PAIN 2010; 149:100-6.
7. Muscoli C, Dagostino C, Ilari S, et al. Post-translational nitration of tyrosine residues modulates glutamate transmission and contributes to N-methyl-D-aspartate-mediated thermal hyperalgesia. Mediators Inflamm 2013; 950947.
8. El SN, Karakaya S. Olive tree (Olea europaea) leaves: potential beneficial effects on human health. Nutri Rev 2009; 67(11):632-8.
9. Zare L, Esmaeili-Mahani S, Abbasnejad M, Rasoulian B, Sheibani V, Sahraei H, Kaeidi A. Oleuropein, chief constituent of olive leaf extract, prevents the development of morphine antinociceptive tolerance through inhibition of morphine-induced L-type calcium channel overexpression. Phytother Res 2012; 26(11):1731-7.

10. Visioli F, Galli C, Galli G, Caruso D. Biological activities and metabolic fate of olive oil phenols. Eur J Lipid Sci Technol 2002; 104:677-84.
11. Visioli F, Bogani P, Galli C. Healthful properties of olive oil minor components. In: Olive Oil, Chemistry and Technology, Boskou D, editor. AOCS Press; Champaign 2006; 173-90.
12. Wang ZQ, Porreca F, Cuzzocrea S, et al. A newly identified role for superoxide in inflammatory pain. J Pharmacol Exp Ther 2004; 309(3):869-78.
13. Muscoli C, Mollace V, Wheatley J, Masini E, Ndengele M, Wang ZQ, Salvemini D. Superoxide-mediated nitration of spinal manganese superoxide dismutase: a novel pathway in N-methyl-D-aspartate-mediated hyperalgesia. Pain 2004; 111(1-2):96-103.
14. Takagi N, Logan R, Teves L, Wallace MC, Gurd JW. Altered interaction between PSD-95 and the NMDA receptor following transient global Ischemia. J Neurochem 2000; 74:169-178.
15. Moncada S, Palmer RM, Higgs EA. Nitric oxide: physiology, pathophysiology, and pharmacology. Pharmacol Rev 1991; 43:109-42.
16. Faulkner KM, Liochev SI, Fridovich I. Stable Mn(III) porphyrins mimic superoxide dismutase *in vitro* and substitute for it *in vivo*. J Biol Chem 1994; 269:23471-6.
17. Muscoli C, Cuzzocrea S, Riley DP, Zweier JL, Thiemermann C, Wang ZQ, Salvemini D. On the selectivity of superoxide dismutase mimetics and its importance in pharmacological studies. British Journal of Pharmacology 2003; 140(3):445-60.
18. Ndengele MM, Cuzzocrea S, Masini E, et al. Spinal ceramide modulates the development of morphine antinociceptive tolerance via peroxynitrite-mediated nitroxidative stress and neuroimmune activation. J. Pharmacol Exp Ther 2009; 329(1):64-75.
19. Ripamonti C, Dickerson ED. Strategies for the treatment of cancer pain in the new millennium. Drugs 2001; 61(7):955-77.
20. Hanks GW, Conno F, Chemy N, et al. Morphine and alternative opioids in cancer pain: the EAPC recommendations. Br J Cancer 2001; 84(5):587-93.
21. Breivik H. Opioids in cancer and chronic non-cancer pain therapy-indications and controversies. Acta Anaesthesiol Scand 2001; 45(9):1059-66.
22. Salvemini D, Neumann W. Targeting peroxynitrite driven nitroxidative stress with synzymes: A novel therapeutic approach in chronic pain management. Life Sci 2010; 86:604-14.
23. Salvemini D, Neumann WL. Peroxynitrite: a strategic linchpin of opioid analgesic tolerance. Trends Pharmacol Sci 2009; 30:194-202.
24. Tang N, Ong WY, Yeo JF, Farooqui AA. Anti-allodynic effect of intracerebroventricular administered antioxidant and free radical scavenger in a mouse model of orofacial pain. J Orofac Pain 2009; 23:167-73.
25. Ndengele MM, Cuzzocrea S, Masini E, et al. Spinal ceramide modulates the development of morphine antinociceptive tolerance via peroxynitrite-mediated nitroxidative stress and neuroimmune activation. J Pharmacol Exp Ther 2009; 329:64-75.
26. Batinic-Haberle I, Ndengele MM, Cuzzocrea S, Reboucas JS, Spasojevic I, Salvemini D. Lipophilicity is a crucial parameter that dominates the efficacy of metalloporphyrins in blocking the development of morphine antinociceptive tolerance through peroxynitrite-mediated pathways. Free Radic Biol Med 2009; 46:212-9.
27. Doyle T, Bryant L, Muscoli C, Cuzzocrea S, Esposito E, Chen Z, Salvemini D. Spinal NADPH oxidase is a source of superoxide in the development of morphine-induced hyperalgesia and antinociceptive tolerance. Neuroscience Letters 2010; 483:85-9.
28. Visioli F, Poli A, Galli C. Antioxidant and other biological activities of phenols from olives and olive oil. Med Res Rev 2002; 22:65-75.
29. Khalatbary AR, Ahmadvand H. Neuroprotective effect of oleuropein following spinal cord injury in rats. Neurol Res 2012; 34(1):44-51.
30. Gonzalez-Correa JA, Navas MD, Lopez-Villodres JA, Truillo M, Espartero JL, De La Cruz JP. Neuroprotective effect of hydroxytyrosol acetate in rat brain slices subjected to hypoxia-reoxygenation. Neurosci. Lett 2008; 446:143-6.
31. Bu Y, Rho S, Kim J, Kim MY, Lee DH, Kim SY, Choi H, Kim H. Neuroprotective effect of tyrosol on transient focal cerebral ischemia in rats. Neurosci Lett 2007; 414:218-21.
32. Chiricozzi A, Zhang S, Dattola S, Gabellini M, Chimenti S, Nisticò SP. Role of Th17 in the pathogenesis of cutaneous inflammatory diseases J Biol Regul Homeost Agents 2012; 26(3):313-8.
33. Chiricozzi A, Zhang S, Dattola A, Cannizzaro MV, Gabellini M, Chimenti S, Nisticò S. New insights in the pathogenesis of cutaneous autoimmune disorders.

J Biol Regul Homeost Agents 2012; 26(2):165-70.
34. Saraceno R, Nisticò SP, Capriotti E, Chimenti S. Monochromatic excimer light 308 nm in monotherapy and combined with topical khellin 4% in the treatment of vitiligo: A controlled study. Dermatol Ther 2009; 22:391-4.
35. Saraceno R, Nisticò SP, Capriotti E, de Felice C, Rhodes LE, Chimenti S. Monochromatic excimer light (308 nm) in the treatment of prurigo nodularis. Photodermatol Photoimmunol Photomed 2009; 24:43-5.
36. Nisticò S, Chiricozzi A, Saraceno R, Schipani C, Chimenti S. Vitiligo treatment with monochromatic excimer light and tacrolimus: Results of an open randomized controlled study. Photomed Laser Surg 2012; 30:26-30.
37. Chiricozzi A, Pitocco R, Saraceno R, Nisticò SP, Giunta A, Chimenti S. New topical treatments for psoriasis. Expert Opin Pharmacother 2014; 15(4):461-70.

LETTER TO THE EDITOR

EVALUATION OF THE EFFECTS OF A PROBIOTIC SUPPLEMENTATION WITH RESPECT TO PLACEBO ON INTESTINAL MICROFLORA AND SECRETORY IgA PRODUCTION, DURING ANTIBIOTIC THERAPY, IN CHILDREN AFFECTED BY RECURRENT AIRWAY INFECTIONS AND SKIN SYMPTOMS

C. VALSECCHI[1], A. MARSEGLIA[1], L. MONTAGNA[1], S.C. TAGLIACARNE[1], M. ELLI[2], A. LICARI[1], G.L. MARSEGLIA[1] and A.M. CASTELLAZZI[1]

[1]Department of Clinical, Surgical, Diagnostic and Pediatric Sciences, University of Pavia, Pavia, Italy; [2]AAT (Advanced Analytical Technologies) Institute, Piacenza, Italy

Received November 7, 2012 – Accepted February 14, 2014

Antibiotic therapy, especially in pediatric patients, is often associated with significant modifications of the gut microflora, which can lead to intestinal dysbiosis and influence intestinal physiology and immune system functionality. Herein we report the results from a double blind controlled clinical trial in 77 pediatric patients affected by recurrent airway infections, receiving antibiotic therapy with amoxicillin and clavulanic acid. A group was treated with an oral probiotic preparation composed of *Lactobacillus paracasei* ssp.*paracasei* CRL-431, *Bifidobacterium* BB-12, *Streptococcus thermophilus* TH-4 and a fructooligosaccharide (FOS) during and after antibiotic therapy for seven days, while the other group received placebo. The study revealed a reduction in the Clostridia population, with a contemporary increase in Bifidobacteria and Lactobacilli in fecal samples in the probiotic group and an increase in the Enterobacteria population in the placebo group. Moreover, there was a decreasing trend in secretory IgA production in the probiotic group. Some relevant, but not statistically significant probiotic supplementation effects were identified.

Probiotics are defined as "live micro-organisms which, when administered in adequate amounts, confer a health benefit to the host" (1). Among probiotic bacteria, Lactobacilli and Bifidobacteria are normal components of the human intestinal microflora, and can actively modulate the immune system. Even if it is a well established fact that the biological effects of probiotics are strain-specific, probiotic bacteria share several common properties, for example: the ability to eliminate pathogens and reduce their adhesion capacity in the intestinal epithelium, they produce bacteriocines and hydrogen peroxide which diminishes pathogen development and their ability to modulate the intestinal microflora (2). Moreover, the linkage between Lactobacilli surface proteins (SLP) and glycoprotein and glycolipids receptors on enterocyte surface membranes can stimulate cytokine synthesis (3).

Recently it has been shown that antibiotic therapy for recurrent airway infections can promote the development of antibiotic resistant microorganisms and induce intestinal microflora alterations, which lead to the colonization of other pathogenic microorganisms (4). The administration of probiotics could be useful in restoring the correct intestinal microflora and prevention of infections (5).

Keywords: Probiotics, antibiotic therapy, intestinal microflora, salivary IgA

Mailing address: Dr. Chiara Valsecchi, Department of Clinical, Surgical, Diagnostic and Pediatric Sciences, University of Pavia, Piazzale Golgi 2, 27100 Pavia, Italy
Tel.: +39 0382 502909 Fax: +39 0382-502876
e-mail: chiara.valsecchi@unipv.it

0393-974X (2014)

DISCLOSURE: ALL AUTHORS REPORT NO CONFLICTS OF INTEREST RELEVANT TO THIS ARTICLE.

Intestinal microflora plays the role of "barrier" protecting intestinal mucosa against pathogenic colonization. The disruption of the microbic intestinal barrier can lead to intestinal infections caused by opportunistic pathogens in susceptible patients. Probiotic bacteria could be useful in treating AAD and *Clostridium difficile* infection through the stimulation of intestinal microflora reconstitution, stimulation of the immune system and direct elimination of the pathogenic microorganisms and their toxins (6).

A randomized double blinded controlled trial conducted by Nord et al (7) showed that the administration of *Lactobacillus acidophilus* LA-5, *Bifidobacterium* BB-12, *Lactobacillus bulgaricus* LBY-27 and *Streptococcus termophilus* STY-31 in association with antibiotic therapy could have positive effects on the intestinal microflora inducing the proliferation of Bifidobacteria.

It has been demonstrated that *Lactobacillus paracasei* ssp.*paracasei* CRL-431 is able to join with the intestinal epithelial mucosa and eliminate several intestinal pathogens such as *E.Coli*, *Listeria monocytogenes*, *Shigella sonnei* and *Salmonella typhimurium* through a competitive exclusion mechanism and also increases phagocytic activity of macrophages, secretory IgA production and reduces diarrhea induced by intestinal pathogens (8). The aim of this study was to evaluate the effects of a probiotic product with respect to placebo, on the intestinal microflora and immune system in pediatric patients affected by recurrent upper airway bacterial infections.

MATERIALS AND METHODS

Patients and setting

Eligible patients were children between 1-13 years of age, affected by skin or respiratory symptoms such as urticaria, bronchial asthma, bronchospasm, atopic dermatitis, airways inflammation, who were undergoing antibiotic therapy. Symptoms could be caused by recurrent airway infections e.g.: otitis, bronchopneumonia, laryngitis, pharyngitis, tonsillitis, rhinosinusitis. The participants were enrolled from the Pediatric Immuno-Allergology Outpatients of the Pediatric Clinic at the University Hospital IRCCS Policlinico S. Matteo (Pavia) from 2009 to 2011.

The patients' parents gave written informed consent for their children to participate in the study. The study was approved by the Ethical Committee of the Pavia University .

The following exclusion criteria were adopted :

- pediatric patients affected by immunodeficiency, chronic metabolic diseases (eg. diabetes) or genetic disease;
- pediatric patients undergoing a different antibiotic therapy and taking probiotics one month prior to the study;
- pediatric patients whose parents were unwilling to give written informed consent.

Interventions

All patients enrolled were treated with antibiotic therapy, amoxicillin and clavulanic acid (50mg/kg) twice daily for 7 days, in association with probiotic or placebo.

The probiotic product contained *Lactobacillus paracasei* ssp.*paracasei* CRL-431 ($1{,}75x10^9$CFU/dose), *Bifidobacterium* BB-12 ($1{,}75x10^9$CFU/dose), *Streptococcus thermophilus* TH-4 ($1{,}50x10^9$CFU/dose), and a fructooligosaccharide (FOS) (1gr/dose). The placebo was composed by maltodextrins, without probiotic strains or FOS.

All enrolled patients received 1 dose (3gr) of the probiotic product or placebo daily according to randomization, associated with the antibiotic therapy that stopped after 7 days, while the probiotic and placebo administration followed for the next 30 days.

Study design, randomization and blinding

A randomized double-blinded controlled trial was conducted. The enrolled patients were randomized to probiotic supplementation or to placebo treatment by the independent statistician who designed the study. Probiotic and placebo boxes were provided free of charge and marked with the letter A or B. At the end of the study the researchers were informed that product A was the probiotic preparation and product B was the placebo composed of maltodextrins.

Endpoint

In order to evaluate the efficacy of the probiotic product with respect to placebo on the intestinal microflora, different bacterial populations in faecal samples were detected. In particular the primary endpoint of the study was to evaluate the variation in percent concentration of *Bifidobacteria* with respect to baseline in patients treated with antibiotic therapy and probiotic supplementation compared to a placebo group, preserving a concentration of *Bifidobacteria* in feces greater than 10^4 CFU/gr. Furthermore, the efficacy of probiotic supplementation with respect to placebo on mucosal immune system was detected by IgA titration on saliva samples (secondary endpoint). Biological samples, saliva and fecal, were collected regularly according to the following scheme:

- T0 (baseline) = before the beginning of antibiotic

therapy and assumption of the probiotic preparation/placebo;

- T1 (end of antibiotic therapy) = after 7 days of antibiotic therapy and contemporary assumption of the probiotic preparation/placebo;
- T2 (end of probiotic/placebo supplementation) = after assuming the probiotic preparation/ placebo alone for 30 days.

Saliva samples (ca. 500 µl) were collected in 15 ml polystyrene tubes and centrifuged at 3000 rpm for 15 min. Supernatants were then collected in 1.5 ml tubes and frozen at -20°C until use.

Fecal samples were collected in sterile tubes containing Amies buffer, and stored at 4°C. The fecal samples were delivered within 24 h to the Advanced Analytical Technologies Institute S.r.l. (AAT), Piacenza, for the microbiological analysis of fecal microflora.

Characterization of intestinal microflora

Fecal samples were delivered within 24 h to AAT for microbiological analysis. All samples were preserved in Amies buffer at 4°C. Before the analysis, the net weight of the fecal sample was measured. Colonies of Bifidobacteria, Lactobacilli, Clostridia and Enterobateria were evaluated and expressed in CFU(colony-forming unit)/g (of feces).

The fecal samples were diluted in physiological solution in serial dilutions and seeded in plates using a selective medium for the particular bacterial species. In particular, a TPY agar (trypticase-peptone-yeast extract medium) was used for the evaluation of the presence of Bifidobacteria, as described by Scardovi (9). The samples were seeded and incubated at 37°C under anaerobic conditions for 72 h. The presence of Lactobacilli was evaluated after seeding in Rogosa medium (De Man, Rogosa & Sharp) (Difco). The samples were incubated for 48 hours at 37°C under anaerobic conditions. Enterobacteria were grown in MacConkey Agar (Oxoid) medium for 24 hat 37°C under anaerobic conditions.

To analyze the presence of Clostridium spores, fecal samples were subjected to heat treatment at 80°C for 10 min, for the inactivation of vegetative forms and to promote sporulation. The samples were serially diluted in Reinforced Clostridial Medium Agar (RCM) (Oxoid) and incubated for 72 h at 37°C under anaerobic conditions. After incubation, the colonies present in significant dilutions (between 15 and 300) were evaluated. The amount of each bacteria species was expressed as CFU/g feces.

IgA titration

The IgA level (µg/ml) was evaluated by ELISA assay, as described previously (10). Briefly, saliva samples were thawed before use and diluted in PBS (Phosphate Buffered Saline, Euroclone) + 10% FCS (Foetal Calf Serum, Euroclone) + 0.1%Tween 20 (Sigma). The 96 multiwell plates were labelled with a monoclonal goat anti-human IgA (Dako, Denmark) at a concentration of 2.3 µg/ml. The secondary antibody was a HRP-conjugated polyclonal rabbit anti-human IgA antibody (Dako Denmark) 0.3µg/ml. O-phenylenediammine Dihydrochloride (OPD, Sigma) was used as a substrate for enzymatic reaction.

Sample size

The sample size was calculated assuming an improvement in the primary endpoint in the probiotic group of 70% and in the placebo one of 30%. At least twenty three subjects were required in each study group to provide a statistical power of 80% to detect the hypothesized difference between the two groups, assuming a two-sided alpha of 0.05 and using a continuity-corrected chi-squared statistic. It was planned to enrol 77 patients to compensate the higher discontinuation rate generally found in the follow-up study on babies. Since to a simple randomization was applied, the arms resulted unbalanced: forty two patients were enrolled in the probiotic group and 35 in the placebo one. In figures 1 the study flow-chart was reported (Fig. 1).

Statistical analysis

Quantitative variables were summarized as median and interquartile range (IQR) and qualitative as percentage. Comparison between two groups at baseline were made by unpaired non parametric *t* test (Mann-Whitney's test) for quantitative variables and Chi-squared test for qualitative ones.

The Skillings-Mack test (SM) was applied to evaluate differences in fecal microflora amount and IgA level between baseline and the two follow-up times within each group (11). The Skillings-Mack test utilizes a general Friedman-type statistic, the analogous non-parametric analysis of variance for repeated measures. If significant differences were identified by the Skillings-Mack test, multiple comparison tests using the Bonferroni method were investigated by non-parametric Wilcoxon's test for paired data or sign test if symmetry of distribution was lacking. According to Bonferroni's method a multiple comparison was significant if the p-value was equal or less than 0.017 given by the reference p-value (0.05) over the number comparisons made (end of antibiotic therapy *vs* baseline, end of probiotic/placebo supplementation *vs* baseline, end of probiotic/placebo supplementation vs. end of antibiotic therapy).

The efficacy of probiotic preparation with respect to placebo on change in fecal microflora concentrations and IgA levels was assessed by unpaired *t* test (with Satterthwaite's correction for degree of freedom) at the

end of antibiotic therapy (T1) and end of follow-up (T2). Precisely, efficacy was measured as net-change in the amount of fecal bacteria at the two time points with respect to baseline. The net-changes were log-transformated to satisfy normal distribution. So, the results were reported as the ratio of the mean (RM) with 95% Confidence Intervals to reflect the original scale. The differences between the two groups was significant if one was not included in the 95%CI of RM.

Finally, the efficacy of probiotic supplementation at the end of follow-up was adjusted by gender using multiple regression models in which the dependent variables was each time the log transformed net-change in the amount of fecal bacteria or IgA with respect to baseline. The results were expressed again as RM and 95% CI. These analyses were conducted only on subjects who completed the study.

A p-value of less than 0.05 was considered significant (two-side) a part from the multiple comparisons test. All analyses were carried out using STATA 10 [Stata Corporation. STATA 10. College Station, Texas (US); 2008].

RESULTS

Seventy-seven pediatric patients (54 males and 23 females) were enrolled: 42 patients were given probiotic preparation (group A) and 35 patients placebo (group B). Fifty patients completed the study (Fig.1). Approximately 68% of the patients completed the study without significant differences between the two groups: 66.7% probiotic supplementation and 68.6% placebo (*Chi*-squared= 0.03, p = 0.86). The drop-out rate was greater in the probiotic group than in the control group (38.1% *vs* 31.4%, *Chi*-squared=0.54) . At baseline no differences in fecal microflora as well as in IgA were evidenced between two groups (Table I).

Fecal microflora

Enterobacteria median concentration increased after 7 days of treatment with respect to baseline and then it declined in both groups (Table II), but differences across three time points were relevant only for the placebo group. In particular, at the first follow-up time (end of antibiotic therapy) the Enterobacteria concentration was significantly elevated with respect to baseline (p=0.0177), while this excess was not relevant at the end of follow-up (p=0.046). The median Clostridia concentration varied significantly within the probiotic group (Table II). In particular, a significant decline in the concentration was evidenced with respect to baseline and the first follow-up time (T1) (p=0.0011), whereas the increase recorded at the end of follow-up time (T2) was never significant both with respect to baseline (p=0.02) or to the previous follow-up time (p=0.11). In the placebo group, a similar trend was observed however not significant. Even if the Lactobacilli median concentration

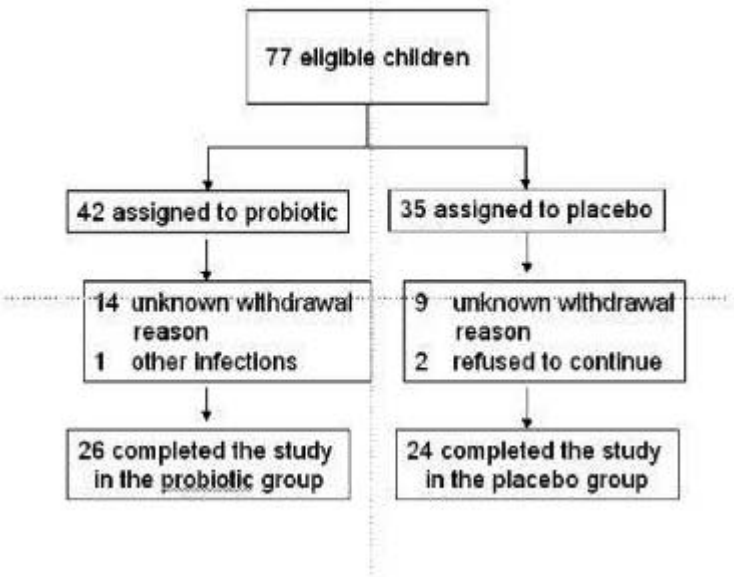

Fig. 1. *Participant flow.*

Table I. *Baseline characteristics of the subjects who completed the study.*

	A (n=37)	B (n=28)	p-value
Enterococcus, median and IQR, CFU/gr	21.2×10^4 (2.21×10^4-417×10^4)	12.85×10^4 (0.96×10^4-796.5×10^4)	0.61
Clostridium, median and IQR, CFU/gr	4.76×10^4 (1.34×10^4-60.2×10^4)	3.34×10^4 (0.44×10^4-12.1×10^4)	0.29
Lactobacillus, median and IQR, CFU/gr	68×10^4 (7.05×10^4-2000×10^4)	425×10^4 (42.5×10^4-3520×10^4)	0.21
Bifidus, median and IQR, CFU/gr	2440×10^4 (158.0×10^4-14100×10^4)	2660×10^4 (43.05×10^4-9590×10^4)	0.70
IgA, median and IQR, µg/ml	61.04 (37.31-68.08)	62.18 (31.91-93.07)	0.79

Probiotic = A; Placbo = B.

Table II. *Median values and inter quartile range (Q1-Q3) of microbacteria in fecal samples and secretory IgA at baseline and at two follow-up times within each group.*

		Baseline (T0)	End of antibiotic therapy (T1)	End of follow-up (T2)	Test and p-value
Enterobacteria (CFU/gr)	A	21.2×10^4 (2.21×10^4-417×10^4)	271×10^4 (14.1×10^4-698×10^4)	22.9×10^4 (0.351×10^4-319×10^4)	SM test=2.00, p=0.37
	B	**12.85×10^4 (0.96×10^4-796.5×10^4)**	**146.65×10^4 (21.35×10^4-2070×10^4)**	**23.5×10^4 (0.226×10^4-237×10^4)**	SM=6.431, p=0.04
Clostridia (CFU/gr)	A	**4.76×10^4 (1.34×10^4-60.2×10^4)**	**1.30×10^4 (0.077×10^4-4.26×10^4)**	**6.34×10^4 (0.44×10^4-22.8×10^4)**	SM=9.647, p=0.008
	B	3.34×10^4 (0.44×10^4-12.1×10^4)	0.70×10^4 (0.12×10^4-6.08×10^4)	6.99×10^4 (0.19×10^4-43.5×10^4)	SM=3.476, p=0.18
Lactobacilli (CFU/gr)	A	68×10^4 (7.05×10^4-2000×10^4)	258.5×10^4 (8.04×10^4-4370×10^4)	845×10^4 (16.7×10^4-4000×10^4)	SM=0.436, p=0.80
	B	425×10^4 (42.5×10^4-3520×10^4)	1550×10^4 (25.3×10^4-10100×10^4)	1000×10^4 (26.9×10^4-12300×10^4)	SM=0.041, p=0.978
Bifidobacteria (CFU/gr)	A	**2440×10^4 (158×10^4-14100×10^4)**	**3150×10^4 (330×10^4-12900×10^4)**	**4340×10^4 (120×10^4-24100×10^4)**	SM=4.659, p=0.10
	B	2660×10^4 (43.05×10^4-9590×10^4)	7760×10^4 (143.2×10^4-36400×10^4)	6960×10^4 (27.4×10^4-42000×10^4)	SM=1.129, p=0.55
IgA (µg/ml)	A	61.07 (37.73-68.92)	59.49 (30.49-69.63)	56.43 (35.11-89.72)	SM test=0.785, p=0.68
	B	61 (31.91-86.33)	55.49 (35.71-68.67)	64.53 (42.39-96.42)	SM test=1.390, p=0.57

(probiotic=A and placebo=B). Skillings-Mack test (SM) and p-value was also reported.

increased in the probiotic group, the variations were never statistically important (Table II). In the placebo group, the pattern was different: an increase in Lactobacilli at the first follow-up time was followed by a fall at the end of the study (T2).

Bifidobacteria showed the same trend as Lactobacilli in the probiotic group, but in this case the increased trend was borderline significant. In the placebo group, Bifidobacteria concentration didn't change over time (Table II).

At the first follow-up time (end of antibiotic therapy) children supplemented with probiotic preparation always exhibited a lower net-change with respect to baseline in the mean amount of bacteria compared with those supplemented with placebo (Table III). Precisely, the mean net-increase in the

Table III. *The Ratio of the Mean (RM) for the net-change log-transformed bacteria amount of with the 95% Confidence Interval was reported at the two follow-up times.*

		T1 (End of antibiotic therapy)			T2 (End of follow-up)		
		n	RM* (95% CI)	Test and p	n	RM* (95% CI)	Test and p
Enterobacteria	A	19	0.69	t=-0.35;	11	3.63	t=0.83;
	B	19	(0.08-5.71)	p=0.727	11	(0.14-93.11)	p=0.417
Clostridia	A	7	0.61	t=-0.31;	9	0.18	t=-1.57;
	B	10	(0.02-16.74)	p=0.757	11	(0.02-1.79)	p=0.135
Lactobacilli	A	19	**0.04**	**t=-2.12;**	14	1.06	t=0.05;
	B	14	**(0.002-0.89)**	**p=0.042**	11	(0.07-16.01)	p=0.963
Bifidobacteria	A	16	0.59	t=-0.55;	19	0.60	t=-0.49;
	B	17	(0.08-4.21)	p=0.585	12	(0.07-5.10)	p=0.627

** The Ratio of the mean was computed as probiotic (A) over placebo (B). The unpaired t test and p-value was also indicated.*

Table IV. *The Ratio of the Mean (RM) for the net-change log-transformed bacteria amount adjusted for gender with the 95% Confidence Interval was reported at the two follow-up time.*

	T2 (End of follow-up)	
	RM per A/B (IC95%)	Test e p-value
Enterobacteria	2.23 (0.21-23.17)***	t=0.72; p=0.48
Clostridia	**0.09 (0.01-0.59)****	**t=-2.71; p=0.015**
Lactobacilli	0.82 (0.06-10.32)*	t=-0.16; p=0.87
Bifidobacteria	0.53 (0.07-3.80)*	t=-0.66; p=0.52
IgA	0.35 (0.07-1.89)	t=-1.30; p=0.21

The test and p-value was also indicated for each estimated RM. The Ratio of the mean was computed as probiotic (A) over placebo (B).^ Stars indicated the significance level for gender: p<0.05=; p<0.01=**; p<0.001=****

amount of fecal microflora in probiotic group was always less than in placebo one (RM<1) and only for Lactobacilli this was significant. At the end of follow-up (T2) the mean net-increase of Enterobacteria and Lactobocilli in the probiotic group was higher than in placebo, but never relevant (Table III).

To take into account a possible selection bias due to unequal distribution by genders between groups at the last follow-up time (females: probiotic group=17.9% *vs* placebo group=45.8%, Chi-squared=4.75, p=0.029), the efficacy of probiotic with respect to placebo was adjusted for gender (Table IV). It was evidenced that the difference between two groups disappeared for Lactobacilli and became significant for Clostridia. Precisely:

- the mean net-increase for Clostridia concentration in probiotic group was less than 91% than in placebo group;
- the mean net-increase for Lactobacilli was smaller in probiotic group than in the placebo one and not relevant.

Secretory IgA

The median secretory IgA levels in patients supplemented with probiotic did not show a significant decrease from baseline to the end of follow-up. In patients assigned to the placebo group, secretory IgA after an early decrease found at the first follow-up time raised again at the end of follow-up (Table II). The mean net-decrease in IgA at the first follow-up time was smaller in probiotic group with respect to placebo (RM=0.93; t= -0.12, p=0.90) as well as at the end of follow-up (RM=0.57; t= -0.82, p=0.42), however never significant. The adjustment by gen-

der did not modify the results.

DISCUSSION

Several studies have demonstrated the efficacy of probiotics in the normalization of the gut microbiota composition and their interaction with the innate and adaptive immune systems, which may promote resistance against pathogens in childhood (12, 13). In particular, probiotics are thought to be effective in the prevention or treatment of viral gastrointestinal infections even more so than for bacterial infections (14).

In this study salivary secretory IgA (sIgA) did not exhibit a significant decrease from the beginning of the trial to the end of probiotic supplementation, while in patients from the placebo group, sIgA levels decreased after antibiotic therapy and rose after 30 additional days of treatment. Similarly, a previous study reported that the supplementation of formula milk with *Bifidobacterium* Bb12 alone or together with *Streptococcus thermophilus* protected children from symptomatic rotavirus infections without an increase in rotavirus-specific IgA antibody titre (15).

Several studies have focused on the beneficial effects of probiotics on intestinal microflora and their ability to restore imbalance caused by antibiotics, thus increasing the scientific interest in their application in the prevention and treatment of AAD in adults and children (16, 17). In particular, antibiotic therapy with amoxicillin, in association or not with clavulanic acid, clindamycin and cephalosporines is often associated with a high risk of AAD, due to an antibiotic-induced dysbiosis of intestinal microflora (18).

Our results on intestinal microflora showed that the supplementation with probiotics could strongly enhance the Bifidobacteria and Lactobacilli populations after antibiotic therapy. Conversely this effect is not long-lasting in the placebo group. The presence of FOS in the probiotic preparation could reinforce their action through the increased Lactobacilli and Bifidobacteria colonization of the gastrointestinal tract (19).

Both Enterobacteria and Clostridia represent two extremely heterogeneous genres, comprehending also several strains usually present in the microbioma of healthy subjects. At the end of the supplementation, despite the antibiotic therapy, the concentrations of these populations were similar to baseline levels. This is particularly important in order to demonstrate the role of probiotics in the maintenance of intestinal homeostasis, enhancing the proliferation of beneficial bacterial strains and restoring the heterogeneity of an healthy microflora.

The study presents several limitations. First the small number of patients enrolled suggests that the findings could not be conclusive and others study with a greater sample size should be conducted. Second, the unbalanced randomization introduced at the end of follow up a possible bias due to genders. A randomized balanced design should be prefer for following greater study.

In conclusion, our results suggest that a probiotic preparation containing different bacterial strains and FOS as prebiotic could be useful as support during antibiotic therapy in pediatric patients affected by recurrent respiratory infections.

Further clinical trials with longer periods of probiotic supplementation and greater samples would be useful to induce a prolonged probiotic effect on the maintenance of GI equilibrium during and after antibiotic therapy.

ACKNOWLEDGEMENTS

The authors thank Dr. Laurene Kelly for correcting the English of the manuscript and Professor Simona Villani for the statistical support.

REFERENCES

1. Joint FAO/WHO Expert Consultation on Evaluation of Health and Nutritional Properties of Probiotics in Food Including Powder Milk with Live Lactic Acid Bacteria. Health and Nutritional Properties of Probiotics in Food including Powder Milk with Live Lactic Acid Bacteria. FAO Food and Nutrition paper 2001; 85:1-50.
2. Kelly D, Conway S, Aminov R. Commensal gut bacteria: mechanisms of immune modulation. Trends Immunol 2005; 26:326-33
3. Annuk H, Hynes SO, Hirmo S, Mikelsaar M, Wadstrom T. Characterization and differentation of lactobacilli by lectin typing. J Med Microbiol 2001;

50: 1069-74.
4. Neu HC.The crisis in antibiotic resistance. Science (1992); 257:1064-73.
5. Tagg JR, Dierksen KP. Bacterial replacement therapy: adapting "germ warfare" to infection prevention. Trends Biotecnol 2003; 21:217-23.
6. Qamar A, Aboudola S, Warny M, Michetti P, Pothoulakis C, LaMont JT, Kelly CP. Saccharomyces boulardii stimulates intestinal immunoglobulin A immune response to Clostridium difficile toxin A in mice. Infect Immun 2001; 69:2762-5.
7. Nord CE, Lidbeck A, Orrhange K, Sjostedt S. Oral supplementation with lactic acid bacteria during intake of clindamycin. Clin Microbiol and Inf 1997; 3:124-32.
8. Schiffrin EJ, Brassart D, Servin AL, Rochat F, Donnet-Hughes A. mmune modulation of blood leucocytes in humans by lactic acid bacteria: criteria for strain selection. Am J Clin Nutr 1997; 66:515S-20S.
9. Scardovi V. Genus Bifidobacterium Orla Jensen 1924, 472[al]. In Bergey's systematic bacteriology 2. Eds. Sneath PHA, Mair NS, Sharpe NE, Holt JG. Williams and Wilkins Baltimore MD USA 1997;1418-34.
10. Ciardelli L, Garofoli F, Avanzini MA, De Silvestri A, Gasparoni A, Sabatino G, Stronati M. Escherichia coli specific secretory IgA and cytokines in human milk from mothers of different ethnic groups resident in northern Italy. Int J Immunopathol Pharmacol 2007; 20:335-40.
11. Chatfield M, Mander A. The Skillings-Mack test (Friedman test when there are missing data). Stata J 2009; 9:299-305.
12. Rautava S. Potential uses of probiotics in the neonate. Semin Fetal Neonatal Med.2007; 12:45-53.
13. Hatakka K, Saxelin M. Probiotics in intestinal and non-intestinal infectious diseases-clinical evidence. Curr Pharm Des 2008; 14:1351-67.
14. Szajewska H, Mrukowicz JZ. Probiotics in the treatment and prevention of acute infectious diarrhea in infants and children: a systematic review of published randomized, double-blind, placebo-controlled trials. J Pediatr Gastroenterol Nutr 2001; 33(S)2:S17-25.
15. Phuapradit P, Varavithya W, Vathanophas K, et al. Reduction of rotavirus infection in children receiving bifidobacteria-supplemented formula. J Med Assoc Thai 1999; 82:(1): S43-8.
16. McFarland LV. Evidence-based review of probiotics for antibiotic-associated diarrhea and Clostridium difficile infections. Anaerobe 2009; 15:274-80.
17. Koning CJ, Jonkers DM, Stobberinghm EE, Mulderm L, Rombouts FM, Stockbrügger RW. The effect of a multispecies probiotic on the intestinal microbiota and bowel movements in healthy volunteers taking the antibiotic amoxycillin. Am J Gastroenterol 2008; 103:178-89.
18. McFarland LV. Epidemiology of infectious and iatrogenic nosocomial diarrhea in a cohort of general medicine patients. Am J Infect Control. 1995; 23:295-305.
19. Bañuelos O, Fernández L, Corral JM, Valdivieso-Ugarte M, Adrio JL, Velasco J. Metabolism of prebiotic products containing beta (2-1) fructan mixtures by two Lactobacillus strains. Anaerobe 2008; 14:184-9.

THE EFFECT OF HYDROXYAPATITE-COATED SCREW IN THE LATERAL FRAGILITY FRACTURES OF THE FEMUR. A PROSPECTIVE RANDOMIZED CLINICAL STUDY

V. PESCE[1], G. MACCAGNANO[1], G. VICENTI[1], A. NOTARNICOLA[1], L. MORETTI[1], S. TAFURI[2], D. VANNI[3], V. SALINI[3] and B. MORETTI[1]

[1]Department of Basic Medical Sciences, Neurosciences and Organs of Sense, "Aldo Moro" University of Bari, Italy; [2]Department of Biomedical Sciences and Human Oncology, "Aldo Moro" University of Bari, Italy; [3]Orthopaedics and Traumatology Division, "G. d'Annunzio" University of Chieti, Italy

Received December 23, 2012 – Accepted February 28, 2014

Due to a growing numbers of lateral fragility fractures of the femur and their high social costs the need to work out an effective strategy in order to find a better solution for these patients is warranted. From January 2010 to July 2011, we carried out a prospective randomized clinical study comparing the results of patients with femoral lateral fractures treated by nail and cephalic hydroxyapatite coated screws (study group including 27 patients) compared to the patients with the same fractures treated with nail and head standard screws (control group including 27 patients). We defined the two parts of the femoral neck as ROI 1 (under the head screw) and ROI 2 (above the femoral screw) on the AP view. The bone density of the two areas was calculated using DEXA at T0 (1st day post-surgery), at T1 (40th day post-surgery), at T2 (3 months later), at T3 (1 year later). The clinical-radiography evaluations were based on the Harris Hip Score (HHS), ADL test and x-ray views of the hip. As far as the bone mineral density average of ROI 1 and ROI 2 is concerned, we found a significant statistical increase at T1 and T3 in the study group, while it was not significant in the control group. We could account for this data through the higher mechanical stability of hydroxyapatite coated screws than standard screws. In fact, this material was responsible for improved implant osteointegration. Thanks to a 1 year follow-up we were able to demonstrate the implant utility associated with augmentation and the importance of densitometry exams such as easily repeatable and low cost diagnostics to prevent the onset of complications linked to screw loosening.

Fragility fractures of the proximal femur are continually increasing due to the higher average life expectancy and of the functional needs of the population (1, 2). The high economic impact on the National Health Service has made it the centre of attention and a central figure in various articles and studies (3, 4). The 2010 Annual National report has shown 93.355 admissions due to femoral neck fractures, a total daily number of in-patients equal to 1.201.010 and an average for a single admission

Key words: fragility fractures, lateral femoral fractures, hydroxyapatite coated screws, bone density

Mailing address: Angela Notarnicola, Ph.D., Department of Basic Medical Sciences, Neurosciences and Organs of Sense, "Aldo Moro" University of Bari, Bari General Hospital, Piazza Giulio Cesare 11, 70124 Bari, Italy.
Tel.: +39 080 5592938 Fax: +39 080 5592938
e-mail: angelanotarnicola@yahoo.it

0393-974X (2014)

is 12.9 days in hospital (5). In 2010, Tarantino et al. estimated that the relative cost of a single femur fracture in the over 65's to be 13.500 euro (6). Researches by Tafuri S. et al., 2008 (7) in Italy, highlighted that the highest number of this type of lesion is found in the 70-89 age range. The main cause of fragility fractures is osteoporosis which gives negative results of osteosynthesis, reducing stability and the time-scale of bone re-growth. Instead, the issue of surgical treatment of lateral fractures needs to be included in the bigger picture of the osteoporosis disease and is always subject to discussion.

At the moment, the most common synthesis for such fractures are slide-plate with a screw and nail. In previous studies there are a lots of papers comparing the results of different treatments. Studies have shown that the best clinical and biomechanical results are obtained using nails rather than using plates (8, 9). In fact the nail allows us to reproduce the shorter arm, thus reducing the risk of failure caused by the rupture and varus deformity of the implant (10, 11). The quality of the bone and the mechanical efficiency of the synthesis are very important to the recovery process because the stabilizing function is linked to the bone-implant interface especially in the case of femur neck fractures. When the nail is positioned correctly, the osteoporosis disease can cause the failure of biological substrate and clinical functional results.

We did a lot of research, using lots of articles that analysed clinical results linked to implant stability of different augmentation techniques. These procedures are able to reinforce the bone structure through the application of cement (Norian Skeletal Repair, bisfenol-dimetacryl cement with spiral blade) or Hydroxyapatite-coated screws or cylinder hydroxyapatite. A great deal of studies analyse the indications and limits of these techniques (12, 13, 14, 15, 16, 17). The aim of this work is to evaluate the effectiveness of using hydroxyapatite during these stabilization procedures comparing the clinical and functional results of two groups of patients with inter-throcanteric fractures. Both of them were treated with femoral nails and we used a head hydroxyapatite coated screw in one of them. For the other group we implanted a femoral nail with standard screw. We were able to follow-up the patients through densitometry exams of the femoral neck as well as through x-rays and a functional question test. As far as instrumental evaluation is concerned, in 1979 Gruen et al. (18) described 7 areas ROI of femoral component in PTH for the first time. In 2010 Cadossi et al. (19), introduced the new periprosthetic area called ROI 8 and they revealed bone mineral densitometry, discovering a direct connection between bone density and the position of the femoral component prosthesis. Furthermore in our study, the definition of the two areas (called ROI 1 and ROI 2) for densitometry analysis, is the first reference in the bibliography associated with the femoral nail. In this context, our end point is to confirm the effectiveness of the densitometry exam to detect the onset of early complications linked to screw loosening.

MATERIALS AND METHODS

From January 2010 to July 2011, we carried out a prospective randomized clinical study comparing the results of patients with femoral lateral fractures treated using nail and cephalic hydroxyapatite coated screws (study group) compared to the patients with the same fractures treated with nail and head standard screws (control group). The inclusion criteria was:

-age 60 - 94 years;

-according to AO classification, all of the fractures were 31-A3 (20);

-co-operative patients;

-patients with osteoporosis disease if T- Score < -2.5 DS;

-Body Mass Index (BMI) < 30.0 Kg/m2

The exclusion criteria was:

-patients with heart, kidney, neurological diseases, diabetes and systemic diseases who were able to follow the rehabilitation programme;

-previous surgery or severe osteoarthritis of lower limbs;

-specifics drugs treatments such as anticoagulants or psychiatric drugs.

We used the same nail for all the patients, namely the Uninail (Lima Corporate S.P.A.-Villanova di San Daniele del Friuli-Udine®). It is an anatomic nail in titanium alloy ($Ti6Al4V$), available in the 20.5 cm standard version and in a 18 cm short version. The proximal diameter is 16.5 mm, the distal 11 mm; the valgus angle is 4° and the cervico-diaphyseal is available in 125° and 130°. The diameter of the cephalic screw is 12 mm and it is possible to use the hydroxyapatite coated screw. The features of

these materials are: crystallinity index 76.9%, calcium-phosphorus ratio 1.67, porosity 7.6%, rugosity 48.5 μm, adhesion 33.1 Mpa. The method of application is plasma spray.

For all patients the surgery was performed within 48 h of injury. Under spinal anesthesia we placed the patients on a traction bed and, after reducing the fracture, we stabilized the lesion with a nail and cephalic screws (standard for the control group and hydroxyapatite-coated screws for the study group) and dynamic distal screw. Through the fluoroscopy view, the correct position of the head screw was verified according to the Cleveland and Bosworth method (21). We calculated the Tip Apex Distance (TAD), that the bibliography defines in the range of 11-25 mm in order to decrease the risk of screw cut out (22). We discharged all the patients with the same osteoporosis drug prescription (clodronic acid), weight-bearing was delayed until 10 days then we permitted progressive weight bearing with crutches. We defined the two parts of the femoral neck ROI 1 (under the head screw) and ROI 2 (above the femoral screw) on the AP view. The bone density of the two areas was calculated using DEXA (Fig. 1). In this way it was possible to follow the changes of the bone mineral density near the cephalic screws caused by hydroxyapatite.

In analysing the densitometry value of the two areas at T0 (1st day post-surgery), T1 (40th day post-surgery), T2 (3 months later), and T3 (1 year later), the dimensions revealed at T0 were kept the same, reducing the operator's possibility to add or take off bone tissue. The clinical-radiography evaluations were based on the Harris Hip Score (HHS) (23), ADL test and x-rays view of the hip. Recorded at T0, T1, T2 and T3 we detected complications such as malunion, the cutting-out of the cephalic screw, the implant rupture or femoral neck reduction. For every patient we completed a form reporting demographic data, date of surgery, densitometry value and HHS at the different times. These files were inserted into a database using FileMaker pro 11 software and analyzed using Software Stata MP 11.2.

Continuous variables were described as mean and standard deviation values were reported. Categorical variables were described as percentages. Before the statistical analysis, we performed Barlett's test and results of the test showed that the distribution was normal; then we used parametric tests for the analysis.

To compare the average densitometry value between the two groups at the same times, we used the *t* student test for independents samples. To compare the average densitometry values within the same group at different times, we used the *t* student test for paired samples. For all tests, a p value of less than <0.05 was considered to be statistically significant.

RESULTS

We enrolled 54 patients (42 females and 12 males) with an age range from 60 to 94 years (average 77.56). These patients were under our observation due to proximal femur fractures who fitted the necessary criteria. The control group was composed of 27 patients (20 females, 7 males, aged between 65-90 years), while the study group was made up of 27 patients (22 females, 5 males, aged between 60-94 years).

At T0 the ROI 1 bone density, was 0.89±0.20 gr/cm2, with no statistical differences between the study group (0.87 ±0.15 gr/cm2) and the control group (0.89 ±0.24 gr/cm2; t=0.36; p=0.35); in ROI 2 bone density was 0.77 ±0.03 gr/cm2 and this was higher in the control group (0.81±0.20 gr/cm2) than in the study group (0.72 ±0.18 gr/cm2; t=1.69; p=0.04). The average of the two values was 0.87±0.02 gr/cm2, higher in the control group (0.92±0.15 gr/cm2) than in the study group (0.81±0.14 gr/cm2; t=2.55; p=0.007; Table I and II).

At T1 the ROI 1 bone density was 0.97±0.17 gr/cm2, with no statistical differences between the study group(1.04±0.12 gr/cm2) and the control group(0.93±0.18 gr/cm2; t=-1.36; p=0.09); in ROI

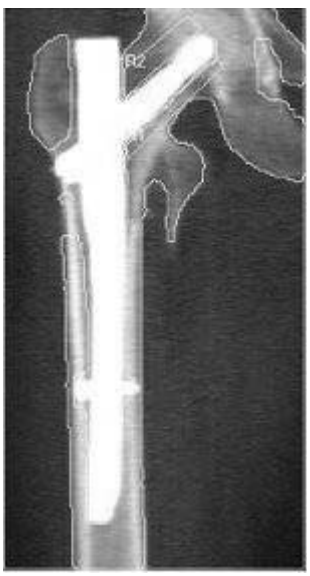

Fig. 1. *Division of the femoral neck in two parts (ROI 1 under the head screw and ROI 2 above the femoral screw) on the AP view. The bone density is calculated using DEXA.*

Table I. *The average BMD in the study group on the first day post-surgery (**T0**); at 40 days (**T1**); at 3 months later (**T2**); at 1 year later (**T3**).*

	T0	**T1**	T2	**T3**
Roi1	0.87±0.15	1.04±0.12	0.93±0.12	0.97±0.16
Roi2	0.72±0.18	0.90±0.08	0.78±0.20	0.83±0.16
average	0.77±0.20	0.97±0.10	0.86±0.12	0.91±0.14

Table II. *The average BMD in the control group on the first day post-surgery (**T0**); at 40 days (**T1**); at 3 months later (**T2**); at 1 year later (**T3**).*

	T0	**T1**	**T2**	**T3**
Roi1	0.89±0.25	0.93±0.18	0.97±0.20	0.90±0.34
Roi2	0.81±0.21	0.91±0.27	0.91±0.33	0.81±0.26
average	0.87±0.16	0.92±0.20	1.56±2.43	0.90±0.23

Table III. *The percentage of the patients of the two groups that presented Harris Hip Score included in the different ranges (excellent-good-acceptable-insufficient).*

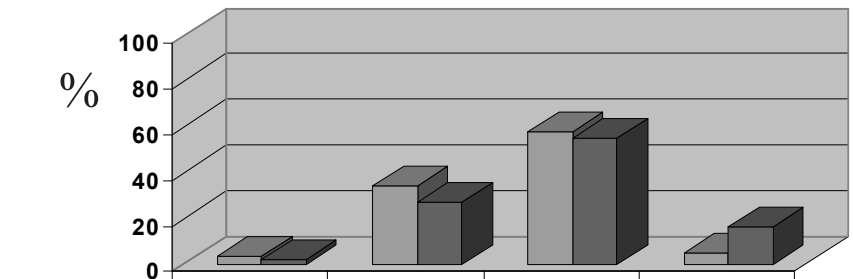

	EXCELL.	GOOD	ACCEPT.	INSUFF.
STUDY GR.	3	34	58	5
CONTROL GR.	2	27	55	16

2 bone density was 0.91±0.27 gr/cm2 also showing no differences between the study group (0.90 ±0.08 gr/cm2) and the control group (0.91±0.27 gr/cm2; t=0.12; p=0.45). The average of each value was 0.93 ±0.18 gr/cm2, the same results were found in the patients operated on using hydroxyapatite coated screws (0.97±0.10 gr/cm2) and standard screws (0.92±0.05 gr/cm2; t=-0.53; p=0.30; Table I and II).

As far as ROI 1 is concerned, in the control group we did not find any significant statistical differences between the two average bone densities calculated at T0 and T1(t=-0.49; p=0.31); however in the study groups we noted a significant statistical increase of the density value between T0 et T1(t=-2.46; p=0.01).

With reference to ROI 2, the averages of density value at T0 and T1 differed in the study group (t=-2.1; p=0.04), but there were no major statistical differences in the control group(t=-0.72; p=0.24).

At T2, the average bone density in ROI 1 was 0.95±0.17 gr/cm2, with no statistical differences between the study group (0.93±0.12 gr/cm2) and the control group (0.97±0.20 gr/cm2; t=0.57; p=0.29). As far as ROI 2 is concerned, the average bone density was 0.85±0.28 gr/cm2, higher in the control group (0.91±0.33 gr/cm2) than in the study group (0.78±0.20 gr/cm2; t=1.18; p=0.12; Tab. 1 and 2), but with no significant statistical differences

The average bone density of the two groups was 1.23±0.12 gr/cm2. We did not observe any significant statistical differences between study

group (0.86±0.12 gr/cm2) and the control group (1.56±2.43 gr/cm2; t=1.04; p=0.15; Table I and II).

Comparing the measurements of the BMD at T0 and T1, we did not find any significant statistical differences neither in the study group (ROI 1: t=0.56; p=0.31- ROI 2: t=-0.92; p=0.22- average: t=0.25; p=0.41) nor in the control group (ROI 1: t=0.33; p=0.37- ROI 2: t= -0.27; p=0.39- average: t=-1.01; p=0.17).

At T3 the average of bone density in ROI 1 was 0.94 ±0.26 gr/cm2, with no statistical differences between the study group (0.97±0.16 gr/cm2) and the control group (0.90±0.34 gr/cm2; t=-0.79; p=0.21); in ROI 2 was 0.82±0.21 gr/cm2. In detail it was 0.83±0.16 gr/cm2 in the study group and 0.81±0.26 gr/cm2 in the control group (t=-0.25; p=0.40). The average bone density of the two groups was 0.91±0.19 gr/cm2 and neither in this case were there any differences between the study group (0.91±0.14 gr/cm2) and the control group (0.90±0.23 gr/cm2; t=-0.06; p=0.48; Table I and II).

And so comparing the value of bone density at T1 and T2 in ROI 1, we noted a significant statistical difference in the study group (t=-1.97; p=0.04) whilst there was not any difference in the control group (t=0.76; p=0.23); in ROI 2 we found no difference either in the study group (t=-0.62; p=0.27) or in the control group (t=1.58; p=0.07). As far as average bone density is concerned, we did not notice any significant statistical difference neither in the study group (t=-1.35; p=0.10) nor in the control group (t=1.06; p=0.15).

If we compare the bone density average at T0 et T3, while the increase found in ROI 1 is significant statistically in the study group (t=-2.31; p=0.02), it is not significant in the control group (t=-0.89; p=0.19). Also in ROI 2 we can see a significant statistical increase in the study group (t=-2.59; p=0.01) but not in the control group (t=0.82; p=0.21). The different BMD average at the two times is significant in the study group (t=-2.53; p=0.01), but less so significant in the control group (t=-0.90; t=0.19).

Throughout the clinical and functional analysis carried out at T0-T1-T2-T3 highlighted in the study group, the HHS was excellent in 3% of patients, good in 34%, acceptable in 58% and insufficient in 5%; within the control group 2% of patients we found had an excellent score, 27% good, 55% sufficient and 16% was unacceptable (Table III).

DISCUSSION

Due to a growing numbers of lateral fragility fractures of the femur and their high social costs we need to work out a good strategy in order to come up with a better solution for these patients. Bad bone quality increases the risk of failure of the synthesis for which the type of implant must be decided, based on the type of fracture, bone quality and the overall health of the patient. Higher life expectancy in older patients and continual developments of biomaterials have made this subject the centre of attention in recent studies. In fact, at the moment the surgeon can choose the correct implant and the option of augmentation to achieve a larger bone-implant interface and better mechanical resistance of the bone. In 1970 Harrington already suggested the use of metacryl cement for the treatment of instable inter-trochanteric fracture in patients with osteoporosis. In 1989 Cheng used both a screw and polymetacryl cement (PMMA) and analysed the results over 5 years, pointing out the complications in 16% of patients, attributing the principle cause of exothermic reaction effects to the healing of the bone. In 2008 Moroni discovered an increase of the mechanical resistance in the neck after using PMMA. These days biological cements are preferred despite being characterized as having a longer solidification time and less mechanical resistance. They have a lower polymerization temperature (50°-60°) and they are absorbed without interfering with the healing process of the bone.

In 2000, Elder et al. carried out a corpse study using the Norian Skeletal repair system. These authors used this cement for the patients with instable lateral femur fractures, increasing the stability of synthesis. Through strain gauges analysis, they confirmed that the application of Ca/P cement upgrades the stability of the implant by 83% compared to not using it and posteromedial cortical bone. Lastly they verified the reduction of the screw by bending moment that is responsible for cut-out. In 2005 Moroni et Faldini enrolled 60 patients with a neck femur fracture type I-II according to the Garden Classification. For the synthesis they used standard or hydroxyapatite coated screws. They revealed high a complication

count for screw loosening in the joint and head hip necrosis for the control group. These complications caused an increased recovery time, a second surgery to remove the implant or the need to perform a hip prosthesis surgery.

As for the study group treated by the coated screw, the authors did not observe any complications and got good clinical results. In the control group they discovered the reduction of the femur neck due to mechanical instability of bone-implant interface, above all in patients with osteoporosis. The other device is Lag-Fix. It is a synthetic bone cylinder with a synthetic body made of granules of hydroxyapatite granules [Ca10(PO4)2(OH)2], which is the main inorganic component of normal osseous tissue. This material is being used to fill the bone gap in cancellous bone because it is biocompatible. It is designed to be used in conjunction with nails for a lateral femur fracture in osteoporotic patients, because this device does not sufficiently protect the mechanical stability to cope with the weight forces. In 2006 Kwok-Sui Leung enrolled 12 osteoporotic patients with lateral femur fractures, 8 out of 12 were unstable. He used Gamma nails with Lag-Fix. His results were good and there were no complications.

Through the introduction of nails, we obtained biomechanical advantages with plates but, at the same time, in literature it is described the presence of different complications such as cut-out, the rupture or loosening of the implant and pseudo-arthritis disease (24). Thanks to our study, which is the first of its kind on live human subjects, we are able to reveal the same ROI 1 bone density value between the two groups at T0, whilst the ROI 2 density was higher in the control group than the study group. As far as the BMD average of ROI 1 is concerned, in the control group we did not find any significant statistical differences at T0 at T1, while in the study group we discovered a significant statistic increase at T1. As for ROI 2 we noted a higher bone density in the study group that was significant. These results underlined the principle role of hydroxyapatite to increase the primary stability of implant. At T2 we did not notice any significant statistic differences for the ROI 1 and ROI 2 average bone densities, even when compared to T0 and T1. Comparing the average bone density at T0 and T3, we noted a significant statistical increase in both areas in the study group, whilst it was not significant in the control group. We could explain this through the higher mechanical stability of hydroxyapatite coated screws compared to standard screws. In fact this material was responsible for the improved osteointegration of the implant (25).

According to literature (Capone at al., 2006), we detected that the main complications of nails were caused by cephalic screw loosening (3,1%), diaphyseal fracture under the implant (5,3%) and nail rupture (1%). The first complication is the principle cause of osteosynthesis failure and the authors identified the strain in relationship between the morphology of the fracture, the quality of reduction, osteoporosis disease and the position of the cephalic screw. The bone trabecular density near the implant is responsible for the assurance of biological support for the implant and its reduction causes unstable bone implant interface (26).

Through this study we were able to describe the absence of complications in the study group, whilst in the control group we found 2 patients out of 27 (7,407%) with the cutting-out of cephalic screw at 1 year after the surgery. Both of them had a good TAD value of the head screw included in the optimal range as defined by literature. For this reason we concluded that screw loosening could be connected to the mechanical instability of the bone and not a bad positioning of the nail.

As far as clinical and functional analysis is concerned, in the control group we found insufficient clinical results. In fact these patients lost the ability to walk. Although we allowed weight bearing at the same time for both groups, we observed that in the control group the ADL test showed a reduction in the ability to get washed and dressed or to do the shopping unaided compared to those in the study group.

Bone quality is a very important aspect in terms of the fixation and stability of the implant. For this reason the evaluation of bone mineral density and bone remodeling plays a central role in the primary prevention of fragility fractures and in limiting the failure of the synthesis, especially during the high risk post-surgery period during the first year (27).

The administration of adequate drug therapy reduces these lesions by 50% and this information is noteworthy, whether we consider the fact that the percentage of second fractures in patients doubles

within 1 year of the first fragility fracture whether not adequately treated. Because of this it is very important when dealing with patients who have this problem to treat not only the lesion with surgery, but also to prescribe the correct calciotropic therapy in order to control the bone remodeling and reabsorption process. In our study we used clodronic acid for each patient involved (28).

The growing number of the osteoporotic patients and occurrence of fragility fractures has determined an ever growing interest in the development of synthesis techniques and implantations effective on osteoporotic bone. Through the different techniques we focused our attention on femoral nails with hydroxyapatite coated screws analyzing the biological and mechanical reaction of bone-implant interface. In the study group we did not observe any complications and the clinical-biological results that we evaluated through densitometry, were superior to the control group.

As described in the bibliography (29, 30), these results refer to a better mechanical stability of the bone-implants interface obtained by hydroxyapatite which at the same time reduces the risk of complications such as loosening and screw cut-out.

The data of these study support the effectiveness, in terms of biological response and stability of bone-implant interface, of the hydroxiapatite coated screw using an instrumental exam of the first level (DEXA). Thanks to a 1 year follow up, we were able to demonstrate the implant utility associated with augmentation and the importance of densitometry exams such as an easily repeatable and low cost diagnostic to prevent the onset of complications linked to screw loosening.

REFERENCES

1. Spira AP, Covinsky K, Rebok GW, Punjabi NM, Stone KL, Hillier TA, Ensrud KE, Yaffe K. Poor sleep quality and functional decline in older women. J Am Geriatr Soc 2012; 60(6):1092-8.
2. Gauthier A, Kanis JA, Jiang Y, Martin M, Compston JE, Borgström F, Cooper C, McCloskey EV. Epidemiological burden of postmenopausal osteoporosis in the UK from 2010 to 2021: estimations from a disease model. Arch Osteoporos 2011; 6(1-2):179-88.
3. Lötters FJ, Lenoir-Wijnkoop I, Fardellone P, Rizzoli R, Rocher E, Poley MJ. Dairy foods and osteoporosis: an example of assessing the health-economic impact of food products. Osteoporos Int 2013; 24(1):139-50.
4. Viswanathan HN, Curtis JR, Yu J, et al. Direct healthcare costs of osteoporosis-related fractures in managed care patients receiving pharmacological osteoporosis therapy. Appl Health Econ Health Policy 2012; 10(3):163-73.
5. http://www.salute.gov.it/ricoveriospedalieri.jsp.
6. Tarantino U, Cerocchi I, Celi M, Rao C. Dimensione attuale del fenomeno osteoporosi in Italia. G.I.O.T. 2010; 36:263-7.
7. Tafuri S. Martinelli D, Balducci MT, Fortunato F, Prato R, Germinario C. Ig Sanita Pubbl 2008; 64(5):623-36.
8. Yuan GX, Shen YH, Chen B, Zhang WB. Biomechanical comparison of internal fixations in osteoporotic intertrochanteric fracture. A finite element analysis. Saudi Med J 2012; 33(7):732-9.
9. Zhu QL, Yan MH, Zhao LL, Xu B, Rong LJ, Luo JM. Analysis of treatment of osteoporotic intertrochanteric fracture of femur with the locking compression plate (LCP). Zhongguo Gu Shang 2011; 24(5):378-81.
10. Davis TR, Sher JL, Horsman A, Simpson M, Porter BB, Checketts RG. Intertrochanteric femoral fractures: mechanical failure after internal fixation. J Bone Joint Surg Br 1990; 72(1):26-31.
11. Pogrund H, Kenan S, Frankl U, Amir D. Another look at the pertrochanteric fracture of the femur: the relationship to osteoporosis. Injury 1987; 18:36-9.
12. Yetkinler DN, Goodman SB, Reindel ES, Carter D, Poser RD, Constantz BR. Mechanical evaluation of a carbonated apatite cement in the fixation of unstable intertrochanteric fractures. Acta Orthop Scand 2002; 73:157-64.
13. Cheng CL, Chow SP, Pun WK, Leong JCY. Long-term results and complications of cement augmentation in the treatment of unstable trochanteric fractures. Injury 1989; 20:134-8.
14. Moroni A, Hoang-Kim A, Orsini R, Micera G, Giannini S. Aumento delle tecniche di fissazione nel paziente osteoporotico. G.I.O.T. 2008; 34(1):S255-8.
15. Elder S, Frankenburg E, Goulet J et al. Biomechanical

evaluation of calcium phospate cement augmented fixation of unstable intertrochanteric fractures. J Orthop Trauma 2000; 14:386-93.
16. Faldini C, Moroni A, Grandi G, Biagini C, Digennaro V, Leonetti D, Nanni M, Himmelmann M. Trattamento chirugico delle fratture mediali del collo del femore Garden tipo I-II mediante osteosintesi con viti percutanee rivestite di idrossiapatite. G.I.O.T. 2005; 31:247-52.
17. Leung KS. Osteoporotic bone fixation with Lag Fix in proximal femoral fractures. Department of Orthopaedics and Traumatology. The Chinese University of Hong Kong 2006.
18. Gruen TA, McNeice GM, Amstutz HC. Modes of failures of cemented stem-type femoral components: a radiographic analysis of loosening. Clin Orthop 1979; 141:17-27.
19. Cadossi M, Moroni A, Romagnoli M, Chiarello E, Faldini C, Giannini S. Bone mineral density of the proximal femur recovers after metal-on-metal hip resurfacing. Clin Cases Miner Bone Metab 2010; 7(2):135-9.
20. Müller ME, Nazarian S, Koch P, et al. The comprehensive classification of fractures of the long bones. Berlin. Springer-Verlog 1990.
21. Cleveland M, Bosworth DM, Thompson FR. Interthrocanteric fractures of the femur: survey of treatment in traetin and by internal fixation. J Bone Joint Surg Am 1947; 29(4):1049-67.
22. Baumgaertuer R. The value of the tip apex distance predective failure of per-trochanteric fracture. J Bone Joint Surg Am 1995; 77:1058-63.
23. Harris WH. Traumatic arthrits of the hip after dislocation and acetabular fractures: treatment by mold arthroplasty. an end-result study using a new method of result evaluation. J Bone Joint Surg Am 1969; 51:737-55.
24. Muhammad Khon Pahore. Evalation of risk of lag screw cut out in ustable intertrochanteric fractures. JLUMHS 2011; 10(3):157-162.
25. Moroni A, Faldini C, Pegreffi F, Giannini S. HA coated screws decrease the incidence of fixation failure in osteoporotic trochanteric fractures. Clin Orthop Relat Res 2004; 425:87-92.
26. Capone A, Padda D, Cabras E, Civinini R, Scharchini M. Criteri di scelta degli impianti nei pazienti con fratture laterali del femore ed osteoporosi severa. G.I.O.T. 2006; 32(1):S272-6.
27. Goldhahn J, Suhm N, Goldhahn S, Blauth M, Hanson B. Influence of osteoporosis on fracture fixation - a systematic literature review Osteoporos Int 2008; 19:761-72.
28. Tarantino U, Cannata G, Lecce D, Celi M, Cerocchi I, Iundusi R. Incidence of fragility fractures. Aging Clin Exp Res 2007;19(4):7-11.
29. Moroni A, Faldini C, Chilò V, Rocca M, Stea S, Giannini S. The effect of surface material and roughness on bone screws stability. J Orthop Trauma 1999; 13:477-82.
30. Moroni A, Faldini C, Marchetti S, Manca M, Consoli V, Giannini S. Improvement of the bone-pins interface strenght in osteoporotic bone using hydroxyapatite coated tapered external fixation pins. A prospective randomized clinical study of wrist fractures. J Bone Joint Surg Am 2001; 83-A(5):717-21.

IMMUNOMODULATING TREATMENT WITH LOW DOSE INTERLEUKIN-4, INTERLEUKIN-10 AND INTERLEUKIN-11 IN PSORIASIS VULGARIS

M.L. ROBERTI[1], L. RICOTTINI[2], A. CAPPONI[3], E. SCLAUZERO[4], P. VICENTI[5], E. FIORENTINI[6], C. SAVOIA[7], G. SCORNAVACCA[8], D. BRAZIOLI[9], L. GAIO[10], R. GIANNETTI[11], C. IGNAZZI[12], G. MELONI[13] and L.M. CHINNI[14]

[1]Private Practice, Rome, Italy; [2]"Sinergheia" Medical Center, Rome, Italy; [3]Private Practice, Latina, Italy; [4]OSTEMDA, Therapeutic Strategies Empowerment and Advanced Diagnostic Methods Organization, Udine, Italy; [5]Private Practice, Altamura, Bari, Italy; [6]Dermatological Health Clinic, Aversa, Caserta, Italy; [7]Private Practice, Fino Mornasco, Como, Italy; [8]Private Practice, Catania, Italy; [9]Private Practice, Turin, Italy; [10]Private Practice, Caserta, Italy; [11]"Aurelia" Medical Center, Rome, Italy; [12]Local Health Unit (ASL), Putignano, Bari, Italy; [13]"GEA Medica" Medical Center, Montebelluna, Treviso, Italy; [14]Istituto Dermopatico dell'Immacolata (IDI), Rome, Italy

Received October 21, 2013 - Accepted January 21, 2014

Psoriasis is a chronic inflammatory skin disease affecting approximately 2-3% of the world population; it is characterised by hyperproliferation and hyperplasia of the superficial layers of the epidermis. Inappropriate signals released by the immune system determine an altered keratinocyte differentiation, resulting in the formation of desquamating, thickened, inflamed and erythematous plaques. The aim of this investigation was to study the pharmacological activity and safety of three low dose cytokines, Guna-Interleukin 4, Guna-Interleukin 10 and Guna-Interleukin 11 at the concentration of 10 fg/ml in patients affected by moderate to slight psoriasis vulgaris. The multicenter, double-blind, randomized, placebo-controlled clinical trial involved 48 patients who were enrolled and followed up according to a 8-month experimental project. All patients received, according to a cross-over model, either the experimental treatment or placebo, alternatively. Globally, in the 41 evaluated patients it was observed a PASI significant reduction (Friedman test: p=0.00960). The DLQI too decreased significantly in all subjects compared to baseline (Friedman test: p=0.00007). The safety of the treatment with three low dose cytokines administered simultaneously was proved; no adverse event was reported during the whole trial.

Psoriasis is a common chronic inflammatory skin disease, most often characterized by thickened erythematous scaly plaques, and appears in a variety of forms with distinct characteristics. The most common form, psoriasis vulgaris, affects 1-3% of the Caucasian population, usually persists, with 40% developing seronegative arthritis, and has a very negative impact on quality of life (1).

The existence of familial cases of psoriasis and the occurrence of the pathology in monozygotic twins demonstrates the role of genetic factors. The mode of inheritance of psoriasis is complex. In the multifactorial hypotesis environmental triggering factors (traumas, infections, stress, climate) interplays with genetic factors (2).

The pathogenesis of disease is still not clear,

Key words: Psoriasis vulgaris, interleukin-4, interleukin-10, interleukin-11, PASI score, DLQI

Mailing address:
Maria Luisa Roberti MD,
Private Practitioner,
Piazza di Villa Carpegna, 42/B,
00165 Roma, Italy
Tel.: +39 06 6634750
e-mail: mlroberti@gmail.com

0393-974X (2014)

therefore psoriasis is generally regarded as a T-cell mediated autoimmune disease. Although psoriasis was initially classified as a Th-1-polarized disease, a clear role for CD4+ T cells that produce IL-2, IL-6, IL-17 and IL-22 has been demonstrated. The cytokines show a key role in the development and maintenance of psoriasic lesions. The hypothesis of a cytokine network in psoriasis proposes a central role of pro-inflammatory cytokines, including TNF-α. In this disease, three predominant cytokines seem to be at play: type I interferons, IFN-γ and TNF-α. In psoriasis, IFN-γ, the prototype Th-1 cytokine, interplays with TNF-α, IL-17, IL-22, and IL-6 to inflammatory process (3, 4). Therapies targeting T cells seem to be very effective in the treatment of skin lesions and arthritis involvement. Strategies for intervention into the cytokine network have included antagonism of pro-inflammatory cytokines (e.g. TNF-α, IL-1, IL-6, IL-8, IL-12, IL-18, IL-23) with neutralizing antibodies and soluble receptors; application of recombinant cytokines (e.g. IL-4, IL-10, IL-11, IFN-γ) to shift the cytokine balance; and administration of small molecules to modulate cytokine expression or signaling (5). The treatment with IL-4, IL-10 and IL-11 down-regulates type I cytokine pro-inflammatory pathways in psoriasis lesions. IL-11 therapy has demonstrated immunomodulatory activity to regulate both T cell and macrophage function (6).

Aims of this study were to assess the safety and efficacy of oral low-dose cytokines (IL-4, IL-10 e IL-11) in the treatment of psoriasis and to evaluate the effects of this therapy in the quality of life.

MATERIALS AND METHODS

Subjects

Forty-eight patients with moderate to slight psoriasis, according to the psoriasis area and severity index (PASI), were enrolled in this study, 41 (17 females and 24 males; mean age 46.2± std.dev. 11.7 years) were evaluated. Table I shows the patients' epidemiological and clinical features.

Patients with guttate psoriasis, palmoplantar, pustular and erythrodermic psoriasis and other skin diseases were excluded.

Patients who underwent topic or systemic therapies specific for psoriasis, respectively in 15 and 90 days prior the enrolment.

Other exclusion criteria: subjects under 18 years of age and subjects in therapy for other pathologies with steroid (topical or systemic), anti-TNF-α therapies, immunosuppressive agents (e.g., cyclosporine, tacrolimus or methotrexate).

Protocol inclusion criteria concerned also patients in more serious conditions, in order to assess whether patients not responding to phototherapy treatment could benefit from the studied therapy.

Study design

This is a multicenter, double-blind, randomized, placebo-controlled clinical trial, alternated according to a cross-over model, lasting eight months overall. Since the beginning of the trial, for a period of 3 months, all individuals enrolled in the study were treated with low dose cytokines or with placebo solution. After a wash-out period of 60 days, the administration of the experimental product was resumed for a further three-month period, thus implementing the cross-over experimental model. After signing an informed consent the patients were enrolled progressively in the different experimental sites and identified with their initials as well as through a serial number.

A randomization procedure performed using a tailored software has generated two equal parts, one containing cytokines and one containing placebo. These preparations were marked with a serial number and an identifying code of the three products. Each preparation was allocated to the related subject. The chief of the Guna Labs (GUNA Spa, Milan - Italy) was the only one aware of the product content. A yellow label identified the products prepared for the first period of treatment; a green label identified the products prepared for the second period of treatment.

One group was treated with Guna-Interleukin 4, Guna-Interleukin 10, Guna-Interleukin 11 at the concentration of 10 fg/ml in a hydroalcoholic solution 30% for oral use (GUNA Spa, Milan, Italy) administered at a dose of 20 drops twice daily, taken on an empty stomach from 8.00 to 10.00 and from 19.00 to 21.00. The other group was treated with placebo (hydroalcoholic solution at 30% containing no active ingredients) with the same mode of administration. Neither the doctor nor the patient were aware of the nature of the preparation assigned.

At the end of the first 3 months of treatment, patients underwent a new clinical control and after a wash-out period of 60 days, the 2 experimental groups were inverted (cross-over model). This in order to reduce the possible error factors in the evaluation, as well as to give the possibility to both groups to benefit from the therapy (Fig. 1).

Since our primary goal was to assess the activity of the three interleukins, the sample size was calculated considering the possible reduction of PASI score within treated patients by means of a crossover design. On the

other hand, from our previous experiences, we suspected a possible long lasting carry-over effect exerted by the interleukins (so interfering with the crossover results), and therefore we chose a sample size as we were measuring the PASI score in a "before-after" design. Assuming to recruit 20 subjects, in which the average reduction of PASI score at end of protocol should have been 1.5, with a standard deviation of reduction equal to 2, a sample of 20 patients would have reached a 87% power (with an error α=0.05) to detect the expected difference (before-after) within the group starting with interleukins. Then, the same sample size was chosen also for the other group, bearing in mind that our focus would have been on group firstly treated with interleukins.

Clinical assessment

Disease severity was assessed using the psoriasis area and severity index (PASI). The PASI is a dermatological index conventionally used, through which are evaluated extension, erythema, infiltration and desquamation in the areas of the head, arms, trunk and legs. The degree of severity of psoriatic manifestations provides a score ranging from 0 (no psoriasis) to 72 (maximum value, severe psoriasis). Higher scores represent greater degrees of disease severity (7). Severe psoriasis is defined as a PASI score >12 (8).

For the evaluation of individual distress it was used a Dermatology Life Quality Index (DLQI). This questionnaire fulfils reliability, validity, repeatability, and internal consistency requirements. It is meant for adults older than 16 years. It is self-administered and consists of 10 questions and measures 6 categories: symptoms and feelings (questions 1 and 2), daily activities (questions 3 and 4), leisure (questions 5 and 6), work and school (question 7), personal relationships (questions 8 and 9), and treatment (question 10). All questions relate "to the last week." Each question is answered using a tick box, with not at all, a little, a lot or very much, being scored from 0 to 3. The DLQI is calculated by summing the scores of each question, resulting in a minimum score of 0 (no impairment) to a maximum score of 30 (maximum impairment) in order to measure Heath Related Quality of Life (HRQoL) in patients. Higher scores represent greater degrees of HRQoL impairment (14). Severe impact on HRQoL by psoriasis is defined as a DLQI >10 (9).

Statistical analysis

All data were analyzed with usual descriptive statistics. D'Agostino-Pearson test, together with visual inspection of the histogram, were used to check the variable distributions: mean and standard deviation were used for the normally distributed variables, while median and IQR (InterQuartile Range) were used for non-normal ones. The Friedman test was used to analyze the within-group repeated measure variation of both PASI and DLQI scores; the post-hoc test according to Conover was used to check the pairwise comparisons. The Mann-Whitney U test was used to evaluate the difference of the scores between groups at baseline. Statistical significance was assumed with $p<0.05$.

RESULTS

Forty-eight patients were enrolled in the study in a period of 12 months; of these, 41 patients completed the entire experimental design and could be evaluated (Fig. 2). 34 subjects had a PASI score at enrollment <10; 7 had a PASI score at enrollment <30. All the recruited patients were divided in two groups, group A and group B. Group A, consisting of 23 individuals, performed the experimental design taking at time T0-T3 active preparation and at time T3-T6 the placebo. Group B, consisting of 18 subjects, conversely began with placebo in the first time and then took the cytokines in the second time (Fig. 1).

The global PASI score for the 41 patients at baseline (T0) ranged from a minimum of 1 to a maximum of 21 (median=5). Considering the 2 groups separately, the PASI of group A (n=23) is 5 (1-18, IQR 2-8). In group B (n=18) the PASI at baseline (T0) is 5 ranged (1-21, IQR 2-8). No significant differences are observed at baseline between two groups (Mann-Whitney U test: $p>0.9999$).

Globally, in the 41 evaluated patients, who completed the study, it is observed a PASI significant reduction (Friedman test: $p=0.0096$). According to the Conover's post-hoc test, significant difference ($p<0.05$) is evident between values at time T0 and at time T3 and between values at time T0 and at time T6, but not between T3 and T6 time values (Table II).

Group A (n=23), treated during the first period, shows a PASI significant reduction (Friedman test: $p=0.0275$) (Table III). A significant difference according to Conover ($p<0.05$) was found only between values at T0 and at T6, whereas variations at T3 are not significant.

In group B (n=18) no significant differences between values at T0 and at T3 and between values at T0 and at T6 are observed (Friedman test: $p=0.23348$) (Table III).

Table I. *Epidemiological and clinical features of patients with psoriasis.*

Sex (female/male)	17/24
Age, years	46.2 ±11.7
Disease duration <5 years	9
Disease duration 5>years<15	13
Disease duration >15 years	18
Smokers, n (%)	8 (19.5%)
Patients with intermittent psoriasis, n (%)	21 (51%)

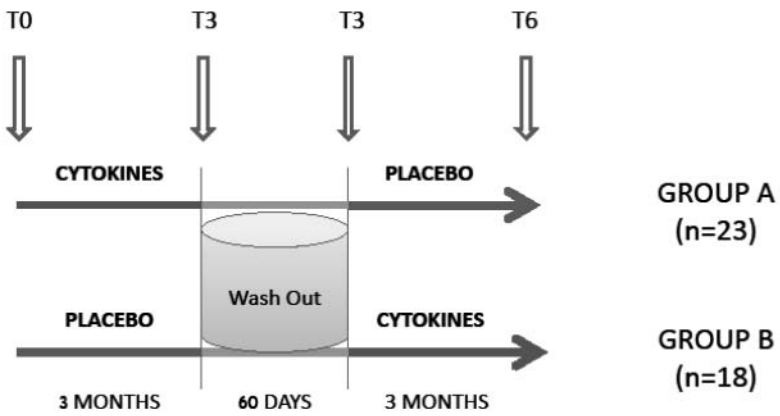

Fig. 1. *Study design.*

The DLQI for all patients (n=41) at baseline is 5 (0-23, IQR 2-10) (Table II). In group A, the DLQI is 4 (0-14, IQR 1.25-10) (Table III). In group B, the DLQI is 6 (0-23, IQR 3-10) (Table IV). The DLQI at baseline did not show any difference between the 2 groups (Mann-Whitney U test: p=0.2688).

The DLQI decreased significantly in all subjects (n=41) compared to baseline (p<0.0001). A significant difference according to Conover (p<0.05) was observed between values at T0 and at T3 and between values at T0 and at T6, but not between T3 and T6 (Table II).

In group A (n=23) we observed a DLQI significant reduction (p=0.0134) between values at T0 and at

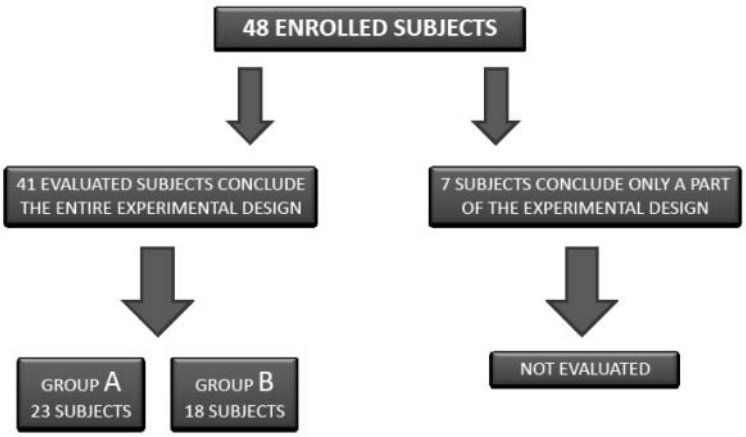

Fig. 2. *Flow chart of enrolled patients.*

Table II. *The PASI and DLQI in all subjects.*

N=41	Basal	3 months	6 months	p
PASI	5 (1-21)	3 (0-11)	3 (0-12)	p<0.05 (bas. vs 3/ 6 m.)
DLQI	5 (0-23)	3 (0-14)	3 (0-18)	p<0.05 (bas. vs 3/ 6 m.)

Data are expressed in median with range (minimum and maximum).

Table III. *The PASI and DLQI in group A subjects.*

N=23	Basal	3 months	6 months	p
PASI	5 (1-18)	4(1-11)	3 (0-12)	p<0.05 (bas. vs 6 m.)
DLQI	4 (0-14)	4 (0-14)	3 (0-17)	p<0.05 (bas. vs 6 m.)

Data are expressed in median with range (minimum and maximum).

Table IV. *The PASI and DLQI in group B subjects.*

N=18	Basal	3 months	6 months	p
PASI	5 (1-21)	2 (0-11)	3.5 (0-7)	p>0.05 (bas. vs 3/ 6 m.)
DLQI	6 (0-10)	3 (0-9)	2.5 (0-18)	p<0.05 (bas. vs 3/ 6 m.)

Data are expressed in median with range (minimum and maximum).

T6. A significant pairwise difference ($p<0.05$) was found between baseline and values at 6 months, but not between baseline and values at 3 months, nor between 3 and 6 months (Table III).

In group B (n=18) the variation is still significant ($p=0.0005$) and the significant difference is kept between baseline and 3 months and between baseline and 6 months (Table IV).

DISCUSSION

In this study we demonstrated that therapy with low dose of cytokines (IL-4, IL-10 and IL-11) was safe and reduced severity of psoriasis vulgaris. In addition, this therapy improved the quality of life.

No adverse event was reported during the study in patients with psoriasis vulgaris. At our knowledge

this is the first study who demonstrated the safety of low dose cytokine.

In this study the low dose cytokine ameliorate the PASI score significantly (p=0.00960) between baseline and 3 months and between baseline and 6 months. These results confirmed the hypothesis that anti-inflammatory cytokines (IL-4, IL-10, IL-11) showed a key role in the pathogenesis of psoriasis. A network of pro-inflammatory cytokines is a central feature in the pathophysiology of cutaneous inflammatory diseases. While anti-TNF therapeutics have proven to be effective for the treatment of psoriasis, clinical investigations have now begun with other cytokine-directed therapies, such as those targeting IFN-γ, IL-12, and IL-18.

Since the IL-4 and IL-10 have reduced psoriatic plaques, we can suppose that the administration of these low dose cytokines restores the normal balance of cytokine network (10).

Ghoreschi et al. demonstrated that in patients with psoriasis IL-4 therapy was well tolerated and within six weeks all patients showed decreased clinical scores. IL-4 therapy can induce Th2 differentiation in human CD4+ T cells and is promising as a potential treatment for psoriasis (11).

IL-10 is an important immunoregulatory cytokine produced by many cell populations. Its main biological function seem to be the limitation and termination of inflammatory responses and the regulation of differentiation and proliferation of several immune cells such as T cells, B cells, natural killers, antigen-presenting cells, mast cells, and granulocytes. Recombinant human IL-10 has been produced and is currently being tested in clinical trials. This includes rheumatoid arthritis, inflammatory bowel disease, psoriasis, organ transplantation, and chronic hepatitis C (12, 13). A study involving 28 patients with moderate-to severe psoriasis showed that treatment with rhIL-10 resulted in only temporary clinical improvement in psoriasis, despite sustained systemic decreases in pro-inflammatory and type 1 cytokine production (14).

IL-11, a multifunctional cytokine, modulates macrophage and type 1 T-lymphocyte function in cell culture and shows anti-inflammatory activity in animal models. Trepicchio et al. evaluated the effect of subcutaneous delivery of rhIL-11 in patients with psoriasis. Seven of 12 patients responded well to rhIL-11 treatment. Amelioration of disease by rhIL-11, as shown by reduced keratinocyte proliferation and cutaneous inflammation, was associated with decreased expression of products of disease-related genes, including K16, iNOS, IFN-γ, IL-8, IL-12, TNF-α, IL-1β, and CD8+, and with increased expression of endogenous IL-11 (6). The ability of rhIL-11 to modulate cytokine production from activated CD4+ T cells provides a mechanism through which rhIL-11 may ameliorate such inflammatory diseases as psoriasis (15). Conversely, in comparison with normal controls, bone marrow stromal cells from patients with psoriasis showed no alteration in the levels of GM-CSF, IL-11, IL-7 (16).

Our data confirm that most patients with psoriasis have poor quality of life prior to treatment, and that improvement in psoriasis lesion and symptoms (e.g. pruritus, restlessness) with treatment significantly correlates with improvement in DLQI.

We can conclude that low dose cytokines are safe and effective in the treatment of psoriasis vulgaris. Considering the initial suspect of carry over effect, the results of this exploratory study seemed to highlight a long time action of interleukins. The latter is shown also after stopping the treatment. Further trials with a longer observational period are necessary to confirm our preliminary data.

ACKNOWLEDGEMENTS

We wish to thank M.Assirati, B.Fiorentino, A.Crippa, A Nazari, B.Arsuffi, G.Tomasini, M.Passafaro, S.Cangemi, R.Malvicini, M.Siffredi, C.Gremita, F.Mazzola, L.Morlando, L.Cendret for their valuable clinical contribution to the achievement of this work. We wish to thank V.Miranda (Clinical Research Unit Guna S.p.a Milan-Italy) for his helpful scientific discussion and critical revision of the manuscript. We also thank M.Nichelatti and C.Mattana for the bioinformatic analysis, M.Campanella (Clinical Research Unit Guna S.p.a Milan-Italy) for her scientific and technical support in data management, F.Melzi (Guna S.p.a) for her linguistic assistance.

REFERENCES

1. Kurd SK, Gelfand JM. The prevalence of previously

diagnosed and undiagnosed psoriasis in US adults: results from NHANES 2003-2004. J Am Acad Dermatol 2009; 60:218-24.
2. Krueger GG, Duvic M. Epidemiology of psoriasis: clinical issues. J. Invest Dermatol 1994; 102:14-18S.
3. Gudjonsson JE, Johnston A, Sigmundsdottir H et al. Immunopathogenic mechanisms in psoriasis. Clin Exp Immunol 2004; 135:1-8.
4. Nestle FO, Kaplan DH, Barker J. Psoriasis. N Engl J Med 2009; 30(361):496-509.
5. Numerof RP, Asadullah K. Cytokine and anti-cytokine therapies for psoriasis and atopic dermatitis. BioDrugs 2006; 20:93-103.
6. Trepicchio WL, Ozawa M, Walters IB. Interleukin-11 therapy selectively downregulates type I cytokine proinflammatory pathways in psoriasis lesions. J Clin Invest 1999; 104:1527-37.
7. Fredriksson T, Petersson U. Severe psoriasis oral therapy with a new retinoid. Dermatologica 1978; 157: 238-44.
8. Schmitt J, Wozel G. The Psoriasis Area and Severity Index Is the Adequate Criterion to Define Severity in Chronic Plaque-Type Psoriasis. Dermatology 2005; 210:194-9
9. Finlay AY, Khan GK. Dermatology Life Quality Index (DLQI)-a simple practical measure for routine clinical use. Clin Exp Dermatol 1994; 19:210-6.
10. Numerof RP, Dinarello CA, Asadullah K. Cytokines as potential therapeutic targets for inflammatory skin diseases. Eur Cytokine Netw 2005; 16:101-3.
11. Ghoreschi K, Thomas P, Breit S, Dugas M, Mailhammer R, van Eden W, et al. Interleukin-4 therapy of psoriasis induces Th2 responses and improves human autoimmune disease. Nat Med 2003; 9:40.
12. Asadullah K, Sterry W, Volk HD. Interleukin-10 therapy – review of a new approach. Pharmacol Rev 2003; 55:241.
13. Asadullah K, Sabat R, Friedrich M, Volk HD, Sterry W. Interleukin-10: an important immunoregulatory cytokine with major impact on psoriasis. Curr Drug Targets Inflamm Allergy 2004; 3:185-92.
14. Kimball AB, Kawamura T, Tejura K, et al. Clinical and immunologic assessment of patients with psoriasis in a randomized, double-blind, placebo-controlled trial using recombinant human interleukin 10. Arch Dermatol 2002; 138:41.
15. Bozza M, Bliss JL, Dorner AJ, Trepicchio WL. Interleukin-11 modulates Th1/Th2 cytokine production from activated CD4+ T cells. J Interferon Cytokine Res 2001; 21:21-30.
16. Zhang K, Liu R, Yin G, Li X, Li J, Zhang J. Differential cytokine secretion of cultured bone marrow stromal cells from patients with psoriasis and healthy volunteers. Eur J Dermatol 2010; 20:49-53.

JOURNAL OF BIOLOGICAL REGULATORS & HOMEOSTATIC AGENTS Vol. 28, no. 1, 143-147 (2014)

LETTER TO THE EDITOR

WHITE MULBERRY SUPPLEMENTATION AS ADJUVANT TREATMENT OF OBESITY

G. DA VILLA[1], G. IANIRO[2], F. MANGIOLA[2], E. DEL TOMA[1], A. VITALE[1], A. GASBARRINI[2] and G. GASBARRINI[3]

[1]F. De Ritis Institute, Afragola, Naples, Italy; [2]Division of Internal Medicine and Gastroenterology, Catholic University of Sacred Heart, Rome, Italy; [3]Medical Research ONLUS Foundation, Bologna, Italy

Received February 20, 2013 – Accepted January 8, 2014

Body weight is controlled by our genes and managed by a neuro-hormonal system, in particular by insulin and glucagon. The meristematic extract of Japanese white mulberry blocks the alpha-glucosidase and then the intestinal hydrolysis of polysaccharides, thereby reducing the glycaemic index of carbohydrates. The target of our research was to evaluate the adjuvant slimming effect of the extract of white Japanese mulberry in the dietetic treatment of some patients who are obese or overweight. 46 overweight people were enrolled and divided into two subgroups: the subjects of both subgroups were given an identical balanced diet of 1300 kcal: subjects of the subgroup α received 2400 mg of white Japanese mulberry extract, the subgroup b subjects receive placebo. Each subgroup was followed-up every 30 days at 30, 60 and 90 days of treatment. Both in the periodic inspections and in the final inspection measurements of body weight and waist circumference in all the subjects and thigh circumference in women only were repeated. All subjects repeated blood tests. In the subgroup α,weight loss was about 9 kg in 3 months, equal to approximately 10% of the initial weight, significantly higher than subgroup β (P<0.0001); moreover, the plasma insulin and glucose curves of the volunteers in this subgroup at the end of the trial were lower than those performed at the time of enrolment. In the 20 women of the β subgroup treated with only low-calorie diet and with placebo, weight reduction was globally of 3.2 kg, approximately equal to 3% of the initial weight; moreover, the blood glucose curves and the insulin curves showed a slight decline compared to baseline, but not so significantly as was the case for group α. Waist circumference and thigh circumference (in women) decreased in all participants, obviously more evidently in subjects who lost more kg. The extract of white Japanese mulberry may represent a reliable adjuvant therapy in the dietetic treatment of some patients who are obese or overweight.

Obesity is a pathological condition, characterized by an excess in the human organism of body fat (1), defined as a BMI exceeding 30 kg/m2. It has been classified as a Disease by the American Medical association, representing one of the most severe public health problems of our century that can seriously reduce the life expectancy (1-3). Indeed, the excess of body fat represents a preventable risk factor for many diseases, particularly cardiovascular disease, type 2 diabetes, osteoarthritis and some types of neoplasia (4). The mechanisms that lead to obesity can be reached commonly in an improper

Key words: White mulberry, insulin, obesity, weight loss

Mailing address: Gianluca Ianiro, MD,
Division of Internal Medicine and Gastroenterology,
Catholic University of Sacred Heart,
Largo Gemelli 8,
00168 Rome, Italy
Tel.: +39 06 30156018 Fax: +39 063 0157249
e-mail: gianluca.ianiro@hotmail.it

0393-974X (2014)

lifestyle, characterized by an excessive food intake and a lack of physical activity, often supported by a genetic susceptibility (5, 6).

Body weight is controlled by our genes and managed by a neuro-hormonal system represented by the diencephalic regulatory centers, which constantly receive information from the periphery by many appetite-hormone, particularly leptin and ghrelin). These peripheral hormones act regulating the food intake thought the signalling modulation of several circuits of the hypothalamus. Among those, the melanocortin pathway is the most clearly understood: from the arcuate nucleus the signal reaches the feeding and satiety centers of the brain, localized in the lateral (LH) and ventromedial (VMH) hypothalamus, respectively (7, 8)

In addition to leptin and ghrelin, other mediators such as insulin, orexin, PYY 3-36, cholecystokinin and adiponectin contribute to this regulatory system (9).

Insulin is a peptide hormone produced by the beta cells of the pancreas which has a central role on the metabolism regulation of carbohydrate and fat in the human body. It has a lipogenic function because it stimulates the liver to produce cholesterol and triglycerides from calories of unused nutrients, and also sensitizes lipase of the adipose tissue to allow entry of fats in adipocytes (10). Consequently, it would seem desirable to direct therapeutic approaches against obesity to reduce insulin circulating in the patient's blood, believing that insulin triggers the increase of body weight.

In recent decades several molecules have been put on the market, each of which boasted a slimming capacity or because of limiting the absorption of carbohydrates or lipids, or because it reduced the sense of hunger or as it was able to perform both of these activities, without significant results (11).

The most effective and safest treatment for obesity consists of dieting and physical exercise (6), but the most difficult step remains to maintain the reached weight loss, goal possible only with a permanent changes of lifestyle (12, 13). Therefore, the aim of this research was to identify a natural substance, without side effects, that would be able to act indirectly on the hyperinsulinemic conditions of obese or overweight patients in order to obtain their weight loss and, once they had lost weight, maintaining the achieved weight without the risk of re-fattening.

The diencephalon, in fact, has in memory the setting of the body weight before slimming treatment and, at the same time, receives peripheral information about the emptying of fat already present in the fat deposits due to the previous slimming cure. Consequently, his reaction is to reduce energy consumption and increase the feeling of hunger to fight weight loss by making patients gain weight back. Thus we have experienced the slimming effect of the meristematic extract of Japanese white mulberry (Morus Alba) which is characterized by the presence of Deoxynojirimycin (DNJ). This molecule is a D-glucose analogue that blocks the alpha-glucosidase and then the intestinal hydrolysis of polysaccharides, thereby reducing the glycaemic index of carbohydrates (14, 15). As already shown by Kimura et al, the dietary intake of mulberry DNJ has a suppressive effect on the post prandial glucose increase in blood (16, 17) and, through the activation of β-oxidation system, it reduces the plasma triacylglycerol and the lipid storage in the liver (18). Additionally, it seems to have a positive effect also on lipid metabolism in normal rats (19).

Through this method, according to our working hypothesis, it is possible to enhance the slimming effect of a low-calorie diet both in obese subjects and in slimmed down subjects, making the effect of reducing the rate of circulating insulin produced by natural DNJ. Also, once obtained the desired result, the continuous integration of white mulberry meals may avoid the re-fattening of slimmed down obese patients.

Rationale and objectives

The target of our research was to evaluate the adjuvant slimming effect of the extract of white Japanese mulberry in the dietetic treatment of some patients who are obese or overweight. The objective of this experiment was to obtain the weight loss in obese patients, reducing their rate of circulating insulin through the administration at mealtimes of 800 mg of extract of Japanese white mulberry (8 mg of natural DNJ).

MATERIALS AND METHODS

The clinical trial lasted 3 months (January to March

2012) and involved 46 overweight people including 40 women and 6 men, chosen on the basis of therapeutic compliance, that is the ability to follow a low-calorie dietetic treatment plus drug treatment for 3 months. All subjects included in the study were aged between 35 and 55 years and had no noteworthy illnesses. At the time of enrolment, for every subject body weight, waist and abdominal circumference, and - only in women- thigh circumference were measured.

The body mass index of the group ranged on average between 28 and 34 and their plasma insulin and glucose curves at the time of recruitment were all abnormal.

The patients have been divided into two subgroups: subgroup α consisted of 20 women and 3 men and 20 women and 3 men represented subgroup β. The subjects of both subgroups were given an identical balanced diet of 1300 kcal: subjects of the subgroup α received 2400 mg of white Japanese mulberry extract (800 mg divided in three administrations paid out after the three main meals, 8 mg of natural DNJ for three times a day); participants of the subgroup β instead received two placebo tablets at the 3 main meals (6 tablets at day).

After one month all the men (3) of the subgroup β left the experimentation. Each subgroup had follow-up every 30 days at 30°, 60° and 90° days of treatment; both in the periodic and final inspections, measurements of body weight and waist circumference in all the subjects and thigh circumference in women only were repeated. All subjects repeated blood tests: blood glucose curve and insulin glucose load, complete blood count, blood urea nitrogen, creatinine and electrolytes (sodium and potassium).

RESULTS

Fig. 1 shows the mean values of blood glucose curve and the insulin curve that have been highlighted in the whole group of 40 women and 6 men before the division into two subgroups. Fig. 2 shows the average values of insulin and glucose curve performed on 20 participants and three volunteers of the subgroup α at the end of the trial. Fig. 3 shows the average of the values of the blood glucose curve and the insulin curve practiced to 20 volunteers belonging to the subgroup β.

In the subgroup α (low-calorie diet plus the intake of natural DNJ 8 mg thrice at meals), weight loss was about 9 kg in 3 months, equal to approximately 10% of the initial weight, significantly higher than subgroup β ($P<0.0001$); moreover, the plasma insulin and glucose curves of the volunteers in this subgroup at the end of the trial were lower than those performed at the time of enrollment (Fig. 2). In the 20 women in the β subgroup treated with only low-calorie diet and with placebo, weight reduction was globally of 3.2 kg, approximately equal to 3% of the initial weight; moreover, the blood glucose curves and the insulin curves (Fig. 3) showed a slight decline compared to baseline, but not so strong as was the case for the group α.

Waist circumference and thigh circumference (in women) decreased in all participants, obviously

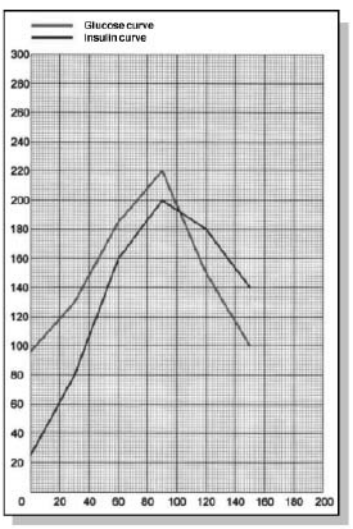

Time	Glucose	Insulin
0	98	25
30	130	80
60	185	160
90	220	200
120	150	180
150	100	140

Fig. 1. *Blood glucose and insulin curve in the whole study population after 3 months of treatment.*

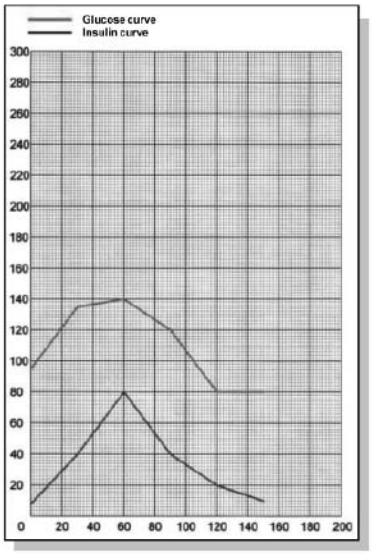

Time	Glucose	Insulin
0	95	8
30	135	40
60	140	80
90	120	40
120	80	20
150	80	10

Fig. 2. *Blood glucose and insulin curve in group A after 3 months of treatment.*

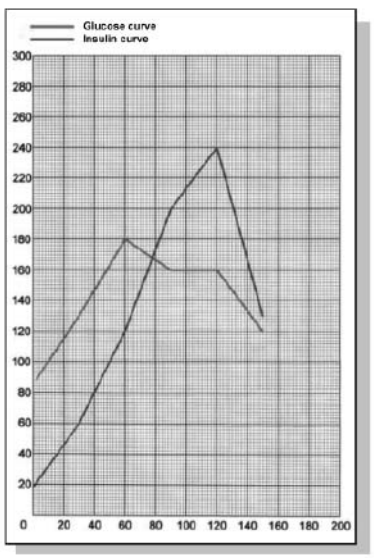

Time	Glucose	Insulin
0	85	18
30	130	60
60	180	120
90	160	200
120	160	240
150	120	130

Fig. 3. *Blood glucose and insulin curve in group B after 3 months of treatment.*

more evidently in subjects who lost more kg. Finally, among the subjects who took DNJ no undesirable side effects were observed, except for a slight bloating of the colon, probably related to the fermentation of polysaccharides hydrolysed in the small intestine.

CONCLUSIONS

In this study, it is evident that in the subgroup α, treated with 1300 Kcal diet and 2400 mg of extract of Japanese white mulberry, the weight loss was typically higher (about 3 times) compared to subgroup β control, treated only with the low-calorie diet and placebo. In addition, the insulin curve in the subgroup α showed after 3 months of treatment with DNJ a significant reduction compared to the curve tested at the time of recruitment, especially in the subgroup β.

The slimming effect observed in the subgroup α, in our opinion, may derive from the reduction of the glycaemic index of meals consumed by this subgroup due to the molecule Deoxynojirimycin (natural DNJ)

that, as we have seen, is able to prevent hydrolysis of the polysaccharides in the digestive tract. It is evident that in such a case the rate of blood insulin is reduced, as shown in Fig. 2, and then, consequently, the fat cells are emptied of the fat since there is no more blockage of insulin-dependent lipase.

We therefore hypothesize that the reduction rate of the blood insulin produced by the effect of DNJ has been the cause of reversal of triglycerides blood flow from the liver to adipose cells with consequent reduction of fat.

Finally, among the subjects who took DNJ no undesirable side effects were observed, except for a slight bloating of the colon, probably related to the fermentation of polysaccharides hydrolysed in the small intestine; this process, if not annoying, is an additional advantage for the health of consumers in view of the fact that the fermentation of polysaccharides causes the release of short-chain fatty acids, such as butyrate which, as we know, have a preventive effect on colon cancer.

REFERENCES

1. Haslam DW, James WP. Obesity. Lancet 2005; 366(9492):1197-209.
2. Barness LA, Opitz JM, Gilbert-Barness E. Obesity: genetic, molecular, and environmental aspects. Am J Med Genet A 2007; 143(24):3016-33.
3. Pollack. A.M.A. Recognizes Obesity as a Disease. The New York Times 2013.
4. Poulain M, Doucet M, Major GC, et al. The effect of obesity on chronic respiratory diseases: pathophysiology and therapeutic strategies. CMAJ 2006; 174(9):1293-9.
5. Keith SW, Redden DT, Katzmarzyk PT, et al. Putative contributors to the secular increase in obesity: exploring the roads less traveled. Int J Obes 2006; 30(11):1585-94.
6. Lau DC, Douketis JD, Morrison KM, Hramiak IM, Sharma AM, Ur E, et al. 2006 Canadian clinical practice guidelines on the management and prevention of obesity in adults and children. CMAJ 2007; 176(8):S1-13.
7. Flier JS. Obesity wars: molecular progress confronts an expanding epidemic. Cell 2004; 116(2):337-50.
8. Ahima RS, Flier JS. Adipose tissue as an endocrine organ. Trends Endocrinol Metab 2000;11(8):327-32.
9. Tchernof A, Despres JP. Pathophysiology of human visceral obesity: an update. Physiol Rev 2013; 93(1):359-404.
10. Svacina S. Treatment of obese diabetics. Adv Exp Med Biol 2012; 771:459-64.
11. Martinez-Augustin O, Aguilera CM, Gil-Campos M, Sanchez de Medina F, Gil A. Bioactive anti-obesity food components. Int J Vitam Nutr Res 2012; 82(3):148-56.
12. Shick SM, Wing RR, Klem ML, McGuire MT, Hill JO, Seagle H. Persons successful at long-term weight loss and maintenance continue to consume a low-energy, low-fat diet. J Am Diet Assoc 1998; 98(4):408-13.
13. Tate DF, Jeffery RW, Sherwood NE, Wing RR. Long-term weight losses associated with prescription of higher physical activity goals. Are higher levels of physical activity protective against weight regain? Am J Clin Nutr 2007; 85(4):954-9.
14. Zhong L, Furne JK, Levitt MD. An extract of black, green, and mulberry teas causes malabsorption of carbohydrate but not of triacylglycerol in healthy volunteers. Am J Clin Nutr 2006; 84(3):551-5.
15. Hunyadi A, Veres K, Danko B, Kele Z, Weber E, Hetenyi A, et al. In vitro anti-diabetic activity and chemical characterization of an apolar fraction of Morus alba leaf water extract. Phytother Res 2013; 27(6):847-51.
16. Singab AN, El-Beshbishy HA, Yonekawa M, Nomura T, Fukai T. Hypoglycemic effect of Egyptian Morus alba root bark extract: effect on diabetes and lipid peroxidation of streptozotocin-induced diabetic rats. J Ethnopharmacol 2005; 100(3):333-8.
17. Asano N, Kato A, Watson AA. Therapeutic applications of sugar-mimicking glycosidase inhibitors. Mini Rev Med Chem 2001; 1(2):145-54.
18. Tsuduki T, Kikuchi I, Kimura T, Nakagawa K, Miyazawa T. Intake of mulberry 1-deoxynojirimycin prevents diet-induced obesity through increases in adiponectin in mice. Food Chem 2013; 139(1-4):16-23.
19. Tsuduki T, Nakamura Y, Honma T, et al. Intake of 1-deoxynojirimycin suppresses lipid accumulation through activation of the beta-oxidation system in rat liver. J Agric Food Chem 2009; 57(22):11024-9.

JOURNAL OF BIOLOGICAL REGULATORS & HOMEOSTATIC AGENTS Vol. 28, no. 1, 149-156 (2014)

LETTER TO THE EDITOR

DIURNAL TRAJECTORIES OF SALIVARY CORTISOL, SALIVARY α-AMYLASE, AND PSYCHOLOGICAL PROFILES IN ORAL LICHEN PLANUS PATIENTS

R. PIPPI[1], R. PATINI[1], C.M. GHICIUC[2], R.B. SANDU[2], V. PASQUALI[3], S. SCACCIANOCE[4], L.C. DIMA-COZMA[5] and F.R. PATACCHIOLI[4]

[1]Department of Oral and Maxillo-Facial Sciences Faculty of Medicine and Dentistry, Sapienza University of Rome, Italy; [2]Department of Pharmacology, School of Medicine, University of Medicine and Pharmacy "Grigore T. Popa", Iasi, Romania; [3]Department of Psychology, Sapienza University of Rome, Italy; [4]Department of Physiology and Pharmacology "V. Erspamer", Sapienza University of Rome, Italy; [5]Department of Internal Medicine, School of Medicine, University of Medicine and Pharmacy "Grigore T. Popa", Iasi, Romania

Received May 29, 2013 – Accepted December 16, 2013

Although many reports have been published on the link between oral lichen planus (OLP) and the stress-related neuro-psycho-endocrine clinical features of the disease over the last 20 years, the data still remain controversial. Therefore, the aim of this study was to explore the personality traits of OLP subjects and assess the subjects' capability of coping with stress challenges. Cortisol and α-amylase were measured as reliable markers of the hypothalamic-pituitary-adrenal (HPA) axis and autonomic nervous system (ANS) activities in salivary samples collected by the participants at their home during the sampling day (07:30, 12:00, and 19:30). Compared with the healthy controls, the OLP patients demonstrated a less effective coping ability, had higher scores in stress perception and loneliness, and had no significant variation in their anxiety and depressive symptoms. The OLP patients also showed dysregulation of the HPA axis activity with a significant reduction of diurnal salivary cortisol production, which was particularly significant in the morning hours. No significant variation was found in the OLP salivary α-amylase diurnal fluctuation and production, which was measured at the same time point as that for cortisol. In conclusion, we report that OLP subjects had a reduced capability of coping with stress events and presented a dysregulation of HPA axis activity with hypocortisolism detected in the morning hours.

The prevalence of oral lichen planus (OLP) in the population varies from 0.1-4% (1, 2). OLP is a chronic inflammatory disease of the oral mucosa, the etiology of which has not been clearly defined (3). OLP involved in pathogenetically cell-mediated autoimmune responses and is frequently associated with many functional somatic syndromes. In addition, worsening of OLP symptoms has been described after stressful life events (4), which impairs an individual's capacity to suppress stress-increased immune activity. Although there is currently a large focus on the social-behavioural, autonomic, and/or endocrine factors that may have a potential effect on oral health (5) there are only partial and

Key words: Salivary cortisol, salivary α-amylase, oral lichen planus, psychological profile

Mailing address: Prof. Francesca Romana Patacchioli, MD, Department of Physiology and Pharmacology "V. Erspamer", "Sapienza" University of Rome, Piazza A. Moro 5, 00185, Rome, Italy
Tel.: +39 06 49912506
Fax: +39 06 49912506
e-mail: francesca.patacchioli@uniroma1.it

0393-974X (2014)

largely conflicting data present in the literature on the link between OLP and the stress-induced neuro-psycho-endocrine clinical features associated with the disease; these data are mainly characterized by confounding methodological approaches (6, 7).

People differ widely in how well they manage their emotional experiences in everyday life, not only due to differences in their skills but also due to differences in their perceived capabilities to regulate their emotions. In the present study, we examined the OLP patient psychological profile through standardized self-report questionnaires aimed at identifying depressive and anxiety symptoms (8) and subjective stress perceptions by evaluating the management of emotional experiences, loneliness, and coping strategies for life events (9-12). The purpose of this study was also to evaluate whether the psychological profile of OLP subjects was associated with changes in the circadian fluctuation of salivary cortisol and/or in its overall diurnal secretion (13, 14). We studied cortisol, which is the primary end product of the hypothalamic-pituitary-adrenal (HPA) axis because it is widely considered as a biological regulator of adaptation and of the maintenance of homeostasis in response to psychological and physiopathological challenges (15). Complex reciprocal counterbalances between the HPA axis and the autonomic nervous system (ANS) have been described (16). Therefore, we also studied the ANS activity in OLP patients through the analysis of salivary α-amylase circadian fluctuation and production, which were measured at the same time point as cortisol (13, 17-19).

MATERIALS AND METHODS

Study population

This study was formally approved by the local ethics committee (prot n° 393/13) and was conducted over a period of three months from March-May 2013. We studied 20 outpatients (OLP group) referred to the Department of Oral and Maxillo-Facial Sciences of "Sapienza" University of Rome, who were enrolled according to the following inclusion criteria to avoid confounding effects of ulcerative-erosive lesions of oral mucosa on salivary cortisol: 44-66-year-old women and men, non-smokers, and affected by OLP in the inactive state (with the histological diagnosis of OLP between 2-10 years before the enrollment).

None of the study participants was affected by neoplastic or immunological diseases or had received in the previous two months any steroidal, immunosuppressive, psychoactive, or vasoactive drugs (e.g., anti-hypertensives or thyroid agents), which could influence the cortisol and α-amylase. Saliva was collected in fertile women during the follicular phase. Among the outpatients referred to the same department for general periodic dental procedures, we selected 14 adult subjects for the control group who shared the same somatic characteristics of the OLP group and did not suffer from any ulcerative-erosive lesions of the oral mucosa. We previously estimated that at least 24 subjects (12 per group) were required to detect a mean absolute difference corresponding to a 30% variation in the expected peak concentration of salivary cortisol in healthy subjects (6.00 ng/ml; SD=2) with a two-tailed α of 0.05 and a power of 80%.

Psychometric testing paradigms

Eligible subjects were invited to the psychometric testing session at our laboratory from 09:00 to 12:00 am. Upon arrival, the participants were seated in a comfortable chair and given a full explanation of the test that they were about to undertake. The participants completed standardized self-report questionnaires to assess their depressive and anxiety symptoms and their perception of their own stress. The management of their emotional experiences, loneliness, and life event coping strategies was explored.

The State and Trait Anxiety Inventory (STAI, 20) yields separate measures of situational (state) and enduring (trait) anxiety. In the state anxiety test, the subjects were asked to describe how they felt at a particular moment. In the trait anxiety test, the participants were asked to describe how they generally feel. The 20 state anxiety and 20 trait anxiety items were each rated on a 4-point intensity scale, from 1 ("not at all") to 4 ("very much so"). The range of the scores for each of the 2 scales was 20-80.

The Beck Depression Inventory-II (21) is a self-reported measure that was designed to assess depression. It consists of 84 self-evaluative statements grouped into 21 categories that assess the affective and cognitive symptoms of depression. The items were rated in terms of increasing severity from 0 to 3, with 0 indicating the absence of a particular symptom. The scores for each item were summed, resulting in a score range from 0-63.

The participants' coping ability was assessed using a modified version of the Coping Orientation to Problems Experienced (COPE, 12), which consisted of 56 items and 7 factors: active coping, social support, alcohol and drug disengagement, avoidance, turning to religion, venting emotions and acceptance. The participants were specifically asked to rate how often they were engaged in the strategy described by each item on a 4-point Likert-

type scale ranging from 1 ("I usually do not do this at all") to 4 ("I usually do this a lot").

The Perceived Stress Scale (PSS) was used to assess the degree to which life situations were perceived as stressful (9). The items in the PSS were designed to assess how unpredictable, uncontrollable, and overloading the subjects found their lives to be. The participants responded on a 5-point scale ranging from 0 ("never") to 4 ("very often"). The responses to the items represented a psychological stress score, with higher scores indicating greater psychological stress.

Loneliness was assessed using the University of California at Los Angeles (UCLA) Loneliness Scale (22). This scale includes 20 Likert-type questions on a 4-point scale (1 - "strongly disagree", 4 - "strongly agree"). The sum of the responses to the 20 questions was used to determine loneliness. For emotional self-efficacy (ESE), which could contribute to effective emotion regulation, the participants rated (1 – "not well at all", 5 – "very well") their capability to manage shame/embarrassment, fear and guilt. The sum of the responses to the 18 questions was used to determine ESE total and 3 factor scores (10).

Salivary sampling procedure and cortisol and α-amylase measurement

During the three days before the "saliva sampling day", the participants were asked to maintain a completely quiet resting state without engaging in any intense physical activity or receiving any significant psychological input. The diet was similar among the study population. The subjects were asked to avoid food, coffee or alcohol consumption, teeth brushing, smoking, and any physical exercise for 30 minutes prior to each saliva collection (23).

After completing the psychometric testing, the participants were instructed on how to collect their saliva at home using the Salivette sampling device (Sarstedt, Italy). On the day after the psychometric assessment, all of the patients underwent three salivary collections: the saliva was collected at 07:30 (at least 60 minutes after awakening), 12:00 (before lunch), and 19:30 (before dinner). The participants were asked to store the samples in their home refrigerators and to deliver the samples to the laboratory on the day after collection.

The saliva was recovered from the polyester swab devices by centrifugation at 3,000 rpm for 15 minutes (24). The salivary samples were immediately frozen at a temperature of -20°C until they were analyzed.

For each sample, duplicate measurements were performed on 25 µl of saliva using commercial immunoenzymatic kits (Diametra, Italy) for the direct salivary assay of cortisol; the inter- and intra-assay coefficients of variation were < 10% and < 7%, respectively, with a minimum detectable concentration of 0.5 ng/ml. The salivary α-amylase was measured by a commercially available assay kit (Diametra, Italy) that was specifically designed to quantify α-amylase activity via a colorimetric assay; the inter-assay coefficient of variation was < 1.5%, and the minimum detectable concentration of α-amylase that could be distinguished from the blank standard at a 95% confidence interval was 2.5 U/ml.

Data and statistical analysis

All of the data are reported as the means±SEM unless otherwise specified. The statistical analyses and graphics were performed using SigmaPlot 11 software (SxST. it, Italy). The comparisons between the demographic characteristics of the OLP and control groups and between their psychometric parameters were performed using the Student's t-test or the Mann-Whitney test. The categorical data for gender were compared using the chi-square test. The GROUP, TIME, and GROUP x TIME effects on salivary cortisol and salivary α-amylase diurnal trajectories measured in the study population were determined using the two-way ANOVA for repeated measures followed by the Fischer LSD method for multiple comparisons.

The salivary cortisol and salivary α-amylase diurnal production were calculated from the area under the curve (AUC) of the salivary cortisol (ng/ml/h) and the α-amylase (U/ml/h) calculated for each subject using the trapezoidal method for the three samples collected from awakening to 19:30 (25). The statistical significance was set at $p < 0.05$.

RESULTS

As reported in Table I, the men and women were equally distributed between the control and OLP groups, which were homogenous for age, body mass index (BMI), and cardiovascular parameters (systemic blood pressure and heart rate). The psychometric profile of the study population is also presented in Table I. Compared with the control group, the OLP subjects showed a slight and non-significant increase in the state and trait components of anxiety symptoms and the somatic and cognitive components of depression.

When exploring the processes by which people face a stressful event, a significantly lower capability of active coping was found in the OLP subjects compared with the controls. However, non-significant differences were found between the two groups in social support, alcohol/drug disengagement, avoidance, turning to religion, and emotional and acceptance coping strategies. Furthermore, the OLP patients exhibited higher scores than those of the

Table I. *Somatic and psychometric variables of the study population.*

		Control (n=14)	OLP (n=20)	*p*
Men/women		4/10	6/14	1.000
Age, y		53 (7)	57 (6)	0.171
BMI, kg/m^2		25.5 (2.1)	26.7 (3.3)	0.233
SBP, mmHg		127.5 (9.6)	130 (7)	0.106
DBP, mmHg		76.5 (8.6)	85 (9.5)	0.111
HR, beats/min		67 (6)	72 (8)	0.108
STAI	Anxiety state	35±2	40±2.2	0.143
	Anxiety trait	36±3	40±1.9	0.321
BDI	Depression	5.9±1.7	8.9±1.5	0.195
	Somatic-affective	3.9±1.1	5.6±0.9	0.236
	Cognitive	1.4±0.6	1.8±0.6	0.672
COPING	Coping	2.4±0.1	2.2±0.1	0.341
	Active coping	3.1±0.1	2.6±0.1	0.024
	Social support	2.4±0.2	2.4±0.2	0.978
	Alcohol-drug disengagement	1.0±0.1	1.1±0.1	0.314
	Avoidance	1.7±0.1	1.6±0.1	0.746
	Turning to religion	2.5±0.3	2.5±0.2	0.875
	Venting emotion	2.1±0.1	2.2±0.2	0.763
	Acceptance	2.9±0.2	2.6±0.2	0.233
PSS	Perceived stress	20.1±2	25.4±2	0.031
UCLA	Loneliness	1.9±0.1	2.3±0.1	0.037
ESE	Emotional Self-Efficacy	2.8±0.2	2.9±0.1	0.651
	Guilt	2.4±0.2	2.4±0.2	0.957
	Fear	3.3±0.2	3±0.2	0.406
	Shame	2.6±0.2	3±0.2	0.151

The data are presented as the mean values ± SD or SE. ***BMI****=Body Mass Index;* ***SBP****: Systolic Blood Pressure;* ***DBP****: Diastolic Blood Pressure;* ***HR:*** *Heart Rate,* ***STAI:*** *State and Trait Anxiety Inventory;* ***BDI:*** *Beck Depression Inventory;* ***PSS:*** *Perceived Stress Scale;* ***SEE:*** *Self Emotional Efficacy,* ***UCLA:*** *University of California at Los Angeles.*

Table II. *Diurnal salivary cortisol and α-amylase AUCs in the study population.*

	Control (n=14)	OLP (n=20)	t	*p*
Cortisol diurnal AUC (ng/ml/h)	42±2	36±2	2.044	0.049
α-Amylase diurnal AUC (U/ml/h)	483±47	426±37	0.981	0.334

The data are shown as the mean values ± SEM. Student's t-test was used for the statistical analysis. ***AUC****: Area Under the Curve.*

controls in the PSS and the UCLA loneliness scale. Non-significant differences were found when self-emotional efficacy was explored as a general dimension and with regard to its sub-rating scales for guilt, fear, and shame.

Salivary cortisol and α-amylase daily trajectories

Fig. 1 (upper part) shows salivary cortisol

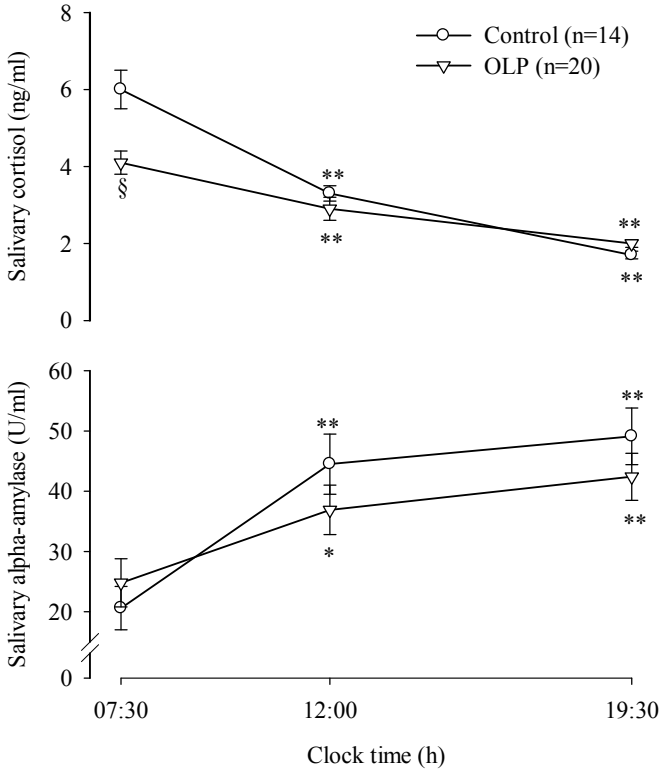

Fig. 1. *Diurnal trajectories of salivary cortisol and salivary α-amylase in the study population. Data are presented as mean ± SEM. * and **: P <0.05 and <0.01, respectively, vs 7:30; §: P <0.01 vs Control.*

daily trajectories in the study population. The two-way ANOVA for repeated measures, which was applied for the statistical evaluation of salivary cortisol variations during the sampling day, showed significant effects for the factor GROUP ($F_{1,101.}$ = 4.886; $p < 0.05$), the factor TIME ($F_{2,101.}$ = 69.626; $p < 0.001$), and their interactions (GROUP x TIME; $F_{2,101}$= 7.817; $p < 0.001$).

The post-hoc Fischer LSD method for multiple comparisons showed that the salivary cortisol concentration measured in the control group reflected a typical salivary cortisol diurnal trajectory; the evening value (1.6±0.1 ng/ml) was significantly lower than the morning value (6.0±0.5 ng/ml; $p <$ 0.001) and 12:00 value (3.3±0.2 ng/ml; $p < 0.001$). The OLP subjects showed a comparable trend with a significant diurnal decrease in the salivary cortisol concentration during the day ($p < 0.001$) and a salivary cortisol concentration in the morning (4.1±0.3 ng/ml) that was significantly higher than the concentrations at noon (2.9±0.3 ng/ml; $p < 0.001$) and in the evening (2.0±0.1 ng/ml; $p < 0.001$). As seen in Fig. 1, a statistically significant difference was found between the salivary cortisol levels of the OLP and control groups ($p < 0.001$).

With regard to the salivary α-amylase concentrations (Fig. 1, lower part), the ANOVA for repeated measures revealed no significant effects for the factor GROUP ($F_{1,101}$ = 0.498; p = 0.486), statistically significant effects for the factor TIME ($F_{2,101}$ = 25.320; $p < 0.001$), and no significant effects for the interaction GROUP x TIME ($F_{2,101}$ = 1.863; p = 0.164). The post-hoc Fischer LSD method for multiple comparisons showed a statistically significant difference between the salivary α-amylase concentrations in the morning and evening for all of the groups (morning controls 20.6±3.6 U/ml versus noon controls 44.5±5.3 U/ml, $p < 0.001$, and evening

controls 49.1±5.0 U/ml, $p < 0.001$) (morning OLP 24.8±4.0 U/ml versus noon OLP 36.9±4.1 U/ml, $p < 0.05$, and evening OLP 42.4±3.9 U/ml, $p < 0.001$).

AUCs of diurnal production of salivary cortisol and α-amylase

Table II demonstrates that the diurnal salivary cortisol production was significantly decreased in the OLP subjects compared with the controls and that OLP induced no significant effects in the salivary α-amylase diurnal production.

DISCUSSION

The main finding of this pilot study was that, compared to the controls, the OLP patients presented psychopathological disturbances affecting their social and personal dimensions because they showed a significantly lower capability of active coping that was associated with higher scores in stress perception and loneliness. In agreement with a previous report, this study showed that the anxiety and depressive symptoms were slightly, but not significantly, altered in the OLP group. This psychometric outcome is not in accordance with other studies (7). However, the discrepancy may be due to the differences in the inclusion criteria of the study populations.

In addition to the psychological dimensions involved in OLP, we also showed that the OLP-affected subjects had a reduced diurnal production of salivary cortisol, which occurred primarily in the morning hours. On the contrary, non-significant variations were found in the salivary α-amylase diurnal fluctuation and production measured at the same time points as cortisol.

The endocrine outcomes of this study differed from previous reports in which no changes (26) or increased (7) cortisol levels were demonstrated. However, biological and analytical-procedural factors, which can influence hormonal measurements, may have contributed to the variance in the outcomes of these studies (23). Although the individual increased stress sensitivity and related psychopathologies have been more obviously to hypercorticism, this association somewhat controversial. Consistent with McEwen's allostatic load model (15), the dysregulation of the HPA axis associated with psychopathologies may be manifested in a reduced diurnal pattern of cortisol production (27). Thus, we have shown that the OLP subjects were more sensitive to subjective stress perception, unable to cope with the stress, and presented a blunted salivary cortisol diurnal production compared with healthy controls.

Cortisol and α-amylase production is characterized by a circadian fluctuation (13, 17). In this study, we showed that the OLP subjects maintained the physiological circadian activity of the HPA axis, with the highest cortisol concentrations produced in the morning and the lowest produced in the evening. Moreover, the OLP subjects maintained the overall physiological pattern of the salivary α-amylase diurnal fluctuation observed in the controls, with a morning level that was significantly lower than the evening level.

From a methodological point of view, the measurement of the salivary biomarkers provided several advantages over their measurements in blood or urine because it represented a non-invasive, stress-free, and reliable source for monitoring changes in the HPA axis and ANS activities (14, 17, 18, 28). We studied the subjects who were chronically affected by OLP during the inactive state of the disease to avoid the reciprocal confounding effects of ulcerative-erosive oral mucosal lesions on the individual's psychological structure and/or the salivary biomarkers due to the possible blood contamination of the salivary samples. In addition, the potentially confounding effects of hypertension on the HPA axis and ANS activities were avoided in our study.

The blood pressure levels of our study population were categorized as optimal (control n=3; OLP n=2), normal (control n=4; OLP n=1), and high normal (control n=7; OLP n=17), and the participants presented with no or only slight alterations of systemic blood pressure (29).

OLP is a persistent inflammatory disease that is commonly observed in dental practices and is often associated with patient psychological profiles that are particularly susceptible to stressful events (4, 6, 7). Thus, the validation of the findings of the present study on a larger scale may help to aid patient care in the dentistry setting, resulting in a new series of topical symptomatic therapies (30) and a non-pharmacological approach to support patients' psychological need to improve their coping

strategies for challenging life events.

ACKNOWLEDGEMENTS

The authors wish to thank MASOPHRD (The Managing Authority for Sectoral Operational Programme Human Resources Development) for financial support to Raul Sandu in the frame of the POSDRU/107/1.5/S/78702 project, entitled "Inter-university partnership for increasing the medical doctoral research quality and interdisciplinary through doctoral scholarships – DocMed.net".

Dr. M.C. Ghiciuc and Dr. LC. Dima-Cozma participated in this study as visiting scientists, and Dr R.B.Sandu as International Doctorate fellowship, in the frame of the Bilateral Agreement between the Department of Physiology and Pharmacology of Sapienza University and the University of Medicine and Pharmacy "Grigore T. Popa" of Iasi, Romania.

REFERENCES

1. Scully C, Beyli M, Ferreiro MC, et al. Update on oral lichen planus: etiopathogenesis and management. Crit Rew Oral Biol Med 1998; 9:86-122.
2. Kleinman DV, Swango PA, Niessen LC. Epidemiologic studies of oral mucosal conditions--methodologic issues. Community Dent Oral Epidemiol 1991; 19:129-40.
3. Lavanya N, Jayanthi P, Rao UK, Ranganathan K. Oral lichen planus: An update on pathogenesis and treatment. J Oral Maxillofac Pathol 2011; 15:127-32.
4. Chaudhary S. Psychological stressors in oral lichen planus. Aust Dent J 2004; 49:192-5.
5. Ivanovski K, Nakova M, Warburton G, et al. Psychological profile in oral lichen planus. J Clin Periodontol 2005; 32:1034-40.
6. Girardi C, Luz C, Cherubini K, de Figueiredo MA, Nunes ML, Salum FG. Salivary cortisol and dehydroepiandrosterone (DHEA) levels, psychological factors in patients with oral lichen planus. Arch Oral Biol 2011; 56:864-8.
7. Koray M, Dülger O, Ak G, Horasanli S, Uçok A, Tanyeri H, Badur S. The evaluation of anxiety and salivary cortisol levels in patients with oral lichen planus. Oral Dis 2003; 9:298-301.
8. Beck AT, and Steer RA. BDI, Beck depression inventory: manual. New York: Psychological Corporation, 1987.
9. Cohen S, Kamarck T, Mermelstein R. A global measure of perceived stress. J Health Soc Behav 1983; 24:385-396.
10. Caprara GV, Di Giunta L, Pastorelli C, Eisenberg N. Mastery of Negative Affect: A Hierarchical Model of Emotional Self-Efficacy Beliefs. Psych Assess 2013; 25:105-17.
11. Russell DW. UCLA Loneliness Scale (Version 3): Reliability, validity, and factor structure. J Pers Assess 1996; 66:20-40.
12. Carver CS, Scheier MF, Weintraub JK. Assessing coping strategies: A theoretically based approach. J Pers Soc Psychol 1989; 56:267-83.
13. Ghiciuc CM, Cozma-Dima CL, Pasquali V, Renzi P, Simeoni S, Lupusoru CE, Patacchioli FR. Awakening responses and diurnal fluctuations of salivary cortisol, DHEA-S and α-amylase in healthy male subjects. Neuroendocrinol Lett 2011; 32:475-80.
14. Patacchioli FR, Perrone G, Merlino L, Simeoni S, Bevilacqua E, Capri O, Galoppi P, Brunelli R. Dysregulation of Diurnal Salivary Cortisol Production Is Associated with Spontaneous Preterm Delivery: A Pilot Study. Gynecol Obstet Invest 2013; 76:69-73.
15. McEwen BS. Mood disorders and allostatic load. Biol Psychiatry 2003; 54:200-7.
16. Cortelli P, Lombardi C, Montagna P, Parati G. Baroreflex modulation during sleep and in obstructive sleep apnea syndrome. Auton Neurosci 2012; 169:7-11.
17. Nater UM, Rohleder N. Salivary alpha-amylase as a non-invasive biomarker for the sympathetic nervous system: current state of research. Psychoneuroendocrinology 2009; 34:486-96.
18. Ghiciuc CM, Dima-Cozma LC, Bercea RM, Lupusoru CE, Mihaescu T, Szalontay A, Gianfreda A, Patacchioli FR. Restoring of salivary cortisol awakening response (CAR) by nasal continuous positive airway pressure (CPAP) therapy in obstructive sleep apnea. Chronobiol Int 2013; 30:1024-31.
19. Schumacher S, Kirschbaum C, Fydrich T, Ströhle A. Is salivary alpha-amylase an indicator of autonomic

nervous system dysregulations in mental disorders? A review of preliminary findings and the interactions with cortisol. Psychoneuroendocrinology 2013; 38:729-43.
20. Spielberger CD. Conceptual and methodological issues in anxiety research. In Anxiety: Current trends in theory and research. C.D. Spielberger, ed. Academic Press New York 1972; 481.
21. Beck AT, Steer RA, Ball R, Ranieri WF. Comparison of Beck Depression Inventories-IA and-II in psychiatric outpatients. J Pers Assess 1996; 67:588-97.
22. Russell D, Peplau L, Cutrona C. The revised UCLA Loneliness Scale: Concurrent and discrimenant validity evidence. J Pers Soc Psychol 1980; 39:472-80.
23. Hackney AC, Viru A. Research methodology: endocrinologic measurements in exercise science and sports medicine. J Athl Train 2008; 43:631-9.
24. Gröschl M, Khöler H, Topf HG, Rupprecht T, Rauh M. Evaluation of saliva collection devices for the analysis of steroids, peptides and therapeutic drugs. J Pharm Biomed Anal 2008; 47:478-86.
25. Fekedulegn DB, Andrew EA, Burchfiel CM, Violanti JM, Hartley TA, Charles LE, Miller DB. Area under the curve and other summary indicators of repeated waking cortisol measurements. Psychosom Med 2007; 69:651-9.
26. Rödström PO, Jontell M, Hakeberg M, Berggren U, Lindstedt G. Erosive oral lichen planus and salivary cortisol. J Oral Pathol Med 2001; 30:257-63.
27. Delle Chiaie R, Trabucchi G, Girardi N, et al. Group psychoeducation normalizes cortisol awakening response in stabilized bipolar patients under pharmacological maintenance treatment. Psychother Psychosom 2013; 82:264-6.
28. Simeoni S, Biselli R, D'Amelio R, Rocca B, Lattanzio S, Mucci L, Davì G, Patacchioli FR. Stress-induced salivary cortisol secretion during hypobaric-hypoxia challenge and in vivo urinary thromboxane production in healthy male subjects. Stress 2011; 14:282-9.
29. ESC/ESH Hypertension Guidelines Committee. Guidelines for the management of arterial hypertension: The Task Force for the Management of Arterial Hypertension of the European Society of Hypertension (ESH) and of the European Society of Cardiology (ESC). Eur Heart J 2007; 28:1462-536.
30. Rodhus NL, Cheng B, Bowles W, Myers S, Miller L, Ondrey F. Proinflammatory cytokine levels in saliva before and after treatment of (erosive) oral lichen planus with dexamethasone. Oral Dis 2006; 12:112-6.

JOURNAL OF BIOLOGICAL REGULATORS & HOMEOSTATIC AGENTS Vol. 28, no. 1, 157-167 (2014)

LETTER TO THE EDITOR

SAFETY PROFILE AND PROTOCOL PREVENTION OF ADVERSE REACTIONS TO UROANGIOGRAPHIC CONTRAST MEDIA IN DIAGNOSTIC IMAGING

C. ROSSI[1], A. REGINELLI[1], M. D'AMORA[1], G. DI GREZIA[1], Y. MANDATO[1], A. D'ANDREA[2], L. BRUNESE[3], R. GRASSI[1] and A. ROTONDO[1]

[1]Second University of Naples, Department of Experimental and Clinical Internistic "F. Magrassi A. Lanzara", Diagnostic Imaging Section, Naples, Italy; [2]S.G. Moscati Hospital, Radiology Department, Aversa, Italy; [3]University of Molise, Department of Health Science, Campobasso, Italy

Received October 17, 2013 – Accepted December 16, 2013

The purpose of the study is to examine the incidence of adverse reactions caused by non-ionic contrast media in selected patients after desensitization treatment and to evaluate the safety profile of organ iodine contrast media (i.c.m.) in a multistep prevention protocol. In a population of 2000 patients that had received a CT scan, 100 patients with moderate/high risk for adverse reactions against iodinated contrast agents followed a premedication protocol and all adverse reactions are reported and classified as mild, moderate or severe. 1.7% of the pre-treated patients reported a mild, immediate type reaction to iodine contrast; of these five patients with allergy 0.71% had received iomeprol, 0.35% received ioversol and 0.71% received iopromide. The incidence of adverse reactions was reported to be higher (4 out of 5 patients) among those that referred a history of hypersensitivity against iodinated i.c.m. Although intravenous contrast materials have greatly improved, especially in terms of their safety profile, they shoud not be administered if there is not a clear or justified indication. In conclusion, even if we know that the majority of these reactions are idiosyncratic and unpredictable we propose, with the aim of improving our knowledge on this subject, a multicenter study, based on skin allergy tests (prick test, patch test, intradermal reaction) in selected patients that have had previous experiences of hypersensitivity against parenteral organ iodine contrast media.

The use of contrast media has significantly increased during the last decades as a direct consequence of many new applications in Radiology, such as computerized tomography, and especially because of the constantly increasing role of Interventional Radiology. Now, notwithstanding their value in diagnostic imaging, it is mandatory to be aware of the possibility of adverse reactions against these compounds, that may range from mild inconveniences, such as itching associated with hives, to real life-threatening emergencies. Fortunately, the rate of adverse events has significantly decreased with the more recently introduced, low osmolality iodinated contrast media (i.c.m.) (3). Nonetheless, the possibility of an immediate or delayed allergy type reaction has not been completely surmounted. For this reason, radiologists and all the other physicians, especially anesthesiology and re-animation specialists, must be aware of the risk factors for adverse reactions, in order to be able to implement

Key words: Contrast media, adverse reactions, hypersensitivity, desensitization treatment

Mailing address: Dr Graziella Di Grezia,
Second University of Naples,
Department of Experimental and Clinical Internistic "F. Magrassi A. Lanzara", Diagnostic Imaging Section,
P.zza Miraglia 2 80138 Naples, Italy
Tel.: +39 081 5665200 Fax: +39 081 5665202
e-mail: graziella.digrezia@yahoo.it

0393-974X (2014)

the best strategies to avoid such undesired events and to recognize and treat immediately any emergency (4). Types of Adverse Reactions are described below (Table I).

Based on the time elapsed between the systemic administration of the i.c.m. and the onset of symptoms, adverse reactions can be classified as acute (onset within 1 h) or delayed (onset after 1 h and within 7 days from the administration) (1, 19). Obviously, acute reactions are dose- independent and potentially life-threatening.

Allergic-like Reactions

On account of their chemical structure and relative osmolality, contrast agents can be classified as ionic or non-ionic. Respect to the blood, ionic compounds have higher osmolality and non-ionic compounds have a lower osmolality, and it is well known that high osmolality contrast media (HOCM) are more frequently responsible of adverse events and nephrotoxicity as compared to low osmolality contrast media (LOCM). With the introduction of these LOCM has also diminished the incidence of cardiovascular undesired effects and allergic-type reactions. In adult subjects, adverse reactions are less frequent with ionic agents than with non-ionic agents.

Lethal reactions after contrast media administration are extremely rare (1:170,000) and no differences have been reported for the incidence of lethal events between ionic and no-ionic contrast agents (1). Still, the physiopathological mechanism of adverse reactions related to uroangiographic contrast media remains largely unclear.

Although adverse reactions to iodinated contrast media usually present with symptoms similar to those typical of type 1 hypersensitivity reactions (anaphylaxis) (24), they should not be considered real allergic reactions, because even if in these events a release or activation of several mediators typically involved in allergic reactions has been observed, it seems that they are not mediated by any antigen-antibody complex. Immunoglobulin E (IgE) are not involved and it seems that a reaction can occur even in absence of a previous sensitization (2). Only in a few cases it has been actually demonstrated that the undesired effects were actually antibody-mediated reactions against iodinated radiological contrast medium. For this reason, the undesired events usually referred to as an allergic reaction against contrast medium containing iodine are actually anaphylactoid reactions, often defined "allergy-type reactions".

As already mentioned, the precise mechanism of these anaphylactoid reactions is still largely unknown. Symptoms usually appear within a few minutes after administration and reflect the activity of various chemotactic, vasoactive and spasmogenic compounds released or activated in these circumstances.

The principal mediator in these anaphylactic/anaphylactoid reactions is probably histamine and it is most likely responsible for the rapid onset of the clinical manifestations. Histamine is released from basophil and mast cells after degranulation of the cells caused by various stimuli. However, the precise mechanism by which contrast agents activate basophils and mast cells, with subsequent release of histamine and other mediators, is still unknown, even if it has been hypothesized that they act directly on the cell membrane in some way. One of the hypotheses is that contrast agents might be involved in active secretory processes, without causing a real cytotoxic effect. It seems that increasing dimensions and complexity of the compound is related to an increase in cell membrane receptor interactions and release of histamine.

Another important factor that might stimulate histamine release seems to be the higher osmolality, while water solubility and protein binding don't appear to be determinant. Another mechanism suggested to explain anaphylactoid reactions is a direct activation of the immune system, but data available is still not conclusive. However, even if occasionally described in the literature, the ability of these compounds to induce synthesis of antibodies is extremely rare. It is also unlikely that these molecules act as haptens, because they are generally chemically inactive and don't establish strong covalent bonds with proteins. Nonetheless they can activate complement and induce formation of anaphylotoxins, such as C3a, C4a e C5a, that in turn increase release of histamine. They could also activate coagulation factor XII (Hageman factor), with subsequent activation of the kinin system and synthesis of bradykinin (12), that causes

vasodilation, increased blood vessel permeability and bronchospasm. Bradykinin also activates the arachidonic acid cascade, that brings to the production of prostaglandins and leukotrienes. Bradykinin can also stimulate the activation of coagulation factor XII, thus stimulating autocatalytic amplification of the initial triggering factor.

Allergic-like reactions are also called "breakthrough reactions", and these have been observed both in children and adults (24). According to the American College of Radiology (13), symptoms may be classified as mild, moderate and severe, as illustrated in table 3. Although the majority of allergy-type reactions are mild, they can occasionally be so severe to become a risk for patients' life (13) (Table II).

From this point of view, two important things must be kept in mind; the first is that mild forms of allergy-like reactions often are not recognized, because the symptoms may be very common and self-limited, and the second is that besides their unpredictability, these conditions can evolve towards more severe stages if not immediately and appropriately treated. Furthermore, the onset of these undesired effects can also be delayed from one hour to one week after the administration of the contrast agent.

Because of these aspects that it becomes difficult to establish the real incidence of allergy-type reactions; anyway, it seems that they range from 0.5 to 9%, depending on the interval of time considered between administration of the contrast and the onset of symptoms (up to seven days). In any case, they're usually transitory and resolve with appropriate treatment, while life threatening delayed allergy-like reactions are extremely rare (0.0004-0.0008%).

The most severe adverse reactions reported include erythema multiforme, cutaneous vasculitis, Steven-Johnson syndrome, toxic epidermal necrolysis and papulo-pustular eruption.

The objective of this study is to examine the incidence of adverse reactions caused by non-ionic contrast media in selected patients after desensitization treatment and to evaluate the safety profile of organiodine contrast media in a multistep prevention protocol.

MATERIALS AND METHODS

In a retrospective study we reviewed 2000 patients that had received a CT scan with non-ionic i.c.m. during the previous two years (Table III). In this patient population we selected those individuals whose personal history revealed a moderate/high risk for allergy-like adverse reactions against a contrast agent containing organic iodine and that had already reported a previous adverse event related to contrast imaging. In all patients observed (m=1178; f=822; mean age: 55 years) were applied stepwise prevention measures as follows:

Selection of risk patients

After an accurate clinical history, patients furnished informed consent by answering a questionnaire dealing with the most recent European Recommendation on use of Contrast Agents, carefully filled out by medical personnel (informed consent, ESUR Guidelines). This procedure allowed to identify 280 patients at risk; 100 of these had moderate/high risk for adverse reactions against iodinated contrast agents. This risk was stratified in mild, moderate or severe, according to the updated European Society of Urogenital Radiology (USUR) and the American College of Radiology (ACR) Guidelines (13).

Pre-medication protocol

Patients considered at risk for an adverse event against iodinated contrast media (n=280) received the following pharmacological treatment with cortisone and anti-histamine drugs, as suggested by ACR guidelines (2008): Prednisone (50 mg p.o. every 6h the day before the procedure and one h before the i.c.m administration); Diphenhydramine (50 mg i.m. one h before i.c.m administration).

In our operative unit we usually use three different types of non-ionic iodinated i.c.m., as needed: iomeprol (400 mgI/ml in 780 patients), ioversol (350 mgI/ml in 350 patients) or iopromide (300 mgI/ml in 650 patients), administered *iv* at a dosage varying between 10 and 100 ml (2 ml/kg), at a rate of 1-2 ml/s with the aid of an automatic pump.

From our database we selected 2000 patients that had received a CT scan of the region of interest between October 2008 and May 2010 with a TC-Aquilion 4S scanner by Toshiba Medican System.

For all patients we previously obtained and registered the following data: date of procedure, age, sex, body weight, region examined, related diseases (i.e. diabetes, cardiovascular disease, liver disorders), history of hypersensitivity, history of previous undesired reactions related to organ iodine contrast material, other drug therapies and type, dose and route of administration of the contrast agent used (Table IV).

All adverse reactions reported within one hour after the administration of the iodine contrast medium were

classified as mild, moderate or severe, according to the criteria established by ESUR and ACR and registered, as required by the principles of "good practice". Patient monitoring was extended for at least 30 min after i.c.m. in case of mild adverse reactions and for at least one hour in case of moderate reactions.

Statistical analysis

Chi-square test (χ^2 test) was used to compare the incidence of acute adverse reactions, with results statistically significant when $p < 0.005$.

RESULTS

Of the 2000 patients enrolled in the study, only 280 received desensitizing treatment (age range 27-56 years) of which 5 pre-treated patients (1.7%) reported a mild, immediate type reaction to iodine contrast, characterized by variously associated symptoms, such as itching, hives, nasal congestion, vomiting and sweating. Of these five patients with allergy 2 (0.71%) (1 male and 1 female; age 28 and 35, respectively) had received iomeprol, 1 (0.35%) (male, age 31) received ioversol and 2 (0.71%) (1 male and 1 female; age 39 and 44, respectively) received iopromide (Table V). No moderate/severe or fatal reactions were reported, nor were observed statistically significant differences respect to sex, body weight or site examined. No patients that did

Table I. *Characteristics of chemotoxic and anaphylactoid adverse reactions.*

CHEMOTOXIC REACTIONS	- dose and plasma concentration-dependent - influenced by the physical-chemical properties of the molecule (osmolality, viscosity, water- solubility, pH) - likely related to the intrinsic chemotoxicity of the compound - involve mainly the nephrovascular system, the central nervous system and the cardiovascular system
ALLERGIC-LIKE OR ANAPHYLACTOID REACTIONS	- not dose-dependent and not predictable - related to the release of histamine and other biological mediators usually involve in allergies
IDIOSYNCRATIC REACTIONS	- abnormal, individual reactions to a substance and are unpredictable and not dose-dependent

Tab. II. *Classification of the severity of adverse reactions to contrast media.*

MILD	MODERATE	SEVERE
Nausea	Bronchospasm	Convulsions
Itching	Hypotension	Symptomatic tachycardia
Dyspnea	Dysgeusia	Arythmias
Erythema Urticaria	Mild laryngeal edema Cough	Symptomatic bradycardia Cardiorespiratory arrest
Vomiting	Anxiousness	Progressive angioedema
Sweating, fever, mild eye and facial edema	Hypertension	Loss of senses
Nasal congestion Flushing Sneezing		Sever respiratory distress

Table III. *Design of the study.*

	DESENSITIZING TREATMENT	*NO DESENSITIZING TREATMENT*	*TOT*
Patients no.	280	1720	2000 pts. (1178 m; 822 f; mean age 55yo)
High risk patients	100	0	100
Mild immediate reactions	5	0	5
Moderate/Severe reactions	0	0	0

Table IV. *Contrast media administered to patients with and without desensitizing treatment.*

Patients. no.	*2000*	
	DT	*No DT*
	280	*1720*
Iomeprol	172	1383
Ioversol	27	46
Iopromide	81	291

DT*: no of patients that received desensitizing treatment.*
No DT*: no of patients that did not receive desensitizing treatment.*

Table V. *Features of patients with mild immediate reactions and type of contrast media administered (no.5).*

MALE	FEMALE	y.o.	CONTRAST MEDIA
1		28	IOMEPROL
	1	35	IOMEPROL
1		31	IOVERSOL
1		39	IOPROMIDE
	1	44	IOPROMIDE

not receive desensitizing treatment reported mild or severe reactions (Table III). The results were also quite similar for type of iodinated contrast agent used, rate of administration or dosage.

Although results did show a slight difference regarding the incidence (0.71% versus 0.35%) between ioversol and iomeprol and iopromide, the values cannot be considered significant, nor do they allow to reach a definite conclusion because of the low number of adverse reactions reported.

The highest incidence of immediate, non-renal, mild reactions was observed in subjects between 20 and 45 years of age, independently of sex. Therefore, it seems acceptable to conclude that younger patients are those more psychologically influenced, as already described in literature (1). Furthermore, the incidence of adverse reactions was reported to be higher (4 of 5 patients) among those that referred a history of hypersensitivity against iodinated i.c.m.; the fifth patient that developed a mild adverse

reaction referred a history of asthma.

DISCUSSION

The data gathered in this study shows that adverse reactions to non-ionic iodinated contrast media has significantly decreased in patients pre-treated with cortisone (prednisone) and antihistamine drugs (diphenydramine). In fact, the patient population that received pretreatment (280 of the approximately 2000 considered) reported an incidence of adverse events of only 1.7%, mostly characterized by itching, hives, vomiting, sweating and nasal congestion.

These adverse reactions were associated to iomeprol, ioversol and iopromide for 0.71%, 0.35% and 0.71%, respectively, and reported mainly in risk patients with known history of hypersensitivity. Other important factors that influence the incidence of adverse reactions are related to the particular characteristics of each individual iodinated compound, such as osmolality, viscosity, water-solubility, iodine concentration and pH.

The three contrast agents used in this study are all non-ionic monomers and therefore they all have similar properties. The osmolality in particular ranged from 610 to 770 mOsm/kg H_2O. Comparing ionic with non-ionic contrast material it appears evident that increasing osmolality is directly proportional to increase of incidence of adverse events; in our study, however, the factor did not seem to be relevant, because quite similar for all three contrast agents.

Since up-to-date or sufficient information does not exist in literature, describing the advantages of one iodinated compound respect to another, in terms of incidence of acute allergy-like reactions, we decided to evaluate the prevalence of adverse reactions against contrast agents routinely used in our Operative Unit, all non-ionic monomers. The non-ionic contrast materials used had all similar molecular structure, while only ioversol had an extra hydroxyl group (-OH) in position 5 (a total of 6 hydroxyl groups versus 5 of the other compounds) and an amide side chain bound to the same radical group as in iomeprol and iopromide.

Although not yet found in literature, it may be hypothesized that the properties of the molecular structure of an organ iodine contrast agent (23) that assure higher water solubility and high stability are the factors that determine a minor incidence of immediate adverse reactions. On the other hand, prevention of adverse events related to i.c.m. is also very vital and the most important moment of such a prevention is the preliminary evaluation of each individual patient from both a clinical and anamnestic point of view, especially of those at risk, done in collaboration between the family or prescribing physician and the radiologist (7-8).

A simple but specific investigation done a few days before the imaging procedure (2 days), with the aid of a patient history questionnaire, is surely useful, but a direct evaluation by the radiologist remains essential, because often it is the only way to resolve any doubts about the patient, frequently related to inadequate compliance. This would allow, for example, to distinguish a mild "food intolerance", a very common diagnosis among dietitians and very popular among patients nowadays, from a real allergic diathesis (7). It's also necessary to debunk the myth that iodine can cause allergy (21), because it is not and cannot become an allergen. As an element, iodine is present in aminoacids and is a fundamental component of thyroid hormones and its absence is not compatible with life.

Until now, it was believed that i.c.m. adverse events were not really allergic reactions (i.e. IgE-mediated), nor that it was necessary a second contact for them to occur; rather, they were defined anaphylactoid, mediated by histamine released from mast cells and basophils because of the higher osmolality of the iodinated compound respect to blood. In fact, evidence suggests that a positive history of allergy against shellfish or iodine is not more important than any other type of allergy or atopy. Adverse reactions to i.c.m. may be avoided by obtaining a detailed clinical history and by an appropriate pharmacological treatment before administration of the contrast agent. Various protocols have been proposed to lower the incidence of i.c.m. Adverse events (1, 2, 11-15). Those most frequently prescribed in high-risk patients are based on corticosteroids and antihistamines (20-21). Antihistamine drugs showed to be able to prevent cutaneous symptoms, while steroids resulted efficacious against respiratory tract symptoms. Corticosteroid prophylaxis (methylprednisolone, betamethasone, dexamethasone, prednisolone) is

frequently recommended, even though the precise mechanism of action remains unknown.

A single dose of prednisolone does not seem to be sufficient to reduce the incidence of adverse events, but on the other hand it is not wise to underestimate the potential of undesired effects of high doses of corticosteroids.

As far as the pharmacological treatment is concerned, there are only few accurate randomized clinical studies that have investigated the possibility of an efficient and optimal regime to prevent adverse reactions against iodinated contrast material. A recent metanalysis revealed that the efficacy of a pre-treatment in non-selected patients is quite uncertain (17). Therefore, it seems appropriate to conclude that there are no clear and widely accepted indications on how to manage patients with previous reactions to i.c.m.. However, it is still common practice to electively schedule contrast imaging only after appropriate pharmacological pretreatment in patients classified "at risk" after a careful and detailed clinical history (7, 8, 18). As for the drugs used to presumably reduce as much as possible the incidence or severity of adverse reactions, even if these are widely used in patients with previous episodes or known allergies, there is not sufficient evidence as yet to establish the real benefit of the pharmacological pretreatment in patients undergoing contrast imaging procedures (1, 5, 9, 12). A systematic review (15) concluded that H1 antihistamine drugs can prevent anaphylactoid reactions when administered before i.c.m.. Similar results can be obtained with steroids (methylprednbisolone), but only if administered in two doses, six hours and two hours before the i.c.m.. In fact, results show that administration of corticosteroids immediately before administration of a contrast medium is void of any protective effect and therefore brings no real benefit in terms of reduction of the incidence of adverse reactions. So, if they are to be used they must be administered at least 6 hours before the i.c.m. The use of H2 receptor antagonists is optional, but recommended only in association with H1 receptor antagonists.

The prophylactic regime proposed by the ACR (a) is: methylprednisolone 32 mg, 12 h and 2 h before administration of i.c.m, or: prednisone 50 mg, 13, 7 and 1 h before the procedure, associated with thediphenydramine 50 mg i.m. 1 h before the imaging test.

The prophylactic treatment proposed by ESUR is prednisolone 30 mg or methylprednisolone 32 mg po, 12 and 2 h before the administration of i.c.m.

Athough pharmacological prophylaxis for adverse reactions against i.c.m. is common practice in patients with moderate/high risk, a questionnaire given to 202 radiologists, all ESUR members, revealed that prophylaxis with corticosteroids, histamine H1 receptor antagonists and histamine H2 receptor antagonists was done by 76%, 37% and 10%, respectively. The rationale behind the use of corticosteroids is that they increase production of the C-1 esterase inhibitor (C1-inh), whose mechanism of action is the inhibition of activated factor XII and kallikrein, the plasmatic proteasis that activates bradykinin, the principal mediator involved in the typical anaphylactoid reaction.

However, data in literature definitely supporting the role of corticosteroids in allergy prophylaxis in patients undergoing contrast imaging is still lacking. In a study conducted in 1987, Lasser et al. (17) randomized 6763 patients to receive an ionic i.m.c. plus a corticosteroid drug or only the ionic contrast agent and observed a significant decrease of adverse events in pretreated patients, with an incidence very similar to that described in literature for non-ionic contrast material.

On the other hand, the benefit of the association of a corticosteroid and a non-ionic i.c.m. appeared less evident. In a subsequent non randomized study (18) on 1155 patients, Lasser reported a significantly lower incidence of adverse reactions in the group undergoing imaging procedure with a non-ionic contrast agent and pretreated with a corticosteroid respect to those not receiving cortisone prophylaxis (1.7% versus 4.9%).

Katayama et al. (10) reached conclusions completely different. Reviewing the Japanese registry containing a very large number of patients (337,647) they did not find any benefit of corticosteroid pre-medication in patients receiving a non-ionic i.c.m.

So, considering the discrepancy between the results reported by various authors and since there are no data in literature indicating that one non-ionic i.c.m. is "safer" than another, we decided to re-examine prospectively CT scans performed with one of the three contrast agents routinely used in

our operative unit. In the cases examined, all of the patients had been adequately informed and for all were implemented all the preventive measures necessary to reduce the risk of adverse reactions, such evaluation for allergy, pharmacological history and the use of non-ionic i.c.m., in compliance with the ACR Guidelines-2008. The results reported correlated with most of the data existing in literature, according to which the incidence of immediate mild adverse reactions associated with a non-ionic contrast agent is lower in patients receiving desensitizing pretreatment respect to those not receiving any pre-medication (1.7 versus 2.5 - 3.5%).

Contrary to other authors (24), in our patient population we registered a rate of adverse events after pharmacological pretreatment of 0.7% for iomeprol and iopromide and of 0.35% for ioversol. Other important aspects observed were a discrete correlation between the incidence of adverse reactions and both young age and known allergy to organiodine contrast media.

Nonetheless, it is very important to keep in mind that a drug or pharmacological regime able to avoid fatal events is not available at the moment, mainly because adverse actions to contrast materials are absolutely unpredictable. Moreover, even if the fatal events associated with i.c.m. are actually rare (1:170,000), with a rather similar risk for ionic and non-ionic compounds, they are more frequently registered in white, old aged women and in those with concurrent debilitating diseases (the 4 W: women, white, wrinkled, weakened) (25).

Deaths consequent to administration of an organ iodine compound can often be attributed to acute renal failure and anaphylaxis. According to a recent review (25) of 48 cases of death caused by uro-angiographic contrast media, the reasons of death were renal failure (58%), anaphylaxis and allergy (19%), cardiorespiratory arrest (10%), respiratory failure (8%) and stroke and cerebral hypoxia (4%). So, the data in literature is not unequivocal, as is not the radiologists' behavior in the specific cases. For this reason, ESUR established its guidelines (37,23), prepared by experts and discussed at the USER European Symposium in 2001 and recently updated.

Considering the low risk and low cost of a brief prophylaxis, these guidelines do suggest a steroid therapy as a precautionary measure in high-risk patients, excluding those with certain health conditions, such as peptic ulcer, tuberculosis or systemic infection. Due to the mechanism of action of corticosteroids (plasma receptor binding, migration into the nucleus, activation of DNA-dependent RNA synthesis, translation of specific inhibitory enzymes) these guidelines however suggest that such treatment be implemented at least 6 hours before the imaging test.

Regarding prophylaxis with H1 and H2 receptor antagonists, to date there is no convincing evidence of the advantages of this treatment in patients with high risk for i.c.m. adverse reactions. Even if experts have different opinion concerning antihistamine drugs, the guidelines suggest an optional use, but in association with corticosteroids: the incidence of acute anaphylactoid reactions has decreased with the use of non-ionic, low osmolality agents, independently from the presence or absence of risk factors, making it difficult today to justify the use of ionic i.c.m.; high risk patients must use non-ionic i.c.m.; delayed adverse reactions are generally less severe and independent from the contrast material used; it is always necessary to follow the patients for a few hours after the administration of a contrast agent, as undesired events may also appear after several hours from the procedure (20); in high risk patients, corticosteroid prophylaxis is still recommended and must be started at least six hours before the administration of the i.c.m.

Anaphylaxis and "anaphylactoid" (not immunoglobulin-mediated) adverse reactions against uro-angiographic intravenous contrast media is still an unsolved problem that raises much concern, also because the real etiopathogenetic mechanisms behind these events are still not clear.

Although much time and efforts have been dedicated to this problem and many studies have been performed with the objective of disclosing such mechanisms, no one single desensitizing pretreatment regime showed significant benefits in terms of reduction of the incidence of severe or fatal adverse reactions (21, 22).

So we still need more clinical and experimental studies to improve our knowledge of the physiopathological mechanism of these undesired reactions, in order to be able to offer the best protection possible for patients undergoing imaging

procedures.

Thus, even if we know that the majority of these reactions are idiosyncratic and unpredictable (at least 50% of these are immune-mediated) and that their development, at least those more severe or fatal, independently from any prophylaxis, we propose, with the aim of improving our knowledge on this subject, a multicenter study, based on skin allergy tests (prick test, patch test, intradermoreaction) in selected patients that have had previous experiences of hypersensitivity against parenteral organ iodine contrast media. This screening procedure might result useful to diagnose an allergy towards a specific iodinated contrast medium and will allow to identify agents showing the highest tolerability and therefore a consequently lower incidence of repeated adverse reactions.

In the light of the recent directives of SIRM (Italian Society of Clinical Radiology) regarding the use of *iv* organiodine contrast medium, guidelines widely supported also throughout Europe, we decided to apply in our Operative Unit the suggested updated strategy for prophylaxis against i.c.m. toxicity, that goes from the preparation of the patient to the implementation of a pre-contrast treatment protocol.

Asserting and underlying that the knowledge of the norms and regulations of a certain matter is an essential requirement, we would like to point out that the main objective of our experimental model was to propose a *modus operandi* regarding prophylaxis associated to the use of uro-angiographic contrast agents, also taking into account the essential basic knowledge of the radiologists, that ranges from pharmacology to physiopathology to basic reanimation techniques. That radiology is a highly qualified profession and that it carries certain risks (for example, radioprotection, frequent use of i.c.m., diagnostic- therapeutic interventions) is a well-known fact, and this amply justifies the attention given to the subject in question, and not only for operators directly involved.

If we just stop and think that since their introduction in the 1950s, today over 80 million contrast procedures are carried out the world over. If it is true that the majority of the adverse reactions related to contrast materials are mild/moderate and therefore self-limiting, but it's also true that, notwithstanding the extremely low incidence, patients may develop severe life-threatening reactions. Thus, such events represent an important chapter in medical urgencies because of their fast onset, unpredictability, variability of the clinical picture and the possibility of death, despite an adequate prophylaxis. All of these considerations obviously require continuous attention from both medical personnel and not. Without wanting to cause excessive alarm, it seems appropriate to remember what Sidhu and Dowson said in 2002: "anyone who administers i.c.m. will sooner or later have to deal with an unexpected and severe or even a potentially fatal reaction".

The clinical role of the radiology physician must be strongly emphasized today: if we just consider that there are not really any absolute counter indications for the use of intravenous contrast material, (maybe the only one valid reason not to do contrast imaging is the lack of any true indication for such a procedure) we must also accept the fact that the radiologists is the only one who can make a considered decisions, obviously taking into account the risk/benefit ratio, that is the risk of using versus the risk of not using an intravenous contrast medium.

Although we might believe that a prescribing physician will continue to suggest procedures and technique to confirm his suspected diagnosis, it is important to recognize that each case must be considered individually, and the radiologists is the only one who can do so.

This particular aspect is also underlined in recent literature, adding that i.c.m. should not be administered if there is not a clear or justified indication. Moreover, since non contrast procedures are constantly improving and always more widely available, these should be preferred to contrast procedures if they can furnish the same information. It must however be acknowledged that intravenous contrast materials have greatly improved since they were first introduced, especially in terms of their safety profile. On the one hand, industry has implemented a continuous and qualified research program to always find newer and safer contrast agents (the route toward the ideal contrast medium: optimal contrast, optimal tolerability), on the other hand the explosion of the number of procedures performed, technical improvements (i.e. TCMD) and the diffusion of intervention radiology: these are the factors that have determined a significant increase in

the use of i.c.m. oriented in improving diagnostic-therapeutic accuracy, something that the modern image-guided medicine can longer do without.

In as much and in compliance with the new European GuidelinesESUR 2009 and with the SIRM – 2009 "Use Recommendations" and by initiative of the Italian Society of Clinical Radiology and other Scientific Societies (SIAARTI, SIN, AINR) it seemed appropriate to implement in our own department the new guidelines for the use of iodinated intravenous contrast media, starting by activating a specific approach to patient preparation and prevention.

In fact, SIRM strongly wanted to underline the responsibilities of the radiologists as "first operators", absolutely not to create excessive alarm, but to suggest a series of recommendations that would allow them to carry out their work with caution, confidence and awareness, both in diagnostic and interventional radiology. From this point of view, a determining factor seems to be the knowledge of the characteristics of the various i.c.m. currently available, as well as the continuous update by the radiology physicians regarding technological progress. Not of secondary importance is the no longer deferrable necessity to refer, in compliance with current regulations, eventual adverse reactions, with the only aim to learn from past experience and to share such experience with others, so to avoid that such events might repeat. Finally, it is essential to become aware that adverse drug reactions, and contrast agents are real drugs, are considered a health emergency over the world and that in Italy in particular this awareness is still insufficient.

REFERENCES

1. Delaney A, Carter A, Fisher M. The prevention of anaphylactoid reactions to iodinate radiological contrast media: a systematic review. BMC Medical Imaging 2006; 6:2.
2. Trcka J, Schmidt C, Seitz CS, Bröcker EB, Gross GE, Trautmann A. Anaphylaxis to iodinated contrast material: nonallergic hypersensitivity or IgE-mediated allergy? AJR Am J Roentgenol 2008; 190(3):666-70.
3. M.G. Bonetti, A. Vesprini, M. Concetti, S. New guidelines on the use of iodinated contrast media: a report on an implementation project. RadioIogia Medica 2009; 114:496-508.
4. Namasivayam S, Kalra MK, Torres WE, Small WC. Adverse re action to intravenous iodinated contrast media: a primer for radiologists, Emerg Radial 2006; 12(5):210-5.
5. Tramèr MR, von Elm E, Loubeyre P, Hauser C. Pharmacological prevention of serious anaphylactic reactions due to iodinated contrast media: systematic review. BMJ 2006; 333(7570):675.
6. Freed KS, Leder RA, Alexander C, DeLong DM, Kliewer MA. Breakthrough adverse reactions to low-osmolar contrast media after steroid premedication. AJR 2001; 176(6):1389-92.
7. Scherer K, Harr T, Bach S, Bircher AJ. The role of iodine in hypersensitivity reactions to radio contrast media. Clinic and Exper Allergy 2010; 40(3):468-75.
8. Callahan MJ, Poznauskis L, Zurakowski D, Taylor GA. Nonionic iodinated intravenous contrast material-related reactions: incidence in large urban children's hospital - retrospective analysis of data in 12,494 patients. Radiology 2009; 250(3):674-81.
9. Davenport MS, Cohan RH, Caoili EM, Ellis JH. Repeat contrast medium reactions in premedicated patients: frequency and severity. Radiology 2009; 253(2):372-9.
10. Brockow K, Romano A, Aberer W. European Network of Drug Allergy and the EAACI interest group on drug hypersensitivity. Skin testing in patients with hypersensitivity reactions to iodinated contrast media - a European multicenter study. Allergy 2009; 64(2):234-41.
11. Bui KL, Horner JD, Herts BR, Einstein DM. Intravenous iodinated contrast agents: risks and problematic situations. Clevel din J Med 2007; 74(5):361-7.
12. Dewachter P, Laroche D, Mouton-Faivre C. Immediate reactions following iodinated contrast media injection: a study of 38 cases. EJR 2011; 77(3):495-501.
13. Namasivayam S, Kalra MK, Torres WE, Small WC. Adverse reactions to intravenous iodinated contrast media: an update, Curr Probi Diagn Radiol 2006; 35(4):164-9.
14. Loh S, Bagheri S, Katzberg RW, Fung MA, Li CS. Delayed adverse reaction to contrast-enhanced CT: a prospective single center study comparison to control group without enhancement. Radiology 2010; 255(3):764-71.
15. Caimmi S, Benyahia B, Suau D, Bousquet-Rouanet

L, Caimmi D, Bousquet PJ, Demoly P. Clinical value of negative skin tests to iodinated contrast media. Clinic and Exper Allergy 2010; 40(5):805-10.
16. Feltrin GP, Zandonà M, Borile V, Rettore C, Miotto D. Fondamenti sui mezzi di contrasto iodati e reazioni avverse. Radiol Med 2004; 107(1-4):8-31.
17. Schabelman E, Witting M. The relationship of rodiocontrast, lodine and seafood allergies: a medical myth exposed. JEM 2010; 39(5):701-7.
18. Brockow K, Christiansen C, Kanny G, et al. Management of hypersensitivity reactions to iodinated contrast media. Allergy 2005; 60(2):150-8.
19. Torres MJ, Mayorga C, Cornejo-Garcia JA, Lopez S, Chaves P, Rondon C, Fernandez T, Blanca M. Monitoring non-immediate allergic reactions to iodine contrast media. Clin Experim Immunol 2008; 152(2):233-8.
20. Brockow K. Contrast media hypersensitivity – scope of the problem. Toxicology 2005; 209(2):189-92.
21. Thomsen HS, Morcos SK, Contrast Media Safety Committee of European Society of Urogenital Radiology. Management of acute adverse reactions to contrast media. Eur Radiol 2004; 14(3):476-81.
22. Morcos SK, Thomsen HS, Webb JA; Contrast Media Safety Committee of the European Society of Urogenital Radiology. Prevention of generalized reactions to contrast media: a consensus report and guidelines. Eur Radiol 2001; 11(9):1720-8.
23. Cohan RH, Ellis JH, Dunnick NR. Use of low-osmolar agents and premedication to reduce the frequency of adverse reactions to radiographic contrast media: a survey of the Society of Uroradiology. Radiology 1995; 194(2):357-64.
24. Dillman JR, Strouse PJ, Ellis JH, Cohan RH, Jan SC. Incidence and severity of acute allergic-like reactions to *iv* nonionic iodinated contrast material in children. AJR 2007; 188(6):1643-7.
25. Brockow K, Ring J. Classification and pathophysiology of radiocontrast media hypersensitivity. Chem Immimol Allergy 2010; 95:157-69.